"THE DYNAMICS AND CONTROL OF CHEMICAL EVAPORATORS"

A THESIS PRESENTED IN CANDIDATURE FOR THE DEGREE

OF DOCTOR OF PHILOSOPHY

by

REGINALD EDWARD UNDERDOWN,

M.Sc., B.Tech., A.U.A.

Department of Chemical Engineering,

University of Adelaide

March 1972

SUMMARY

A mathematical model for the investigation of control system design on concentrating evaporators is developed and demonstrated by reference to two principal types using analogue and digital simulation methods.

The theoretical model is verified on the basis of experimental work performed on a laboratory scale forced-circulation external calandria evaporator.

The frequency responses of the experimental evaporator, to a range of disturbances, are calculated, and checked by comparison with experimentally determined frequency responses. Frequency responses are measured over a ten-fold change in process liquor flow rate for disturbances in steam temperature and liquid flow rate. The occurrence of resonance is demonstrated in the experimental evaporator.

A digital simulation technique developed during the study is applied to an examination of several alternative multi-loop control schemes with the forced-circulation evaporator.

A linearised theoretical model is simulated on analogue computer allowing a comparison of alternative control schemes for the internal-calandria evaporator. The possible use of cascade control systems and of combined feedforward-feedback control is studied in relation to the standard evaporator. A study is made of a wide range of disturbances. Interaction is demonstrated between the control loops in certain configurations and a controller arrangement previously described as unstable is shown to be stable within a restricted region.

It is believed that the model described here is applicable to standard and forced-circulation concentrating evaporators, and by

taking into account the modifications proposed, is applicable to evaporators where solids are present. It is also believed to have relevance in assessing the dynamic behaviour of distillation column reboilers. The linearised model is thought to be applicable to making qualitative predictions for control purposes under normal industrial operating conditions.

PREFACE

The work described in this dissertation was carried out while the author was a lecturer in the School of Chemical Technology, South Australian Institute of Technology. It describes his original work and no part has been submitted to any other University or Institution for a higher degree.

The author wishes to acknowledge the advice and helpful discussions of his supervisor, Professor R.W.F. Tait, during the preparation of this thesis.

INDEX

	Page
SUMMARY	(i)
1. INTRODUCTION	1
1.1 Origin of disturbances	2
1.2 The control problem	3
1.2.1 Density control	4
1.2.2 Pressure control	4
1.2.3 Level control	5
1.3 Selection of control loops	6
1.3.1 Density control	6
1.3.2 Pressure control	7
1.3.3 Level control	8
1.4 Operating limitations	8
2. REVIEW OF PREVIOUS WORK	10
3. THEORETICAL STUDY	27
3.1 Assumptions	31
3.2 The basic equations	40
3.3 The dynamic equations	51
3.3.1 Retaining distributed parameter characteristic	51
3.3.2 Impulse response	55
3.3.3 Linearised dynamic model	59
3.3.4 Reduction of dynamic equations	61
3.4 Derivation of transfer functions for linearised model	67
3.4.1 Response of product density	67
3.4.2 Response of pan level	70
3.4.3 Response of product flow	72

4. DESCRIPTION OF EXPERIMENTAL PLANT 74

5. ESTIMATION OF HEAT TRANSFER COEFFICIENTS 79

6. FREQUENCY RESPONSE ANALYSIS OF FORCED-CIRCULATION EVAPORATOR 84

6.1 Calculation of theoretical responses 84

6.1.1 Theoretical responses based on simplified model 85

6.1.1.1 Product density 85

6.1.1.2 Pan level 91

6.1.1.3 Product flow 92

6.2 Experimental frequency response analysis of forced-circulation evaporator 93

6.2.1 The apparatus 93

6.2.2 The experimental procedure 94

6.2.3 Results and discussion 96

6.2.3.1 Shell-side dynamics 96

6.2.3.2 Product liquor response to feed temperature disturbances 102

6.2.3.3 Product liquor response to steam temperature disturbances 102

6.2.3.4 Response of product liquor temperature to feed flow rate disturbances 104

6.2.4 Accuracy of frequency response measurements 108

7. EVAPORATOR BEHAVIOUR WITH ALTERNATIVE CONTROL SCHEMES 109

7.1 Introduction 109

7.2 Analogue computer simulation 113

7.2.1 Results and discussion 117

7.2.1.1 Case 1 120

7.2.1.2 Case 2 121

7.2.1.3 Case 3 123

7.2.1.4 Case 4 124

7.2.1.5 Case 5 125

7.2.1.6 Case 6 126

7.2.1.7 Response to pressure disturbances 126

7.2.1.8 Cascade control schemes 129

7.2.1.9 Feedforward-feedback control 132

7.2.1.10 Summary 133

7.3 DIGSIM : Digital computer simulation 135

7.3.1 Results and discussion 141

8. CONCLUSIONS 148

Figures - In sequence 153-218

Nomenclature 219

Appendix A : Plant parameters etc. for forced-circulation evaporator 223

Appendix B : Evaporation with solids present 227

Appendix C : Specimen DIGSIM programme 230

Appendix D : Computer programme IMPULSE 236

Bibliography 250

INDEX OF TABLES

TABLE NO.	DESCRIPTION	PAGE
1.	Response of tube fluid temperature to impulse disturbance in steam temperature	59
2.	Wall and fluid temperatures	80
3.	Heat transfer coefficients	83
4.	Frequency response of simplified model (Response of product density)	90
5.	Experimental data for vapour flow response to steam flow variations	97
6.	Experimental data for steam flow response to steam pressure variations	97
7.	Summary of controller configurations used in initial analogue simulation	118-119

1. INTRODUCTION

The main aim of most evaporator control systems is to regulate conditions within the evaporator so that the product stream meets a particular specification. This requires that the control system minimises fluctuations in the product composition arising from disturbances in the input stream or in the plant itself. The nature of the fluid, the operating conditions, the equipment design, and the manner of association with other plant, all influence the detailed nature of the control scheme. This is why the plant and its associated control equipment should be considered together at the design stage. In particular where the process is associated with other processes in a plant with little or no storage capacity to act as a buffer between processes, care must be taken to guard against interaction between control loops. Even in the course of this work involving only a single process, certain control schemes showed pronounced interaction between control loops.

Figure 1 is a diagrammatic representation of a natural-circulation internal-calandria evaporator which also indicates the symbols used in this study.

Generally an evaporator is designed to produce product of a specified grade from a feedstock whose flow rate, composition, and enthalpy are all specified. At the design stage, given this information together with a selected operating pressure, the calandria and condenser heat loads and heat transfer areas can be calculated. Once these areas are fixed, provided the specified input variables remain constant the evaporator should always produce

material of the required concentration. However, under normal operating conditions disturbances arise which alter these parameters from their design values, and in the absence of effective controllers faulty product may result. It is worthwhile to consider where and how these disturbances may arise. It is also well to remember that control schemes which are effective for small disturbances may fail if the disturbances become larger, generally because a process which is inherently non-linear behaves linearly until excited by signals with a sufficiently large amplitude.

1.1 Origin of Disturbances

Disturbances may arise in any of the following variables:

(a) Feed flow rate, density and enthalpy.

(b) Calandria heat input rate, which may vary through changes in the heating medium supply pressure or temperature.

(c) Condenser heat removal rate, which may vary because of changes in flow rate or temperature of the cooling medium (surface condenser) or flow rate (contact condenser).

(d) Pan pressure, through changes occurring in the condenser-ejector system.

(e) Ambient conditions, which affect the rate of heat transfer from the equipment, or the operating pressure of any plant vented to the atmosphere.

(f) Variations in product withdrawal rate, originating in changing demands by some succeeding process.

Of these, the main source of disturbances is the feed stream, particularly as most evaporators have their own subsidiary control loops regulating the heating medium conditions, and the

condenser-ejector conditions. In a similar fashion it would be possible to control separately the feed flow rate and temperature, but at the risk of controller redundancy. Figures 2 and 3 summarise these comments in block diagram form for the main output variables, namely product density, level, and product flow.

1.2 The Control Problem

As already stated the object is to maintain one, or more, of the specified variables at some desired value by manipulating some other control variable. The basic problem is to choose the controlled and controlling or manipulated variables in such a way as to minimize the magnitude of the initial deviation and the time required to return to the desired value. Other measures of controllability have been proposed and may have special merit in particular cases, but in general the two criteria proposed ensure satisfactory performance. It is necessary to study the dynamic behaviour of the equipment, in this case evaporator, to determine which combinations of controlled manipulated variables give the best performance.

Generally the controlled conditions are specified in the initial design, e.g. product density. However measurement of this variable is not always satisfactory and an inferential measurement may have to be made. The pan pressure, which is also generally specified, is readily measured, the problem in this case reduces to selecting the control loop to give the fastest response. To ensure that the density and pressure control loops operate properly, it is also necessary to control the

liquid level in the evaporator. The level loop ensures that the vapour boil-up rate does not vary due to uncontrolled changes in the available heat transfer surface.

1.2.1 Density Control

Direct measurement of density is possible, but commonly the density is inferred from temperature measurements, since at a given pressure and under equilibrium conditions, the temperature of the liquid at any point is a function of the composition of the liquid at that point. Having decided on the measurement technique it is necessary to consider the dynamics of the system to determine whether the density should be controlled by regulating the heating medium rate, the feed rate, or the product withdrawal rate.

1.2.2 Pressure Control

The pressure in an evaporator must be controlled to meet three requirements.

(a) Any measurement of temperature is a function of composition only when the pressure is constant at the point of measurement.

(b) Under transient pressure conditions the vapour rate is dependent mainly on such pressure variations and not on the heat input as under steady state conditions.

(c) The pressure difference between the evaporator and its associated plant items should be kept sensibly constant to reduce unwanted flow fluctuations.

The pan pressure is determined by the quantity of vapour in the system so that the manipulated variable for any control loop can be selected from those variables which affect the vapour content directly, viz. heat input rate, and vapour withdrawal rate. The heat input rate is not generally used for pressure control as it is usually specified either as the correcting condition or at a fixed value, for the more important density control scheme. Where the vapour contains inerts, regulation of the vapour withdrawal rate affects the partial pressure of the condensables in the condenser. Any pressure control loop will affect the vapour rate during transient conditions even if the heat input is held constant. Thus strong interaction can be expected between the pressure and density control loops when the temperature is controlled (as a means of controlling density) by regulating the heat input to the calandria. The existence of such interaction is seen clearly in the traces obtained during the digital simulation.

1.2.3 Level Control

Considered in isolation the liquid level in an evaporator need not be specified, provided it remains between the two limited conditions of exposed calandria tubes or flooded evaporator, and provided always that transient changes do not take the pan off the boil. However in the total system it performs two important duties.

(a) It ensures that the density and pressure loops operate as designed.

(b) It ensures that large fluctuations in product withdrawal rate do not disturb the flow rate where the evaporator product is the feed to succeeding processes.

The level controller in fact assists to satisfy the mass balances in the pan and condenser systems. It is undesirable to tie the vapour rate to the feed conditions by using a ratio controller since under transient conditions these flows are not related directly because of the system. In addition if feed composition changes occur, any attempt to control the product stream as a ratio of the vapour rate or feed flow rate will generally give a product outside the specifications.

1.3 Selection of Control Loops

There is a number of possible combinations of controlled and manipulated variables. In essence two general conditions must be satisfied to secure adequate concentration and good controllability.

(a) The product must meet the quality specified.

(b) The number and magnitude of lags in the control loops must be kept to a minimum.

1.3.1 Density Control

There are four possible control schemes.

(a) Constant vapour withdrawal rate - regulation of steam supply to calandria.

(b) Constant product withdrawal rate - regulation of feed.

(c) Constant feed rate - regulation of product withdrawal.

(d) Constant feed rate - regulation of steam supply to calandria.

The choice between (b) and (c) would depend on the dynamic behaviour of the two loops. In the case of (d) the main lags would be associated with heat transfer in the calandria and mass transfer within the evaporator pan. The delay in vapour propagation could be expected to be negligible.

1.3.2 Pressure Control

The methods available are similar to those applicable in distillation column control, except that in evaporation one does not generally have liquid top products, or even mixed liquid and vapour top products. This tends to reduce the applicability of the technique found most effective in distillation practice, viz. varying the proportion of non-condensables in the condenser. Under these circumstances two methods seem applicable.

(a) Regulation of coolant flow rate.

(b) Variation of total pressure in the condenser.

Method (a) requires a condenser design such that there is a small difference between the coolant outlet temperature and the condensing temperature of the vapour to achieve good controllability. Where untreated water is

used as the coolant the water outlet temperature is usually limited to 35°C to minimise scaling. This limits the operating pressure range. Further, since the regulation is achieved by a supply side change the loop response will be slow.

Method (b) is more applicable to systems operating at high pressure and is most useful where the temperature difference in the condenser is small, since in such case, any increase in coolant flow will only cause a slight fall in condensing pressure, and thus condensing temperature, without affecting the boil-up rate materially. However, in general, method (a) is to be preferred.

1.3.3 Level Control

The liquid level is controlled by regulating the feed rate or product withdrawal rate, the choice must depend on the respective loop dynamics and the alternatives have been compared in the simulation studies. Generally any attempt to control the liquid level by adjusting the heat input is considered undesirable because it places greater reliance on maintaining the liquid level than on securing the desired concentration.

1.4 Operating Limitations

Apart from the particular features commented on already, there are some operational requirements which influence the detailed design of control systems.

(a) Any correcting condition which limits the rate of production should not be used for control but should be adjusted to its optimum value. Such a condition would be the heat input rate to an evaporator operating at the minimum hold-up time. Apart from dynamic considerations this would tend to count against an overall control scheme in which the density control loop modulates the steam supply.

(b) It is preferable to operate with the heat transfer tubes fully covered. The effect of this requirement is that a level control loop generally forms part of the overall evaporator control scheme even though, as discussed elsewhere, the actual level is not critical under open-loop conditions and only affects product density through the controllers, under normal closed-loop operation.

(c) If disturbances are anticipated in the condenser cooling medium supply, or in the vapour withdrawal rate, the pressure control loop should act on the variable that is most disturbed. In general it would be anticipated that with level control, a uniform and adequate heating medium supply, and feed admitted at its boiling temperature, the boil-up rate should not fluctuate wildly. In this case the pressure control loop would manipulate the coolant flow rate, as previously intimated.

2. REVIEW OF PREVIOUS WORK

The majority of the publications describing the behaviour of chemical evaporators have dealt with the dynamics of the heat exchanger portion. Other papers have dealt with operating aspects such as examining the conditions under which solids are deposited.[38] Not surprisingly the results of such studies indicate that the solids are deposited in regions associated with the regimes of flow and heat transfer. It is partly for this reason that recommended industrial practice is to maintain a minimum fluid velocity of 8 feet per second to minimise solids deposition.[7]

A few workers have also concerned themselves with the establishment of optimum production conditions for a specific product,[28,40] or with contrasting the merits of particular classes of evaporator for various kinds of tasks.[13,27,33] Parker[33] considered the factors which influence the selection of evaporation plant and proposed guide-lines for writing industrial specifications, while Newman[31] summarised the more common operating difficulties and suggested appropriate test procedures.

Only three research papers are known to the writer which touch on the central theme of this study.

The report of Andersen et al[1] is the most complete investigation reported previously. It describes the analogue simulation of a natural-circulation internal-calandria evaporator together with certain responses of the simulated model and some limited frequency response data. The transient responses of product density and flow to feed density disturbances are reported for four controller configurations, and to steam supply for three of these cases plus a fifth controller arrangement. One experiment examined feed flow disturbances, but disturbances in

pressure or feed temperature were not considered. In fact pressure was assumed to be constant throughout the study. The frequency response results concern the response of product density to feed flow disturbances. Theoretical curves are presented for this case and for density response to steam supply disturbances.

The experimental results were not normalised in the usual way because the large time constant of the evaporator would have necessitated holding plant conditions steady for several hours. The procedure used was to regard the point on the experimental curve which corresponded to a phase lag of 45^{o} as having an attenuation of 1.41 and to plot the remaining experimental points accordingly. This technique is sound enough if the system is a single transfer stage, as was assumed, but is less certain if a distance-velocity lag is present. Comparison of the experimental and theoretical phase curves shows some deviation over the frequency range 2π-4π radians per hour. In fact at the latter frequency the experimental value is 98^{o} compared with the theoretical value of 83^{o}. The phase lag of a single transfer stage should approach 90^{o} as a limiting angle. There is thus a possibility that the system is not a single transfer stage. Unfortunately no further experimental phase lag readings are indicated in the published figure although amplitude points are recorded up to a frequency of 12.5π radians per hour.

The same evaporator was the subject of a further study, applying a cross-correlation analyser, by Hazlerigg and Noton.[15] The results were somewhat inconclusive. The experimental work concerned the response of product density and pan temperature to feed flow disturbances. The latter results were discarded as not being suitable for analysis. It was found

that the assumed weighting function could only be fitted to the test results if a lag of 3½ minutes was assumed to be in series with the measurements. Evaporator time constants for the response of product density to feed flow of 1½ and 4½ minutes respectively were determined, whereas the earlier work of Andersen et al found a single time constant of approximately 43 minutes. The claimed time constants are hard to reconcile and one is led to conclude that the two groups measured different phenomena. There is nothing in either report to suggest whether either technique was in error, but from a consideration of the physical features of the evaporator studies, the figures cited by Andersen et al would seem the more realistic.

The earlier study used an empirical proportional relationship between the product density and concentration. There is the possibility that some dynamic effect is involved, such that during transient disturbances of feed flow the pan concentration changes more rapidly than the product density despite the direct proportionality assumed in the steady state expression. Hazelrigg and Noton in fact advanced the hypothesis that since density is a function of concentration and temperature, an increase in feed flow causes a drop in both concentration and temperature. Neither group reports any results that could provide a check on this suggestion. It is true that for ammonium nitrate, the solution being treated in the evaporator, a fall in concentration means a fall in density, whereas a drop in temperature means an increase in density. The observed density is thus the resultant of two conflicting effects and might exhibit a larger time constant as observed in the product line, where measured by Andersen, than the density measured in the pan. Even so, the time constants reported by Hazlerigg and Noton seem unreasonable when one considers that

the hold-up time (volume/throughput) is about 1.65 hours.

In view of the magnitude of the principal time constant in the evaporator, and the effect of this on the actual performance of a frequency response analysis, the agreement between the theoretical curve and experimental results for the response of product density to feed flow variation is good. For the interval between 0.04 and 0.2 radians per minute the scatter in the phase lag measurements is about 10%, while the attenuation points are distributed evenly about the theoretical curve. The break frequency for the amplitude ratio curve drawn through the points is 0.023 radians per minute which indicates an effective time constant of 0.725 hours, and compares reasonably well with the theoretical value of 0.745 hours. No experimental phase points are presented beyond 0.12 radians per minute, making it difficult to assess if there is a distance-velocity lag involved in the actual system.

Hazlerigg and Noton report that they found the greatest lag occurred at a period of 0.2 hours; at this period the difference between the experimental and calculated results was $(120^{o} - 98^{o}) = 22^{o}$. This phase angle would be contributed by a D-V lag of only 0.74 minutes. Stated another way, the assumed time delay of 3.5 minutes would contribute 105^{o} at this period compared with their measured total phase lag of 120^{o}. Clearly there is some discrepancy here. Andersen does not record a value at this period. However from the trend of the last few phase values reported, we can anticipate a difference between his experimental and theoretical results of about 33^{o}, which would arise from a D-V lag of about 1.1 minutes. Admittedly this is a crude approximation, but if we

refer to the value reported for the period 0.8 hours, which seems to be a reasonable compromise, we note a difference of 11° which corresponds to a D-V lag of 1.47 minutes approximately. There is insufficient information in the paper to calculate the time required for the solution to pass through the calandria tubes, but the linear flow rate can be estimated to be about 0.24 feet per minute assuming single-phase flow. A time delay of the right order could arise at this point.

Johnson[17] described the investigation of an evaporator installation which was subject to an instability. The controller arrangement was similar to that described in this study as Case 6. However there was an additional controller loop in which air loading of the vacuum ejector was used to regulate the pan pressure. The system behaviour was quite different from that expected, the process becoming inoperable at times as the pump lost suction.

Frequency response tests on the plant over the range 0.025 to 2 cycles per minute led to the following transfer function for the response of level to changes in feed flow.

$$\frac{L}{V_f} = \frac{6.0\ e^{-0.63s}}{s(1 + 0.88s)} \quad \text{inches/min-psi}$$

According to Johnson the level control loop was not able to cope with disturbance of about one cycle per minute. He attributed this to interaction with the vacuum system.

Simulation experiments carried out during the present programme using this controller configuration showed that the controller settings were critical because of interaction between the loops. However the level response was acceptable despite large variations in product density. This would support Johnson's conclusion that the vacuum control loop was

involved, and from the tests made, that the source of the pressure disturbances was not the variations in feed flow rate but arose in the ejector.

Johnson observed a strong interaction between vacuum and level, a 0.1 inch (Hg) vacuum change causing an 8.5 inch level change over the entire test frequency range. This interaction did not show on the normal plant records because vacuum upsets sufficient to saturate the level system were less than the pen line width on the vacuum recorder. Although it was first thought that the disturbances might originate in the steam supply to the ejector, later tests showed that they arose in the ejector itself.

Little has been published concerning the dynamics of steam ejectors.[12,20] One of these papers[12] presents a model and design curves for a constant-area ejector. Most commercially available ejectors are of the constant-pressure mixing type. Keenan et al[19] showed experimentally that this type realised 85% of the calculated entrainment and compression. In practice, once the maximum discharge pressure is reached a small additional increase in discharge pressure causes a marked decrease in suction flow. Discharge pressures below the maximum have little effect on the capacity. In this sense ejectors behave like "critical-flow" nozzles, but the two cases are not analogous.

The study of ejectors was considered to be outside the scope of this programme, but the dynamics of vapour withdrawal were included during the development of the mathematical model.

Another potential source of disturbance that could arise in evaporator operation has been described by Danilova and Belsky[10] who reported

that the boiling heat flux exhibits hysteresis during the transition from convective heating to nucleate boiling. This means that if an evaporator is operating normally under natural convection conditions the temperature difference between the tube wall and the boiling liquid increases gradually until some critical value is reached. At this point the heat flux increases suddenly and nucleate boiling is observed. The reverse happens if we begin with a large temperature difference and allow it to decrease in magnitude. This implies that an evaporator should not be operated close to, or below, the critical temperature difference. The particular value can be found only by experiment, however it is of the same order as the minimum temperature difference needed to establish boiling.

There will also be a marked difference between the behaviour of single-tube and multitube evaporators. For single-tube evaporators the heat flux increases steadily with increasing temperature difference up to a critical heat flux. This can be calculated from one of the correlations for boiling heat transfer.[30] At the critical value the tube surface is covered with vapour and any further increase in the temperature difference increases the thickness of the vapour film. Increasing the film thickness increases the thermal resistance to heat transfer. This more than outweighs the increase in temperature difference and the heat flux drops off. Where several tubes are involved a certain amount of vapour binding can be anticipated. Starczenski[42] reported that Abbot and Comley found that blanketing started to have an appreciable effect in a 60-tube evaporator at about half the heat flux reached by a single-tube evaporator, for water at one atmosphere. In the light of the present trend towards more compact evaporators using heat fluxes approaching the critical level it would seem

that further research is desirable into the vapour blanketing problem.

When one turns to consideration of the forced-circulation external-calandria evaporator it is possible to draw on the heat exchanger literature while considering load changes such as feed temperature or feed flow. The important load variable not included in such literature is feed density.

The dynamics of heat exchangers have been the subject of many studies in recent years.[8,9,16,43,44] Most of these were concerned with temperature-forced processes whose mathematical models are linear with constant coefficients (where the heat transfer coefficients are independent of temperature). A small number of papers has been concerned with velocity-forced exchangers. Thus only one of forty-two papers reviewed by Williams and Morris[47] in 1961 dealt with flow disturbances. The models for such exchangers involve variable coefficients, even if the heat transfer coefficients are independent of temperature, and are mathematically nonlinear where they are temperature dependent. In general, models which are non-linear from a process dynamics point of view are not amenable to solution by conventional analytical techniques. In most cases linearised models with constant coefficients are developed by a technique such as perturbation analysis. Almost all studies of velocity-forced processes described in the literature have involved such linearised models.

Hempel,[16] and Stermole and Larson,[43,44] studied steam-heated exchangers with velocity forcing. Their studies involved theoretical treatment with linearised models, validated in part by experimental studies. Hempel found that the theoretical frequency response curves for outlet temperature response to steam temperature changes fitted the experimental data satis-

factorily only at low frequencies, the departure, especially for the attenuation values, becoming marked once the resonance effect was initiated. The situation for the response to inlet temperature changes was less satisfactory, the theoretical curve for attenuation bearing no relation to the experimental data. This arose from the fact that the theoretical values were calculated using the expression

$$|G| = e^{-\beta \frac{L}{v}}$$

and β is proportional to the liquid heat transfer coefficient. Hempel suggested that his mean inlet temperatures may have been different at the different test frequencies. If this were so the attenuation points would have been affected. The phase angle values were not influenced by this variation and the theoretical curves fitted the data very closely.

Hempel simplified his model further, by assuming that the liquid heat transfer coefficient was independent of variations in liquid flow rate, to calculate the response of outlet temperature to flow rate changes. Under these circumstances the only parameter which determines the dynamics is the residence time. A similar observation is probably the basis of the suggestion by Thal-Larsen[45] that this parameter is sufficient to describe the dynamics of heat exchangers.

The experimental attenuation data for the flow-forced case had positive values above 0.2 radians per second. The theoretical did not, even when the simplifying assumption was removed. Apart from this the theoretical and experimental curves agreed well, especially the phase curves.

The discussion by Stermole and Larson[44] was based on a single partial differential equation model for the analysis of flow variations. The agreement with experimental data was good for both amplitude ratio and phase lag, especially for small perturbations. The occurrence of resonance was also predicted. Comparison of the results with those obtained by Hempel using a two-equation model, showed that the simpler single-equation model agreed as well with the experimental data. When the theoretical model was simplified further to an ordinary differential equation it did not predict resonance but the agreement with experiment was still very good for all frequencies less than resonance frequency. At the resonant frequencies average values were calculated.

Yang[49] derived general analytical expressions for a linerarised treatment of steam-water exchangers with flow forcing, while Koppel[21] made an analytical study of a simplified nonlinear model of a flow-forced steam-water exchanger. The latter results suggested that the approximate solution presented should not be used for large step inputs, or for exchangers with high heat exchange to heat capacity ratios. However using more typical values, with 10% step changes and values of around 0.5 for the index for dependence of the heat transfer coefficient upon velocity, Koppel concluded that the approximate solution was quite adequate.

It is worthwhile commenting at this point on the index just mentioned. The heat transfer coefficient (U) is a function of velocity. Writing U_o for its value at r = 0, i.e. at steady state, then,

$$U = U_o (1 + r)^b$$

on the basis of the usual heat transfer correlations.

Expanding the latter term as a Taylor's series

$$(1 + r)^b = 1 + br + \frac{b(b-1)}{2!} r^2 + \frac{b(b-1)(b-2)}{3!} r^3 + \ldots$$

we can write for small r,

$$(1 + r)^b = 1 + br.$$

This approximation represents the dependence of the heat transfer coefficient on flow rate fairly well. For example, for a 100% increase in flow, and with b = 0.53 (its worst value), the approximation gives an error of only 8%, which is less than the error inherent in heat transfer correlations.

Privott and Ferrell solved both linearised and nonlinear models on analogue and digital computers, and compared the model solutions with experimental data. The rigorous model was shown to be a good representation, while the approximate model predicted responses to step changes with substantial error even with small velocity changes. However when the flows were forced sinusoidally the response of the linearised model showed the correct overall trends and order-of-magnitude values. Privott and Ferrell concluded that the approximate model could be used to make qualitative predictions about the nonlinear system for control purposes.

Analysis retaining the distributed-parameter characteristic of a heat exchanger necessitates lengthy and laborious calculations. From a practical viewpoint the question that arises is under what circumstances will a lumped-parameter linearised model give answers of sufficient accuracy.

Mozley[31] concluded that the ratio of one fluid outlet temperature to the inlet temperature of the other fluid, in the case of a concentric

tube heat exchanger, could be represented by a simple second-order lag. The approximation is fairly good up to the frequency at which the time phase lag is 180°. It then deteriorates rapidly. However the particular exchanger studied had a length-volume ratio of 71 ft/ft^3. Many commercial exchangers have a smaller ratio and the lumped-parameter model should be a better approximation to them. Mozley also showed that for flow variations up to 50 percent of the mean flow the response of the exchange might be linearised.

Koppel[22] also examined a class of chemical reactor to determine whether linearisation did require a significant sacrifice in accuracy, and to examine the relationship of the simplified dynamics to the true dynamics. He concluded that the agreement between linearised and actual responses for disturbances of less than 25% of the design values, showed that controllers designed on the basis of linear system analysis should operate as designed over a practical range of fluctuations for the particular nonlinear reactors studied. This, despite the fact that the system investigated was nonlinear and parametrically forced, and had distributed reactance.

Most of the studies discussed above have dealt with concentric tube exchangers which makes the analysis easier, but leaves open the question whether the transfer functions obtained are applicable to multipass exchangers. Stainthorp and Axon[41] examined this aspect for a multitube multipass steam-heated exchanger, in terms of disturbances in steam temperatures and flow. They found that the inclusion of individual passes and reversal chambers gave only a slight improvement over the simpler single-pass model, the latter being recommended because of the

reduced computation time. Another conclusion was that the shell wall should be included in the mathematical model for steam flow variations, it being sufficient to add the shell-wall capacity to the steam capacity.

One of the most interesting aspects of the frequency response curves for flow-forced systems is the appearance of resonance peaks. Earlier experimentalists failed to observe the effect, possibly because their apparatus was not sufficiently sensitive, for the heights of the peaks are small, particularly where the fluid exit temperature is close to the steam temperature. The effect can be predicted from an examination of the transfer functions for such systems, and the occurrence of the resonance peaks has been observed in several studies including the present one.[41,43,46,49] However there is some conflict between the various observers concerning the origin of the effect.

Stainthorp and Axon[41] attribute the peaks to an interference process analogous to the well-known optical case, contending that with the kind of heat exchanger they studied (a 5-pass steam heated exchanger), the gain could not exceed unity nor the maxima-minima effects for the phase changes arise by a purely resonance effect. It can perhaps be interpolated that in no case do the peaks appearing in any published papers indicate a gain greater than unity, in short this is not a necessary condition.

Thomasson[46] considers that the exchanger response consists of two temperature wave systems, coinciding with the directions of travel of the two fluids, whose amplitudes are determined by the boundary conditions. The effect of the thermal capacity of the exchanger wall is to increase the attenuation, particularly at high frequencies. The mechanism

postulated for this effect at high frequencies is as follows. If we assume zero wall thermal capacity and let the inlet temperature of the secondary fluid be zero, then heat will flow from each small segment of the primary fluid at a rate which depends on its temperature. If we now consider the wall has thermal capacity which can be regarded as lumped, then at high frequencies the wall centre temperature will be zero. Therefore the thermal resistance path to heat flow from the primary fluid is halved, and the attentuation is doubled. However for accurate representation the system must be considered as a distributed system.

Extending the argument to an n-section model where n tends to infinity, it becomes apparent that the attenuation for a given incremental length of heat exchanger also tends to a limit which depends only on the heat transfer coefficient from the fluid to the wall. The "wobble" on the loci at high frequencies is due to the relative phases of the two temperature waves changing with changes in frequency. The sinusoidal variation in the primary fluid induces a similar wave on the secondary side which travels to the secondary inlet. Here the temperature is zero by definition. To cancel out the induced temperature a secondary-side wave is generated, an effect analogous to short-circuit reflection in a transmission line. This travels back to the secondary side outlet where its phase relative to the primary side depends on the frequency, thus causing the resonance effects. If this model is correct the effect should be less apparent where the thermal capacity of the exchanger walls is taken into account. Judging from the results presented by Stermole and Larson this seems to be the case. Thomasson's mechanism has the merit that it points to the importance of the heat transfer coeffi-

cient and thermal capacitances in the system.

Stermole and Larson[43] advanced an explanation which is widely supported, in which resonance is attributed to variations in the length of time an element of fluid takes to pass through the shell or tube of an heat exchanger. The implications of this are most readily explained by reference to a steam heated exchanger. If the flow rate of the tube fluid is varied some fluid elements will take longer to pass through the exchanger than others, and will be heated more, giving rise to a periodic temperature response curve. The resonant frequencies correspond to integral numbers of half-cycles in the exchanger. At the resonant frequency, defined by Stermole and Larson as the reciprocal of the residence time for a fluid element at the mean flow rate, each fluid element takes the same time to pass through the exchanger irrespective of the flow rate with which it enters the exchanger. Increase of frequency induces further variation in residence time. The experimental results obtained by Stermole and Larson, and also in the evaporator study reported here, verify that resonance depends upon the L/V ratio of the fluid whose temperature is being measured, resonance occurring when $\omega L/V = 2n\pi$, where n is an integer and ω is the forcing frequency in radians per unit time. This resonant frequency can be predicted from the system transfer functions. The delay term, $e^{\frac{L}{V}}$, which appears in most derivations, is a non-phase limiting component, which can be written as $\cos \omega L/V - i \sin \omega L/V$. The sine and cosine terms repeat at multiples of 2π thus accounting for the periodicity of the resonance. The same term occurs when the transfer function is derived for steam temperature disturbances.

Where two fluids are involved each fluid will have its own separate resonant frequency and there may well be some sort of cross-linking as proposed by Thomasson.

Stermole and Larson claim that for the constant shell temperature case (steam heating or high flow rate of shell fluid) variations in heat transfer coefficient and wall capacitance have a negligible effect on the normalised frequency response results. However examination of their results shows that including the wall thermal capacitance softens the severity of the dips in the theoretical response curves, while neglecting the heat transfer coefficient softens them still further. This is more in conformity with the observed process behaviour.

The significance of the resonance effect in control system design is not assessed easily. The expression $\frac{\omega L}{V} = 2n\pi$ suggests that a short heat exchanger with high fluid velocity would show resonance only at a very high upset frequency, whereas a long heat exchanger with low fluid velocity would show resonance at very low frequencies. This could be important in the design of exchangers and their control systems. In addition resonance could be expected to exert an unstabilising effect on the closed-loop response. Certainly resonance in the magnitude ratio curves implies that a lower controller gain setting must be applied if the usual gain margin criteria are to be met. On the other hand it is conceivable that resonance in the phase curve may be a stabilising influence because of its effect on the phase margin. Clearly it is impossible to generalise and each particular installation would need to be examined over the anticipated range of operating frequencies. Possibly it has not proved a nuisance in industrial practice because

when the fluid circulation rate is raised to suppress boiling in the tube or to reduce scale deposition, the likelihood of resonance is also suppressed.

3. THEORETICAL STUDY

The object of the theoretical study was to derive a set of equations which would describe the dynamic behaviour of an evaporator. It was intended that the mathematical model should indicate the response of the principal output variables, viz. product flow and density, to disturbances in the input variables such as feed flow, concentration, and temperature, also to steam flow and pressure. In addition, although level control is almost imperative in the operation of evaporators, it is desirable that the model admit the possibility of level variation since this will affect product flow markedly. Similarly it is desirable that the pressure in the pan or flash vessel should not be regarded as a constant. Pressure is an important thermodynamic variable which must be controlled. In practice the pressure may be expected to fluctuate as the boil-up rate varies, or in response to disturbances originating in the ejector. While it seems clear that a critical vacuum evaporation might require consideration of the ejector dynamics it was thought to take the problem outside the scope of this study. A mass balance equation was not needed for the vapour space in the disengagement region because the amount of vapour hold-up is small compared with the vapour withdrawal rate. However, arbitrary variations in pressure were taken into account in deriving the mathematical model, and during the simulation experiments pan pressure disturbances were introduced to determine the response of the main output variables. These results are presented and discussed at a later stage.

Generally the steam pressure to the calandria is controlled, and during the development of the theoretical model the steam supply pressure was assumed to be constant. However during the experimental determinations of the frequency response of the forced-circulation evaporator the

response to sinusoidal disturbances in steam pressure was determined and compared with the calculated response. These results also are presented and discussed later.

No attempt was made to include the heat of concentration. This is negligible for the solutions examined but could be introduced into the model if desired. Similarly the case where solids are present in the evaporator was not considered generally. However in this event the model will be simpler, since the boiling point of the slurry will be independent of the density. There has been some conflict about the range of validity of a standard correlation such as the Dittus-Boelter equation to heat transfer to slurries in pipes. Bonilla et al[4] investigated chalk in water as a system free from the tendency to cake onto the tube walls yet similar in nature to many industrial slurries. Their results indicated that above the critical Reynolds number, which incidentally increases with concentration, the heat transfer coefficient agreed well with that of the suspending medium alone. The modifications that should be made to the model when solids are present are discussed later.

The equations presented here were derived by the usual procedure of writing mass and energy balances for the system, together with equations describing the various physical relationships. For example, the boiling point was regarded as a function of density and pressure and an empirical density-concentration relationship used. The conservation equations were derived by taking the balances across the boundaries of an element of length dz of the fluid, tube wall, vapour space, and outer wall respectively.

The method of small perturbations was used to linearise the equations in all variables. There are two areas where linearisation may introduce large errors. It is possible for rapid variations in pan pressure to cause the vapour flow rate to vary widely from its mean value. This is not likely to be serious unless a very rapid increase in pressure causes the pan to go off the boil, which would upset the thermodynamic equilibrium in the system and invalidate the boiling-point relationship used in the model. The other problem area is in the steam side equations.

Steam flow into the calandria will depend on three variables, the steam supply pressure, the steam pressure in the calandria, and the valve stem position. If, as is generally the case, the steam supply pressure is held constant by the use of a self-actuating pressure regulator, the steam flow rate will become a function of the remaining two variables. Since it has been assumed that the steam in the calandria is always saturated, which means that the calandria steam pressure is a function of the steam temperature, then the steam flow rate will be a function of the steam temperature and of the valve stem position. Usually this function will be nonlinear. In general if an analytical expression can be deduced it can be linearised; for instance, by making a Taylor's series expansion about the operating point. In the absence of such an analytical expression the necessary relationships need to be determined experimentally as was done during this study. In any case difficulties will arise if the control valve is part of a control loop where the supply pressure is high and the pressure drop across the valve is small. Under such circumstances large pressure changes will be necessary to effect small temperature changes. In turn the temperature change necessary to

secure a given change in heat flow will depend upon the temperature drop across the tube wall. If this is large the term eliminated during the linearisation of the steam valve equation, namely the product of a change in pressure drop and a change in valve resistance, will no longer be a negligible quantity. The experimental evaporator was adjusted to secure critical flow conditions through the steam control valve. Under such circumstances the flow is proportional to the valve stem position.

Examination of the literature in the field of chemical process dynamics and control shows that when semi-quantitative results are wanted either linear or linearised models are used. This is necessary if generality is sought, since nonlinear systems must be handled by direct computation or simulation leading to specific results for specific problems. The consequences of linearisation are not serious because most of the non-linearities encountered are smooth and particularly in controlled processes, depart only slightly from being linear. The most notable exceptions are reaction processes where the reaction kinetics may introduce severe non-linearities. Attempts to proceed beyond semi-quantitative solutions may lead to unwarrantedly complex mathematical manipulation which does not give any better insight into the dynamics of the process nor lead to better practically-achievable results. There are many published instances where even the linear model is too complex to handle and approximation procedures such as Neumann series or Taylor diffusion models are used to simplify computation and to allow the qualitative estimation of the system behaviour. There are also many papers comparing the results obtained using exact and linearised models; several have been mentioned already. In most cases the results are such as to support the above assertion that the linearised models are adequate for practical purposes.

The following assumptions were made in the course of developing the mathematical model.

3.1 Assumptions

1. Liquor contains no suspended solids.
2. Liquor is perfectly mixed and admitted at its boiling point.
3. Heat transfer areas and coefficients are constant.
4. Heat losses from the pan or flash vessel are negligible.
5. Pressure-temperature equilibrium is maintained in the steam. This implies that the steam supply pressure is constant and the steam dry saturated.
6. Steam condensate is negligible in volume and at its boiling point, that is, it is in thermal equilibrium with the vapour.
7. Latent heat of condensation of steam and of vaporisation of solvent are constant.
8. All physical properties of fluids and evaporator walls are constant over the range of temperatures considered.
9. Heat of concentration of solution is negligible.
10. Atmospheric pressure is constant.
11. Heat losses from jacket of external calandria are small, and constant for small changes in temperature, and the jacket metal is at the steam temperature.
12. Plug flow prevails in the downcomer, i.e. the temperature and velocity profiles of fluid are uniform over any given cross-section normal to the flow.
13. Heat transfer in the direction of flow can be neglected.

The first two assumptions are general. However the necessary modification of the model with the first restriction removed is discussed in Appendix B.

Assumptions (3) and (4) were verified experimentally for a distillation column reboiler.[11] Work cited by Thomasson[46] suggests the possibility that the heat transfer coefficients are not constant under some conditions even with steady liquid flow. For instance, the coefficient is likely to be considerably higher than the steady state value for a short interval following a sudden change in the surface temperature of a duct through which a liquid is flowing. However Thomasson assumed, and his results tend to confirm the assumption, that this is not a serious hazard under normal working conditions. Furthermore Paynter and Takahashi[34] claim that calculations on the static characteristics of shell-and-tube heat exchangers indicate that variations in heat transfer coefficients along the length of the tube due to the temperature profile are unlikely to affect the dynamic characteristics significantly, a conclusion which seems to be supported by the work of Hempel.[16]

The major mechanism involved in heat transfer in evaporators is forced convention. For turbulent flow in pipes and tubes we may write

$$Nu = 0.027\ (Re)^{0.8}\ (Pr)^{1/3}$$

where,

Nu = Nusselt number = $\frac{hD}{k}$

Re = Reynolds number = $\frac{DG}{\mu}$ (> 2100)

Pr = Prandtl number = $\frac{C\mu}{k}$

The correlation shows that the heat transfer coefficient varies directly with the mass flow rate and inversely with the viscosity. This dependence on mass flow is important since control is effected usually by modulating a fluid flow rate which will thus vary the heat transfer coefficient. Since viscosity decreases with temperature, the heat transfer coefficient will increase, while the specific heat and thermal conductivity are affected negligibly. Overall convective heat transfer will be nonlinearly dependent on temperature. However unless viscosity is a strong function of temperature the temperature dependence of h can be ignored.

The validity of assumption (5) rests on the fact that the steam supply line has its own control loop. Measurement of the steam temperature and pressure at the entry point to the calandria suggests that the control loop was effective. In any event the sensible heat is small compared with the latent heat over the temperature range used experimentally. A general attitude is that temperature deviations of the steam may be assumed dependent on time alone, because the flow and pressure transients (momentum transfer) in the vapour phase are very rapid compared with the thermal transients. The validity of these assumptions can be tested by representing the system by a stirred tank model, in which it is assumed that two tanks representing the two sides of the heat exchanger portion of the evaporator are in contact at the transfer wall. It may be presumed that if the fluid transients are found to be negligible in the lumped model they can be ignored in the more exact distributed model, which is to that extent

simplified. The assumptions were tested in this way, the fluid transients proving about twenty-five times faster than the thermal transients, bearing out the validity of the basic assumptions.

In any case an attempt was made to determine the frequency response between the calandria steam pressure and the steam flow rate and this will be mentioned in the experimental section. However at quite high frequencies (35 radians/minute) the phase lag between the steam flow variations and the steam pressure was only 42°. The same conclusion could be reached qualitatively, by observing the lag between the variations indicated by the pressure transducer and those indicated by the steam temperature thermocouple. This was generally too small to measure, and suggests that the dynamics of the steam temperature measurement system could be neglected with little error. Hempel measured the temperature and pressure simultaneously at several points along the inside of the shell of a steam-heated exchanger without detecting any measurable deviation. During these experiments steam pressures were measured at the top and bottom of the shell and converted to temperatures, with the thought that they might be used to take some account of the steam side dynamics. However there was little difference between the readings and these attempts were abandoned.

In steam-heated exchangers the fluid and thermal transients are coupled through two mechanisms. First, the vapour pressure and temperature are related through the saturation curve of the two-phase fluid. Secondly, the volume of the condensate on the steam

side can change if the inlet and outlet rates change momentarily. Should this happen the heat transfer area will change thus altering the heat transfer rate. This eventuality can be included in any proposed model either by considering that the available heat transfer area changes, or by assuming that the heat transfer coefficient on the steam side decreases as the condensation rate increases.

In the case of chemical evaporators or distillation column reboilers the second coupling mechanism is not applicable since the calandria tubes are always submerged in, filled with, or the walls are wetted by, the (boiling) process fluid to guard against burnout. In addition steam condensate is removed as it collects in the bottom of the steam jacket and the instantaneous hold-up on the tube wall is small and reasonably constant. These circumstances ensure that the area available for heat transfer is constant.

The heat of concentration of the solution (assumption (9)) will not always be negligible, although it was in the systems studied. However if desired it could be included in the model. The enthalpy-concentration relationship could be assumed to be linear in form. Even were the relationship markedly nonlinear it would still be practicable to approximate it by a series of linear relationships, particularly since numerical methods are sufficiently well-developed to allow constants to be changed part way through a computation.

Assumption (11) should be nearly true if the jacket is insulated. The losses through the insulated jacket were calculated in the early stages of the experimental work and found to be small; the value obtained is presented later. It can be contended that the important thing is the total flow of heat to the shell wall rather than the temperature on the outside surface. If necessary this could be calculated by making a heat balance between the heat flux to the wall and the heat losses by convection and radiation. If it is desired to take the shell dynamics into account they could be handled in several ways. Stainthorp and Axon[41] treated the shell of their exchanger as a distributed lag but concluded that they could equally well have regarded it as a lumped capacity, or added the shell wall capacity to that of the steam.

Catheron et al[6] maintain that the shell response has only a small effect on exchanger dynamics, because the shell capacity is in parallel with the capacities in the tube and fluid.

Cohen and Johnson[8] go further and contend that heat transfer between the vapour and the heat exchanger jacket wall does not affect the vapour temperature, which is dependent on the thermodynamic pressure, and maintain that the shell wall dynamics do not enter into consideration. Day examined the transient heat flow into the jacket wall of a distillation column reboiler, and concluded that if the transfer resistance can be assumed to be negligible, and the shell wall resistance is negligible also, the heat flux to the wall is proportional to the steam temperature and to the thermal capacitance of the shell wall, and the tempera-

ture changes in the wall should be identical with those in the steam. Day's experimental work[11] indicated that the approximation agreed fairly closely with the experimental data at moderate to long periods, the phase lag results fitting somewhat better than the amplitude ratio. In the light of these several assertions assumption (11) appears to be justified.

The remaining assumptions (12) and (13) are made generally, but it is desirable to examine them as they raise important issues concerning radial and axial diffusion. In many cases the flow pattern is sufficiently turbulent to imply that the radial distribution of physical properties is effectively uniform. This leaves the one spatial dimension, axial distance from the inlet, which simplifies the mathematical treatment while retaining the essential features of the physical behaviour of the system.

Further simplification results if "plug flow" conditions, i.e. the absence of axial diffusion, are assumed. This is said to be an accurate representation except in plant such as packed-bed reactors where channelling and by-passing can occur leading to axial diffusion.

To ignore axial diffusion completely may lead to analytical difficulties that have nothing to do with the physical process itself. These arise because in the complete absence of diffusion the observed parameters are cyclic in nature. This implies discontinuities in the distribution of temperature, concentration, etc. which are propagated throughout the system. Attempts to solve the differential equation numerically under these circumstances

leads to a situation where the discontinuities are represented accurately at the expense of large errors in other parts of the response. The decision whether or not to include axial diffusion depends upon the particular system. A guide as to the relative importance of diffusion is given by the Peclet number which is infinite for zero diffusion.[14].

For a fluid the Peclet number

$$P = \frac{G\, C_p\, L}{k} = \frac{W\, C_p\, L}{A\, k}$$

where,

W = total mass flow rate, lb/sec.

C_p = specific heat at constant pressure, Btu/lb. ^{o}F.

L = length of exchanger, ft.

A = cross-sectional area of pipe normal to the axis, ft^2.

k = thermal conductivity of fluid, Btu/sec.ft ^{o}F.

Where two fluids are separated by a wall, as in a heat exchanger, it is necessary to determine whether axial diffusion along the tube walls can be ignored. The simplest approach is to determine the Peclet number for a single fluid percolating with its surrounding wall with axial conduction. From the literature it seems that axial wall conduction can be ignored if

$$\text{"P"} = \frac{W\, L\, \rho_w\, C_w}{\rho\, A\, k} \gg 1.$$

Here the symbols have their previous meanings except that the subscript w denotes wall properties, k is the thermal conductivity of the wall, and "P" is a nominal Peclet number.

Generally this inequality is very strong in practical situations, implying that all effects arising from axial wall conduction can be ignored. In the experimental evaporator for the lowest flow rate of the range used (the worst case), the Peclet number for the fluid was 2×10^6 and "P" was 5×10^3 for the tube wall. On this basis it is reasonable to ignore the possibility of axial diffusion in the liquid or axial conduction along the tube wall. That is, "plug flow" was assumed for the tube fluid and zero conductance longitudinally for the tube wall. A further significance of the Peclet number is that as it becomes larger the response of the mean temperature is approximated more closely by a pure D-V lag.

Another argument advanced to justify the assumption of zero axial conduction is that although the wall is constructed of metal with a high thermal conductivity it is assumed to have a small cross-section normal to the axis so that heat flowing axially by conduction is small compared with the heat flowing radially into and out of the wall.

Generally thick tube walls would be used in heat exchangers and similar vessels only where one fluid is at a high pressure relative to the other. In the case of an evaporator if the dividing wall is sufficiently thick the film resistances on either side can be neglected and the temperatures of the wall surfaces will be equal to those of the steam and boiling liquid respectively. Any change in steam temperature would cause a change in heat flow through the wall but the temperature of the wall surface in con-

tact with the boiling liquid would remain constant, the change in heat flow producing a change in the boil-up rate.

In view of this, and recalling that the fluid transients are much faster than the thermal transients, it would seem that in normal applications two-phase isothermal fluids can be treated as though no dynamic effects are involved. In cases where, as here, both sides of the exchanger involve two-phase fluids, it would seem that the dominant thermal dynamics are due to the wall, and for engineering purposes the fluids could be represented by instantaneous models, and the dynamic effects accounted for by analysis of the wall separating the fluids.

3.2 The basic equations

The circulating pump

If it be desired to include specifically in the model, the circulating pump used with the forced-circulation evaporator, it may be done as follows.

Assuming negligible heat losses from the pump and negligible hold-up in the pump, equating the rates of heat flow at the inlet and outlet of the pump gives,

$$m\ Cp\ \theta_1 = m\ Cp\ \theta_2 = (m - m_1)\ Cp\ \theta_f + m_1\ Cp\ \theta_4$$

i.e. $$m\ \theta_2 = m\ \theta_f + m_1\ (\theta_4 - \theta_f)$$

or $$\theta_2 = \theta_f + \frac{m_1}{m}\ (\theta_4 - \theta_f) \qquad (1.1)$$

where,

m_1 = mass flow rate of recycle liquor

m_f = mass flow rate of make-up feed

m = mass flow rate to evaporator = $m_1 + m_f$

$\theta_{1,2}$ = the pump inlet and outlet temperatures

θ_4 = the recycle liquor temperature

θ_f = the make-up liquor temperature.

With negligible heat loss from the pipe connecting the pump outlet to the calandria a pure distance-velocity lag (D-V lag) exists between the pump outlet (temp. = θ_2) and the calandria entry point (temp. = θ_3),

i.e. $$\theta_3(t) = \theta_2\ (t - T_{d1}) \qquad (1.2)$$

where T_{d1} = the time delay due to the D-V lag.

Similarly a pure D-V lag exists between the pan (flash vessel) and the pump inlet,

i.e. $$\theta_4(t) = \theta_1(t) = \theta_p\ (t - T_{d2}) \qquad (1.3)$$

where θ_p = temperature in the flash vessel.

These D-V lags may be taken into computer models if desired, but at the high circulation rates used in forced-circulation evaporators, and the relatively short pipe runs involved, the D-V lags are small enough to be neglected. In any case good design requires that these lags be reduced to the minimum since they are non-limiting phase components.

Under ordinary circumstances the pump will have only a very small effect on the enthalpy of the fluid, and since we have assumed negligible heat losses equation (1.1) can be dropped with little error. This assumption was confirmed by making a few trial simulations including the pump equation.

Should for some particular reason, it be required to take account of the pump as a resistance element it may be described by a similar equation to that used in describing the steam supply valve.

Where the range of variation is restricted to small variations about a steady state value

$$P_2(s) - P_1(s) = \frac{\partial(\Delta P)}{\partial Q} Q(s)$$

or $P_2(s) - P_1(s) = R_p\, Q(s)$

where R_p = the pump impedance and the other symbols have their usual meanings. If the supply head (P_1) is constant, this equation may be linearised yielding the dynamic equation

$$p_2 = R_p q + Q\, r_p.$$

Steam supply valve

$$Q_s = A_v\, C_v \sqrt{(P_o - P_s)}$$

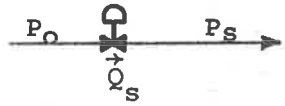

where $A_v = f(x_v)$ and x_v = valve lift,

and P_o, P_s are the steam supply pressure and the pressure in the steam jacket respectively.

Given a linear valve characteristic

$$A_v = k_v\, x_v$$

$$Q_s = k^1\, x_v \sqrt{(P_o - P_s)} \text{ where } k^1 = k_v\, C_v.$$

If a dimensionless relationship is wanted, flow and the valve lift may be normalised with respect to their maximum values, i.e.

$$q = \frac{Q}{Q_m} \quad \text{and} \quad x = \frac{x_v}{x_m}$$

or $Q_s = k\, x \sqrt{(P_o - P_s)}$ where $k = k^1 x_m = k_v\, C_v\, x_m$

and Q_s = normalised steam flow rate

i.e. $Q_s^2\, R_1^2 = (P_o - P_s)$. (1.4)

where R_1 is the valve resistance characteristic whose value is established experimentally.

Steam jacket

Mass balance on steam gives,

$$(M_s - M_{cj})\,dz = \frac{\partial}{\partial t}\left(\frac{V_s}{v_s}\right) dz$$

or $$M_s - M_{cj} = V_s \frac{\partial \rho_s}{\partial t} + \rho_s \frac{\partial V_s}{\partial t} .$$

Mass balance on condensate gives,

$$(M_{cj} - M_c)\,dz = \frac{\partial}{\partial t}\left(\frac{V_c}{v_c}\right) dz$$

or $$M_{cj} - M_c = V_c \frac{\partial \rho_c}{\partial t} + \rho_c \frac{\partial V_c}{\partial t} .$$

Since the amount of condensate hold-up is small and the volume of the jacket is constant the final term in each of the above expressions can be ignored. Combining the expressions to eliminate M_{cj} gives

$$M_s - M_c = V_s \frac{\partial \rho_s}{\partial t} + V_c \frac{\partial \rho_c}{\partial t} .$$

Again if the condensate film is thin and in equilibrium with the vapour, vide Assumption 6, $V_c << V_s$ and the final term in this expression can be eliminated yielding,

$$M_s - M_c = V_s \frac{\partial \rho_s}{\partial t} . \qquad (1.5)$$

Energy balance on steam side

$$(M_s H_s - M_c H_c)dz = h_o A_o (T_s - T_t)dz + Q_{sh}\,dz + V_s \frac{\partial (\rho_s U_1)}{\partial t}\,dz + \frac{\partial (M_c U_c)}{\partial t}\,dz \qquad (1.6)$$

Before proceeding further it is necessary to examine the relationship between the heat loss flux to the shell wall and the jacket temperature.

Assuming that the shell wall can be regarded as a plane, Young[51] has shown that for transient heat flow into the wall,

$$q_{sh} = \frac{m\ C_1\ N(s)\ s\ \theta_s}{1 + N(s)\ s\ \tau_s}$$

where,

$$N(s) = \frac{\tanh \sqrt{(\frac{s}{K})}}{\sqrt{(\frac{s}{K})}}$$

and, $m\ C_1$ = thermal capacity of shell wall

q_{sh} = transient heat flux to shell wall

θ_s = transient disturbance in steam temperature

τ_{sh} = time constant of shell wall

K = thermal diffusivity of metal.

If the thermal capacitance of the shell is small N(s) tends to zero, and if the transfer film resistance is also small, the heat transfer coefficient at the shell wall is large and the time constant (τ_{sh}) becomes negligible. For example,

$$\tau_{sh} = \left(\frac{m\ C_1}{h\ A}\right)_{shell} = \frac{10.8 \times 0.12}{2000 \times 1.045} \times 3600 \doteq 2.2 \text{ secs.}$$

where h is assumed to be 2000 Btu/hr ft^2 ^oF.

Under these conditions

$$q_{sh} = m\ C_1\ s\ \theta_s.$$

Alternatively, if it be assumed (as in Assumption 11), that the shell wall is at the steam temperature, and since it is insulated that the heat losses are small,

$$Q_{sh} = M_1 C_{p1} \frac{\partial T_s}{\partial t}$$ (reverting to our own symbolism)

which is the same as above.

Combining equations (1.5) and (1.6) to eliminate M_c and making the above approximation for Q_{sh} gives,

$$M_s(H_s-H_c) = h_o A_o(T_s-T_t) + V_s\rho_s \frac{\partial U_s}{\partial t} + V_s U_s \frac{\partial \rho_s}{\partial t} + M_1 Cp_1 \frac{\partial T_s}{\partial t} - V_s H_c \frac{\partial \rho_s}{\partial t}$$

or,

$$M_s(H_s-H_c) = (U_s-H_c)\, V_s \frac{\partial \rho_s}{\partial t} + M_1 Cp_1 \frac{\partial T_s}{\partial t} + V_s\rho_s \frac{\partial U_s}{\partial t} + h_o A_o(T_s-T_t) \qquad (1.7)$$

The variables H_s, H_c, ρ_s and U_1, involved in the interaction phenomena are nonlinear functions of the steam pressure (hence temperature). Anticipating that the eventual model will be an incremental linear one the relationships can be written,

$$\rho_s-\rho_{so} = k_a(T_s-T_{so})$$

$$U_s-U_{so} = k_b(T_s-T_{so})$$

$$H_s-H_{so} = k_c(T_s-T_{so})$$

$$H_c-H_{co} = k_d(T_c-T_{co})$$

where the subscript o indicates average values of the respective variables. Assuming that pressure-temperature equilibrium is maintained in the steam (Assumption 5) we have,

$$k_a = \left.\frac{\partial \rho_s}{\partial T_s}\right|_o, \quad k_b = \left.\frac{\partial U_s}{\partial T_s}\right|_o, \quad k_c = \left.\frac{\partial H_s}{\partial T_s}\right|_o, \quad k_d = \left.\frac{\partial H_c}{\partial T_c}\right|_o.$$

which can be evaluated from steam tables.

Assuming further that the condensate is at the same temperature as the steam, i.e. $T_c = T_s$,

$$\left[(H_{so}-H_{co}) + (k_c-k_d)(T_s-T_{so})\right] M_s =$$

$$\left[(U_{so}-H_{co}) + (2k_b-k_d)(T_s-T_{so}) + \frac{k_d}{k_a}\rho_{so} + \frac{M_1 Cp_1}{k_a V_s}\right] k_a V_s \frac{\partial T_s}{\partial t} + h_o A_o(T_s-T_t).$$

Inspection of this expression shows that some of these terms may be neglected. Assuming a ± 10°F change about the operating temperature, $(k_c-k_d)(T_s-T_{so})$ has a value of about 6.5 Btu/lb compared with a value of 950.7 Btu/lb for (H_s-H_c); $(2k_b-k_d)(T_s-T_{so})$ is -4.4 Btu/lb and $(k_d\rho_{so}/k_a)$ is about 16.5 Btu/lb whereas (U_s-H_c) is 875 Btu/lb. If these minor terms are discarded

$$(H_{so}-H_{co})M_s = \left[(U_{so}-H_{co}) + \frac{M_1Cp_1}{k_aV_s}\right]k_aV_s\frac{\partial T_s}{\partial t} + h_oA_o(T_s-T_t) \qquad (1.8)$$

$$\text{i.e. } \tau_1\frac{\partial T_s}{\partial t} = KM_s - (T_s-T_t)$$

$$\text{where } \tau_1 = \frac{(U_{so}-H_{co})k_aV_s + M_1Cp_1}{h_oA_o}$$

$$K = \frac{H_{so}-H_{co}}{h_oA_o} = \frac{\lambda_s}{h_oA_o} .$$

Heat balance on calandria tube wall

As discussed earlier it is assumed that thermal diffusion is zero axially (Assumption 13).

The heat transfer equation is

$$V_tCp_t\rho_t\left(\frac{\partial T_t}{\partial t}\right)dz = h_oA_o(T_s-T_t)dz - h_iA_i(T_t-T_o)dz \qquad (1.9)$$

$$\text{i.e. } \frac{\partial T_t}{\partial t} = \frac{h_oA_o}{V_tCp_t\rho_t}(T_s-T_t) - \frac{h_iA_i}{V_tCp_t\rho_t}(T_t-T_o) \qquad (1.10)$$

$$\text{where } V_t = \frac{\pi(d_o^2 - d_i^2)}{4}dz$$

$$\text{or } \tau_2\left(\frac{\partial T_t}{\partial t}\right) = (T_s-T_t) - \frac{\tau_2}{\tau_3}(T_t-T_o) \qquad (1.11)$$

$$\text{where } \tau_2{}^1 = \frac{V_tCpt\rho_t}{h_oA_o}$$

$$\text{and } \tau_3 = \frac{V_tCpt\rho_t}{h_iA_i}$$

the areas being sq. ft per ft length.

Heat balance on fluid side of evaporator

In normal operation of chemical evaporators boiling occurs in the tubes. Under such circumstances once boiling is established, the process fluid boiling temperature is independent of axial position within the tube. In the case of vertical-tube forced-circulation evaporators the process fluid enters at the saturation temperature in the separator but boiling is suppressed at first, principally because of the hydrostatic head. However the temperature increases as the fluid travels through the tube and finally boiling starts, but if the entrance velocities are high, say 5-15 feet per second, only a small fraction of the feed evaporates in the tube. At lower entrance velocities the boiling zone is extended and the fraction evaporated increases. These effects account for the differing constants reported for heat transfer correlations applicable to evaporators.

Applying the usual conservation approach we can write,

$$Cp_o \frac{\partial (V_3 \rho_o T_o)}{\partial t} dz = M_i Cp_i T_i dz - M_o Cp_o T_o dz + h_i A_i (T_t - T_o) dz - M_v (Cp_w T_o + \lambda) dz$$

where the final term is the enthalpy removed by the vapour. That is,

$$Cp_o \frac{\partial (V_3 \rho_o T_o)}{\partial t} = M_i Cp_i T_i - M_o Cp_o T_o + h_i A_i (T_t - T_o) - M_v (Cp_w T_o + \lambda) \quad (1.12)$$

For systems in which boiling does not occur in the tube, the fluid-side equation is slightly simpler in form, the first two terms on the right hand side can be consolidated and the final term disappears.

Thus considering an incremental slice of tube dz, having an inside diameter d_i,

$$\rho_o Cp_o \left(\frac{\pi d_i^2}{4}\, dz\right) \frac{\partial T_o}{\partial t} = \rho_o Cp_o \left(\frac{\pi d_i^2}{4}\right) v \left[T_o - \left(T_o + \frac{\partial T_o}{\partial z}\, dz\right)\right] - h_i \pi d_i\, dz\, (T_o - T_t)$$

i.e.,

$$\rho_o V_o Cp_o \frac{\partial T_o}{\partial t} = -\rho_o V_o Cp_o\, v \frac{\partial T_o}{\partial z} - h_i A_i (T_o - T_t) \qquad (1.13)$$

$$\text{or} \quad \tau_4 \frac{\partial T_o}{\partial t} + \tau_4 v \frac{\partial T_o}{\partial z} = (T_t - T_o) \qquad (1.14)$$

where $\tau_4 = \dfrac{\rho_o V_o Cp_o}{h_i A_i}$.

The second term in equation (1.14) reflects the distributed nature of the system. Actually the coefficient is time variant, but generally it is regarded as linearisable over the operating range. Several analyses of this equation have been published[18] and treatment along conventional lines leads to the following expressions describing the temperature response of the fluid leaving the tube to variations in the fluid flow rate.

$$\left.\begin{aligned} \left|\frac{\theta_o}{v}\right| &= \frac{R}{\omega} (2 - 2\cos \omega\tau_D)^{\frac{1}{2}} \\ < \frac{\theta_o}{v} &= \tan^{-1} \left(\frac{1 - \cos \omega\tau_D}{\sin \omega\tau_D}\right) \end{aligned}\right\} \qquad (1.15)$$

where τ_D is the distance-velocity lag involved in passage of the fluid through the tube, and

$$R = \frac{T_i - T_o}{v\, \tau_4}\, e^{-\frac{\tau_D}{\tau_4}} .$$

Mass balance on process fluid

$$M_i - M_o - M_v = \frac{\partial}{\partial t} \left(\frac{V_b}{v_b}\right) = \frac{\partial (V_3 \rho_o)}{\partial t} \qquad (1.16)$$

Density-Boiling point relationship

$$T_o = f(P_e, \rho_o)$$

$$= \bar{T}_o + \left(\frac{\partial T_o}{\partial P_e}\right)_{P_e} + \left(\frac{\partial T_o}{\partial P_o}\right)_{P_o}$$

$$\text{i.e. } T_o = \bar{T}_o + \alpha P_e + \gamma \rho_o \qquad (1.17)$$

where $\alpha = \frac{\partial T_o}{\partial P_e}$

$\gamma = \frac{\partial T_o}{\partial \rho_o}$.

Mass balance on solute in the evaporator pan

$$\frac{\partial (V_3 \rho_o K_o)}{\partial t} = M_i K_i - M_o K_o \qquad (1.18)$$

Density-Concentration relationship

$$K = A_1 + A_2 (\rho - \rho_w) \qquad (1.19)$$

where the constants are determined experimentally and assumed to be constant over the operating range.

Product withdrawal

Applying Bernoulli's equation the following expression relates pan level and product flow rate.

$$Q_o^2 \rho_o R_2 = \rho_o H_1 + P_e - P_a \qquad (1.20)$$

Mass flow - Volumetric flow relationship

$$M = Q \rho . \qquad (1.21)$$

This relationship is used with appropriate subscripts at several points during the development of the model, e.g. $M_o = Q_o \rho_o$ refers to the process effluent fluid, etc.

The set of equations is nonlinear. Unless the equations can be uncoupled and rendered linear or quasilinear, the quantitative evaluation of the dynamic response is a fairly intractable problem. In an earlier section attention was directed to the efforts of other workers to establish the extent to which linearisation could be carried without sacrificing the essential features of the system dyanmics. Essentially their results showed that for liquid type exchangers the equations could be linearised so that the performance could be studied from a control viewpoint, provided the flow did not vary greatly, and provided the temperature did not vary over a wide range. However the linearisation of equations describing exchangers with boiling liquids or condensing vapours presents some problems.

To linearise the conservation and state equations, those parameters which are functions of time and distance must be replaced by constants which are both space and time invariant, or independent of time and varying linearly with distance. Even when linearised the equations are partial types necessitating the handling of transcendental functions of complex variables. It is difficult to solve the equations or to prepare the inverse Laplace transformations necessary to derive the transient behaviour of the systems. The approach used generally to overcome these difficulties is to convert the linearised partial-differential equations into linear equivalent ordinary differential equations. These equations can be handled as rational functions in the complex variable which respond to the ordinary direct and inverse Laplace transformation techniques.

3.3 Dynamic equations

3.3.1 Retaining distributed parameter characteristic

The equations describing heat transfer to the process fluid are nonlinear because the film coefficient h_i is a function of both the fluid velocity and the fluid temperature, the frictional forces are a function of temperature and velocity, and velocity is a function of viscosity which in turn is a function of temperature. Of these effects the first, the dependence of the film coefficient on fluid velocity, is the most significant.

Assuming that evaporation is suppressed in the tube the equations of interest here, (1.10) and (1.13) can be written

$$\left.\begin{aligned} \rho_o \frac{\partial T_o}{\partial t} + \rho_o v_o \frac{\partial T_o}{\partial z} + \frac{\pi d_i h_i}{A_i Cp_o} (T_o - T_t) &= 0 \\ \frac{\partial T_t}{\partial t} + \frac{h_o}{\rho_t Cp_t z_t} (T_t - T_s) + \frac{h_i}{\rho_t Cp_t z_t} (T_t - T_o) &= 0 \end{aligned}\right\} \qquad (2.1)$$

where a section of length dz is considered.

These equations become linear if neither v_o nor the variations in temperature are so great that h_i has to be treated as a function of flow rate or temperature. In a controlled system this is the intended objective.

Assuming that the mass flow rate is constant but allowing the shell side temperature to vary, although not sufficiently to negate the assumption that the shell side film coefficient is constant, the dynamic response equations (2.1) can be linearised.

$$\left.\begin{aligned} \rho_o Cp_o A_i \frac{\partial T_o}{\partial t} + \rho_o Cp_o A_i v \frac{\partial T_o}{\partial z} + \pi d_i h_i (T_o - T_t) &= 0 \\ \rho_t Cp_t z_t \pi d_i \frac{\partial T_t}{\partial t} + \pi d_i h_o (T_t - T_s) - \pi d_i h_i (T_o - T_t) &= 0 \end{aligned}\right\} \quad (2.2)$$

These equations can be expressed as Laplace transforms preparatory to examining the response of the exchanger for control purposes. Defining the constants,

$$b_1 = \frac{h_i}{\rho_o Cp_o A_i}$$

$$b_2 = \frac{h_o}{\rho_o Cp_o A_i}$$

$$b_3 = \frac{h_i}{\rho_o Cp_t z_t \pi d_i}$$

$$b_4 = \frac{\rho_o Cp_o A_i v}{\rho_o Cp_o A_i} = v.$$

and writing each temperature as a steady state component and a small variable portion, e.g. $T_s + \theta_s$, and substituting into equation (2.2) gives,

$$\left.\begin{aligned} \frac{\partial \theta_o}{\partial t} + b_4 \frac{\partial \theta_o}{\partial z} + b_1 (\theta_o - \theta_t) + b_4 + b_1 &= 0 \\ \frac{\partial \theta_o}{\partial t} + b_2 (\theta_t - \theta_s) + b_2 + b_3 (\theta_t - \theta_o) + b_3 &= 0 \end{aligned}\right\} \quad (2.3)$$

Since by definition the differential steady-state terms must equal zero, and since the initial value of the variable portion of each temperature can be made zero by assuming that the system is initially at its steady state, the transformed equations become,

$$\left.\begin{aligned} (s+b_1)\theta_o(z,s) + b_4 \frac{\partial \theta_o(z,s)}{\partial z} &= b_1 \theta_t(z,s) \\ (s+b_2+b_3)\theta_t(z,s) &= b_3 \theta_o(z,s) + b_2 \theta_s(z,s) \end{aligned}\right\} \quad (2.4)$$

Eliminating $\theta_t(z,s)$ by combining these equations,

$$b_4 \frac{d\theta_o(z,s)}{dz} + \left[\frac{s^2+(b_1+b_2+b_3)s+b_1b_2}{s+b_2+b_3}\right] \theta_o(z,s)$$

$$= \left(\frac{b_1b_2}{s+b_2+b_3}\right) \theta_s(z,s) \qquad (2.5)$$

Writing

$$\alpha(s) = \left[\frac{s^2+(b_1+b_2+b_3)s+b_1b_2}{s+b_2+b_3}\right]$$

$$= s + b_1 - \frac{b_1b_3}{s+b_2+b_3}$$

$$\beta(s) = \left[\frac{b_1b_2}{s+b_2+b_3}\right]$$

and substituting into (2.5) gives,

$$b_4 \frac{d\theta_o(z,s)}{dz} + \alpha(s)\theta_o(z,s) = \beta(s)\theta_s(z,s) \qquad (2.6)$$

Laplace-transforming a second time with respect to the distance variable z, gives,

$$[b_4p + \alpha(s)]\theta_o(p,s) = \beta(s)\theta_s(p,s) + b_4\theta_o(o,s) \qquad (2.7)$$

With the assumption generally made, Assumption (2), that the shell-side fluid is perfectly mixed, the temperature $\theta_s(p,s)$ is independent of distance. The transform of $\theta_s(p,s)$ then becomes $\frac{1}{p}\theta_s(s)$.

The equation (2.7) can now be used to define the fluid temperature anywhere in the tube, i.e.

$$\theta_o(p,s) = \left[\frac{\beta(s)}{b_4p+\alpha(s)}\right]\frac{1}{p}\theta_s(s) + \left[\frac{b_4}{b_4p+\alpha(s)}\right]\theta_o(o,s) \qquad (2.8)$$

It is now possible to write transfer functions relating the fluid temperature to variations in either the steam temperature or fluid inlet temperature. Thus

$$G_1(p,s) = \frac{\beta(s)}{b_4p+\alpha(s)} \qquad (2.9)$$

describes the relationship between the temperature anywhere in the tube, $0 < z < L$, and changes in $\theta_s(s)$ where $\theta_o(o,s) = 0$, i.e. where the fluid inlet temperature is constant.

$$G_2(p,s) = \frac{b_4}{b_4 p + \alpha(s)} \tag{2.10}$$

defines the relationship between the process fluid outlet and inlet temperatures for constant steam conditions.

Equation (2.8) can be solved by expanding the first term on the right-hand side into a partial fraction and then taking the inverse Laplace transform term by term, yielding,

$$\theta_o(z,s) = \frac{\beta(s)}{\alpha(s)}\left[1 - e^{-\frac{\alpha(s)}{b_4} z}\right]\theta_s(s) + \left[e^{-\frac{\alpha(s)}{b_4} z}\right]\theta_o(o,s) \tag{2.11}$$

from which the temperature of the fluid leaving the tube at $z = L$ is,

$$\theta_o(L,s) = \frac{\beta(s)}{\alpha(s)}\left(1 - e^{-\frac{\alpha(s)}{b_4} L}\right)\theta_s(s) + \left(e^{-\frac{\alpha(s)}{b_4} L}\right)\theta_o(o,s) \tag{2.12}$$

That is, the transfer functions $G_1(s)$ and $G_2(s)$ relate the temperatures $\theta_o(L,s)$, $\theta_o(o,s)$, and $\theta_s(s)$.

The transfer function $G_2(s)$ can be written

$$G_2(s) = e^{-\frac{\alpha(s)}{b_4} L} \tag{2.13}$$

or alternatively as,

$$G_2(s) = e^{-\tau_D s} \cdot e^{-\tau_D b_1} \cdot e^{\tau_D \left(\frac{b_1 b_3}{s+b_2+b_3}\right)} \tag{2.14}$$

where τ_D is the distance-velocity lag, $\frac{L}{b_4}$, i.e. $\frac{L}{v}$, for the flow of fluid through the tube of length L.

The function $G_1(s)$,

$$G_1(s) = \frac{\beta(s)}{\alpha(s)} \left(1 - e^{-\frac{\alpha(s)}{b_4} L} \right) \qquad (2.15)$$

can thus be written in terms of the function $G_2(s)$.

$$G_1(s) = \frac{\beta(s)}{\alpha(s)} (1 - G_2(s)). \qquad (2.16)$$

The various relationships can be summarised by a signal flow diagram where $\frac{V_s}{Q_s}$ is the hold-up time in the shell-side of the exchanger in appropriate units.

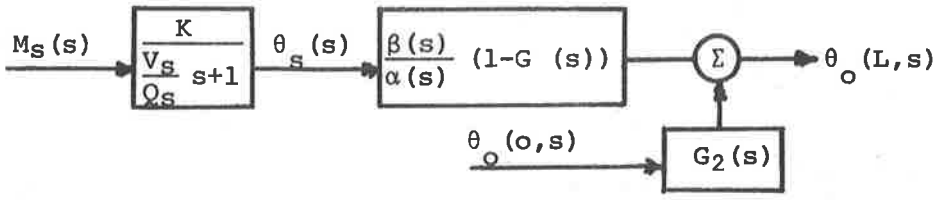

3.3.2 Impulse Response

If $\theta_o(o,s)$ is a unit impulse and $\theta_s(s) = 0$, the impulse response $g_2(t)$ can be found by expanding $G_2(s)$ as an infinite series and inverse-transforming term by term.

Equation (2.14) can be expanded as

$$G_2(s) = e^{-t_d s} \cdot e^{-b_1 t_d} \left[1 + \sum_{n=1}^{\infty} \frac{1}{n!} \left(\frac{b_1 b_3 t_d}{s+b_2+b_3} \right)^n \right] \qquad (2.17)$$

which on inverse transformation becomes

$$g_2(t) = e^{-bt_d} \left([\delta(t-t_d)] + \left[\sum_{n=1}^{\infty} \frac{1}{n!} \mathcal{L}^{-1} \left\{ \left(\frac{b_1 b_3 t_d}{s+b_2+b_3} \right)^n e^{-t_d s} \right\} \right] u(t-t_d) \right) \qquad (2.18)$$

where $u(t-t_d)$ is a unit step at $t = t_d$, and $\delta(t-t_d)$ is a unit impulse at $t = t_d$.

The inverse Laplace transform in equation (2.18) must be evaluated before proceeding further. Under the above conditions this can be written as

$$\mathcal{L}^{-1}\left\{\left(\frac{b_1 b_3 t_d}{s+b_2+b_3}\right)^n e^{-t_d s}\right\} = e^{-(b_2+b_3)(t-t_d)}\left[\frac{(b_1 b_3 t_d)^n (t-t_d)^{n-1}}{(n-1)!}\right]$$

which on substitution into (2.18) gives,

$$g_2(t) = e^{-b_1 t_d}\left(\left[\delta(t-t_d)\right] + \left[e^{-(b_2+b_3)(t-t_d)} \sum_{n=1}^{\infty} \frac{(b_1 b_3 t_d)^n (t-t_d)^{n-1}}{n!\,(n-1)!}\right]\right) \qquad (2.19)$$

This equation describes the response of the exit temperature of the tube fluid to a unit impulse disturbance in the fluid temperature at the point of entry to the tube.

For arbitrary variation of the inlet temperature the outlet temperature variation is given by the superposition integral,

$$\theta_o L(t) = \int_0^{\infty} g_2(x)\,\theta_o(t-x)\,dx \qquad (2.20)$$

The function $G_1(s)$, given by equation (2.16) can be treated similarly to the above to find the impulse response, $g_1(t)$, describing the system behaviour following a unit impulse in steam temperature $\theta_s(s)$. Thus if $\theta_s(s)$ is a unit impulse and $\theta_o(o,s) = 0$,

$$G_1(s) = \left\{\frac{b_1 b_2}{s^2+(b_1+b_2+b_3)s+b_1 b_2}\right\}\left[1 - G_2(s)\right] \qquad (2.21)$$

$$= \left[\frac{K_1}{s-s_1} + \frac{K_2}{s-s_2}\right]\left[1 - G_2(s)\right] \qquad (2.22)$$

where the constants K_1, K_2 and the roots s_1, s_2 must be determined for the specific parameters b_1, b_2, and b_3.

The first two terms can be inverse transformed directly but the third term gives rise eventually to Bessel functions.

Equation (2.22) may be written in the form,

$$G_1(s) = \phi_1(s) + \phi_2(s) + \phi_3(s) \tag{2.23}$$

where,

$$\phi_1(s) = \frac{K_1}{s-s_1} + \frac{K_2}{s-s_2}$$

$$\phi_2(s) = -Ke^{-b_1 t_d}\, e^{-t_d s}\, \frac{1}{s-s_1}\, e^{\frac{C_o}{s+c_1}}$$

$$\phi_3(s) = +Ke^{-b_1 t_d}\, e^{-t_d s}\, \frac{1}{s-s_2}\, e^{\frac{C_o}{s+c_1}}$$

As stated above $\phi_1(s)$ can be inverted directly.

$\phi_2(s)$ and $\phi_3(s)$ both involve a time delay term and a term of the form

$$\frac{1}{s+a}\, e^{\frac{C_o}{s+c_1}}$$

The inverse transform of $\phi_2(s)$ is,[5]

$$\phi_2(t) = -Ke^{-b_1 t_d}\, e^{-c_1(t-t_d)} \sum_{v=0}^{\infty} \beta_1{}^{v} C_o^{\frac{-v}{2}} (t-t_d)^{\frac{-v}{2}} I_v \left(2\sqrt{C_o(t-t_d)}\right) \tag{2.24}$$

where $\beta_1 = (s_1+c_1)$.

A similar expression can be written for $\phi_3(t)$. Hence the impulse response $g_1(t)$ can be written

$$\left.\begin{aligned} g_1(t) &= K(e^{s_1 t} - e^{s_2 t}) \quad \text{for } 0 < t < t_d \\ \text{and} \\ g_1(t) &= K(e^{-s_1 t} - e^{s_2 t}) + Ke^{-b_1 t_d}\, e^{-c_1(t-t_d)} \\ &\quad \sum_{v=0}^{\infty} \left(\frac{\beta_2{}^{v} - \beta_1{}^{v}}{C_o^{\frac{v}{2}}}\right) (t-t_d)^{\frac{v}{2}} I_v \left(2\sqrt{C_o(t-t_d)}\right) \\ &\quad \text{for } t < t_d. \end{aligned}\right\} \tag{2.25}$$

i.e. the impulse response becomes a series of Bessel functions.

A simplification is possible if the exponent in equation (2.13) is expanded as a series

$$G_2(s) = e^{-\frac{\alpha(s)L}{b_4}} = 1 - \frac{\alpha(s)L}{b_4} + \frac{\alpha(s)^2L^2}{2b_4^2} \qquad (2.26)$$

This expression can then be used to write the approximation

$$[1 - G_2(s)] - (1 - e^{-\frac{\alpha(s)L}{b_4}}) = \frac{\alpha(s)L}{b_4} - \frac{\alpha(s)^2L^2}{2b_4^2} + \frac{\alpha(s)^3L^3}{6b_4^3} \qquad (2.27)$$

Thus considering equations (2.16) and (2.27) we can write the approximation

$$G_1(s) \simeq \beta(s)\frac{L}{b_4}$$

$$\simeq \frac{b_1b_2L}{b_4}\left(\frac{1}{s+b_2+b_3}\right) \qquad (2.28)$$

which on inversion gives the impulse response

$$g_1(t) = \left(\frac{b_1b_2L}{b_4}\right) e^{-(b_2+b_3)t} \qquad (2.29)$$

It may be mentioned in passing that attempts to determine experimentally the response to impulse disturbances in steam temperature were unsatisfactory, the problem being to monitor the response. To get a measurable signal the disturbance had to be very large or sustained for some time. These difficulties were attributed to the very small time constant on the steam side and the relatively high flow rate on the liquid side.

However the theoretical response based on equation (2.29) is summarised in the table below. In addition a programme

developed to determine the time-domain response of a system from a knowledge of its s-plane constellation and overall gain is included as an appendix.

Table 1

Time (secs.)	Response of tube fluid temperature to impulse disturbance in steam temp.
0.0	38.62
0.1	2.658
0.2	0.183
0.3	0.013
0.4	0.0

3.3.3 Dynamic model

The basic equations presented in section 3.2 may be linearised by applying the small perturbation technique. This involves writing the dependent variables as a steady-state component and a small deviation. Time derivative terms are treated as independent variables, and second or higher-order terms in the perturbed variables are neglected. Any partial differentials in the coefficients of the perturbed variables are evaluated at the initial steady-state operating condition about which the dynamic behaviour of the plant is being analysed. When the static equations are subtracted from the perturbed equations the set of dynamic equations is obtained. These equations are linear ordinary differential equations with constant coefficients in perturbed variables. To facilitate analysis the equations may be Laplace transformed

and the resultant set of simultaneous equations solved manually or by the use of computers.

Unless otherwise indicated mean values of the variables have been represented by capital letters, variations about these values being indicated by the corresponding lower case character. An exception occurs with temperature, where to allow t to be reserved for time, θ has been used for the small deviations, thus $T_i = T_i + \theta_i$. In the case of density (ρ) the mean values are indicated by a bar, thus $\bar{\rho}$. This has been done also in any instance where uncertainty might arise. Laplace transforms are represented by tilde symbols, e.g. $\tilde{\theta}_i$, wherever this is thought necessary.

The equations used to develop the dynamic model are the equations (1.4) (1.5) (1.8) (1.9) (1.12) (1.16) (1.17) (1.18) (1.19) (1.20) and (1.21), the resulting set of dynamic equations being as follows.

$$p_s = -2Q_s^2 R_1 r_1 - 2Q_s R^2 q_s \tag{3.1}$$

$$V_s \frac{d\rho_s}{dt} = m_s - m_c \tag{3.2}$$

$$m_s \lambda_s = \left[(U_{so} - H_{co}) + \frac{M_1 Cp_1}{k_a V_s}\right] k_a V_s \frac{dT_s}{dt} + h_o A_o (\theta_s - \theta_t) \tag{3.3}$$

$$\bar{\rho}_t V_t Cp_t \frac{d\theta_t}{dt} = h_o A_o (\theta_s - \theta_t) - h_i A_i (\theta_t - \theta_o) \tag{3.4}$$

$$\begin{aligned} \bar{\rho}_o V_3 Cp_o \frac{d\theta_o}{dt} + Cp_o T_o \frac{d(v_3 \rho_o)}{dt} &= M_i Cp_i \theta_i + Cp_i T_i m_i \\ &- M_o Cp_o \theta_o - Cp_o T_o m_o + h_i A_i (\theta_t - \theta_o) \\ &- (Cp_w T_o + \lambda) m_v - M_v Cp_w \theta_o \end{aligned} \tag{3.5}$$

$$\theta_o = \alpha\, p_e + \gamma\, \rho_o \tag{3.6}$$

$$\frac{d(v_3\rho_o)}{dt} = m_i - m_o - m_v \tag{3.7}$$

$$K_o \frac{d(v_3\rho_o)}{dt} + v_3\bar{\rho}_o \frac{dk_o}{dt} = K_i m_i + M_i k_i - K_o m_o - M_o k_o \tag{3.8}$$

$$k = A_2\rho \tag{3.9}$$

$$H_1\rho_o + \bar{\rho}_o h_1 + p_e = 2Q_o\bar{\rho}_o R_2 q_o + Q_o^2 R_2 \rho_o + Q_o^2\bar{\rho}_o r_2 \tag{3.10}$$

$$m = Q\rho + \bar{\rho}q. \tag{3.11}$$

3.3.4 Reduction of dynamic equations

The set of dynamic equations can be combined as described below, to eliminate various intermediate variables producing a set of three simultaneous differential equations which yield the transfer functions relating the major output and input variables. The transfer functions may be used to calculate the response to any nominated forcing function, including the impulse response. However if they are used to calculate the frequency response the plotted data will not show resonance peaks as any distributed character of the system is eliminated during the development of the dynamic equations. However for engineering purposes the linearised model is probably adequate in view of the opinions expressed by other workers.[14,16,34,43]

Steam supply

The equation describing the steam-supply valve (3.1) may be rearranged as follows:

$$p_s = -2Q_s^2 R_1 r_1 - 2Q_s R_1^2 q_s$$

$$\text{i.e. } q_s = -\frac{ps}{2Q_s R_1^2} - \frac{2Q_s^2 R_1 r_1}{2Q_s R_1^2}$$

$$\text{or } q_s = -\frac{\beta}{R_1}\theta_s - Q_s \eta_1$$

where,

$$\beta^1 = \frac{\partial P_s}{\partial T_s} = \frac{ps}{\theta_s} \text{ and } \beta = \frac{1}{2R_1 Q_s}\beta^1$$

$$\eta_1 = \frac{r_1}{R_1}$$

Substituting this expression for q_s in equation (3.11) gives,

$$m_s = Q_s \rho_s + \bar{\rho}_s \left(-\frac{\beta}{R_1}\theta_s - Q_s \eta_1\right)$$

$$\text{i.e. } m_s = Q_s k_a \theta_s - \frac{\beta \bar{\rho}_s}{R_1}\theta_s - M_s \eta_1 \qquad (4.1)$$

where

$$k_a = \frac{\partial \rho_s}{\partial T_s} = \frac{\rho_s}{\theta_s}$$

and $M_s = Q_s \rho_s$, from equation (3.11).

Substituting equation (4.1) for m_s in equation (3.3) yields

$$\gamma s \theta_s = \lambda_s \left(Q_s k_a \theta_s - \frac{\beta \bar{\rho}_s}{R_1}\theta_s - M_s \eta_1\right) - h_o A_o (\theta_s - \theta_t).$$

Writing

$$N_1 = h_o A_o + \frac{\beta \bar{\rho}_s \lambda_s}{R_1} - Q_s k_a \lambda_s$$

$$a = \frac{h_o A_o}{N_1}$$

$$a^1 = \frac{M_s \lambda_s}{N_1}$$

$$\gamma = \left[(U_{so} - H_{co}) + \frac{M_1 Cp_1}{k_a V_s}\right] k_a V_s$$

$$\tau_5 = \frac{\gamma}{N_1}$$

we get, $(1 + \tau_5 s)\tilde{\theta}_s = a\tilde{\theta}_t - a^1\tilde{\eta}_1$. (4.2)

Since τ_5, the time constant for the calandria steam space, is a very small quantity there will be instances where it may be ignored. Under these circumstances equation (4.2) becomes,

$$\tilde{\theta}_s = a\tilde{\theta}_t - a^1\tilde{\eta}_1. \quad (4.3)$$

Substituting for θ_s and θ_o from equations (4.3) and (3.6) respectively in equation (3.4) gives,

$$V_t Cp_t \bar{\rho}_t s\theta_t = h_o A_o(a\theta_t - a^1\eta_1) + h_i A_i(\alpha p_e + \gamma\rho_o) - (h_i A_i + h_o A_o)\theta_t$$

$$= -(h_i A_i + h_o A_o)\theta_t + h_o A_o a\theta_t - h_o A_o a^1\eta_1 + h_i A_i(\alpha p_e + \gamma\rho_o).$$

Writing

$$N_2 = (h_o A_o(1-a) + h_i A_i)$$

$$\tau_6 = \frac{V_t Cpt\bar{\rho}t}{N_2}$$

$$b = \frac{a^1 h_o A_o}{N_2}$$

$$c = \frac{h_i A_i}{N_2} \quad \text{gives,}$$

$$(\tau_6 s+1)\theta_t = c\alpha p_e + c\gamma\rho_o - b\eta_1$$

or writing $E_1(s) = (1+\tau_6 s)$

$$E_1(s)\tilde{\theta}_t = c\alpha\tilde{p}_e + c\gamma\tilde{\rho}_o - b\tilde{\eta}_1 \quad (4.4)$$

Should it be decided that τ_5 cannot be ignored, equation (4.2) must be substituted instead of (4.3) into equation (3.4).

Equation (4.4) will have the same form but the constant b will be changed, as will the constant a in N_2.

Thus

$$a'' = \frac{a}{1+\tau_5 s}$$

$$b'' = \frac{a^1 h_o A_o}{(1+\tau_5 s)N_2}$$

Heat balance equations

The heat balance equations may be reduced by substituting for θ_o, m_v, m_i, m_o from equations (3.6), (3.7), (3.11), and (3.12) respectively into equation (3.5) giving,

$$Cp_o T_o s(v_3\rho_o) + Cp_o V_3 \bar{\rho}_o s(\alpha p_e + \gamma\rho_o) =$$

$$Cp_i T_i (Q_i\rho_i + \bar{\rho}_i q_i) + Cp_i M_i \theta_i - Cp_o T_o (Q_o\rho_o + \bar{\rho}_o q_o)$$

$$- Cp_o M_o (\alpha p_e + \gamma\rho_o) - (Cp_w T_o + \lambda) m_v$$

$$- Cp_w M_v (\alpha p_e + \gamma\rho_o) + h_i A_i \theta_t - h_i A_i (\alpha p_e + \gamma\rho_o).$$

Substituting $m_v = m_i - m_o - \frac{d(v_3\rho_o)}{dt}$ from equation (2.7) $= Q_i\rho_i + \bar{\rho}_i q_i - Q_o\rho_o - \bar{\rho}_o q_o - s(v_3\rho_o)$

and collecting terms,

$$Cp_o T_o s(v_3\rho_o) - (Cp_w T_o + \lambda) s(v_3\rho_o) + (Cp_o V_3 \bar{\rho}_o \gamma) s\rho_o$$

$$+ (Cp_o T_o Q_o + Cp_o M_o \gamma - (Cp_w T_o + \lambda) Q_o + Cp_w M_v \gamma + h_i A_i \gamma)\rho_o$$

$$= (Cp_i T_i Q_i - (Cp_w T_o + \lambda) Q_i)\rho_i + (Cp_i T_i \bar{\rho}_i - (Cp_w T_o + \lambda)\bar{\rho}_i) q_i$$

$$+ Cp_i M_i \theta_i + ((Cp_w T_o + \lambda)\bar{\rho}_o - Cp_o T_o \bar{\rho}_o) q_o$$

$$- ((Cp_o V_3 \bar{\rho}_o s + Cp_o M_o + Cp_w M_v + h_i A_i)\alpha) p_e + h_i A_i \theta_t.$$

Writing $N_4 = \gamma(h_iA_i + Cp_wM_v + Cp_oM_o) - Q_o(\lambda + T_o(Cp_w - Cp_o))$

and dividing through by N_4 we have:

$$\tau_7 s\tilde{\rho}_o - \frac{g}{\bar{\rho}_o} s(\widetilde{v_3\rho_o}) = -\tilde{\rho}_o + d\tilde{\theta}_t + g\tilde{q}_o - f_1Q_i\tilde{\rho}_i - f_1\bar{\rho}_i\tilde{q}_i + e\tilde{\theta}_i - \frac{\alpha}{\gamma}(\tau_7 s + f_2)\tilde{p}_e \qquad (4.5)$$

where,

$$\tau_7 = \frac{Cp_oV_3\bar{\rho}_o\gamma}{N_4}$$

$$d = \frac{h_iA_i}{N_4} \; ; \quad e = \frac{Cp_iM_i}{N_4} \; ; \quad f = \frac{\lambda + Cp_wT_o - Cp_iT_i}{N_4}$$

$$f_2 = \frac{\gamma(h_iA_i + Cp_wM_v + Cp_oM_o)}{N_4}$$

$$g = \frac{\bar{\rho}_o(\lambda + T_o(Cp_w - Cp_o))}{N_4} \; .$$

Mass balance on solute

Substituting for k_i and k_o from equation (3.9) into equation (3.8) yields

$$K_o s(v_3\rho_o) + A_2V_3\bar{\rho}_o s\rho_o = K_im_i + A_2M_i\rho_i - K_om_o - A_2M_o\rho_o.$$

Now at substituting for m_i, m_o from equation (3.11) and for M_i, M_o from equation (1.21) we get

$$K_o s(v_3\rho_o) + A_2V_3\bar{\rho}_o s\rho_o = K_i(Q_i\rho_i + \bar{\rho}_iq_i) + A_2Q_i\bar{\rho}_i\rho_i - K_o(Q_o\rho_o + \bar{\rho}_oq_o) - A_2Q_o\bar{\rho}_o\rho_o$$

$$= Q_i(K_i + A_2\bar{\rho}_i)\rho_i + K_i\bar{\rho}_iq_i - Q_o(K_o + A_2\bar{\rho}_o)\rho_o - K_o\bar{\rho}_oq_o,$$

i.e. $$K_o s(v_3\rho_o) + (A_2V_3\bar{\rho}_o s + Q_o(K_o + A_2\bar{\rho}_o))\rho_o$$

$$= Q_i(K_i + A_2\bar{\rho}_i)\rho_i + K_i\bar{\rho}_iq_i - K_o\bar{\rho}_oq_o.$$

Write $N_5 = (K_o + A_2\bar{\rho}_o)$ and divide through by $Q_o N_5$.

$$\frac{K_o}{Q_o N_5} s(v_3\rho_o) + (\tau_8 s+1)\rho_o = (\frac{Q_i (K_i+A_2\bar{\rho}i)}{Q_o N_5})\rho_i$$

$$+ (\frac{K_i\bar{\rho}_i}{Q_o N_5})q_i - (\frac{K_o\bar{\rho}_o}{Q_o N_5})q_o$$

where,

$$\tau_8 = \frac{A_2 V_3 \bar{\rho}_o}{Q_o N_5} .$$

If

$$h = \frac{Q_i (K_i + A_2\bar{\rho}i)}{Q_o N_5} ; \quad i = \frac{K_i\bar{\rho}_i}{Q_o N_5} ; \quad j = \frac{K_o\bar{\rho}_o}{Q_o N_5}$$

we can write

$$\frac{j}{\bar{\rho}_o} s(\widetilde{v_3\rho_o}) + (\tau_8 s+1)\tilde{\rho}_o = h\tilde{\rho}_i + i\tilde{q}_i - j\tilde{q}_o \qquad (4.6)$$

Relationship between fluid level in pan and product flow

Applying Bernoulli's equation we can write the following expression

$$\rho_o H_1 = (P_a - P_e) = Q_o^2 \rho_o R_2 \qquad (1.20)$$

Assuming,

(1) that the frictional pressure drop between the pan and the product fluid exit point is negligible, and

(2) that variations in atmospheric pressure can be ignored,

yields equation (3.10)

$$\bar{\rho}_o h_1 + H_1\rho_o + p_e = 2Q_o\bar{\rho}_o R_2 q_o + Q_o^2\bar{\rho}_o r_2 + Q_o^2 R_2\rho_o .$$

Rearranging,

$$q_o = \frac{1}{2Q_o\bar{\rho}_o R_2} (\bar{\rho}_o h_1 + H_1\rho_o + p_e - Q_o^2\bar{\rho}_o r_2 - Q_o^2 R_2\rho_o)$$

i.e.

$$\tilde{q}_o = \frac{1}{2Q_o\bar{\rho}_o R_2} ((H_1-Q_o^2 R_2)\tilde{\rho}_o + \tilde{p}_e + \bar{\rho}_o h_1) - \frac{Q_o}{2}\tilde{n}_2$$

where $\tilde{\eta}_2 = \frac{r_2}{R_2}$.

If the level in the pan (or flash vessel) is substantially constant, $h_1 = \frac{V_3}{A_p}$ and the equation becomes

$$\tilde{q}_o = \frac{1}{2Q_o\bar{\rho}_o R_2}\left((H_1 - Q_o^2 R_2)\tilde{\rho}_o + \tilde{p}_e + \frac{\bar{\rho}_o}{A_p}\tilde{v}_3\right) - \frac{Q_o}{2}\tilde{\eta}_2. \qquad (4.7)$$

3.4 Derivation of Transfer Functions

3.4.1 Response of Product Density

To deduce the transfer function describing the response of the product density to the various disturbances entering the system, it is necessary to combine the reduced equations (4.5) and (4.6) in such a way as to secure the simultaneous elimination of the variables $(\widetilde{v_3\rho_o})$ and $\tilde{q}_o$.

Multiply equation (4.5) by j and equation (4.6) by g and add the resulting equations yielding

$$(j\tau_7 + g\tau_8)s\rho_o = -(g + j)\rho_o + dj\theta_2 + (gh - f_1 Q_i j)\rho_i$$
$$+ (ig - f_1\bar{\rho}_i j)q_i + ej\theta_i - \frac{\alpha j}{\gamma}(\tau_7 s + f_2)p_e$$

i.e.

$$(1+\frac{j}{g})\tau_5 s\rho_o = \frac{j}{g}\{-(g + j)\rho_o + dj\theta_2 + (gh - f_1 Q_i j)\rho_i$$
$$+ (ig - f_1\bar{\rho}_i j)q_i + ej\theta_i - ej\theta_i - \frac{\alpha j f_2}{\gamma}E_2(s)\,p_e\}$$

where $\tau_9 = \frac{\tau_7}{f_2}$

and $E_2(s) = (1 + \tau_9 s)$

and $\tau_{10} = \frac{\tau_8(1+\frac{j}{g})\frac{\tau_7}{\tau_8}}{1 + \frac{j}{g}}$.

Substituting for θ_2 from (4.4) gives,

$$(1 + \frac{j}{g}\tau_{10}s\rho_o = \frac{j}{g}\{(\frac{cdj\gamma}{E_1(s)} - (g + j))\rho_o + (ig - f_1\bar{\rho}_i j)q_i$$

$$+ (gh - f_1 Q_i j)\rho_i + ej\theta_i$$

$$- \frac{bdj}{E_1(s)}\eta_1 + (\frac{cdj\alpha}{E_1(s)} - \frac{\alpha j f_2}{\gamma}E_2(s))\ p_e\}$$

i.e.

$$E_1(s)\ (1 + \frac{j}{g})\tau_{10}s\rho_o = \frac{j}{g}\{(cd\gamma - E_1(s)\ (\frac{g}{j} + 1))\rho_o$$

$$+ ((\frac{ig}{j} - f_1\bar{\rho}_i)q_i + (\frac{gh}{j} - f_1 Q_i)\rho_i + e\theta_i)\ E_1(s)$$

$$- bd\eta_1 + (cd\alpha - \frac{\alpha}{\gamma}f_2 E_1(s)E_2(s))\ p_e\}$$

$$E_1(s)\ (1 + \frac{j}{g}\tau_{10}s\rho_o - \frac{j}{g}(cd\gamma - E_1(s)\ (\frac{g}{j} + 1))\rho_o$$

$$= \frac{j}{g}\{E_1(s)\ ((\frac{ig}{j} - f_1\bar{\rho}_i)q_i + (\frac{gh}{j} - f_1 Q_i)\rho_i + e\theta_i)$$

$$- bd\eta_1 + (cd\alpha - \frac{\alpha}{\gamma}f_2 E_1(s)E_2(s))\ p_e\}$$

Dividing through by $(1 + \frac{j}{g})$

$$E_1(s)\ (1 + \tau_{10}s) - \frac{jcd\gamma}{g(1+\frac{j}{g})}\rho_o = \frac{j}{g(1+\frac{j}{g})}\left\{E_1(s)\left[(\frac{ig}{j} - f_1\bar{\rho}_i)q_i\right.\right.$$

$$\left.\left. + (\frac{gh}{j} - f_1 Q_i)\rho_i + e\theta_i\right] - bd\eta_1 + \frac{\alpha}{\gamma}(cd\gamma - f_2 E_1(s)E_2(s))\ p_e\right\}$$

or

$$E_3(s)\rho_o = E_1(s)\left[K_1\rho_i + K_2 q_i + K_3\theta_i\right] - K_4\eta_1 + K_5 E_4(s)\ p_e$$

where $N_8 = \dfrac{1}{(1 + \frac{g}{j} - cd\gamma)}$

$$K_1 = N_8(\frac{gh}{j} - f_1 Q_i)$$

$$K_2 = N_8(\frac{ig}{j} - f_1\bar{\rho}_i)$$

$$K_3 = N_8\ e$$

$$K_4 = N_8\ bd$$

$$K_5 = N_8 \frac{\alpha}{\gamma} (f_2 + cd\gamma)$$

$$E_3(s) = \frac{\tau_{10}\tau_6 s^2 + (\tau_{10} + \tau_6)\, s + 1}{(1 - \frac{cdj\gamma}{g + j})}$$

$$E_4(s) = \frac{\tau_6\tau_7 s^2 + (\tau_6 f_2 + \tau_7)\, s + 1}{(f_2 + dc\gamma)}$$

$$\therefore \tilde{\rho}_o = \frac{E_1(s)}{E_3(s)} \left[K_1\tilde{\rho}_i + K_2\tilde{q}_i + K_3\tilde{\theta}_i\right] - \frac{K_4}{E_3(s)} \tilde{\eta}_1 + \frac{K_5 E_4(s)}{E_3(s)} \tilde{p}_e$$

$$\therefore \tilde{\rho}_o = G_1(s) \left[K_1\tilde{\rho}_i + K_2\tilde{q}_i + K_3\tilde{\theta}_i\right] - K_4 G_2(s)\tilde{\eta}_1 + K_5 G_3(s)\, \tilde{p}_e \qquad (5.1)$$

where $G_1(s) = \frac{E_1(s)}{E_3(s)}$; $G_2(s) = \frac{1}{E_3(s)}$; $G_3(s) = \frac{E_4(s)}{E_3(s)}$.

Since the time constant of the tube wall is considerably smaller than the other time constants involved it may in some instances be neglected, allowing the transfer functions to be simplified. In which case

$$\tau_a = \tau_{10}(\frac{1-cdj\gamma}{g+j})$$

$$E_3(s) \doteq (1 + \tau_a s)(1 + \tau_6 s) \qquad \tau_6 << \tau_{10}, \tau_a$$

$$E_4(s) \doteq (1 + \tau_9 s)(1 + \tau_6 s) \qquad \tau_6 << \tau_9, \tau_7$$

$$G_1(s) = \frac{E_1(s)}{E_3(s)} \doteq \frac{1}{1 + \tau_a s}$$

$$G_3(s) = \frac{E_4(s)}{E_3(s)} \doteq \frac{1 + \tau_9 s}{1 + \tau_a s}$$

Equation (5.1) $\tau_a = \tau_{10}(\frac{1 - cdj\gamma}{(g + j)})$ remains unchanged.

For the purposes of this study the wall time constant was retained. The computed frequency responses are presented in a later section.

3.4.2 Response of pan level

The pan level response is determined by substituting the expression for $\tilde{q}_o$ (4.7) into equation (4.6).

$$\tau_o \left[\frac{\bar{\rho}_o A_2}{K_o + \bar{\rho}_o A_2}\right] s\rho_o + \frac{j}{\rho_o} s\,(\tilde{v}_3 \rho_o) = -\rho_o + h\rho_i + iq_i$$

$$- \frac{j}{2Q_o \bar{\rho}_o R_2}\left[(H_1 - Q_o^2 R_2)\rho_o + p_e + \frac{\bar{\rho}_o}{Ap} v_3\right] + \frac{jQ_o}{2}\eta_2$$

$$\text{i.e. } \tau_o\left[\frac{\bar{\rho}_o A_2}{K_o + \bar{\rho}_o A_2}\right] s\rho_o + \frac{jv_3}{\bar{\rho}_o}\rho_o + jsv_3 = -\rho_o + h\rho_i + iq_i$$

$$- j N_6\left[\frac{N_7}{N_6}\rho_o + p_e + \frac{\bar{\rho}_o}{Ap} v_3\right] + \frac{jQ_o}{2}\eta_2$$

where $N_6 = \left[2Q_o \bar{\rho}_o R_2\right]^{-1}$

$N_7 = (H_1 - Q_o^2 R_2) N_6$

and $\tau_o = \frac{V_3}{Q_o}$

Substituting the earlier definition for j in the second term of the above equation, viz. $j = \frac{K_o \bar{\rho}_o}{Q_o N_5}$, recalling that $N_5 = K_o + \bar{\rho}_o A_2$, and combining the substituted form with the first term of the above equation, we have

$$jsv_3 = -(1 + \tau_o s + jN_7)\rho_o - jN_6\, p_e - \frac{jN_6 \bar{\rho}_o}{Ap} v_3 + \frac{jQ_o}{2}\eta_2$$

$$+ h\rho_i + iq_i$$

$$(js + \frac{jN_6 \bar{\rho}_o}{Ap}) v_3 = -(1 + \tau_o s + jN_7)\rho_o - jN_6\, p_e + \frac{jQ_o}{2}\eta_2$$

$$+ h\rho_i + iq_i.$$

Writing $\tau_b = \frac{Ap}{N_6 \bar{\rho}_o}$ and letting $G_4(s) = (1 + \tau_b s)^{-1}$

gives,

$$v_3 = G_4(s)\left[-K_6 G_5(s)\rho_o + K_7 \rho_i + K_8 q_i + K_9 \eta_2 - K_{10} p_e\right] \quad (5.2)$$

where,

$$\tau_c = \frac{\tau_o}{1 + j\ N_7}$$

$$G_5(s) = (1 + \tau_c s)$$

$$N_9 = \frac{Ap}{j\ N_6 \bar{\rho}_o}$$

$$K_6 = N_9(1 + j\ N_7)$$

$$K_7 = N_9\ h$$

$$K_8 = N_9\ i$$

$$K_9 = N_9\ \frac{j\Omega_o}{2}$$

$$K_{10} = j\ N_6 = \frac{Ap}{\bar{\rho}_o}$$

Because of the occurrence of $\tilde{\rho}_o$ in the R.H.S. of the response equation (5.2) it is necessary to substitute for $\tilde{\rho}_o$ from equation (5.1) to solve for the response of pan level. If this is done the function becomes:

$$v_3 = G_4(s)\ \big[-K_6G_5(s)G_1(s)\ [K_1\rho_i + K_2q_i + K_3\theta_i] + K_4K_6G_2(s)$$

$$G_5(s)\eta_1 - K_5K_6G_3(s)G_5(s)p_e + K_7\rho_i + K_8q_i + K_9\eta_2 - K_{10}p_e\big]$$

which on collecting like terms yields,

$$\therefore\ v_3 = G_4(s)\ \big[(K_7 - K_1K_6G_6(s))\tilde{\rho}_i + (K_8 - K_2K_6G_6(s))\tilde{q}_i$$

$$- (K_3K_6G_6(s))\tilde{\theta}_i + (K_4K_6G_7(s)\tilde{\eta}_1 - (K_{10} + K_5K_6G_8(s))\tilde{p}_e$$

$$+ K_9\tilde{\eta}_2\big] \qquad (5.3)$$

where $G_6(s) = G_1(s)\ .\ G_5(s)$

$G_7(s) = G_2(s)\ .\ G_5(s)$

$G_8(s) = G_3(s)\ .\ G_5(s)$.

3.4.3 Response of Product Flow

This is obtained from equation (4.7) which can be written:

$$q_o = K_{11}\rho_o + K_{12}\, p_e + K_{13}\, v_3 - K_{14}\eta_2 \qquad (5.4)$$

where $K_{11} = N_7$

$K_{12} = N_6$

$K_{13} = \frac{\bar{\rho}_o N_6}{Ap}$

$K_{14} = \frac{Q_o}{2}$.

Once again since $\tilde{\rho}_o$ and $\tilde{v}_3$ appear in this equation it is necessary to substitute for these variables from equations (5.1) and (5.3) in order to determine the product flow response. When this is done the following equation results:

$$\begin{aligned} q_o = {} & K_{11}\ (G_1(s)[K_1\rho_i + K_2 q_i + K_3\theta_i] - K_4 G_2(s)\eta_1 \\ & + K_5 G_3(s) p_e) + K_{12} p_e + K_{13}\ (G_4(s)[(K_7 - K_1K_6G_6(s)\rho_i \\ & + (K_8 - K_2K_6G_6(s))q_i - (K_3K_6G_6(s))\theta_i + (K_4K_6G_7(s))\eta_1 \\ & - (K_{10} + K_5K_6G_8(s))p_e + K_9\eta_2) - K_{14}\eta_2 \end{aligned}$$

which on collecting like terms yields the following transfer function:

$$\begin{aligned} \tilde{q}_o = {} & (K_1K_{11}G_1(s) + K_{13}G_4(s)\ (K_7 - K_6G_6(s))\tilde{\rho}_i + (K_2K_{11}G_1(s) \\ & + K_{13}G_4(s)(K_8 - K_2K_6G_6(s)))\tilde{q}_i + (K_3K_{11}G_1(s) \\ & - K_{13}G_4(s)(K_3K_6G_6(s)))\tilde{\theta}_i + (K_{13}G_4(s)(K_4K_6G_7(s)) \\ & - K_4K_{11}G_2(s))\tilde{\eta}_1 + (K_5K_{11}G_3(s) + K_{12} - K_{13}G_4(s) \\ & (K_{10} - K_5K_6G_8(s)))\tilde{p}_e + (K_9K_{13}G_4(s) - K_{14})\tilde{\eta}_2 \end{aligned} \qquad (5.5)$$

Since there seems little point in the definition of further constants to make the equation look less complicated, it will be left in this form.

The above transfer functions may be used to calculate the response of the output variables to disturbances in the significant input variables. However it must be repeated that they are linearised functions and the resonance peaks appearing in the frequency response of distributed parameter systems will not be present. In many instances this will not matter, particularly as it seems from the published studies mentioned already that the linearised model is good at least to the first resonant frequency, and there seems reason to assume that high frequency disturbances are not significant in the process industries. The linearised model was used for the simulation studies in which various controller configurations were compared.

Should the resonance phenomena be of interest, the transfer functions developed earlier in which the distributed parameter characteristics were retained, should be used. These are equation (1.15) for the response of the temperature of the fluid leaving the exchanger to disturbances in the fluid flow rate, and equations (2.13 and (2.15) for the response to disturbances in the fluid inlet temperature or in the steam temperature. These equations were used to calculate frequency response curves for comparison with the experimental results obtained with the forced-circulation evaporator.

4. DESCRIPTION OF EXPERIMENTAL PLANT

In the standard natural-circulation internal-calandria evaporator the feed enters via a distributor which terminates in a number of short vertical pipes which direct the dilute feed liquor into the calandria. This is a bundle of tubes supported by end-plates. The tubes are heated by steam which condenses on the outside of the tubes, the condensate being removed through a trap. The feed liquor is heated as it passes through the tubes, boils above the upper tube plate and passes downwards through the annular space separating the calandria from the wall of the evaporator thus completing the natural circulation. The concentrated liquor is removed continuously through a stand-pipe. In the case of evaporators working under vacuum this pipe is prolonged to form a barometric leg. The water vapour formed during the boiling process is led to a condenser, in which, under vacuum operation the cooling water flow rate may be regulated to control the pan pressure. Any noncondensable gases are removed by a steam ejector. The natural-circulation evaporator simulated during the study has been described by Andersen et al.[1]

A comparison of the Figures 1 and 4 will show that the forced-circulation external-calandria evaporator is essentially similar to the apparatus described above, except that the calandria is outside the pan, which thus becomes a flash vessel and may be reduced in size. The merits and fields of application of both types have been reviewed elsewhere.[13,28]

For the experimental portion of this study the writer built a forced-circulation evaporator having the following characteristics.

The calandria was a concentric tube heat exchanger consisting of a nine-foot length of copper tube (one-inch outside diameter by 16 gauge)

supported by brass compression fittings in the axis of a 4-inch diameter, schedule 40, wrought-iron pipe. The heater was lagged externally by a layer of polythene foam one-inch thick. The heat transfer area was assumed to be that of the copper pipe only, the end effects being assumed negligible on the basis of calculated heat losses through the gaskets and flanges. The heated section was six feet long.

Micro-pyrotenax copper-constantan thermocouples were used for the temperature measurements. These couples were chosen because of their stability and relatively high electromotive force per degree. The thermocouples were attached at six-inch intervals along the copper tubes, the measuring junctions being silver-soldered into grooves machined in the tube walls so that a minimum thickness of copper separated the thermocouples from the tube liquor. The thermocouples were calibrated in situ and recalibrated at regular intervals throughout the programme. All switches and terminals were mounted in constant-temperature insulated boxes to ensure isothermal conditions. The lead wires were the same material as the thermocouples, and in fact were extensions of the thermocouples themselves; their lengths being adjusted so that all thermocouple circuits were of equal electrical resistance. All temperature readings were corrected for the cold junction reading.

The temperature of the liquid was measured using a travelling thermocouple system. In the early runs a set of five thermocouples were arranged such that one was located in the central axis of the column, one six inches above this to provide a check on the previous reading, and three equispaced radially to keep the system properly located. The tips of these last thermocouples tended to rub through on the tube wall and

the system was replaced by a single central thermocouple, silver-soldered into the end of a length of 1/8-inch outside diameter stainless steel tubing which had locating vanes attached to it. This could be raised and lowered in the column, a ball and detent system ensuring that the thermocouple tip was always locked into the chosen positions. The liquid flow rates were corrected to allow for the effect of immersing the thermocouple probe to different extents. The internal thermocouple measuring points were opposite the thermocouples embedded in the tube wall.

One-eighth inch pipe couplings were brazed to the copper tube near the ends of the heating section to allow the inlet pressure and pressure drop to be measured. Conventional mercury manometers were used to make the measurements, which were corrected in every case for the liquid column which collected above the mercury. The accuracy of the manometer readings was estimated as ±0.25 psi. No particular significance could be attached to these measurements of which a typical set is presented in Figure 5.

The fluid flow rates were measured in the earlier runs by sharp-edge orifice plates constructed in the laboratory workshop. These were used in conjunction with a commercial recording manometer, the combination being calibrated in situ. Eventually this arrangement was replaced by a turbine flowmeter and its associated ratemeter and totalising flowmeter.

The steam used for heating was generated in the laboratory by a "Clayton" steam generator and brought to dry saturated condition by passage through a heat exchanger and catch pot after preliminary reduction

of pressure. This was followed by a further, smaller reduction in pressure, the steam then being admitted to the calandria through a manifold so that the velocity was reduced to a minimum before the steam reached the tube. This was considered necessary since the surface temperature distribution on the copper tube was found to be sensitive to the method of introducing the steam. The condensate was removed through a thermostatic steam trap, and collected in a weight tank where its temperature was also measured. The steam jacket was vented to remove any entrained air.

The copper pipe was extended about eighteen inches beyond each end of the heat exchanger, the upper end terminating in a wrought-iron cross attached to the side of the pan. A double glass window was mounted in one arm of the cross to allow visual observation of conditions at the top of the tube. The travelling thermocouple passed vertically through the cross, as shown in Figure 4. The remaining branch communicated with the flash vessel.

The concentrated liquor was removed from this vessel through a two-inch diameter downcomer. The vapour was removed from the top of the flash vessel and carried to a condenser. The condensed vapour could be collected and weighed if desired. For a while a layer of woven copper was used as a mist entrainer, but this was found to induce periodic surges through the system. Apparently the mesh retained condensed vapour forming a water seal, which was destroyed explosively when the pressure beneath the seal reached a sufficiently high level. This mist entrainer was replaced by a baffle which seemed to prevent entrainment. Tests

were carried out to verify this by measuring the conductance of samples of condensed vapour using tap water as the process liquid. The flash vessel also acts as a separation chamber to reduce the risk of vapour carry-under.

Petrick[36] has examined the circumstances under which carry-under could occur in steam-water and other systems. Although he was concerned with natural convection systems the phenomenon is of significance in forced-circulation systems too, since entrainment of significant amounts of vapour in the circulating liquid in the suction line to the pump could cause caviation problems.

The pump in the system serves to recirculate the concentrating liquor and to introduce make-up feed liquor. A closed-coupled 1½-inch centrifugal pump was used in the experimental apparatus.

Apart from the measurements already indicated, the pressure and temperature of the steam were measured just before admission to the heat exchanger and in the steam space. The temperature and pressure in the flash vessel, and the feed liquor temperature, also the temperature of the liquor leaving the heat exchanger and leaving the evaporator were monitored. The feed liquor was preheated and admitted at its bubble-point.

5. ESTIMATION OF HEAT TRANSFER COEFFICIENTS

The conclusion reached when considering the problem of axial diffusion was that the tube wall could be treated as a lumped rather than distributed system. This is significant enough to warrant experimental investigation. As described earlier, thermocouples were implanted in the wall at six inch intervals. These temperatures were read, together with the liquid temperatures taken at the same levels through the exchanger, for a range of flowrates.

The results show that for a uniform steam temperature the wall temperature fluctuates slightly about a mean temperature. The fluctuations are random and small in magnitude as can be seen from Table 2 which presents a set of typical results. Variations of the magnitude shown could arise from variations in contact resistance, variations at the junctions, or through variation in the thermocouple or leadwire material, even though each of these is within its range of permissible tolerance. Alternatively they could arise from variation in the thickness of the condensate film on the shell-side of the tube wall or from tube fluid phenomena.

The wall mean temperatures vary slightly at different feed flow rates but it is difficult to point to any specific relationship. Reference to the table indicates that the wall mean temperature is slightly higher at higher fluid flow rates. Heat balances were performed at regular intervals throughout the experimental work to determine that the thermocouples and associated instrumentation were functioning correctly, and frequent checks were made on the steam quality. This was done by injecting steam into a tared amount of water in a weigh tank and measuring the temperature of the water over the test period.

TABLE 2: WALL TEMPERATURES (^{o}F)

Steam temp. 242.3^{o}F

Flow rate	gpm 1.73 fps 1.15	3.45 2.30	5.18 3.45	6.91 4.60	8.63 6.58	10.36 6.90	12.10 8.05	13.81 9.20	15.54 10.35	17.27 11.50
	221.9	221.2	220.5	220.9	220.1	227.6	227.8	228.1	227.5	227.2
	220.1	219.1	218.9	220.6	218.5	226.1	225.9	225.5	224.9	224.9
	219.7	218.8	218.8	222.1	217.5	225.1	224.7	224.6	224.0	223.8
	222.3	221.1	220.1	222.1	220.1	226.5	228.0	227.6	227.3	227.3
	221.2	219.8	219.4	220.6	218.5	224.7	226.1	225.6	225.6	225.3
	222.7	220.5	220.3	220.6	219.2	225.5	226.2	225.4	225.0	224.7
	222.1	220.5	220.3	221.0	219.4	225.2	227.2	226.7	226.8	226.4
	221.6	219.6	218.7	220.0	218.5	224.9	226.3	225.8	225.6	225.6
	222.9	221.3	220.1	221.3	220.1	226.7	228.4	228.1	228.2	227.9
	222.7	221.7	220.9	218.9	220.3	226.9	228.7	228.6	228.2	229.1
	221.9	220.5	220.3	219.0	219.0	225.5	226.9	227.2	226.8	226.4
	221.6	220.1	219.3	220.6	218.8	225.4	227.4	226.8	226.8	226.6

FLUID TEMPERATURES AT CORRESPONDING LEVELS

	210.4	211.7	211.7	211.7	211.5	210.8	211.3	211.7	212.2	212.2
	211.3	211.7	211.5	211.3	211.1	210.8	211.1	211.5	211.7	211.7
	211.7	211.3	211.1	211.1	210.9	210.4	210.6	211.5	211.3	211.5
	211.5	210.6	210.4	210.6	210.2	210.2	210.4	210.8	211.1	211.3
	209.7	210.2	210.2	210.2	209.7	210.2	210.2	210.6	211.1	210.8
	209.3	209.5	209.7	210.2	209.7	209.7	210.2	210.4	210.6	210.8
	208.6	209.3	209.5	210.2	209.5	209.5	209.7	210.2	210.4	210.8
	207.7	208.6	209.0	209.5	209.3	209.3	209.5	210.2	210.2	210.6
	207.3	208.0	208.6	209.3	208.8	209.0	209.3	209.7	210.2	210.4
	206.8	207.5	208.0	208.8	208.6	209.0	209.3	209.5	210.2	210.2
	206.4	207.3	208.0	208.6	208.6	208.8	209.3	209.5	210.2	210.2
	206.1	207.3	207.7	208.6	208.4	208.6	209.3	209.5	210.2	210.2

Note: In each column the temperatures correspond to the measurement points in the tube read downwards.

In the majority of studies in forced-circulation heat transfer the data have been correlated according to some form of Dittus-Boelter equation for heat transfer coefficients. This correlation has the general form

$$\frac{hD}{k} = a\left(\frac{\rho VD}{\mu}\right)^{n}\left(\frac{C\mu}{k}\right)^{m}$$

There has been a certain amount of discussion concerning the values to be ascribed to the parameters a, m and n. According to McAdams[27] the best working form seems to be a = 0.0225, n = 0.8 and m = 0.4. Logan et al[26] confirmed this correlation for forced-circulation evaporation under non-boiling conditions, although they modified the value of the coefficient to a = 0.0205. Their work found general support from Boarts et al[3] for water with some boiling, although they in turn proposed the new value a = 0.0278. In the case where appreciable boiling occurred they claimed that the predicted value was less than that found experimentally, at least for flow rates less than 3.5 feet per second. In fact simple heating occurred over 5.5 feet of tube at 2.3 feet per second (fps), over 9.2 feet at 3.5 fps, over 11.5 feet at 5.0 fps, and over practically the whole tube at higher velocities. The tube was 12 feet long and 0.76 inches inside diameter.

Despite the above variations in the values recommended, it seems reasonable to assert that for forced-circulation evaporators, provided the flow rate is kept sufficiently high, the Dittus-Boelter equation provides a reasonable route to the estimation of the heat transfer coefficient.

Heat fluxes were determined for the forced-circulation evaporator at various flow rates within the range 17-248 pound per minute. The

procedure used was to adjust the steam conditions and fluid flow rate and to operate the unit until steady state conditions were established. The inlet and outlet fluid temperatures were then recorded together with the steam and steam condensate temperatures, the wall temperatures and the fluid flow rates.

These data were used to calculate overall heat transfer coefficients from which the wall conductance and steam-side coefficients calculated using equation (10-46) from Perry's Handbook[35] were subtracted, to give an estimate of the fluid-side coefficients. These values are tabulated below together with a set calculated using the Dittus-Boelter correlation (Perry 11-1).

For comparison with the measured overall heat transfer coefficients the Fragen-Badger correlation (Perry 11-2) was used to calculate a range of coefficients which are tabulated in Table 3 together with the experimental values referred to above.

The values listed with the plant data for h_i and h_o are the values corresponding to the operating flow rate adjusted to include half the wall conductance each.

TABLE 3: HEAT TRANSFER COEFFICIENTS

Fluid flow rate (fps)	Overall coefft. (Experimental)	Overall coefft. (Calc'd Perry 11-2)	h_o calc'd (Perry 10-46)	h_i calc'd (Perry 11-1)	h_i estimated (from 1 & 3)
1.15	410	384	1564	515	564
2.30	616	582	1726	897	980
3.45	781	742	1933	1240	1357
4.60	926	882	2131	1561	1708
6.58	1101	1094	2442	2080	2106
6.90	1181	1125	2489	2160	2362
8.05	1296	1234	2652	2443	2698
9.20	1395	1337	2808	2719	2972
10.35	1499	1435	2958	2987	3281
11.50	1591	1528	3100	3250	3554

Units: $Btu/hr.ft^2.{}^oF$

6. FREQUENCY RESPONSE ANALYSIS OF FORCED-CIRCULATION EVAPORATOR

6.1 Calculation of theoretical responses

Theoretical frequency responses relating product density, liquid level, and product flow to a range of input disturbances may be calculated from the transfer functions developed in an earlier section, viz. equations (5.1), (5.3), (5.5). Since these are linearised equations the frequency response results obtained in this way are only indicative of the system behaviour.

Transfer functions,presented as equations (1.15), (2.13) and (2.15) which retain the distributed-parameter feature of the forced-circulation evaporator, were used to calculate the process fluid effluent temperature to cyclic disturbances in the fluid flow rate, fluid influent temperature, and steam temperature respectively. These results are compared with experimentally determined results in the cases of steam temperature and fluid flow oscillations in a later section. As expected, these curves show resonance peaks with increasing frequency the incidence being dependent on the process fluid flow rate.

The usual Laplace transformation and complex variable procedures were used to calculate the frequency responses from the transfer functions, computer programmes being prepared to calculate the attenuation and phase angle values as a function of frequency for the specified plant conditions. Terms of the form $(1 + \tau s)$ can be handled without trouble but the term of the form $(1 - Ke^{-as})$ occurring in equation (2.5) required preliminary manipulation as follows.

Substitution of $s = i\omega$ in $(1 - Ke^{-as})$ gives $(1 - Ke^{-ai\omega})$

which

$$= \frac{e^{ai\omega} - K}{e^{ai\omega}} = \frac{\cos a\omega + i \sin a\omega - K}{\cos a\omega + i \sin a\omega} .$$

Rationalisation gives,

$$\frac{\cos^2 a\omega - i \sin a\omega \cos a\omega + i \sin a\omega \cos a\omega + \sin^2 a\omega - K \cos a\omega + iK \sin a\omega}{\cos^2 a\omega + i \sin a\omega \cos a\omega + \sin^2 a\omega - i \sin a\omega \cos a\omega}$$

$$= 1 - K \cos a\omega + i K \sin a\omega.$$

Separation into parts plus slight manipulation yields

$$|G| = \sqrt{(1 + K^2\cos^2 a\omega - 2K \cos a\omega + K^2\sin^2 a\omega)}$$

i.e. $$|G| = \sqrt{(1 + K^2 - 2K \cos a\omega)}$$

and $$\angle G = \tan^{-1} \frac{K \sin a\omega}{1 - K \cos a\omega}$$

6.1.1 Theoretical responses based on the simplified model

6.1.1.1 Product density

Equation (5.1) is the transfer function relating product density to disturbances in the feed variables (density, flow rate, and temperature), the evaporator pan pressure, and the steam supply rate. It is a condensed form of the full transfer function and is reproduced here for convenience.

$$\tilde{\rho}_o = G_1(s) \ (K_1\tilde{\rho}_i + K_2\tilde{q}_i + K_3\tilde{\theta}_i) - K_4G_2(s)\tilde{\eta}_1 + K_5G_3(s) \ \tilde{p}_e \qquad (5.1)$$

The pertinent relationships can be illustrated most conveniently through the block diagram, Figure 2. The transfer function allows the time-domain responses or frequency responses to be cal-

culated, a point which will be taken up again later. In the above expression $G_1(s)$ relates the product density to the feed variables, $G_2(s)$ to the steam disturbances, and $G_3(s)$ to pressure disturbances respectively.

Considering the various relationships in turn we can write the following equations.

$$G_1(s) = \frac{E_1(s)}{E_3(s)} = \frac{\dfrac{1 + \tau_6 s}{\tau_6\tau_{10}s^2 + (\tau_6+\tau_{10})s + 1}}{(1 - \dfrac{cdj\gamma}{g+j})}$$

$$= \frac{0.92\ (1 + \tau_6 s)}{\tau_6\tau_{10}s^2 + (\tau_6+\tau_{10})s + 1}$$

Similarly,

$$G_2(s) = \frac{1}{E_3(s)} = \frac{0.92}{\tau_6\tau_{10}s^2 + (\tau_6+\tau_{10})s + 1} \quad \text{and}$$

$$G_3(s) = \frac{E_4(s)}{E_3(s)} = \frac{0.92(\tau_6\tau_7 s^2 + (\tau_6 f_2 + \tau_7)s + 1)}{0.19(\tau_6\tau_{10}s^2 + (\tau_6+\tau_{10})s + 1)}$$

Comparing the time constants involved in the above functions we note that,

$\tau_{10} = 0.00356$, $\tau_6 = 0.000234$ and $\tau_7 = 0.00108$ hours respectively for the forced-circulation evaporator.

The time constant for the calandria tube wall, τ_6, is rather smaller than the other two, and if it is regarded as insignificant a set of simpler transfer functions results.

From the linearised transfer functions describing the relationship between product density and the feed parameters, the major time constant

involved is seen to be a function of volume/throughput and feed concentration/product concentration ratios. This time constant is so large compared with that for the wall that the response is effectively that for a single exponential transfer stage. The difference between these two time constants would be more marked in an industrial-sized evaporator. Under such circumstances the decision to ignore the tube wall constant would be valid generally.

The response to steam changes is a product of two first-order stages, one time constant being that already referred to, the other that for the calandria tube wall. Again, if the decision is taken to ignore the tube wall time constant this relationship also reduces to a first order one identical with that relating the product density and feed parameter disturbances.

The response to pan pressure disturbances is rather more complex since it involves a second-order term in the numerator, with one of the time constants involved being relatively large. Consequently rapid changes of pressure are likely to cause large changes in vapour flow. In the extreme a very rapid increase in pressure could cause an evaporator operating under vacuum to go off the boil, upsetting the thermodynamic

equilibrium and invalidating the boiling point-density relationship used in the development of the mathematical model. The experimental evaporator was free from this danger since it was operated at atmospheric pressure, while normal plant practice would depend on an effective pressure control loop.

In the absence of controllers, variations in pan level or product flow will not affect product density, provided the solution continues boiling. If the only controller is one monitoring level and regulating product flow the system would behave identically with the open-loop case, so far as feed flow or steam changes are concerned. However with both density and level controllers in place variations in level and product withdrawal rate affect density through the controllers.

Making the appropriate substitutions for the gain constants and time constants the simplified set of transfer functions describing the product density response can be written,

$$\frac{\tilde{\rho}_o}{\tilde{\rho}_i, \tilde{q}_i, \tilde{\theta}_i} = 0.159,\ 0.0063,\ 0.00265\ \left(\frac{1}{1+0.0128s}\right)$$

respectively.

$$\frac{\tilde{\rho}_o}{\tilde{\eta}_1} = \frac{0.159}{(1+0.0128s)(1+0.00018s)} = \left(\frac{0.159}{1+0.0128s}\right)$$

$$\frac{\tilde{\rho}_o}{\tilde{p}_e} = 0.00053\ \left(\frac{1+0.0126s}{1+0.0128s}\right).$$

These transfer functions were used to calculate the frequency responses for the simplified model, the results being tabulated below. Since the gain constants can be taken into the ordinate factor the responses to ρ_i, q_i, θ_i, η_1 are presented together. The assumption to neglect the tube wall time constant was not made in computing the theoretical responses reported later.

Table 4: Frequency response of simplified model

Response of product density, P_Q, to disturbances in ρ_i, q_i, θ_i, η_1			Response of product density, P_Q, to disturbances in P_e	
Frequency (radians/sec.)	Normalised attenuation	Phase lag	Normalised attenuation	Phase lag
0.001	1.000	-2.7	1.000	-2.5
0.005	0.981	-14.0	0.984	-12.3
0.010	0.903	-25.6	0.984	-23.5
0.020	0.776	-43.8	1.03	-41.1
0.050	0.386	-67.3	0.924	-65.3
0.100	0.205	-78.2	0.914	-77.1
0.200	0.104	-84.0	0.911	-83.5
0.300	0.070	-86.0	0.910	-85.6
0.400	0.052	-87.0	0.910	-86.7
0.500	0.042	-87.6	0.910	-87.4
0.600	0.035	-88.0	0.910	-87.8
0.700	0.030	-88.3	0.910	-88.1
0.800	0.026	-88.5	0.910	-88.4
0.900	0.023	-88.7	0.910	-88.5
1.000	0.021	-88.8	0.910	-88.7
2.000	0.010	-89.4	0.910	-89.3
3.000	0.007	-89.6	0.910	-89.6
4.000	0.005	-89.7	0.910	-89.7
5.000	0.004	-89.8	0.910	-89.7
6.000	0.003	-89.8	0.910	-89.8
7.000	0.003	-89.8	0.910	-89.8
8.000	0.003	-89.9	0.910	-89.8
9.000	0.002	-89.9	0.910	-89.9
10.000	0.002	-89.9	0.910	-89.9

6.1.1.2 Pan level

The response of pan level to disturbances in feed and product densities, feed flow, pan pressure, and product withdrawal rate, may be deduced from equation (5.2) which is the transfer function describing these relationships.

$$\tilde{v}_3 = G_4(s)(-K_6G_5(s)\tilde{\rho}_o + K_7\tilde{\rho}_i + K_8\tilde{q}_i + K_9\tilde{\eta}_2 - K_{10}\tilde{p}_e) \qquad (5.2)$$

where

$$G_4(s) = (1 + \tau_b s)^{-1}$$

$$G_5(s) = (1 + \tau_4 s).$$

It will be observed that the pan level response involves the product density so that an expression relating the two parameters will need to be substituted into the transfer function. This requirement is met by the substitution of equation (5.1) into (5.2), the substitution being detailed in another section.

Equation (5.2) shows that the response to feed density and flow rate, product withdrawal rate, and pan pressure are all similar differing only in the gain constants. These responses were not calculated during this programme but the corresponding transient responses for the closed-loop system, obtained by simulation, are presented in a later section.

6.1.1.3 Product flow

The response of product flow is given by equation (5.5), reproduced here for convenience,

$$\tilde{q}_o = K_{11}\tilde{\rho}_o + K_{12}\tilde{p}_e + K_{13}\tilde{v}_3 - K_{14}\tilde{n}_2. \qquad (5.5)$$

This expression indicates the response to changes in product density, pan level, pan pressure, and product withdrawal rate as determined by the valve opening in the product line. Once again it can be seen that previously determined relationships appear in the expression. Since both product density and pan level are involved, it will be necessary to substitute both equations (5.1) and (5.2) into equation (5.5) to determine the response of product flow. Details of the substitution have been presented already.

The responses of pan level and product flow may be represented conveniently on a single block diagram, Figure 3.

The inclusion of a level controller, which it has been emphasised already is usual practice, will necessitate the inclusion of an expression relating pan level and either feed flow or product flow. Experimentally, alternative configurations of the controller loops are readily incorporated into the simulated models and the cases reported represent such alternatives.

The frequency responses of the approximate model are not presented in detail since a major objective was to compare the behaviour of the exact model with the experimental results and this is done later.

6.2 Experimental frequency response analysis of forced-circulation evaporator

6.2.1 The apparatus

A schematic diagram of the evaporator and the associated instrumentation has been presented already, Figure 4. The working fluids were water and ammonium nitrate solutions. The vapour-liquid mixture was separated in the flash vessel, the vapour being taken off to the condenser and the liquid either withdrawn through the product offtake line or recirculated through a 2 inch nominal bore downcomer. The liquid level was maintained about 12 inches above the top of the evaporator tube and the condenser was vented to the atmosphere. A heat exchanger was installed in the steam supply line to regulate the steam condition.

Standard commercial instruments were used to monitor the designated variables. The measuring elements were all fast response types. Bare miniature thermocouples having a time constant of approximately 0.2 seconds were used to measure the temperatures and turbine flowmeters with a time constant of about 0.01 seconds in water the flowrates. The tachometer output of the flowmeter could be directed to a UV-recorder when flow variations were to be recorded. All

control valves were fitted with valve positioners to improve their response to changes in applied pressure.

The process analyser used to perform the frequency analysis was a Tinsley pneumatic sine-wave generator which had been discarded by an industrial user and rebuilt by the writer. It consisted of a small variable speed electric motor driving a sine-wave potentiometer, also the recorder chart, through a reduction gear box. The electrical signal from the sine potentiometer was fed through a coupling unit to an electro-pneumatic converter and thence to a plant regulating unit. The output pressure was recorded on one pen of a two-pen recorder, the remaining channel being used to record the plant response. As the chart is driven at the same speed as the potentiometer the sine waves produced always have the same length whatever frequency is used.

6.2.2 The experimental procedure

To make a run the system was brought to steady state at the desired mean value by applying a constant air pressure to the appropriate control valve. The process analyser was adjusted to apply a sinusoidal air signal of the chosen frequency and suitable amplitude about the mean value; when stabilised this output signal was then applied to the control valve. The process analyser recorded the test signal and the system response, the record being continued until the transients had disappeared and three or four identical cycles had been recorded. The procedure was repeated for a range

of frequencies, and at a very long period to allow subsequent normalisation.

The phase lags and attenuations were determined by direct measurement from the chart.

The main concern in the analysis of evaporator dynamics is with the response of product density to variations in feed flow rate, feed density, and temperature. Experimentally it is easier to measure the frequency response of product density to feed flow, mainly because of the difficulty of causing the other two input parameters to oscillate sinusoidally.

Since the laboratory lacked suitable instrumentation to monitor product density continuously some runs were made in which the product concentration was determined conductimetrically, the results being compared with the recorded fluid exit temperatures. The agreement was close enough, in terms of trend, to lend support to the idea that the temperature of the fluid leaving the heating tube would determine the extent of vapour formation in the flash vessel and thus the product concentration. Accordingly the fluid exit temperature was recorded throughout the experiments. Experimentally-derived frequency response plots are presented for product temperature as a function of steam supply rate and feed flow rate.

The other main independent variable in the system is the product flow rate. The frequency response of this variable was not determined because of experimental difficulties.

In any case, as mentioned previously, level control is almost mandatory in evaporators for stable operation. Throughout these experiments the level was maintained constant by modulating the product withdrawal rate. This coincides with the usual operating arrangement. Generally this control loop will not affect the product density so long as the liquid continues to boil, and the tubes do not become uncovered, or the evaporator flood. The level control loop should correct for the latter two eventualities. If desired the response of the product flow may be calculated analytically or determined on the simulated system. Results are presented that were obtained by simulation.

6.2.3 Results and discussion

6.2.3.1 Shell-side dynamics

Attempts were made to determine the response of the steam flow rate resulting from a change in steam pressure, and to determine the vapour boil-up in response to variations in steam flow rate.

The steam condensate flow rate was monitored by weighing it. For this series of tests the evaporator was operated under thermosyphon conditions. The experimental data are tabulated below.

Table 5: Experimental data for vapour flow response to steam flow rate variations

ω (radians/sec)	Attenuation (dl)	Phase lag (degrees)
0.45	0.33	-85
0.71	0.23	-98
1.10	0.13	-105
1.60	0.06	-105
3.10	0.03	-108

The vapour rate was determined in a similar fasion by weighing the process liquor condensate. These measurements are probably not very accurate although liquid hold-up was minimised as much as possible. The experimental results are presented in the following table.

Table 6: Experimental data obtained for steam flow response to steam pressure variations

ω (radians/sec)	Attenuation (dl)	Phase lag (degrees)
0.45	0.83	-14
0.57	0.80	-18
0.71	0.71	-33
0.81	0.67	-37
1.10	0.56	-44
1.6	0.45	-52
3.1	0.25	-59
4.5	0.25	-60
5.7	0.146	-57
7.0	0.12	-60
8.0	0.11	-58
10.0	0.10	-56
12.5	0.095	-51
20.0	0.069	-47
35.0	0.05	-36

By considering these results it is possible to examine the effects of two important factors, namely the heat flow into the jacket wall and variations in the liquid-side heat transfer coefficient, both of which probably have a similar effect on the frequency response.

Variations in steam pressure lag changes in the valve stem position because of the vapour volume in the shell and the capacity of the shell wall. However as far as could be determined by observation of the shell temperature and pressure the lag following a step change in valve stem position was less than a second.

Some idea of the relative importance of this time constant can be gained by writing an approximate energy balance for the shell and tube,

$$(C_v + C_w + C_{sh}) \frac{d\theta_s}{dt} = (K_v \bar{F}_s \lambda)x - UA(\theta_s - \theta_f),$$

where,

C_v, C_w, C_{sh} = thermal capacity of vapour, tube wall, and shell respectively,

and the other symbols have their usual meanings. If it is assumed that the shell and wall temperatures are the same as the steam temperature, the error introduced by this assumption can be calculated readily by substituting experimental values if desired, and the temperatures are regar-

ded as deviations about their steady-state values, the expression can be transformed and rearranged to give

$$(\frac{C}{UA}\, s + 1)\theta_s = (\frac{K_v \bar{F}_s \lambda}{UA})x - \theta_f.$$

That is, considering only the dynamic relationship between the steam temperature and valve position, since the steam flow, F_s, depends only on valve position where the flow is critical, we have

$$\frac{\theta_s}{x}(s) = \frac{K}{\tau s + 1}$$

where $K = (\frac{K_v \bar{F}_s \lambda}{UA})$

$$\tau = \frac{C}{UA}$$

and $C = C_v + C_w + C_{sh}$.

For the experimental evaporator with steam at 26 psia the mass of steam in the shell is,

$$M = \frac{\text{volume of shell}}{\text{spec.vol.steam}} = \frac{0.49}{15.72} = 0.0312 \text{ lb.}$$

The vapour capacity is then,

$$C_v = \frac{M}{P}\lambda\,(\frac{\partial P}{\partial \theta_s}) = \frac{0.0312}{26} \times 951.1 \times 0.46$$

$$= 0.53 \text{ Btu/}^{\circ}\text{F.}$$

where $\bar{P}$ = mean pressure of steam in the shell. The tube capacity $C_w = 0.41$ and the shell wall capacity $C_{sh} = 7.8$ Btu/$^{\circ}$F. Thus the time constant $\tau = 0.04$ seconds where $U_o = 1435$ Btu/hr ft^2 $^{\circ}$F. Even if this approximate value is only one-tenth the true value, the time constant involved is

negligible compared with other time constants in the system.

One point that does emerge from the above discussion is that there is appreciable thermal energy storage capacity in the shell wall, particularly with small exchangers. However the shell response has little effect on the exchanger dynamics because the shell capacity is in parallel with the tube and fluid capacities. Catheron et al[6] showed that a ten-fold change in the assumed time constant for the shell produced only a 30-50 per cent shift in the frequency response curves.

The time constant for vapour hold-up in the shell depends on the rate of condensation. It will therefore be affected by variations in the liquid-side heat transfer coefficients. This dependence has been the basis of a number of experimental studies using the Wilson plot[48] approach. Where heat is supplied from a condensing vapour however the unsteady-state is largely self-regulating. For instance, an alteration in the heat transfer coefficient will change the wall temperature and thus the driving force from hot fluid to tube wall. The heat flux changes and a new steady state is established. This leads to smooth operation even in the transition region of boiling.

The attitude of the exchanger is also important. For example the upper portion of an insulated exchanger may have a thin film of condensate and a small time constant. Should the film evaporate following a drop in steam pressure dry wall conditions result with a decrease in the transfer coefficient and thus the response. Meanwhile the lower portion of the shell may be flooded with condensate.

The comments made about the shell response could also apply to transfer across the tube wall if conditions are such that there are transient dry-wall conditions. This makes it imperative to have a subsidiary control loop on the steam supply.

It is difficult to make any positive assertion based on the experimental results. At low frequencies the jacket wall behaves approximately as a single exponential transfer stage. However the increasing scatter with increasing frequency may indicate that the jacket wall no longer maintains equilibrium with the steam, which may be due to the development of an appreciable film resistance. It will be observed from the tabulated data (Table 6) that the phase angle increases at first but eventually begins to decrease with increasing frequency, suggesting the presence of both a pole and zero in the appropriate transfer function.

The only explanation which can be advanced is that the shell wall represents a significant side capacity in this installation.

6.2.3.2 Product liquor response to feed temperature disturbances

The response of the fluid outlet temperature to changes in feed temperature was not examined experimentally. However the theoretical results may be summarised as follows. Resonance occurred at all fluid flow rates, initially at normalised frequencies in excess of 5-6 radians, but was not fully established until about 50 radians. Resonance was established more slowly at lower flow rates and the amplitude of oscillation increased with increasing flow rates. In each case the first peak appeared in the phase lag curves slightly earlier than in the amplitude curve. The phase curves tended to oscillate about a mean phase angle of -160^{o}. Figures 6 - 9 are a selection of the theoretical results.

6.2.3.3 Product liquor temperature response to steam temperature disturbances

The response of the effluent liquor temperature to sinusoidally-forced steam flow was determined over the range of fluid flow rates considered theoretically. A selection from the results is presented in Figures 10 - 14 which compare experimentally-determined points with values calculated

using equations (2.13) to (2.15).

The experimental values show general agreement with the theoretical curves, although the latter show the expected resonance peaks more strongly than the experimental results. This suggests that the distributed-parameter characteristic is not as strong in practice as was assumed during the development of the transfer function.

Examination of the experimental results shows that the flow rate must exceed a certain value, about 2 ft per second, before the peaks appear. In addition when the flow rate exceeds about nine ft per second the peaks become less pronounced again. In all cases resonance is more marked in the phase curves than in the attenuation curves.

The larger flow rates tend to be in the range usually recommended[7] in evaporator operation to minimise the risk of solids deposition in the tubes. It may also explain why the phenomenon of resonance does not seem to have posed any problems in industrial practice. There is the added advantage that operation at very low or very high flow rates tends to avoid the instabilities attendant on operation in the slug flow regime.

6.2.3.4 Response of product fluid temperature to feed flow rate disturbances

Experimental results were obtained over a wide range of flow rates varying from approximately 1-11 fps. A representative set of results is presented with the corresponding theoretical curves in Figures 15 - 18. The theoretical values were calculated on the basis of equation (1.15) which retains the distributed-parameter characteristic of the exchanger section. An energy balance yields differential equations with variable coefficients in the case of flow disturbances. Computers are useful in treating these equations, but some assumptions must be made in order to obtain a solution. In particular the equations involving the flow disturbance effects must be reduced to constant coefficient equations to apply frequency response techniques. The procedure used in calculating the theoretical values was to estimate the heat transfer coefficients corresponding to each mean feed flow rate studied. These values were assumed to be constant for the sinusoidal oscillations about each mean value. This seems reasonable in view of the conclusions reached by Hempel.[16]

The data presented cover a ten-fold change in process fluid flow rate. Agreement between the experimental and theoretical values is reasonably

good for both the amplitude ratio and phase lag, the match with the amplitude ratio curve being good up to a normalised frequency of approximately 5 radians. The deviation begins slightly earlier in the case of the lowest flow rate (1.11 fps) but the fit prior to the first resonance peak improves with increasing flow rate. The phase lag points show more deviation from the theoretical results, but even here the fit is better with increasing flow rate. With the exception of the highest flow rate presented (9.97 fps) the phase points are indicative of the sudden changes exhibited by the theoretical curves, the effect being clearer at the intermediate flow rates.

The divergence between the measured and predicted attenuations at the lower flow rate may be due in part to mixing dynamics in the process fluid. The fluid near the centre of the tube may move faster than that in proximity to the wall. Should there be an axial sinusoidal distribution of temperature along the tube wall the faster moving fluid near the centre would tend to "smear out" the distributed waveform. If this effect is real it would be expected to become more pronounced at slower flow rates, increasing frequency of oscillation, or decreasing Reynolds number, and could

be expected to be more significant in its effect on magnitude ratio than on the phase angle. These features are consistent with the observed results.

Although the flow forcing gave rise to the anticipated resonance effect it was not very evident at 1.11 fps, was quite distinct at intermediate flow rates, and was very slight at 9.97 fps. This suggests a limited flow range within which resonance may be observed with the experimental apparatus used in this study.

The relatively slight effect at the lower flow rate may be attributable to the fluid dynamics effect referred to above but the same observation may be expected on the basis of Law's discussion[23] of resonance where we note that the delay term may be written as cos $\omega L/v$ - i sin $\omega L/v$, and since the sine and cosine terms repeat at multiples of 2π this is the factor which causes the periodicity in the occurrence of resonance peaks. However with longer heat exchanger tubes or lower flow rates the D-V lag becomes less important since e^{-x} tends to zero as x becomes larger. This probably explains the virtual absence of resonance peaks at the lower flow rates examined experimentally, while at the higher flow rates the occurrence of amplitude ratio resonance is delayed to fre-

quencies which are not readily achieved experimentally.

There is another feature which merits comment. Analytical solutions predict peaks at additional frequencies. However these are minor compared with those predicted by the D-V lag and possibly arise from temperature reflections at higher-order terms in the mathematical approximation.

Because resonance occurs when $\omega L/V = 2n\pi$ (with consistent dimensions) for either steam or flow rate disturbances the resonant frequencies may be predicted from the physical parameters of the system involved. Thus for any average fluid flow rate, disturbances in either steam temperature or process fluid flow rate give resonance peaks at the same frequencies and neither wall capacitance nor heat transfer coefficient variations have any effect. However it has been noted[45] that inclusion of wall capacitance in the theoretical model softens the dip in the amplitude curve due to resonance and the omission of variation in the heat transfer coefficient softens it still further.

6.2.4 Accuracy of frequency response measurements

It is difficult to make a quantitative estimate of the accuracy of the frequency response results. At any time the accuracy depends upon the variable being examined, particularly with respect to the "noise" component, and the frequency of oscillation. The frequency is important because the attenuation increases as the frequency increases, thus reducing the accuracy. The signal-noise ratio depends on the nature of the variable. For example, pressure measurements usually yield smooth traces while flow measurements are usually noisy. The records of the effluent liquid temperature measurements were difficult to interpret in some runs, probably because of the release of slugs of vapour as the pressure on the heated liquid column was reduced near the top of the tube.

From a comparison of the theoretical and experimental results for the steam-forced trials it would seem that the accuracy of the attenuation values, neglecting resonance, would be in the order of 10-15%, whereas for the flow-forced case the accuracy was possibly around 20%. The phase lag results were a little better in each instance.

On a semi-quantitative basis it is reasonable to say that the results obtained confirm the validity of the theoretical model.

7. EVAPORATOR BEHAVIOUR WITH ALTERNATIVE CONTROL SCHEMES

7.1 Introduction

One of the main objectives of this study was to examine the behaviour of evaporators using alternative control schemes. Although it is possible to calculate the response of a system to any desired forcing function once the transfer function has been derived, it is difficult to take account of the interactions arising in the case of a multiloop control system.

In addition, once a theoretical model has been shown to represent the behaviour of a system adequately it is considerably quicker and simpler to use one of the simulation techniques to investigate the response to a range of input disturbances, or the behaviour with any of a number of possible control schemes. The techniques are applicable to linear or nonlinear systems or to systems having D-V lags. However analyses of systems involving nonlinearities are unique to the particular case, if generality is sought a linear, or linearised model, is necessary.

In studying practical systems we find that many are nonlinear in that they cannot operate linearly with large magnitude control signals. Often such limitation arises from the saturation of a controller amplifier or of the final control element. The transient response of a nonlinear system may still be calculable using one of the time-domain methods. However there is no general solution for the nonlinear vector differential equation although some particular solutions have been recorded. For higher than second-order systems no general answer is available and each

problem must be analysed separately.

This lack of generality, in terms both of methods of solution and application of the results, is one reason why many published studies still use linearised models, and as mentioned earlier the majority of these accounts have concluded that such models provide sufficient information about the performance of actual systems, at least for general design and control purposes. It is, of course, necessary to establish that the linearised model is adequate for the proposed application by comparison with a more exact model. Comparison of the theoretical frequency response results for the approximate model with those obtained experimentally shows that, ignoring the resonance peaks, the approximate model could be used to examine the system performance with the alternative control schemes. This model was therefore used as the basis of the simulation experiments.

The simulations described were carried out on different computers at different stages of the study depending on availability. Thus the results presented earlier by Andersen et al[1] for an internal calandria evaporator were examined and extended using a Solartron SC-30 analogue computer and later PACE machines. The early work on the forced-circulation evaporator was performed on a pair of PACE TR-10 analogue computers ganged together, but the bulk of the simulation of this evaporator was carried out digitally using the CDC-6400, the model being extended to include the D-V lag involved in the passage of liquor through the tube.

Figure 19 shows a block diagram of the evaporator and Figure 20 the circuit used on the Solartron machine. Because the PACE computers had a 10 V reference compared with 100 V on the Solartron, and fewer available amplifiers, the circuit was revised, the amended version appearing in Figures 21 and 22.

The parameters used to calculate the equation variables for the standard evaporator were those reported by Andersen et al,[1] while those used for the forced circulation evaporator describe the equipment constructed in this laboratory. The parameters for the experimental apparatus are listed in Appendix A.

A general discussion concerning the control of evaporators has already been presented. Mention has been made of the fact that level control is almost mandatory, and a level control loop forms part of every simulation. Level control can be effected by regulation of either feed flow rate or product withdrawal rate. Both possibilities are examined alone and in association with other loops.

The process variable of concern is the product density. This may be controlled by manipulation of feed flow rate, product withdrawal rate or the steam supply. Each possibility is investigated in conjunction with both level control loops.

Auxiliary control loops govern pan pressure, feed temperature, and steam supply pressure. In the case of the pan pressure, control may be effected by regulating the flow rate of cooling water to the condenser, or by varying the rate of bleed-off of noncondensables, or less certainly, the vacuum drawn by the steam ejector or vacuum pump. If the latter approach is used,

better control results from controlled admission of air than by other methods. If a barometric leg forms part of the apparatus the storage tank level might provide an alternative means of controlling the pan pressure. Except where pan pressure disturbances were introduced to determine the response of the output variables such as density, the pan pressure was held constant. This is equivalent to assuming a completely effective auxiliary control loop.

The latter comment also applies to the feed temperature and steam supply rate, both of which would have their own separate control loops apart from the evaporator. Control of feed temperature involves the control of a feed preheater, whose dynamic behaviour will be similar to that of any comparable heat exchanger. Indeed many of the statements made about the heating section of the forced circulation evaporator apply with equal pertinence to the preheater. However the feed preheater is not considered in the model or in the simulation study of the evaporator. Steam supply pressure is usually effected by some kind of non-indicating regulator and is not further treated in this study.

To facilitate comparison of the alternative control systems step disturbances were introduced into the various input variables and the effect observed in the response of product density, product withdrawal rate, and pan level. The same magnitude of step disturbance was made in each case, namely 10% of the theoretical maximum value used in scaling the computer equations.

Figure 23 shows the basic controller configurations that may be used in general industrial practice and are in fact those used earlier by Andersen et al.[1] Figures 24-26 are block diagrams for the controller arrangements referred to as Cases 3, 4 and 5 respectively.

The action of the various controller arrangements will be discussed further but it may be appropriate to comment here concerning the feedforward-feedback configuration. Control of product density is likely to be affected adversely when a composition analyser is used, because the analyser introduces a time delay in the feedback loop. This generally means that a lower controller gain must be used to ensure stability. It was expected that the addition of feedforward control to the usual feedback control might make the analysis delay less critical and allow the use of higher gain controllers. To facilitate comparison between systems the controller settings were adjusted to keep the loop gains approximately equal.

7.2 Analogue Computer Simulation

The system equations cannot be used directly for study by the analogue computer but the nature of the equations actually used can be illustrated by listing those developed to simulate the standard evaporator.

$$[5\tilde{\theta}_o] = 1.33\ [50\tilde{\rho}_o] + 0.0444\ [2\tilde{p}_e] \tag{6.1}$$

$$[10\tilde{\theta}_s] = 0.395\ [10\tilde{\theta}_t] - 0.595\ [100\tilde{\eta}_1] \tag{6.2}$$

$$s[10\tilde{\theta}_t] = -9.52\ [10\tilde{\theta}_t] + 7.15\ [10\tilde{\theta}_s] + 6.27[50\tilde{\rho}_o] + 0.21[\tilde{p}_e] \tag{6.3}$$

$$s[50\tilde{\rho}_o] = -0.06\,[50\tilde{\rho}_o] + 0.014\,[10\tilde{\theta}_t] - 0.0031\,[5q_i] + 0.0081\,[2\tilde{\theta}_i] + 0.02\,[50\tilde{\rho}_i] + 0.61\,E(s)\,[2\tilde{p}_e] \quad (6.4)$$

$$7.38s\,[50\tilde{\rho}_o] + s\,[20\tilde{v}_3] = -0.149\,[50\tilde{\rho}_o] - 0.333[2\tilde{q}_o] + 0.177\,[50\tilde{\rho}_i] + 0.107\,[5\tilde{q}_i] \quad (6.5)$$

$$[2\tilde{q}_o] = 0.0836\,[50\tilde{\rho}_o] + 0.121\,[2\tilde{p}_e] + 0.0128\,[20\tilde{v}_3] - 1.35\,[200\tilde{\eta}_2] \quad (6.6)$$

$$[5\tilde{q}_i],\ [200\tilde{\eta}_2] = \frac{Kg1}{C_1}\,\frac{(1 + 30\tau i_1 s)}{30\tau i_1 s\,(1 + 0.25s)}\,[20\tilde{v}_3] \quad (6.7)$$

where $C_1 = 4,\ 0.1$ respectively.

$$[5\tilde{q}_i],\ [200\tilde{\eta}_2],\ [100\tilde{\eta}_1] = \frac{Kg_2}{C_2}\,\frac{(1 + 30\tau d_2 s + \frac{1}{30\tau i_2 s})}{(1 + 0.25s)}\,[50\tilde{\rho}_o] \quad (6.8)$$

where $C_2 = 10,\ 0.25,\ 0.5$ respectively.

The time scale chosen in this work was 1 hour real time = 30 seconds machine time.

As mentioned earlier the output variables of interest in this work are the product density and product flow, particularly the former. The relationships between these and the input variables are defined by the transfer functions. The development of the analogue computer circuit involves the selection of such of the reduced equations as are necessary to generate the terms occurring in the transfer functions.

The steam side of the system could be represented by the reduced equation (4.2), but where it is assumed that the steam space time constant (τ_1) may be neglected compared with the other time constants, (4.3) would be the equation simulated.

Since this equation generates $\tilde{\theta}_s$ and $\tilde{\theta}_t$ it is more convenient to rearrange equation (4.4) in terms of these variables rather than those previously used. However this is not strictly necessary.

The principal input variables required to generate equation (5.1), the product density response, can be derived by simulating either equation (4.5), the heat balance, or equation (4.6), the mass balance on the solute, since both equations involve the variables of interest. Equation (4.6) was used after preliminary treatment giving

$$\tau_o \, s \, \tilde{\rho}_o + j \, s \, \tilde{v}_3 = - \tilde{\rho}_o - j \, \tilde{q}_o + h \, \tilde{\rho}_i + i \, \tilde{q}_i$$

and this is the equation simulated, together with (5.1) the product density transfer function, and (5.4) the product flow transfer function.

It is necessary to scale these equations before setting-up the analogue model, so that the variables reach as large values as possible without saturating the amplifiers. The following voltage scale factors were used.

$[2p_e]$, $[2q_o]$, $[2\theta_i]$, $[5q_i]$, $[5\theta_o]$, $[10\theta_s]$, $[10\theta_t]$, $[20v_3]$, $[50\rho_i]$, $[50\rho_o]$, $[100\eta_1]$, $[200\eta_2]$.

Time scaling was effected by taking 30 seconds machine time equivalent to 1 hour real time.

Substituting the plant parameters and equation constants and using the above voltage and time scaling factors the analogue equations (6.1) to (6.6) are obtained. These six equations suffice to simulate the evaporator with equations (6.7) and (6.8)

representing the controllers etc. In the basic study there were two controllers, a density controller and a level controller. The controllers were simulated along conventional lines, the level controller as a proportional plus integral action controller, and the density controller as a three-term controller. The measuring elements were simulated as first-order transfer lags at the controller inputs, and the control valve gains were taken into account in computing the controller settings.

Although specific controller settings were used during the simulation experiments no attempt was made to establish controller settings which could be applied to a particular system. Partly this was because our interest was in the development of a general model, but partly it arises from the fact that the computer is virtually free from the random noise which may occur in the process. Therefore it should be possible to operate an analogue at a higher gain and shorter derivative action time than is practicable on the plant. The slow components on the plant act as filters where derivative action is concerned, making large derivative action times necessary. In contrast, during an experimental examination of the effect of derivative action on the simulated model it was actually found to be undesirable, despite the fact that it was apparently thought necessary on the industrial evaporator studied by Andersen.

Potentiometers on the outputs of the controllers are set to give the ratio $\frac{V_1}{V_o}$. Thus considering the level controller, in Cases 3 and 4 where the product offtake valve is positioned by

the controller, the ratio is 0.1; while in Cases 5 and 6, in which the feed flow is regulated, the ratio is 4. In the case of the density controller the ratios are 10, 0.25, 0.5 respectively, for the experiments in which the manipulated variables are the feed flow rate, product withdrawal rate, and steam flow.

To facilitate comparison the response curves were plotted as positive quantities wherever practicable. Also the scales of the plots were kept as uniform as possible, but some variation was necessary, and the scale factors actually used are indicated on the plots.

7.2.1 Results and discussion

It was proposed to confirm the results published by Andersen et al[1] and to extend the study to examine the responses to other disturbance variables. Table 7 summarises the systems studied, the controller constants, the nominal valve constants, and the disturbances introduced in each case. The starred disturbances are the ones cited in Andersen's paper, the others were added to complete the picture. Although Andersen varied the size of the input disturbance it was considered better on the basis of preliminary trials, to standardise on a step disturbance of 10 volts, which is equivalent on the machine used to an upset of 10% of the scaled magnitude for the variables feed density, feed flow, and steam condition.

Any values mentioned in the following discussion are deviations from the steady-state values.

TABLE 7 : Summary of Controller Configurations used in initial simulation

Case	Controller Arrangement	Controller Constants	Valve Gain	Disturbance Variables
1	Level controller regulates product flow.	$K_{g1} = 62.3$ $\tau i_1 = 0.8$ hr	$C_1 = 0.1$	$\rho_i^* = 0.18$ $q_i^* = 1.8$ $\eta_1^* = 0.18$
2	Level controller regulates feed flow.	$K_{g1} = 57.5$ $\tau i_1 = 0.8$ hr	$C_1 = 4$	$\rho_i^* = 0.2$ q_i $\eta_1^* = 0.2$
3	Level controller regulates product flow. Density controller regulates feed flow.	$K_{g1} = 62.3$ $K_{g2} = 22$ $\tau i_1 = 0.8$ hr $\tau i_2 = 0.2$ hr $\tau d_2 = 0.033$ hr	$C_1 = 0.1$ $C_2 = 10$	$\rho_i^* = 0.2$ q_i $\eta_1^* = 0.18$
4	Level controller regulates product flow. Density controller regulates steam flow.	$K_{g1} = 62.3$ $K_{g2} = 22.5$ $\tau i_1 = 0.8$ hr $\tau i_2 = 0.2$ hr $\tau d_2 = 0.033$ hr	$C_1 = 0.1$ $C_2 = 0.5$	$\rho_i^* = 0.2$ q_i η_1

TABLE 7 : Summary of Controller Configurations used in initial simulation Cont..

Case	Controller Arrangement	Controller Constants	Valve Gain	Disturbance Variables
5	Level controller regulates feed flow. Density controller regulates product flow.	$K_{g1} = 57.5$ $K_{g2} = 74$ $\tau i_1 = 0.8$ hr $\tau i_2 = 0.2$ hr $\tau d_2 = 0.033$ hr	$C_1 = 4$ $C_2 = 0.25$	ρ_i q_i $\eta_1^* = 0.2$
6	Level controller regulates feed flow. Density controller regulates steam flow.	Various settings tried.	$C_1 = 4$ $C_2 = 0.5$	ρ_i q_i η_1

7.2.1.1 Case 1

The results obtained are similar to those obtained earlier and are illustrated in Figures 27 and 28. It will be seen that the product density responses are essentially those of first-order transfer stages, thus lending weight to the statement that the calandria wall time constant is insignificant relative to the other, which involves the volume-throughput and the feed-product concentration ratios. In addition the final steady state magnitudes for the density responses to feed flow and steam disturbances are similar and much smaller than to feed density disturbances. In view of the fact that the perturbed variable is feed density this seems reasonable.

The pan level behaviour was not reported by Andersen. It could be anticipated that the level would show variations that reflect the rapid oscillation which occurred in the product flow responses immediately following the step changes in input. The small magnitude of any change and the gradual recovery emphasises the smoothing action of the evaporator capacitance and the small time lag in the level control loop. It should be noted that the product density responses to steam and feed disturbances are essentially open-loop in form and are unaffected by the level controller.

Thus to summarise the system behaviour observed with the single control loop connecting level and product flow, we can say:

(a) following a feed flow disturbance the system returns to equilibrium at a new product flow rate, the product density responds in open-loop fashion, the level is scarcely affected.

(b) a feed density disturbance is uncorrected; the product flow response occurs because of a change in the vapour rate. There is a brief oscillation which is damped out as the level controller takes over, until ~~finally~~ equilibrium is restored at a new level and of course flow rate. The two responses should be similar in form, as indeed the curves show.

(c) a steam supply change, say a sustained increase in steam temperature, causes the level to drop and the density to rise, the controller action reduces the product flow thus restoring the level but the product flow remains low and the product density high.

7.2.1.2 Case 2

The original paper only presents two results, the responses for product flow and density following disturbances in feed density and steam supply. The present results are similar to those reported.

It is useful to compare the results obtained with the Cases 1 and 2, since both involve control with a single level controller operating on product and feed flow respectively. Considering product density we see that the settling times and offset are similar following either feed flow or feed density disturbances, but Case 2 gives less offset after a density disturbance. However after a steam disturbance, Case 1 shows less offset than Case 2, although the latter recovers marginally faster.

As might be expected there is more difference between the responses to a feed flow change. This is hardly surprising, since in Case 2 such a forcing function amounts to the imposition of a step change on the control valve setting, which is analogous to introducing a shift in the set-point. For a feed flow change, Case 1 shows a smaller offset but similar settling time to Case 2, but an initial oscillation is present that is absent from the second case. Following a feed density change Case 2 shows a shorter recovery time and an offset about 60% that of Case 1. The most marked difference follows a steam valve change when Case 2 has a settling time about one-third, and a deviation about 15%, that of Case 1.

Level responses were not reported in the earlier study. It can be seen from the curves that a feed flow disturbance in Case 2 leads to a wider initial deviation accompanied by a small oscillation and followed by a longer recovery time than previously. For a feed density change Case 2 is superior, there being little upset and negligible settling time in contrast to the slow recovery in Case 1. Case 2 is scarcely affected by steam disturbances.

To sum up then, we can say that if disturbances are likely to arise in the steam supply or feed density and particularly if constant product density is important, the level should be controlled by regulating the feed flow. On the other hand if constant product flow is wanted, for instance to maintain supply to a following process, then the level should be maintained by regulating the product flow.

7.2.1.3 Case 3

The results presented in Figure 29 are similar to those reported earlier except that the latter are more lightly damped, the maximum values for the response of product density and flow to a feed density change are reached in 15 and 18 minutes respectively. These results do not compare with the results obtainable by calculation and some

error must have crept into the earlier study.

Another feature merits comment. Following a change in feed flow the product flow curve displays some initial high frequency oscillation which gives way to the more usual long period damped wave. No explanation can be offered for this unless the sudden change in flow causes a transient pressure disturbance.

The responses to a steam flow disturbance are similar with the exception that the "chatter" does not occur.

7.2.1.4 Case 4

Only one result is reported by Andersen, the response of product flow and density to a step change in feed density. The results reported are of the general form that might be expected except for two features, the dead-beat return to the base line of the density curve and the fact that the curves reach their maximum values after about 10 minutes (ρ_o) and 23 minutes (q_o). As with the previous example these peak values seem to occur too early in view of the time constants involved in the evaporator. For example the residence time is 1.65 hours.

The results obtained here (refer Figure 30) for a feed density disturbance show a normal kind

of transient response for an underdamped second-order system with the peak values occurring after 40 minutes (ρ_o) and one hour 10 minutes (q_o) respectively. In addition there is some slight offset when the product flow is finally stabilized.

The remaining results are of the form expected from the transfer function.

7.2.1.5 Case 5

In this case Andersen et al[1] report only the responses to a change in the steam valve setting. Their results show a very short period oscillatory response, the periods of oscillation being about 11 minutes for the product density and approximately 7 minutes for product flow. The peak values occur after about 4 minutes in each case and the settling times are about 24 and 21 minutes respectively. Other than the fact that one can expect the responses to be oscillatory because of interaction between the loops these results are surprising, even allowing for the relatively short time lags in the two control loops.

Figure 31 shows that the responses to feed density disturbances or a steam valve change is a slightly damped sine wave with a period of about 70 minutes which seems more realistic.

With this controller arrangement there is marked interaction between the controller loops, a change in the output of the density controller initiating a sequence of operations involving both loops. This process of interaction is sometimes beneficial in making a system more responsive. More generally though it causes oscillation and makes the system unstable, or restricts the range of useful controller settings. An instance of interaction affecting evaporator operation has been mentioned already.[17]

7.2.1.6 Case 6

No results were reported by Andersen et. al. who claimed that the system seemed to be unstable when first examined, but stated that subsequent trials had indicated that it might be stabilised with difficulty.

The present trials showed (Figure 32) that the controller settings were somewhat critical but that the system could be stabilised.

7.2.1.7 Response to pressure disturbances

To complete the examination of the standard evaporator while it was modelled on the analogue computer the response to pressure disturbances, and the possibility of using cascade, or feedforward systems, was examined. This section deals with

pressure changes. To study these the circuit was revised as described earlier.

Insight into the behaviour of an evaporator subject to transient pressure disturbances might be obtained from consideration of steam generators. Observation soon suggests that the level of liquid indicated in the gauge glass is not a true indication of the level in the steam generator. This is most evident if steam generation is halted suddenly, for the indicated level falls. The reason is that the generation of bubbles of steam below the liquid surface and their rising to the steam space produces a swell during steam generation which collapses when generation is halted. The same mechanism operates when a sudden demand for steam is made.

Analogously, when a pressure decrease occurs in an evaporator, the drop in pressure causes a large amount of water to flash into steam which surging up through the body of fluid raises the level in the gauge glass even though the feed rate is less than the steam output. The apparent increase in level causes the controller to reduce the feed rate when what is really needed is an increased feed rate to restore the balance. This incipient instability is aggravated if the feed is relatively cool, since this causes an increase in the number of steam bubbles below the surface and thus an

increase in the apparent level. As conditions become stabilised the level drops rapidly since more water is leaving the system as steam, than is entering as feed. While this is not likely to be serious in an evaporator it could be serious in high pressure boilers.

Once the level controller senses the drop in level it opens the feed valve admitting fresh solution. The admission of relatively cool feed solution now causes the collapse of some of the steam bubbles below the surface, causing the liquid level to drop at a greater rate for a short time. Thus a change in boil-up rate initiates a cyclic disturbance in the feed flow rate which is reflected in the oscillatory record. This probably accounts for the observation reported in 7.2.1.3. The relatively large capacitance of evaporators tends to damp out these oscillations. However, it is not difficult to visualise systems where the incipient instability may be undesirable.

It seems necessary, especially when a level controller is used to regulate the feed flow rate, to ensure that the feed enters at the boiling point and to guard against fluctuations in evaporator pressure which will alter the boil-up rate, and similarly against undue variations in the steam supply. The above discussion is equally pertinent

as we consider the transient behaviour of the evaporator following pan pressure disturbances.

The experimental programme was restricted to the multiple controller systems previously identified as Cases 3 - 6. In each instance a stepwise reduction in pressure equal to ten per cent of the steady state value was imposed and the responses of product density and product withdrawal rate recorded. The recorder scale factors are indicated on the graphs. The time scale factor was constant for all cases, namely three inches represent one hour on the original charts.

Comparing the four cases (Figures 33-36) it seems that Case 3 is superior in terms of product density response, there being a minimum of off-specification material produced and the recovery times are shorter for both output variables. However there is a substantial increase in product withdrawal rate.

7.2.1.8 Cascade control schemes

Cascade control schemes are effective if the inner loop is much faster than the outer loop and if the main disturbance affects it first. Three possible arrangements suggest themselves.

(a) using the product density signal to modulate the input to the level controller,

(b) using the level signal to modify the input to the density controller,

(c) using the product flow to modify the input to the density controller.

In each case the basic controller configurations of Cases 3, 4, 5 and 6 can be used. Each of the above schemes was simulated on the analogue computer and the results are recorded as Cases 7, 8 and 9. Thus Cases 7-3, 7-4, etc. represent the basic Cases 3 - 6 modified by using the product density to change the input to the level controller, and so on.

The results for Case 7 are presented in Figures 37-39. The results obtained for Cases 8 and 9 are similar except for minor differences in level response and they are not presented. Comparison of the Case 7 results with their counterparts using conventional control schemes shows only minor differences.

Another controller configuration which can be grouped with the cascade schemes is one which uses the density controller to regulate the product withdrawal rate and the level controller to adjust the feed and modify the set-point index of the steam supply controller. The direct control of the steam supply by the level controller is usually

criticised as placing more emphasis on the maintenance of the liquid level than on securing the desired concentration. However, the proposed arrangement has the advantage of reducing the magnitude of the lag in the steam loop while making the principle process variable, i.e. product density, the means of controlling the residence time in the evaporator. Any surges in feed flow are compensated fairly rapidly by the level controller, while the level-steam supply loop should reduce the reaction time following pressure disturbances, because the pan pressure depends on the amount of vapour present and this is affected directly by the heat input rate.

The response curves obtained are shown in Figure 40 and indicate that this system provides better control than any previously considered, in terms of reduced stabilisation time. However, there is a permanent change in outflow following a disturbance. This is not likely to matter where product density is of primary concern. If a constant flow is needed to a subsequent process a surge tank may be used.

With the exception of this particular configuration, which would seem to merit plant trial, the conclusion reached is that cascade control offers little advantage over conventional schemes for the control of a standard evaporator.

7.2.1.9 Feedforward-feedback control

If a process has a large time constant and feed conditions subject to change the possibility of using feedforward control seems attractive, particularly if the main load variable is not controllable directly. However, to use feedforward control effectively the transfer functions need to be known accurately and the dynamics need to remain constant, or be susceptible to continuous correction to compensate for changing process conditions.

The principal input variables in the evaporator are feed flow, feed concentration, and feed temperature. Because of the dead time associated with changes in concentration or temperature, it seemed best to postulate any feedforward control on manipulation of the feed flow rate. Cases 3, 5 and 6 all have control loops operating on the feed rate. Several other factors should be considered. The controllers used in the simulation are based on linear models. They will be effective for small excursions about the steady state values of their inputs and the maximum variations they could handle would need to be established experimentally. Further, with pure feedforward control, any dead time in the measuring elements or control valves would call for predictive actions which could not be realised physically. Finally, there is the

possibility, referred to above, of changing process conditions such as the evaporator tubes becoming fouled and changing the transfer rates. These problems call for some kind of trimming action and this is provided by the feedforward-feedback combination, the latter compensating for the unpredictable variations and possibly for the nonlinearities in the system elements.

Several possible systems were investigated, each of them being some modification of the basic cases 3 - 6. The response curves are illustrated in Figures 41-45, the controller configurations being indicated in each instance.

From the diagrams it appears that the modified Case 3 arrangement in which the density signal is fed forward to the level controller represents the best of the feedforward-feedback systems examined.

However when compared with the original scheme, we note that, while it gives superior control in terms of maximum deviation and settling time, the advantages are not so marked as to justify the use of this system with its greater complexity.

7.2.1.10 Summary

The relative merits of the schemes examined can be assessed in terms of the response of the main output variable, product density. Since the product density is affected by variation of feed

flow, or steam supply, we can assert that in Case 1, where the level is controlled by manipulating the product withdrawal rate, the controller has no effect on the product density which responds in open loop fashion. In Case 2 where the feed flow is the manipulated variable, it does have some effect, the difference being most marked in the behaviour of the product flow, there being a freedom from the initial oscillations apparent in Case 1 and a reduced offset. Generally the level responses in Case 2 are superior to those of Case 1 also.

When a density control loop is added we have several possibilities. In three cases (3, 4 and 6) the density controller acts directly to eliminate disturbances on the feed flow in Case 3, and the steam supply in Cases 4 and 6. In Case 5 it acts indirectly by interaction with the level controller. The density controller alters the level, and the level controller seeing this effect as a disturbance changes the feed flow and consequently the density. As discussed earlier, this makes the system more oscillatory, but our results here, as in all the dual-controller cases, differ from those published originally. This disagreement has been described above. Examining those instances in which the level controller acts on the outflow,

viz. Cases 3 and 4, it seems that Case 3 results in a better density response than Case 4 and there is some superiority in terms of the other process variables recorded. However trials with various controller settings suggest that this is partly a function of the controller settings applied in Case 4. Case 6 was capable of stable operation but care was necessary in the selection of the controller parameters. Case 5 gave the faster response in terms of product flow and density but exhibited strong interaction between the loops.

It seems that the system described as Case 3, where the level controller regulates the product withdrawal rate and the density controller regulates the feed rate, is the most suitable, at least for disturbances in the following input variables; feed flow, feed density, and steam flow.

7.3 DIGSIM : Digital Computer Simulation

The digital simulation techniques developed during this research study is applicable to any dynamic system which can be described by a set of differential equations, which may be linear or non-linear, or any system for which an analogue computer circuit has been developed but which is too large for the available analogue equipment. It uses conventional Fortran instructions. The simulation technique, called DIGSIM was original in its inception but during the course of this research commercial programmes, some

similar in concept, were produced. However none of these was available to the writer during this study.

Most of the digital-analogue simulation programmes which have been proposed, stem from the pioneer work of Selfridge[39] who developed basic routines necessary to simulate analogue computer components and interconnections on a digital computer. In general the simulation programmes proposed differ in the kinds of components simulated, the manner in which the interconnections are made, the way these are used as inputs to the digital programme, the integration method used, and the manner in which the problem is solved. The development of such programmes has been described in a survey by Linebarger and Brennan.[25]

The ease with which a simulation can be modified depends upon the extent to which automatic sorting is used. Published programmes range from those which allow the statements describing a system to be written in any order, to those which require the statements describing certain components to be grouped together and placed in the deck in a particular sequence. Obviously fully automatic sorting is advantageous, since it frees the user from the knowledge that he is using a serial device to simulate a parallel system. Equally obviously, a system of such versatility demands a considerable degree of programming sophistication in its preparation, and the ready availability of programmes and programming assistance if they are to be applied by the occasional user. In the absence of such facilities there is considerable attraction in the idea advanced by Benyon[2] in a letter to a computer journal that standard Fortran might be used by anyone using a functional approach and

prepared to perform manual sorting when organising his problem.

This was the method adopted by the writer. The DIGSIM (Digital Simulation) programme uses standard Fortran statements to prepare Control and Integration Functions, to convey the necessary input information, to control the computation, and to process the results. The Control Function is a normal iterative technique in which the initial and final values, the step length, and the terminating test instruction are specified. The Integration Function assumes normal mode integrators and the integration method is a second-order trapezoidal Runge-Kutta routine requiring two passes per step. The coding is of the form

Y = S (X, YIC)

where Y is the output

X the input

YIC the initial condition.

X must not be an expression but S may be part of a larger expression. This restriction is necessary to prevent the occurrence of implicit loops.

Naturally the standard functions such as the trigonometric functions are available, and any legal Fortran instruction may be used. Numerical values are format free, and may be presented in floating point, fixed point or integer form. Also there is nothing to prevent the programmer from writing his own subroutines and introducing them as functional blocks.

Since data statements may vary from one run to another they must be listed separately from the structure statements which are constant. In order to have the convenience of using source language

names in requesting input and output, all variables required for such purposes must be in COMMON storage and must be prepared in accordance with the usual Fortran rules. This permits the input-output routines to identify source language names during execution and to deduce their storage locations. Any DIMENSION statements used to define arrays must appear in the main programme, and where they apply to variables listed in COMMON statements must follow such statements in the data deck.

Sorting is not automatic but the basic rules concerning ordering are simple. They are :

(1) each integrator must occur before the block that feeds it,

(2) each non-integrator block must occur after the block that feeds it.

Automatic sorting could be provided, using a pre-processor to sort the source language statements into order before compilation, or a post-processor to sort the machine code into order after compilation and loading. The former method has the advantages that it is less machine dependent and allows the use of macro instructions. Both methods would require significant amounts of storage space, which is in fact a characteristic of the more sophisticated digital simulation techniques described previously. For example IBM's DSL/90 seems to use about 8K of storage.

Other improvements which might be considered desirable and which could be introduced are

(1) computation of statement 3 in FUNCTION s in partial double prevision;

(2) provision of a choice of integration methods;

(3) provision of standard functions for function generation, data input, etc. For example a standard library routine was adopted to allow for graphical output of the results obtained in this study;

(4) programming of some of the standard routines in assembly language to improve speed and storage economy.

Broadly the organisation of the simulation programme can be represented as a block diagram as shown on the following page.

The structure of the complete card deck is determined by the requirements of the computer installation. Examination of the annotated sample programme which is presented as Appendix C illustrates the principles of the DIGSIM technique. No claim can be made as to its speed. Obviously the time used on a problem is a function of the step length chosen for the integration and equally obviously, programming the standard routines in an assembly language would improve the speed.

In conclusion, it can be stated that when using the DIGSIM programme the operator need be concerned only with the relationships between inputs and outputs of basic blocks which perform specific mathematical operations. Since the system uses conventional Fortran statements it may be used as part of a larger digital computer programme. It may be used for the typical boundary value problems arising in process and control system simulation, for initial value problems, or applied to nonlinear problems, and to control problems involving large distance-velocity lags. That

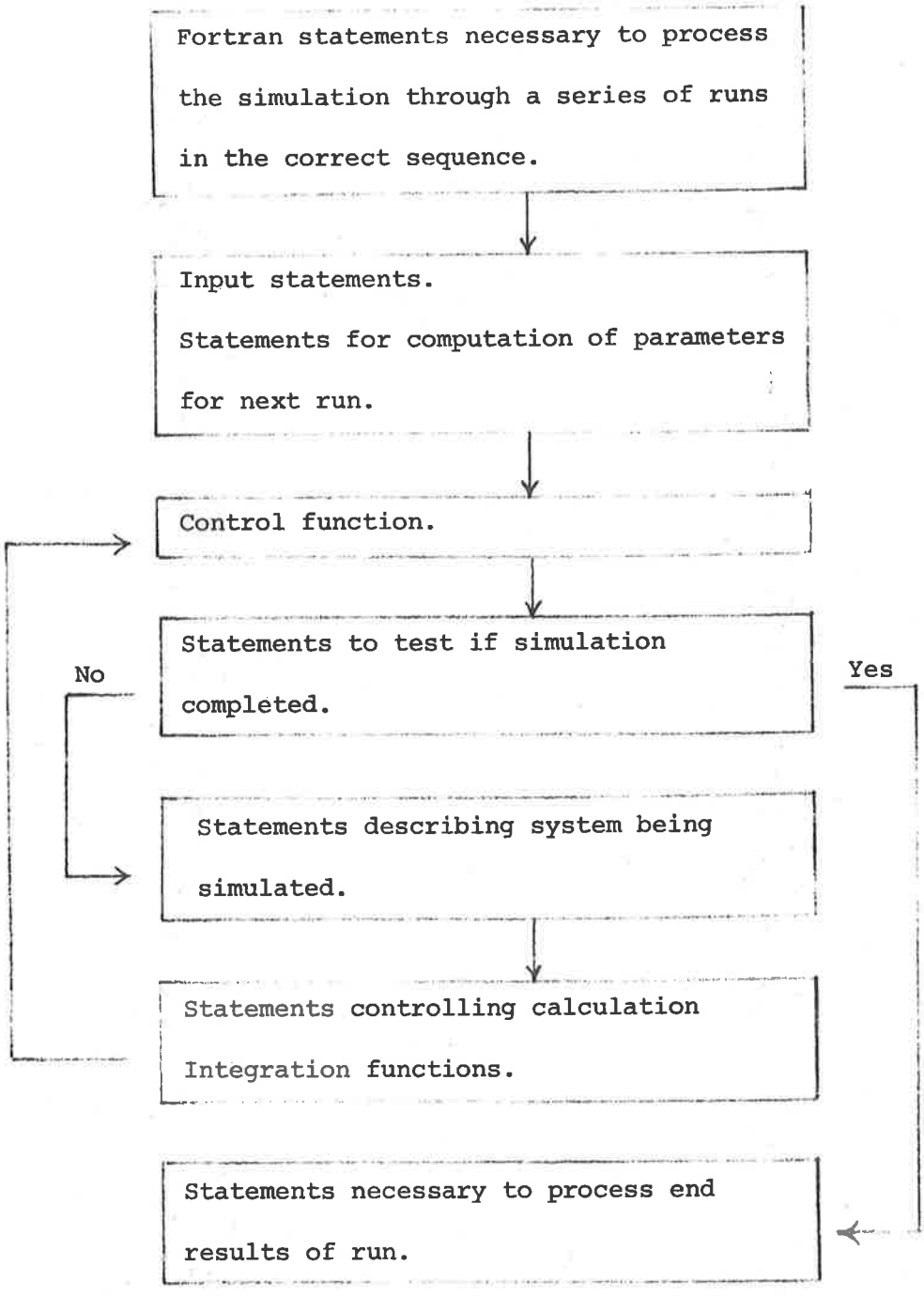

is, the system may be used to simulate a large analogue computer or be regarded simply as a separate technique of problem solution. It was used in this study to examine alternative control systems on a

chemical evaporator in an effort to establish whether some controller arrangements were preferable to others.

7.3.1 Results and discussion

The DIGSIM technique was used to simulate the model for the forced-circulation evaporator including the distance-velocity lag involved in the heat exchanger section and covering the controller configurations identified earlier as Cases 3 - 6.

Two controllers, level and density, are involved. Consideration was given to using a controller to manipulate the pump motor speed, but the idea was discarded because it was believed to be desirable that the fluid flow rate be maintained high enough to achieve several advantages concurrently, viz. enhanced heat transfer, suppression of boiling in the tube, reduction of resonance effects, and minimisation of scaling.

Level control assumes an increased importance with this kind of evaporator. Level control systems fall into two groups, those where the level is an important process variable and those where the flow from the vessel is the important variable. We have already commented that the internal-calandria evaporator is an example of this second group. That is, the actual level is unimportant so long as the tank does not run dry or flood, surges in flow being absorbed by allowing the level to change, at least temporarily. Similar remarks would apply to a distillation column reboiler.

In the case of the forced circulation evaporator the capacity of the flash tank is considerably less than the pan of the internal-calandria type, but it still has three functions to perform. It has to provide adequate vapour disengaging space, it has to maintain sufficient liquid in the pump inlet line to prevent cavitation, and it has to provide a big enough liquid storage to prevent off-specification material being withdrawn. This last requirement is not an onerous one since under-concentrated material will be recycled. One can visualise circumstances, on start-up for instance, where all the fluid is recycled, make-up feed being admitted later as vapour withdrawal occurs. It is difficult to imagine circumstances where the desired concentration might be exceeded other than as a transient condition. In the many hours the experimental rig was operated no trouble was experienced with level control.

The dynamics of the pressure and concentration loops should be relatively the same for both kinds of evaporator, as they should for any subsidiary loops such as steam supply and feed temperature.

In the simulated runs both controllers were arranged as proportional plus integral modes, the controller gains being set at 62.3 in each case, and the integral action being 0.8 hours for the level controller and 0.2 hours for the density controller. For Case 5 these settings had to be varied.

With this particular controller configuration the controller settings were critical. As in the analogue simulations linear control valves were assumed, the valve gains being absorbed in the controller output signals. The measuring elements were simulated as first-order systems with time constants of 30 seconds.

The nature of the programmes submitted to the digital computer are indicated in the annotated specimen enclosed, Appendix C, which was that used for one of the runs. The tables in Appendix A list the plant parameters and equation constants. Once the simulation was operating new controller arrangements could be programmed by renaming the controller outputs, and, if necessary, reading in new data for the controller potentiometer settings. An inspection of the programme will show that the step disturbance required is inserted by a single instruction which varies the value of the variable from its steady state value of zero to a new value of 0.1, assuming that a 10% disturbance is required. In this research the step inputs were all 10% of the magnitude of the steady-state values. As earlier, the variable values represent deviations from the desired steady-state value.

The product density, product withdrawal rate, and the liquid level, were recorded as responses to disturbances in feed flow, feed density, feed temperature, pan pressure, and steam supply. The results are presented graphically.

The time scale is in minutes, the variable scale is in volts, and after taking into account any indicated scale factors, can be expressed in terms of the appropriate steady-state, or design, values. Thus 10 volts is equivalent to $q_0 = 5$ ft^3/hr; $\rho_0 = 0.2$ lb/ft^3; and $v_3 = 0.5$ ft^3 respectively.

Reference to the diagrams, for example those of Case 3, shows what seemed at first to be an unexpected feature, a relatively long period of cycle, where cycling does occur. Further consideration suggested that the important factor in the system response was not the residence time per pass but the time constant involved in the concentration control loop. It was assumed in the preparation of the model that the evaporator was handling the same working solution as used in the laboratory tests.

The results of the simulation are presented as a series of plots in Figures 46-61.

Summarising the results obtained in the digital simulation it can be stated that for the Case 3 arrangement, product density and level were little affected, but product flow was oscillatory and showed residual offset to all disturbances except pan pressure. In the latter case the response took the form of an initial deviation which was eliminated in an apparently critically-damped fashion.

For Case 4 the level was unaffected, there was a small continuing deviation in product density, while in each case,

except in response to a change in feed density, the product flow increased sharply then fell continuously to an offset final steady-state. For the density disturbance the outflow underwent an early inflection then fell to an offset final flow rate.

It was shown earlier in relation to the standard evaporator that there was strong interaction between the control loops in Case 5. The same feature was evident with the forced-circulation evaporator. This interaction may lead to faster response and a shorter stabilisation time in appropriate circumstances but is considered undesirable generally, because of the inability to ensure that the disturbances entering the system are of the right kind. The results showed oscillatory response for all three recorded variables although the magnitudes involved in the cases of level and product density were small enough to ignore in practice. The system was not fully stabilised within the experimental period of 6 minutes in any case and there appeared to be a permanent change in the product flow rate in each instance. This particular controller arrangement is sensitive to the controller settings and no doubt could be stabilised more quickly with further experimenting.

The arrangement described as Case 6 was able to bring the three variables back to their initial values. In particular product flow shows a very slight reaction which was gradually eliminated. The particular configuration poses

problems in that it has a restricted region of stability. There may be installations, such as some reboilers or reactors, where its particular features of constancy of outflow and level are desirable characteristics. In the case of concentrating evaporators the emphasis is on the product density, and variations in product flow rate, if unwanted, may be smoothed out using some sort of holding tank.

The behaviour of the forced-circulation evaporator was so similar to that of the standard evaporator that it was considered to be unnecessary to examine any other controller arrangements.

Of the standard controller arrangements considered there seems little question that Case 3 which combines high stability with rapid response, and particularly close control of product density is the most satisfactory for both types of evaporator. In view of this, it can be said, comparing the two kinds of evaporator on the basis of their performance with the Case 3 scheme, that the forced-circulation external-calandria unit gives much better response in terms of product density, but the product flow cycles for a relatively longer time and shows final offset for disturbances in product density and feed flow. In addition, the product flow shows the same kind of behaviour in response to variations in the other feed variables, flow and temperature, but recovers in critically-damped fashion

from a pan pressure disturbance. The conclusion to be reached is, that where it is important that a minimum of off-specification material be produced, the forced-circulation evaporator, probably because of its lower hold-up volume, is to be preferred to the standard evaporator.

8. CONCLUSIONS

A quantitative method for the investigation of control system design problems related to concentrating evaporators has been described, and its use demonstrated by application to two kinds of evaporator.

A general theory describing the dynamic behaviour of a forced-circulation external-calandria evaporator, and a mathematical description retaining the distributed-parameter characteristics of the heating section, have been developed. The model has been verified by comparison with an experimental evaporator. This seems to be the first published account of such a study on this type of evaporator. A simplified form of the model has been shown to be equally applicable to a natural-circulation internal-calandria evaporator. The modifications necessary to take into account the presence of solids have been indicated.

The mathematical model has been manipulated to yield transfer functions relating the responses of product density, product flow, and level, to disturbances in feed density, feed flow, feed temperature, steam flow, and pan pressure.

A forced-circulation evaporator has been constructed to determine the frequency responses to steam and fluid flow disturbances. Resonance effects were demonstrated in each case, and shown not to occur at the fluid flow rates applicable in normal industrial practice.

Calculations of theoretical frequency responses based on the approximate model have been made and compared with previously published data relating to the natural-circulation evaporator. Theoretical frequency responses based on the exact model have been calculated for the forced-circulation evaporator. No other account is known that describes the behaviour of a similar evaporator. Studies of heat exchangers have

partial relevance but differ in not involving mass transfer, and usually in not involving the possibility of two-phase conditions on both sides of the transfer surface. Comparison of the theoretical and experimental frequency responses has provided a partial check of the theory.

The simplified mathematical model was simulated on an analogue computer using the plant data for the natural-circulation evaporator to scale the model. The transient response of the simulated system has been examined, with a number of alternate control systems, for a comprehensive range of disturbance variables. The transient response analysis has been extended to examine several possible cascade control arrangements and the feasibility of using combined feedforward-feedback control. It was concluded that these latter techniques provide little improvement in the case of the evaporator studied, with the one exception where the Case 3 arrangement was modified to incorporate cascade control of the steam supply.

A digital simulation technique has been developed which allows the study of any system described in the form of an analogue computer circuit. Alternatively the approach can be regarded as an analytical method in its own right. The technique employs standard Fortran instructions. The model is freed from some of the restrictions applying to analogue computer simulation.

The digital simulation procedure has been applied to an examination of the forced-circulation evaporator. The mathematical model was dimensioned and scaled using the parameters of the experimental evaporator. The simulation model has been used to determine the transient response

of the forced-circulation evaporator in association with a number of alternative controller arrangements and for the same wide range of variables as above.

Restricting attention to the multi-loop control systems it can be concluded that if the liquid level is controlled by regulation of either feed or product flow, the concentration may be controlled by regulation of feed, product, or steam flow. There are, therefore, four possible systems.

System	Level regulates	Concentration regulates
Case 3	Product flow	Feed flow
Case 4	Product flow	Steam flow
Case 5	Feed flow	Product flow
Case 6	Feed flow	Steam flow

Of these, Case 6 has been shown to have a limited region of stability. Case 4 is stable, but in common with Case 6, and in contrast to Cases 3 and 5, an additional time constant is introduced by the calandria. Thus controllability can be expected to be inferior under some circumstances. The additional lag becomes significant when the major time lag in the plant, which can be taken very approximately as the ratio of liquor hold-up to liquor throughput, is in the order of minutes instead of hours.

The choice between Cases 3 and 5 is not obvious. Case 5 is characterised by strong interaction between the control loops. This makes choice of the controller settings critical. Case 5 may be better on start-up and thus for batch operation. On start-up the density controller will prevent product withdrawal until the desired concentration is reached,

while the level controller admits sufficient feed to compensate for any evaporation. When the controllers are reversed, i.e. Case 3, no feed will be admitted until correct concentration is reached and the level may become unduly low. However, since most concentrating evaporators are used on a continuous basis the scheme referred to as Case 3 is recommended.

A modification of Case 3 may be considered, in which the level controller regulates the feed supply and operates in cascade on the steam supply controller while the density controller regulates the product withdrawal rate. This places adjustment of the steam supply under control of the fast-acting level control loop. The system has some of the advantages of Case 5 on start-up, since the liquor concentration determines when product withdrawal starts, and feed is admitted to correct for evaporation. However, the level controller may throttle back the steam supply, thus introducing oscillations into the system. This scheme, and that designated Case 3, were examined under continuous operation for some time, while arbitrary disturbances were introduced at several points. The modified Case 3 was marginally more satisfactory and would seem to warrant a plant trial.

The assumptions made in developing the mathematical model are believed to be general. Two factors must be mentioned. One is the assumption that the heat of concentration is negligible. This may not apply in every case but variations may be incorporated readily into the model. The necessary modifications have been indicated. The other is that thermodynamic equilibrium is maintained in the pan. The consequences of variations of these assumptions were discussed.

The evaporators studied had principal time constants in the order of hours and minutes respectively. In this latter case the remaining time constants assume greater relative importance, but since the experimental transient responses involving both approximate and exact models were comparable for both types of evaporator it is postulated that the model is of wide application, and may be equally applicable to distillation reboilers. Indeed it seems that the approximate model may be used to make qualitative predictions for control purposes.

If the dynamic behaviour of the calandria is to be considered in evaporator design the phase lag and attenuation introduced in this section could be reduced by increasing the heat transfer coefficient; reducing the liquid hold-up in the downcomer and pipework associated with the pump in the case of a forced-circulation evaporator; and reducing the mass of metal in the steam jacket and flash vessel walls, or pan wall in the standard evaporator.

It is recommended that any future study of evaporation should examine the dynamics of the condenser-ejector system, and their influence on the evaporator pan pressure.

INDEX TO FIGURES

FIGURE NO.	SUBJECT
1.	Standard natural-circulation internal calandria evaporator and symbols.
2.	Block diagram of evaporator showing relationship between product density and the disturbance variables.
3.	Block diagram of evaporator showing relationship between level or outflow and the disturbance variables.
4.	Forced-circulation external-calandria evaporator.
5.	Pressure drop-Flow. Experimental evaporator.
6.	Response of product liquor temperature to feed temperature disturbances. Flow rate = 3.323 fps.
7.	Response of product liquor temperature to feed temperature disturbances. Flow rate = 5.54 fps.
8.	Response of product liquor temperature to feed temperature disturbances. Flow rate = 7.762 fps.
9.	Response of product liquor temperature to feed temperature disturbances. Flow rate = 9.969 fps.
10.	Response of product liquor temperature to steam temperature disturbances. Flow rate = 2.21 fps.
11.	Response of product liquor temperature to steam temperature disturbances. Flow rate = 3.323 fps.
12.	Response of product liquor temperature to steam temperature disturbances. Flow rate = 5.54 fps.

FIGURE NO.	SUBJECT
13.	Response of product liquor temperature to steam temperature disturbances. Flow rate = 6.65 fps.
14.	Response of product liquor temperature to steam temperature disturbances. Flow rate = 9.969 fps.
15.	Response of product liquor temperature to feed flow rate disturbances. Flow rate = 1.11 fps.
16.	Response of product liquor temperature to feed flow rate disturbances. Flow rate = 3.32 fps.
17.	Response of product liquor temperature to feed flow rate disturbances. Flow rate = 6.65 fps.
18.	Response of product liquor temperature to feed flow rate disturbances. Flow rate = 9.97 fps.
19.	Open-loop block diagram of evaporator.
20.	Analogue computer diagram. Natural-circulation unit with controllers.
21.	Circuit for use on PACE machines for simulation of standard evaporators and controller.
22.	Additional circuitry to add three-term density controller and to introduce P_e.
23.	Basic evaporator control schemes.
24.	Closed-loop block diagram of evaporator. Case 3.
25.	Closed-loop block diagram of evaporator. Case 4.
26.	Closed-loop block diagram of evaporator. Case 5.
27.	Response of control schemes Cases 1 and 2 for natural-circulation evaporator.

FIGURE NO.	SUBJECT
28.	Response of control schemes Cases 1 and 2 for natural-circulation evaporator.
29.	Responses for Case 3, natural-circulation evaporator - all disturbances.
30.	Responses for Case 4, natural-circulation evaporator - all disturbances.
31.	Responses for Case 5, natural-circulation evaporator - all disturbances.
32.	Case 6. Natural-circulation evaporator. Responses using settings detailed for Case 3 - all disturbances.
33.	Case 3. Response of product flow and density to step disturbance in pan pressure. Standard evaporator.
34.	Cases 4 and 5. Response to pan pressure disturbance. Standard evaporator.
35.	Case 6. Response to pan pressure disturbance. Standard evaporator.
36.	Case 6. Response of product flow and density to disturbances in pan pressure and product flow valve setting.
37.	Cascade control schemes Cases 7-3 to 7-6. Response to feed flow disturbance.
38.	Cascade control schemes Cases 7-3 to 7-6. Response to feed density disturbance.
39.	Cascade control schemes Cases 7-3 to 7-6. Response to steam supply disturbance.
40.	Cascade control system. Density regulates product flow. Level cascades onto steam supply controller.

FIGURE NO.	SUBJECT
41.	Feedforward control. Case 3. Density modifying level controller.
42.	Modified Case 3. (a) level modifies density, (b) density modifies level.
43.	Case 4. Level modifies density.
44.	Case 5. Density modifies level.
45.	Case 6. Level modifies density.
46.	Case 3. Response of forced-circulation evaporator to feed flow disturbance.
47.	Case 3. Response of forced-circulation evaporator to feed density disturbance.
48.	Case 3. Response of forced-circulation evaporator to steam disturbance.
49.	Case 3. Response of forced-circulation evaporator to feed temperature disturbance.
50.	Case 3. Response of forced-circulation evaporator to pan pressure disturbance.
51.	Case 4. Response of forced-circulation evaporator to feed temperature disturbance.
52.	Case 4. Response of forced-circulation evaporator to feed density disturbance.
53.	Case 4. Response of forced-circulation evaporator to steam disturbance.
54.	Case 4. Response of forced-circulation evaporator to feed flow disturbance.

FIGURE NO.	SUBJECT
55.	Case 4. Response of forced-circulation evaporator to pan pressure.
56.	Case 5. Response of forced-circulation evaporator to feed flow disturbance.
57.	Case 5. Response of forced-circulation evaporator to feed density disturbance.
58.	Case 5. Response of forced-circulation evaporator to steam disturbance.
59.	Case 5. Response of forced-circulation evaporator to feed temperature disturbance.
60.	Case 5. Response of forced-circulation evaporator to pan pressure disturbance.
61.	Case 6. Response of forced-circulation evaporator to steam, feed flow, and feed density disturbances.

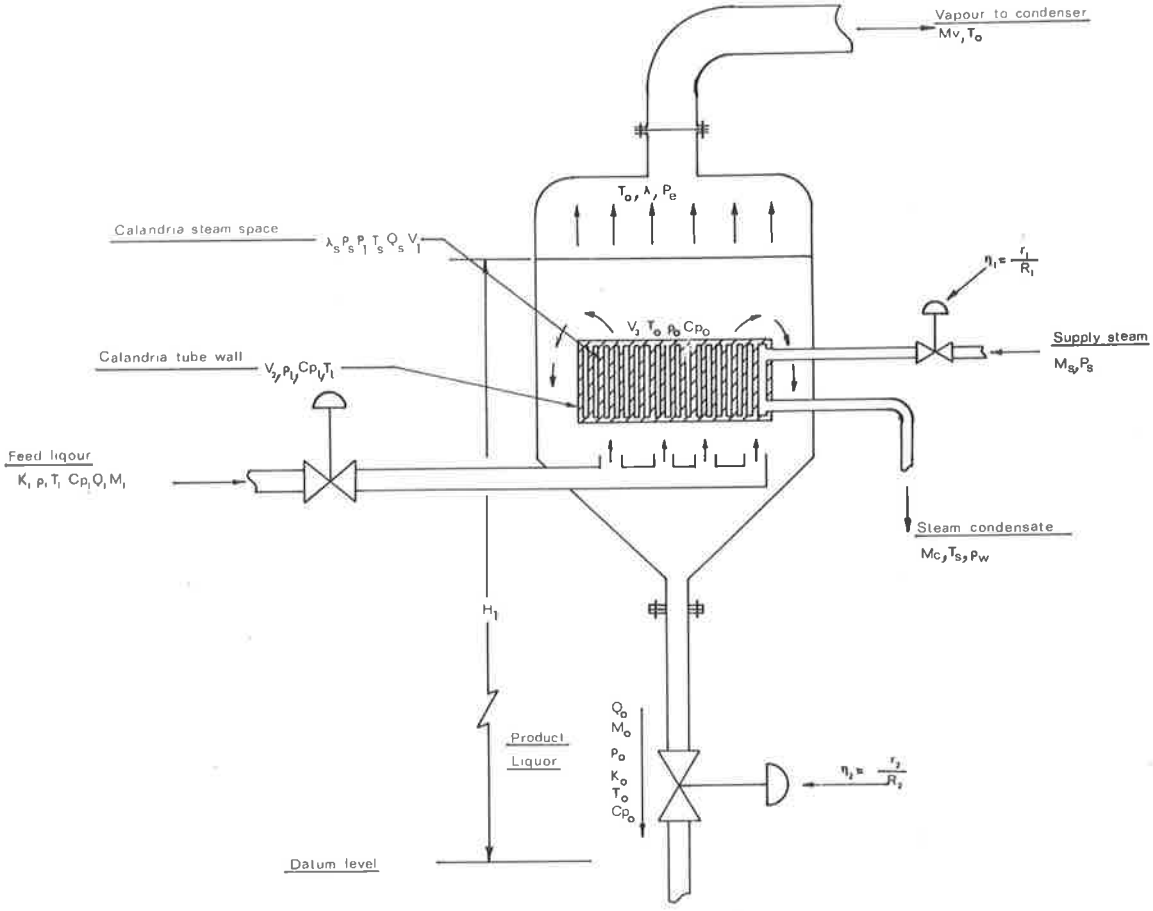

FIG. 1 Standard natural-circulation, internal-calandria evaporator and symbols.

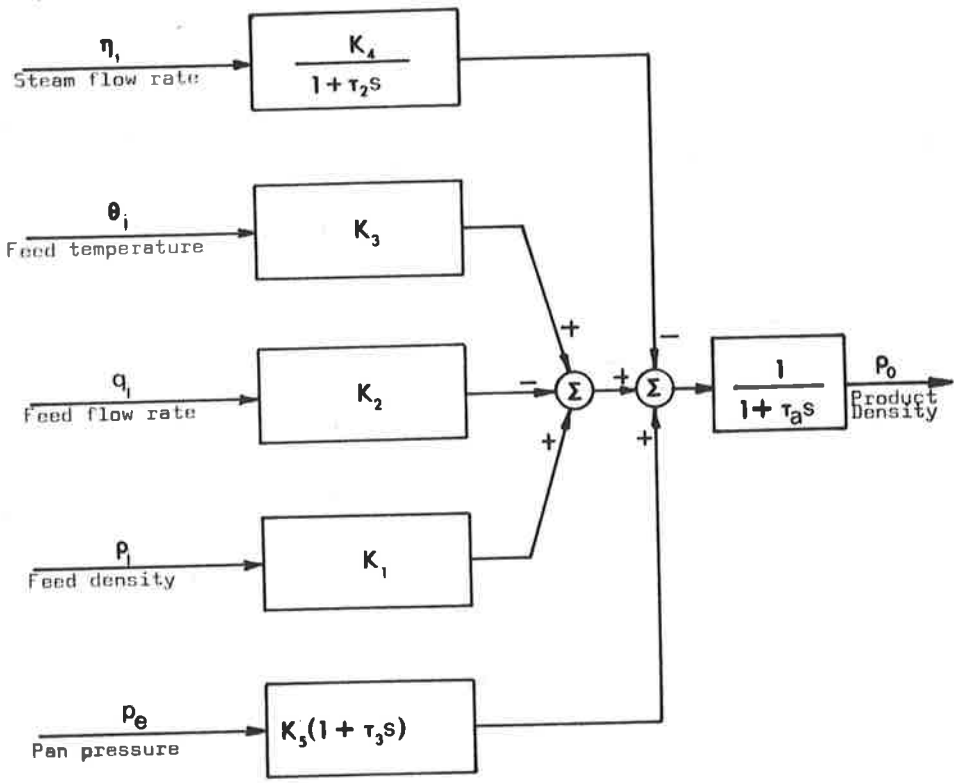

Fig. 2 Block diagram of evaporator showing relationship between product density (ρ_0) and the disturbance variables.

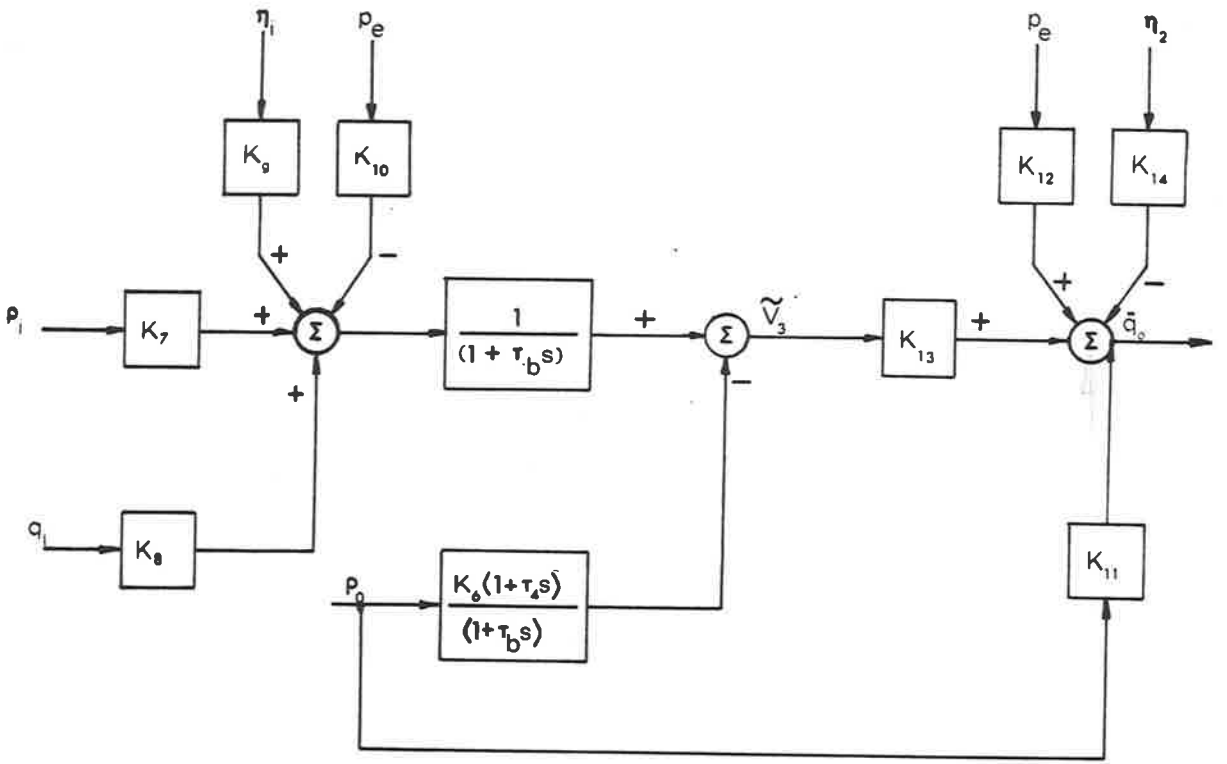

Fig. 3 Block diagram of evaporator showing relationship between level (v_3) or outflow (q_o) and the disturbance variables.

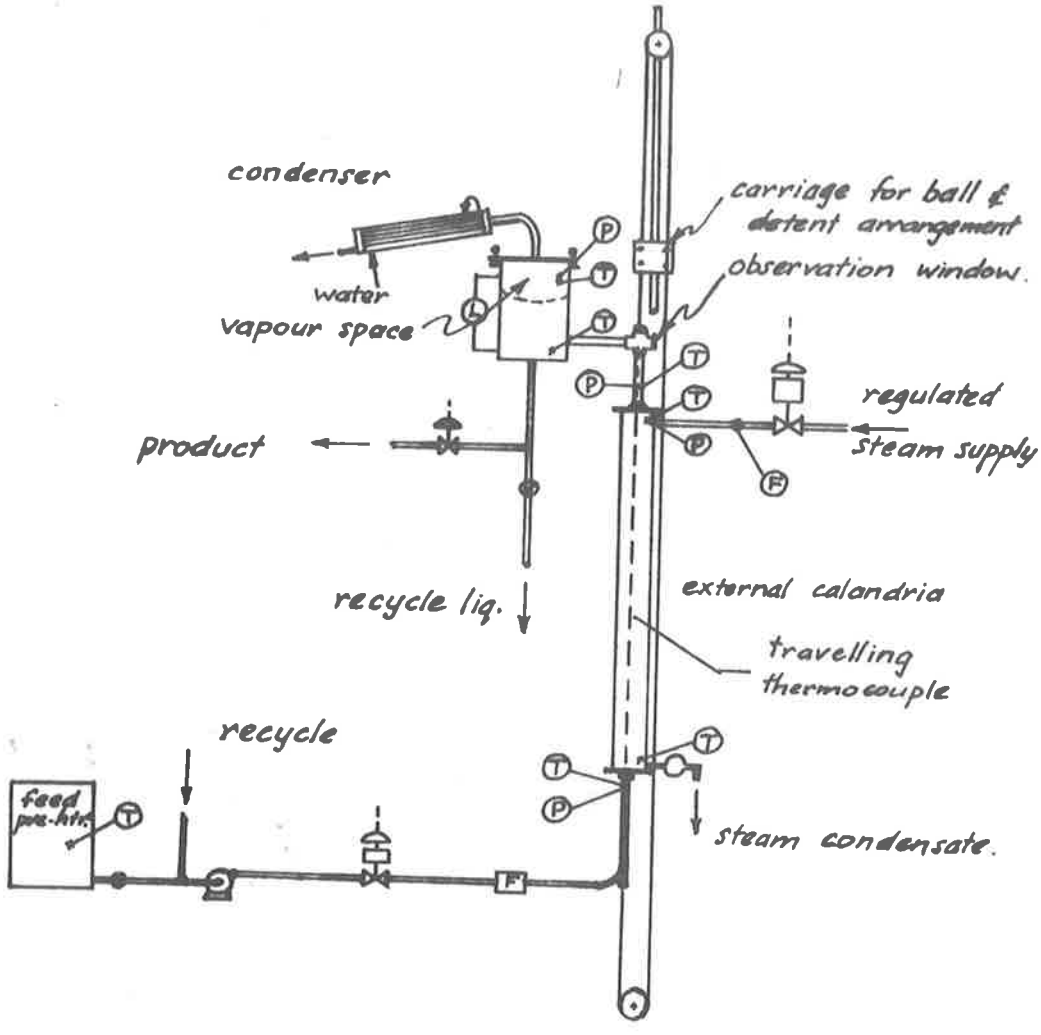

Fig. 4 Forced circulation external-calandria evaporator.

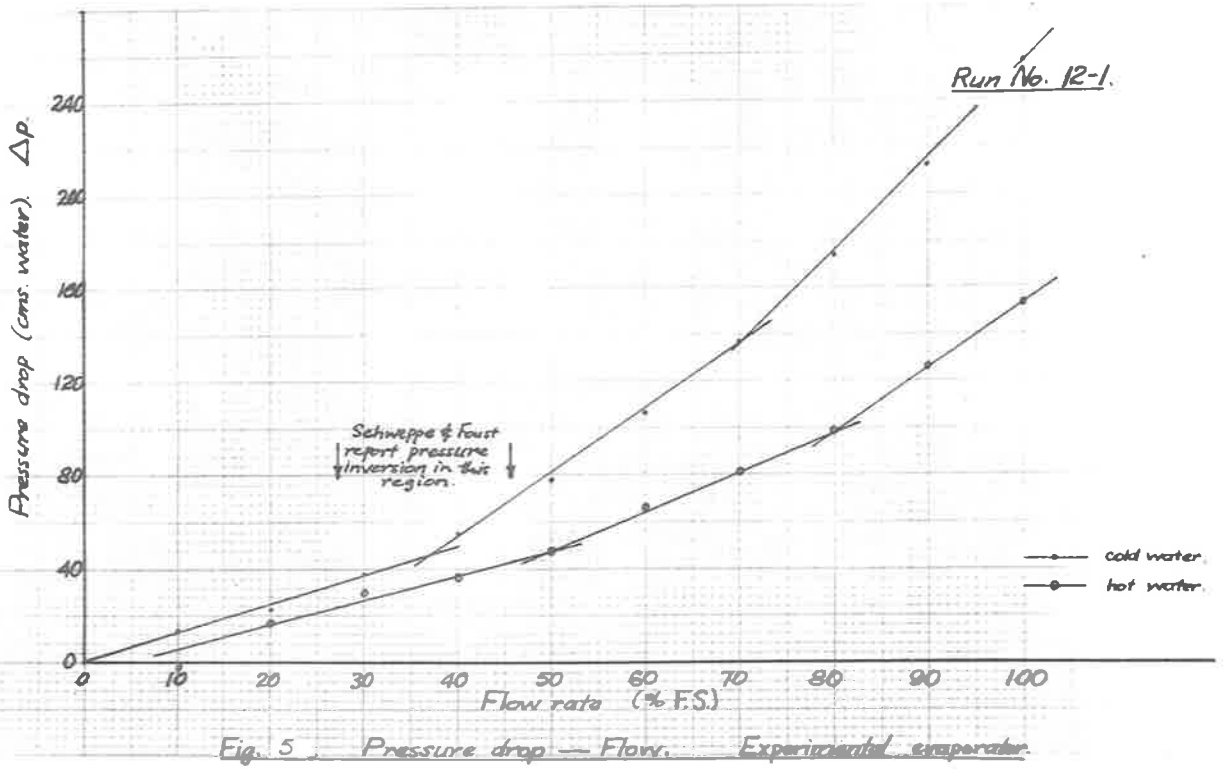

Fig. 5. Pressure drop — Flow. Experimental evaporator.

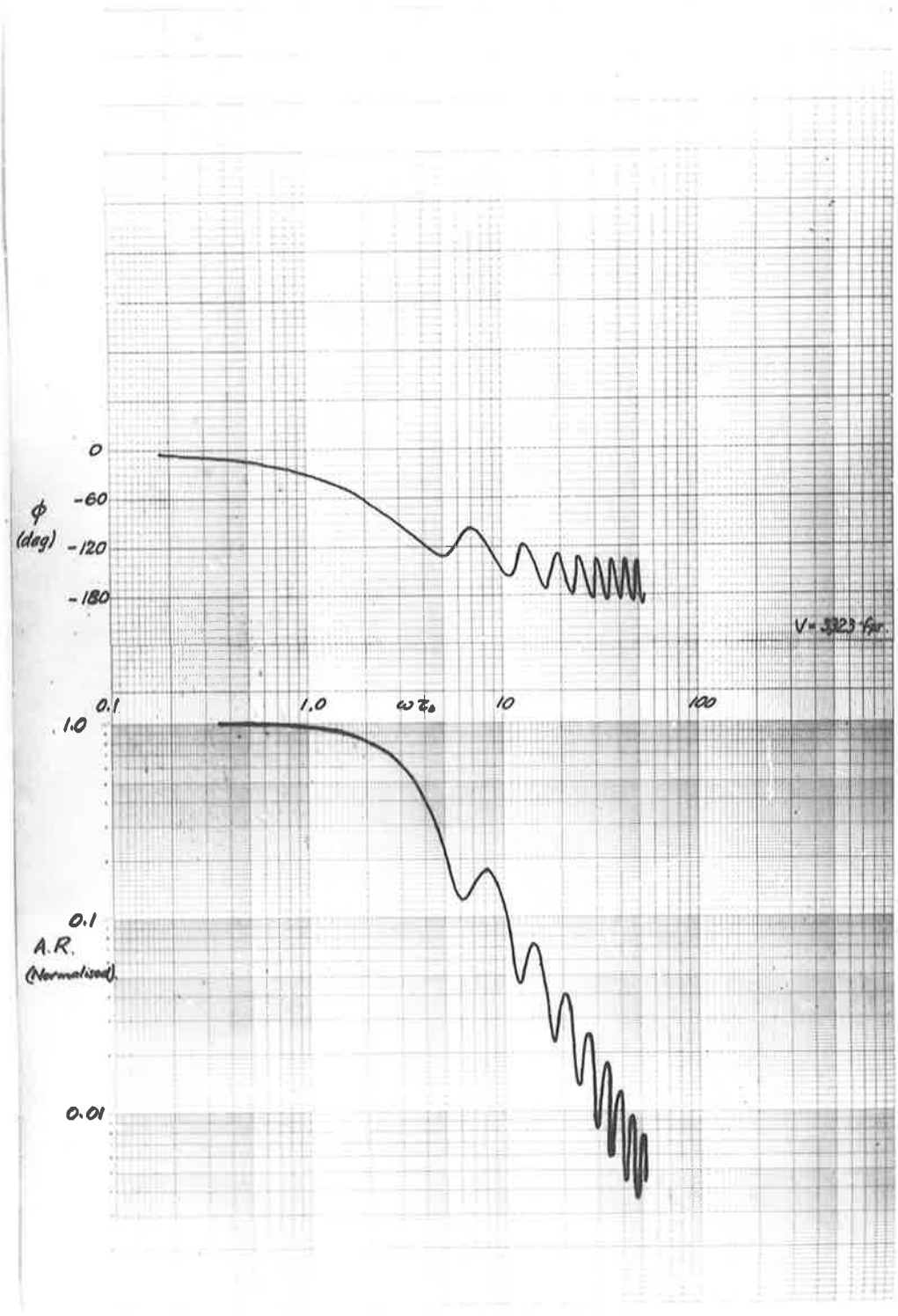
0
-60
-120
-180
φ
(deg)
V = 3323 f/sec.
0.1
1.0
ωτ₀
10
100
1.0
0.1
A.R.
(Normalised)
0.01

Fig 6

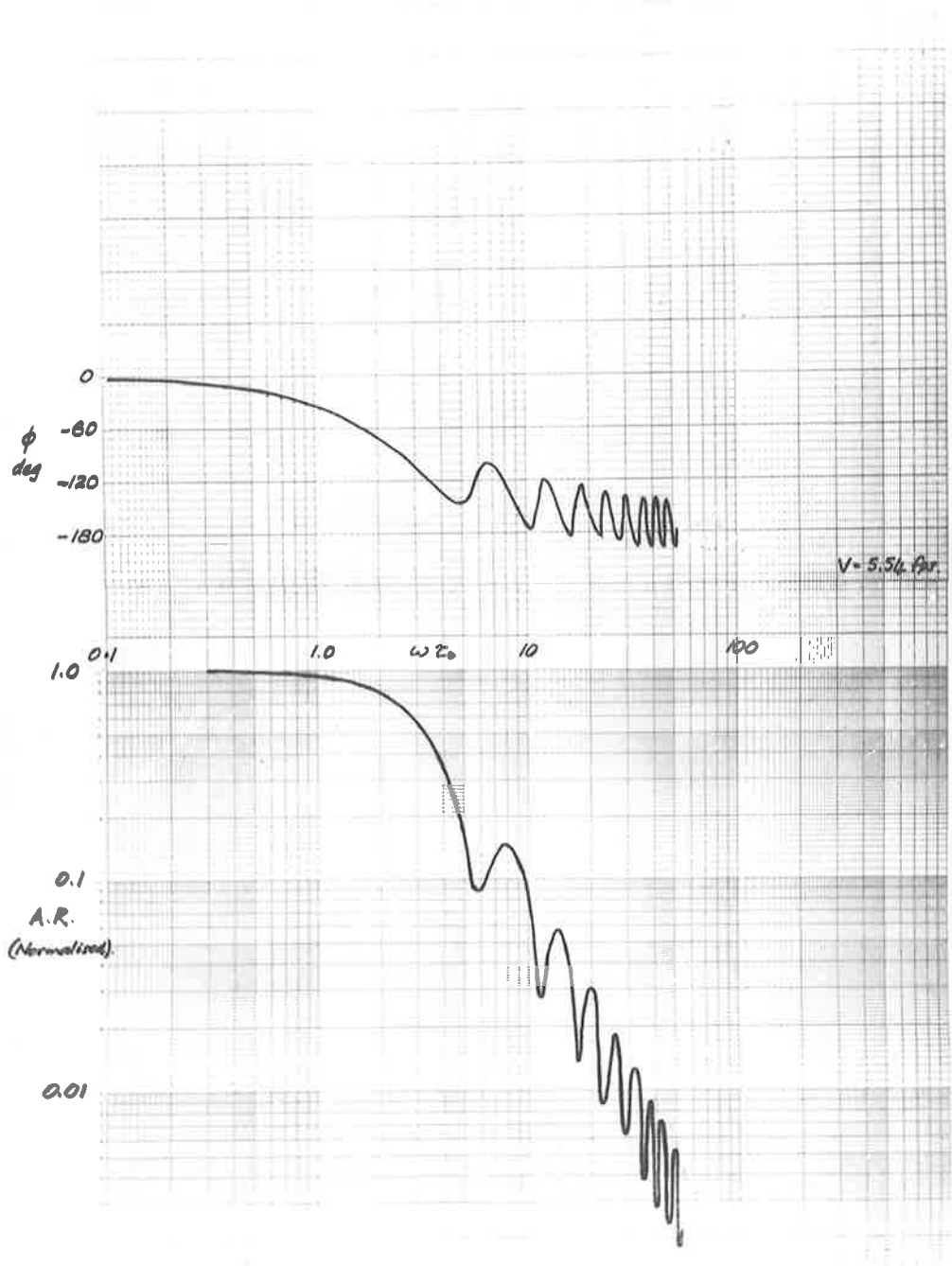
0
-60
-120
-180
φ
deg
V = 5.54 fps
0.1
1.0
ω τ₀
10
100
1.0
0.1
A.R.
(Normalized)
0.01

Fig. 1

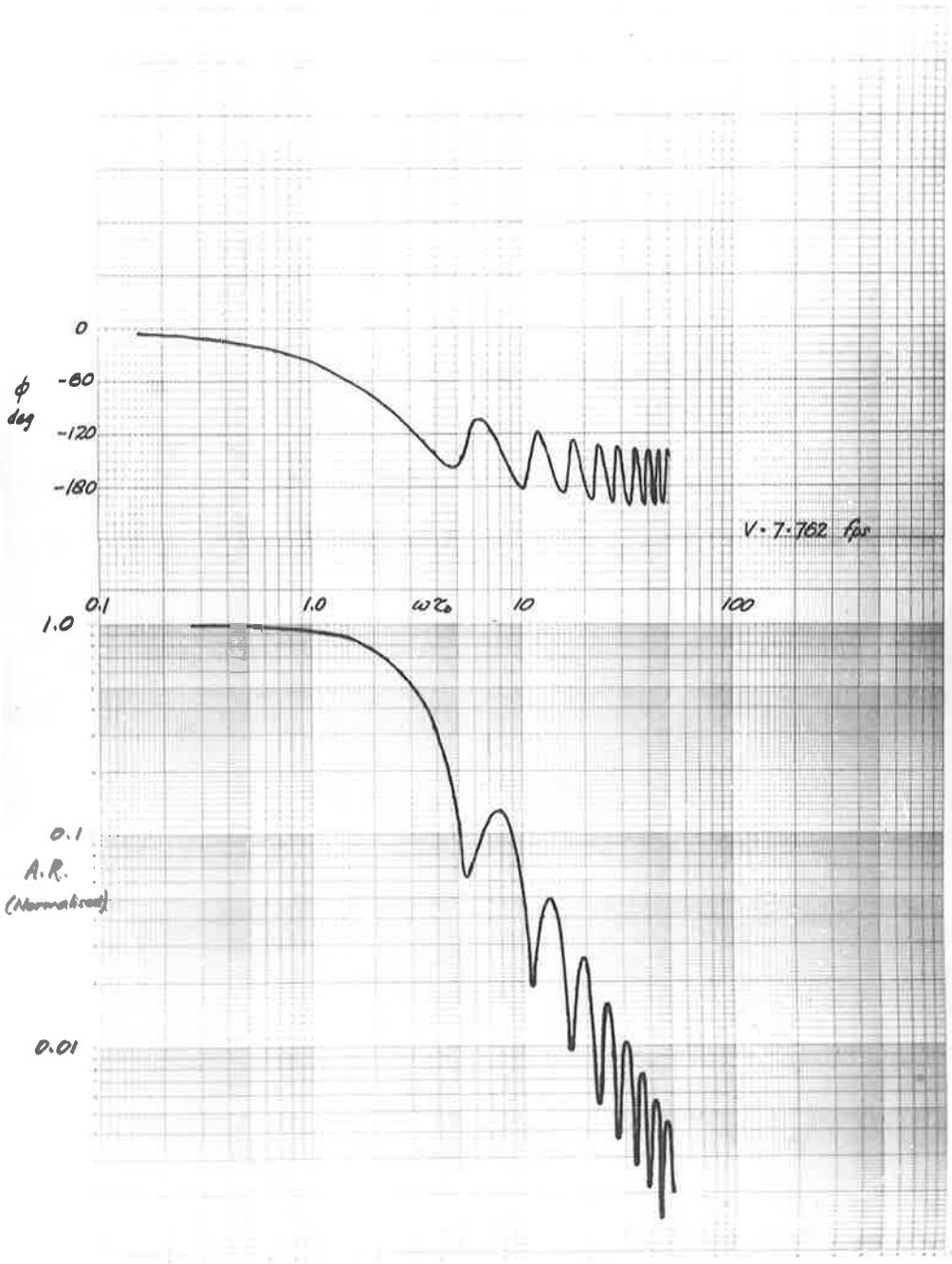
0
-60
-120
-180
φ
deg
V = 7.762 fps
0.1
1.0
ωτ₀
10
100
1.0
0.1
A.R.
(Normalized)
0.01

Fig. 8

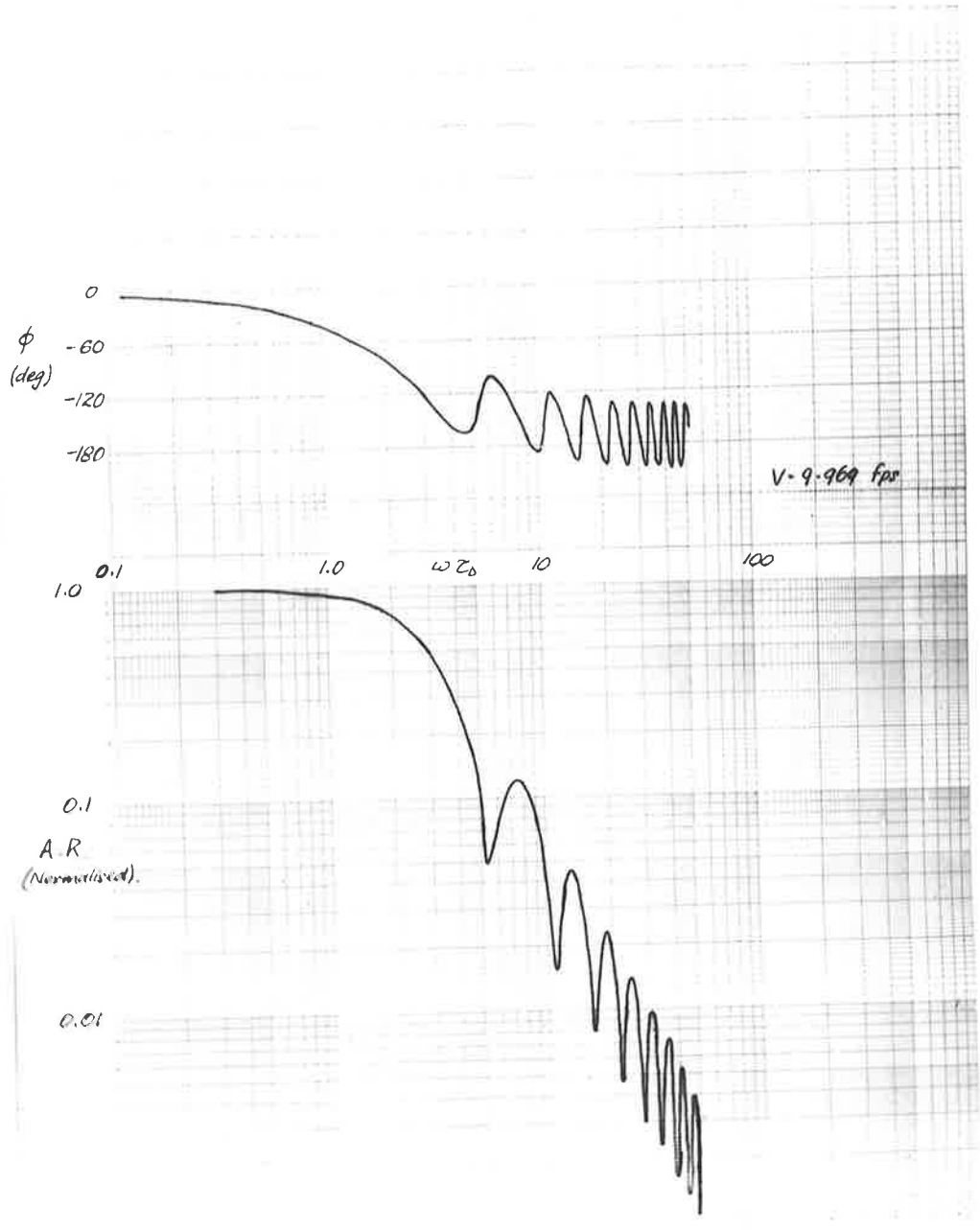
0
-60
-120
-180
φ
(deg)
V- 9·969 fps
0.1
1.0
ω τ_D
10
100
1.0
0.1
A R
(Normalized)
0.01

Fig 9

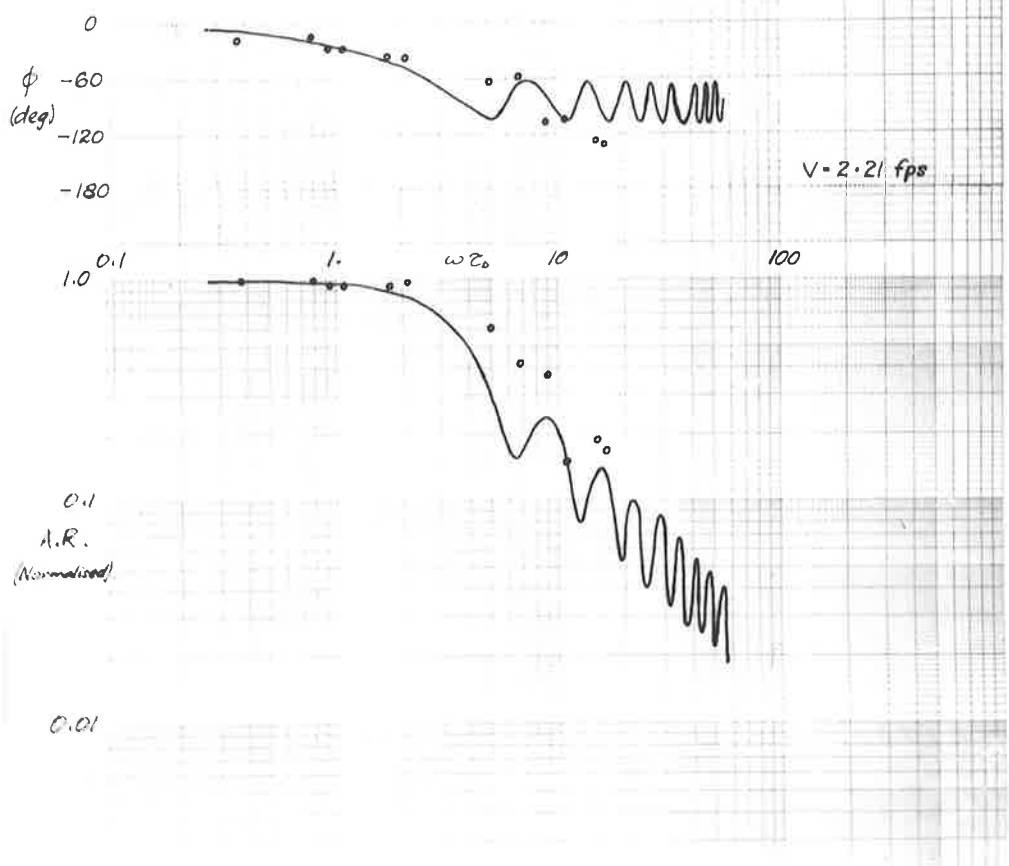
0
φ -60
(deg)
-120
-180
V = 2·21 fps
0·1
1·
ωτ₀
10
100
1·0
0·1
A.R.
(Normalised)
0·01

Fig. 10

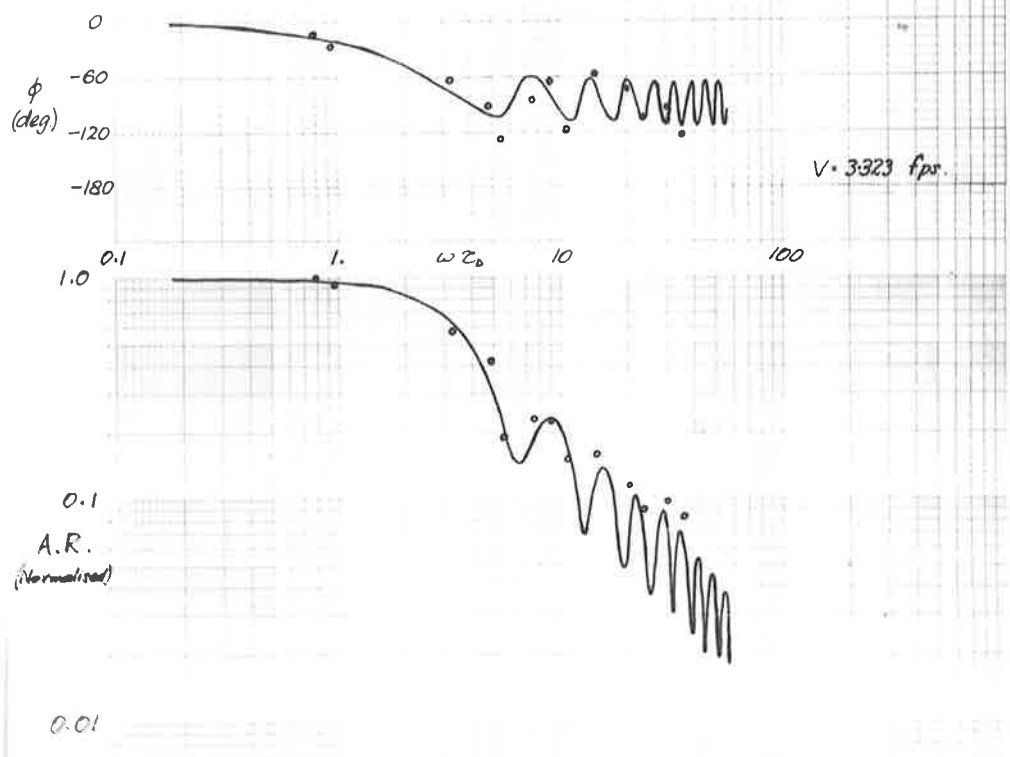
0
-60
-120
-180
φ
(deg)
V = 3.323 fps.
0.1
1.
ωτ₀
10
100
1.0
0.1
A.R.
(Normalized)
0.01

Fig. 11

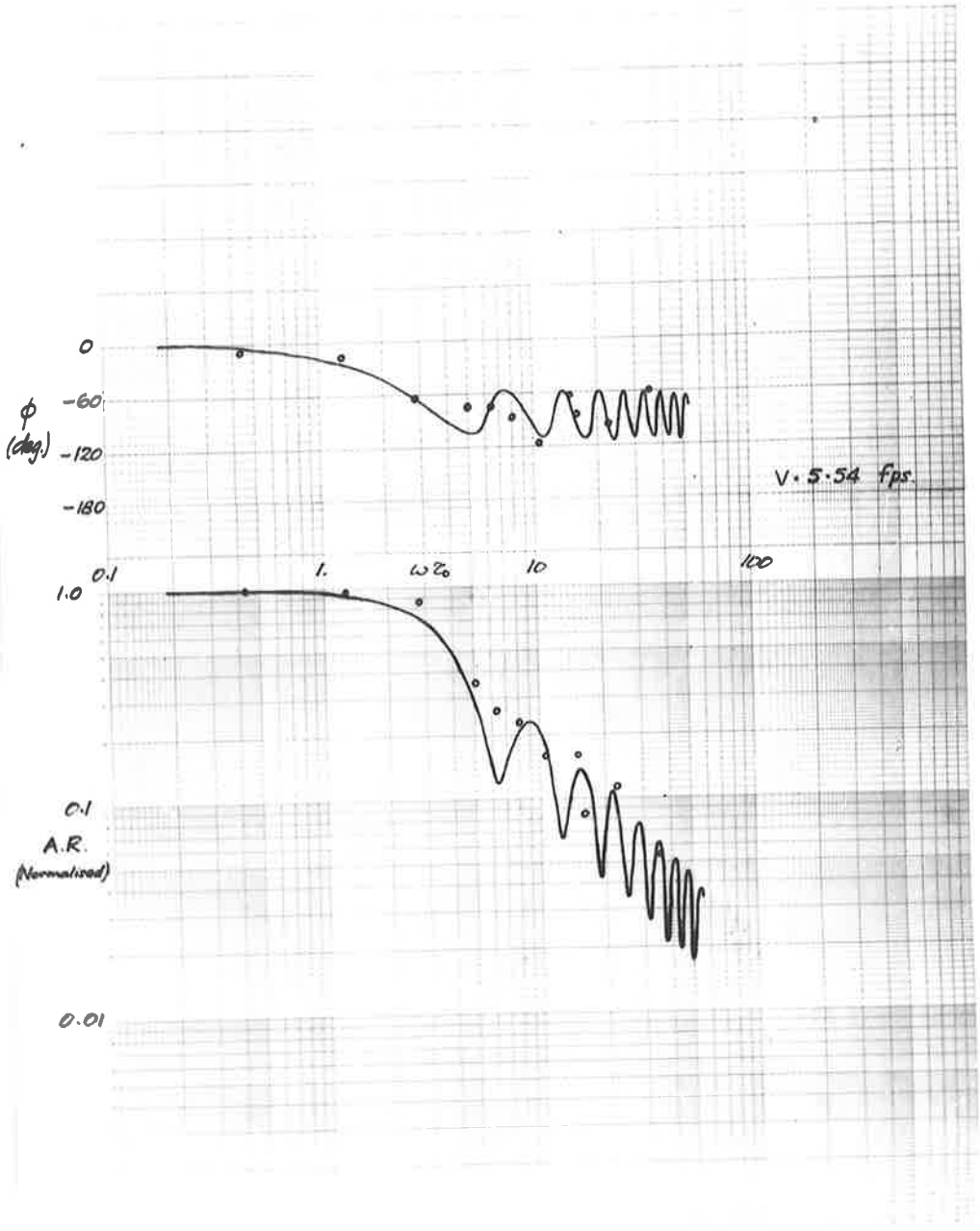
0
-60
-120
-180
φ
(deg.)
V · 5·54 fps.
0.1
1.
ωτ₀
10
100
1.0
0.1
A.R.
(Normalised)
0.01

Fig 12.

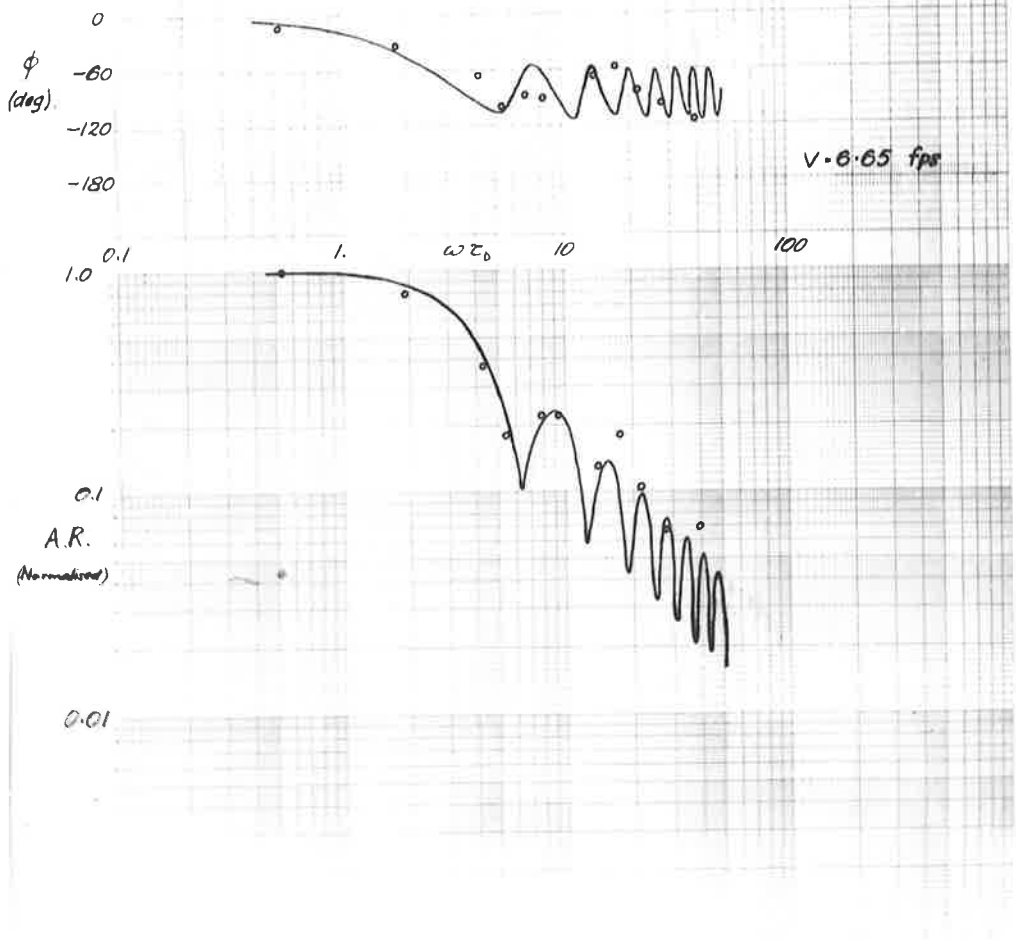
0
ϕ
(deg)
-60
-120
-180
V = 6·65 fps
0.1
1.
$\omega\tau_0$
10
100
1.0
0.1
A.R.
(Normalized)
0.01

Fig. 13

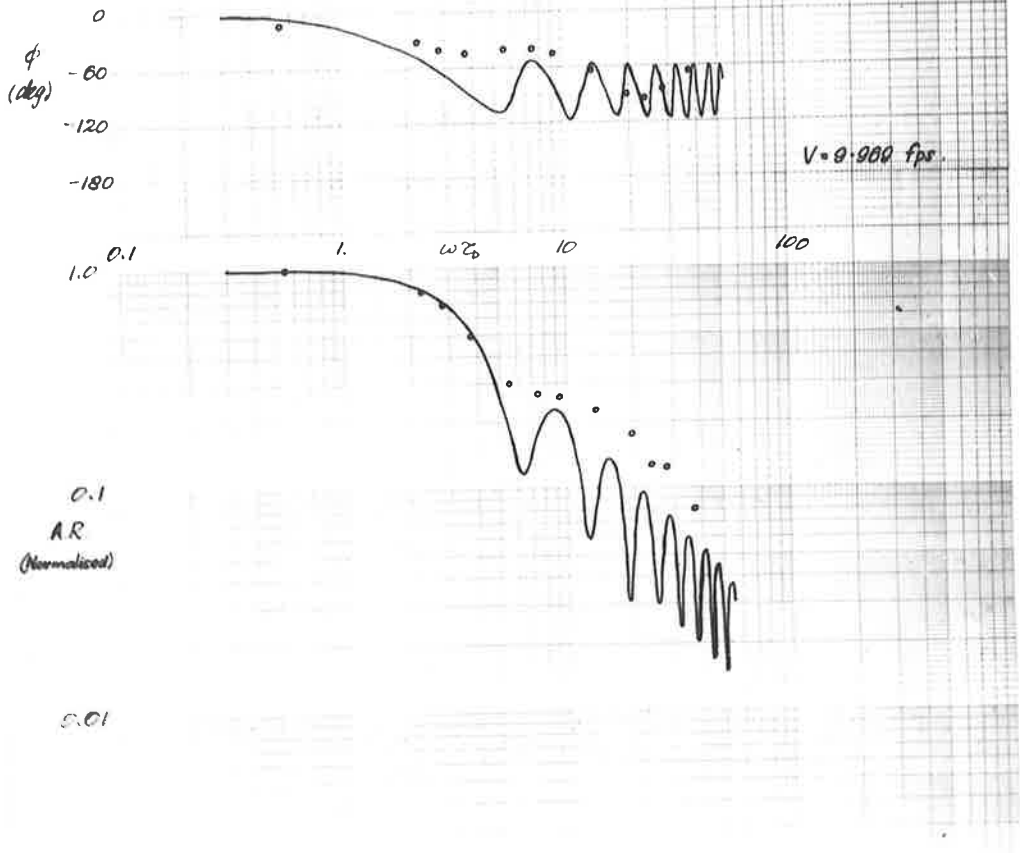
0
-60
-120
-180
φ
(deg)
V = 9,900 fps.
0.1
1.0
1.
ωτ₀
10
100
0.1
1.0
AR
(Normalized)
0.01

Fig. 14

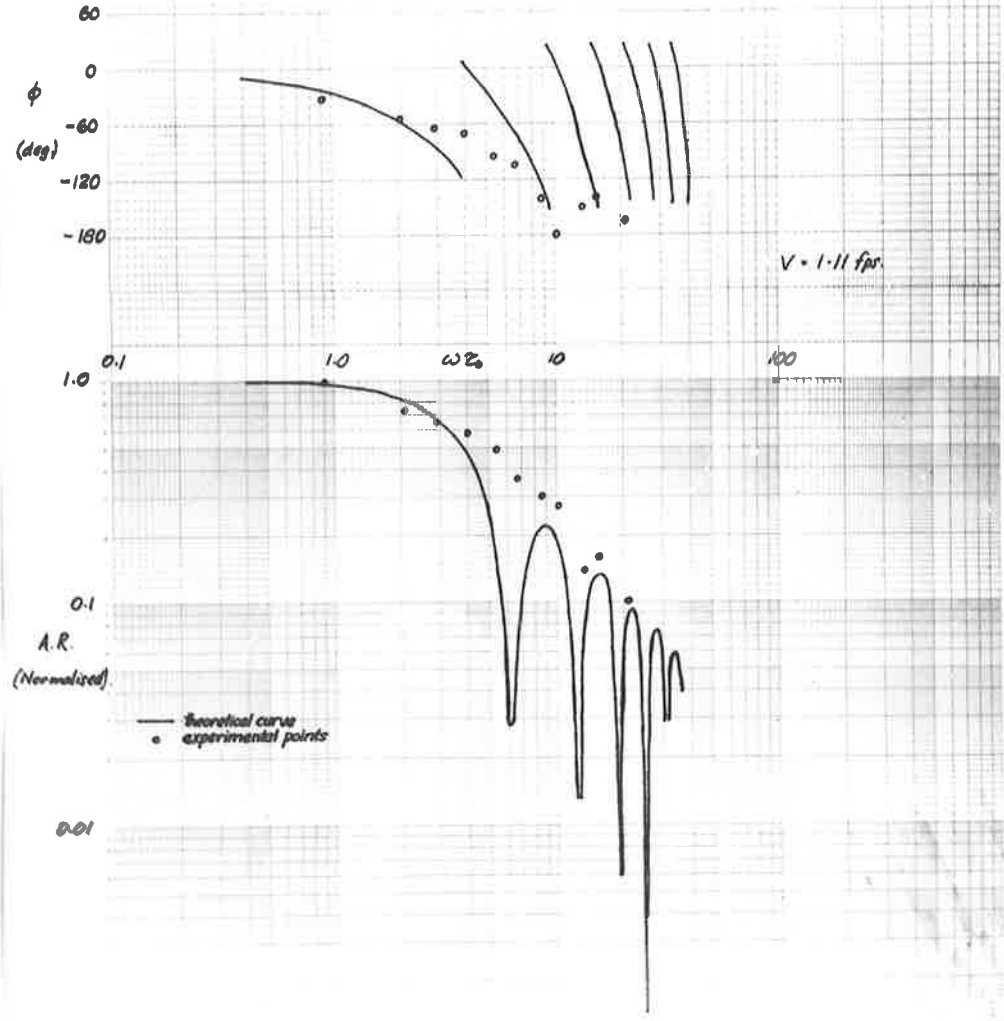
60
0
-60
-120
-180
φ
(deg)
V = 1·11 fps
0·1
1·0
ω τ₀
10
100
1·0
0·1
A.R.
(Normalised)
0·01
Theoretical curve
experimental points

Fig. 15

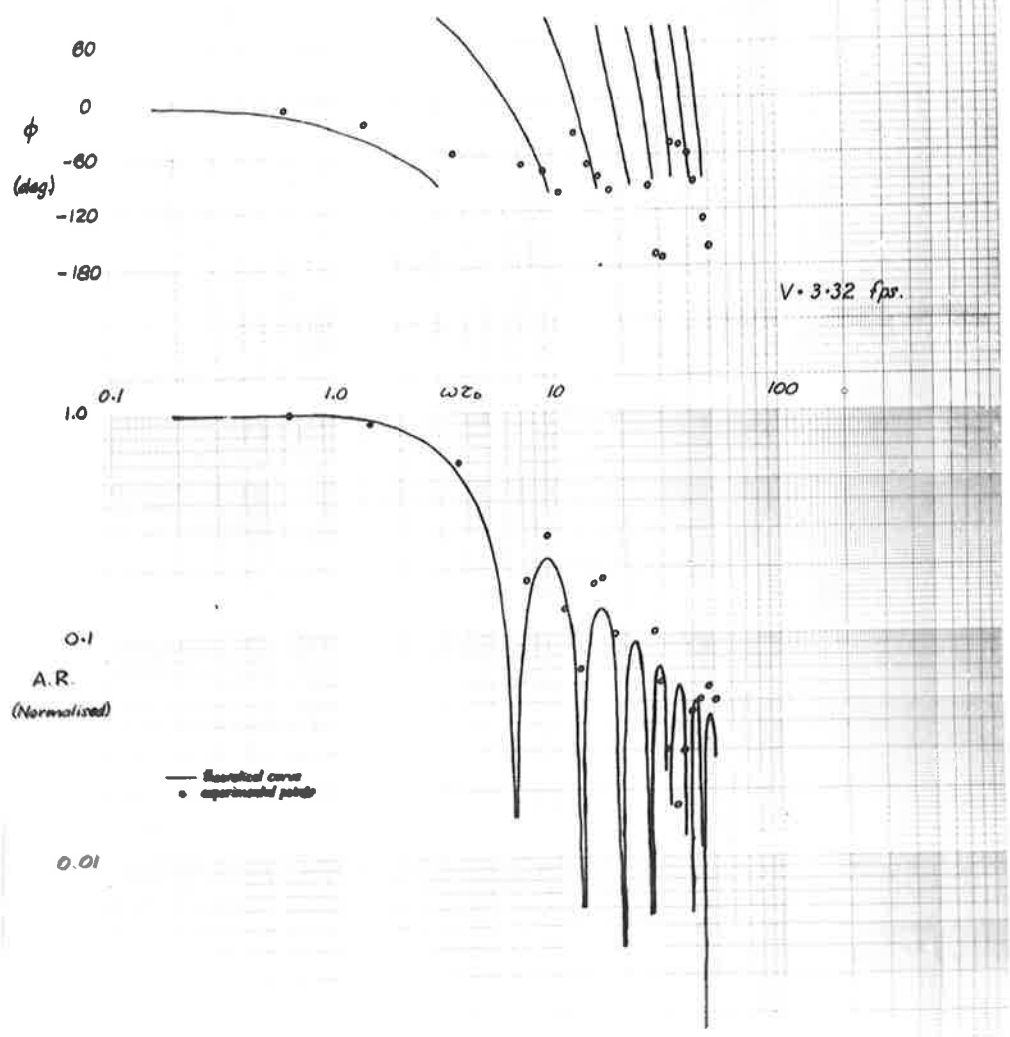
60
0
-60
-120
-180
φ
(deg.)
V • 3·32 fps.
0·1
1.0
ωτ₀
10
100
1.0
0·1
A.R.
(Normalised)
0.01

Fig. 16

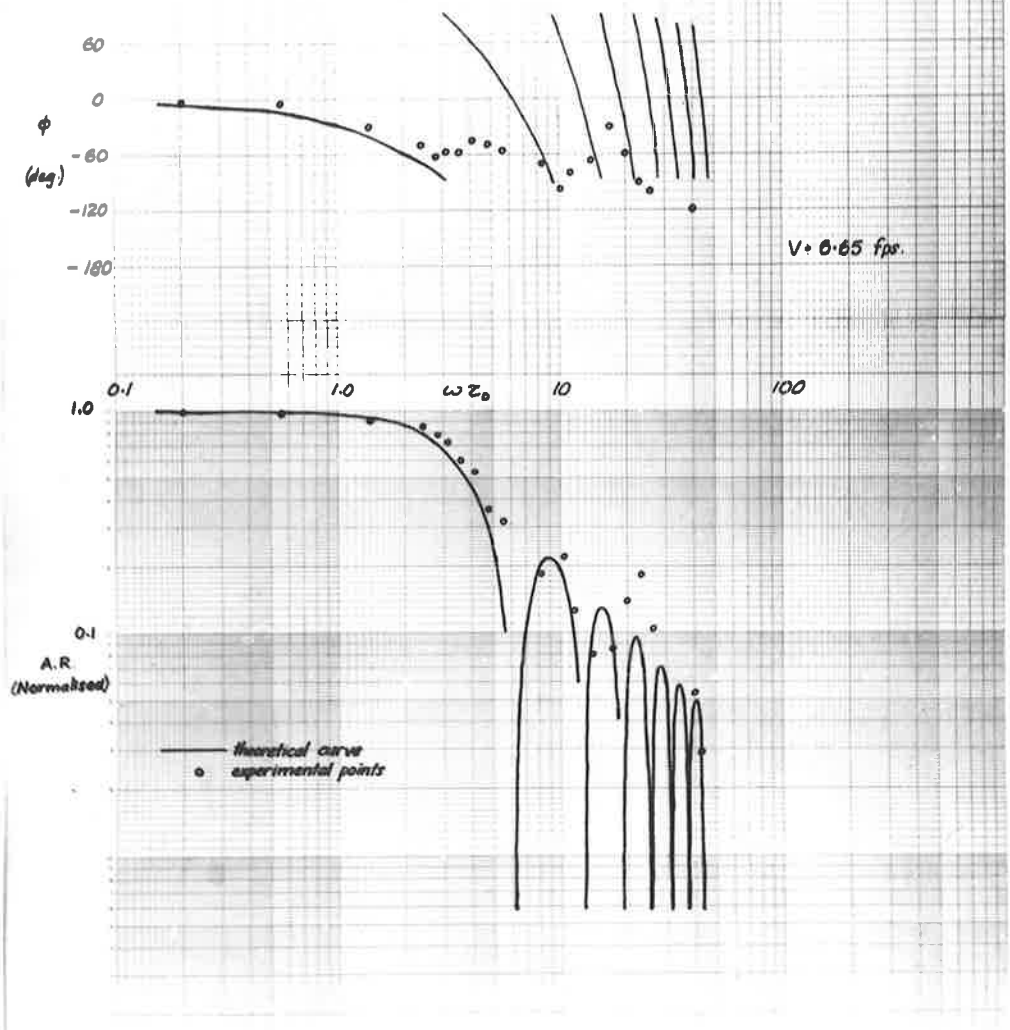
60
0
φ
(deg.)
-60
-120
-180
V = 0·65 fps.
0·1
1·0
ω τ₀
10
100
1·0
0·1
A.R.
(Normalised)
theoretical curve
experimental points

Fig. 17

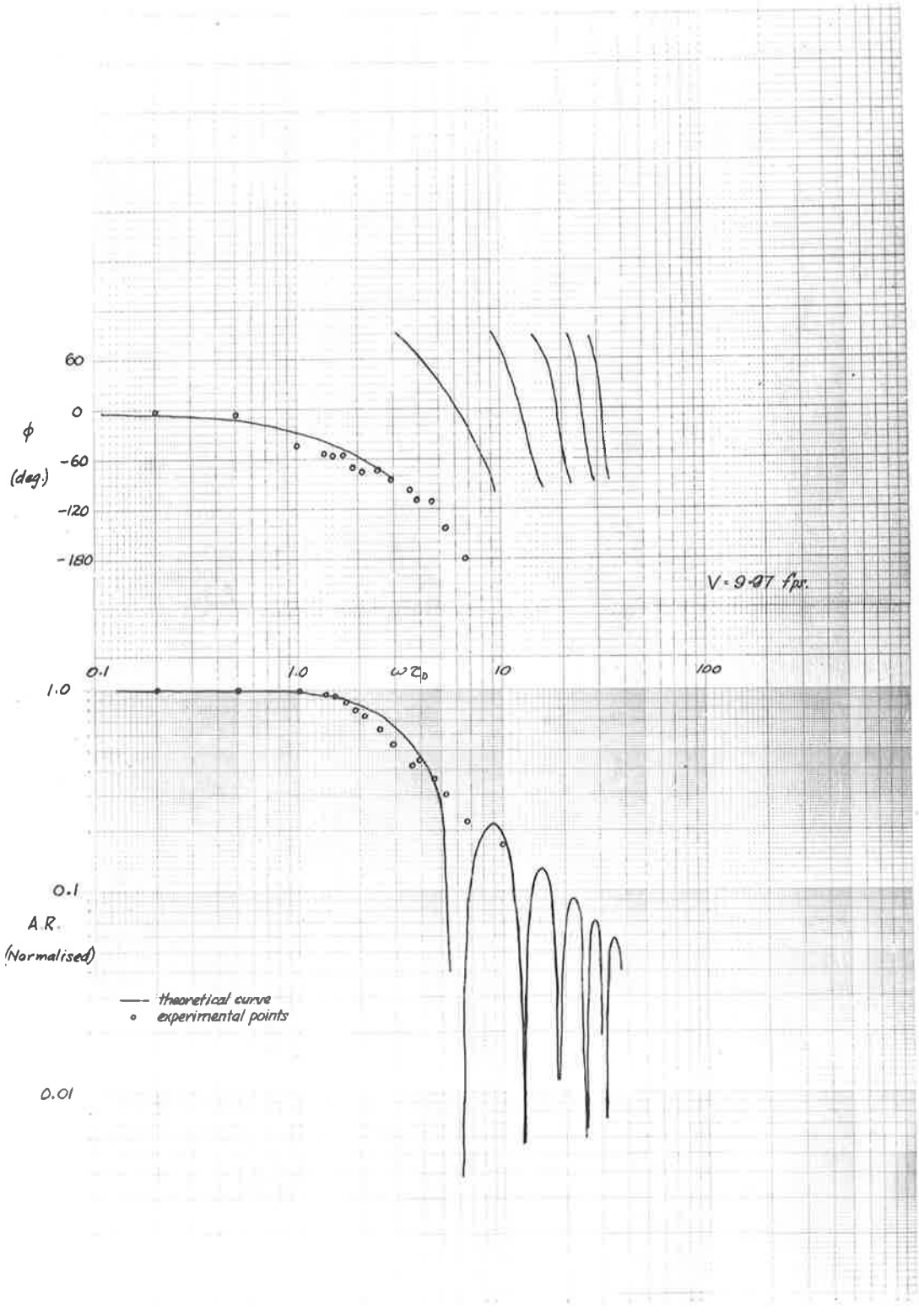
60
0
-60
-120
-180
φ
(deg.)
V = 9.97 fps.
0.1
1.0
ω τ_D
10
100
1.0
0.1
A.R.
(Normalised)
0.01
theoretical curve
experimental points

Fig. 18

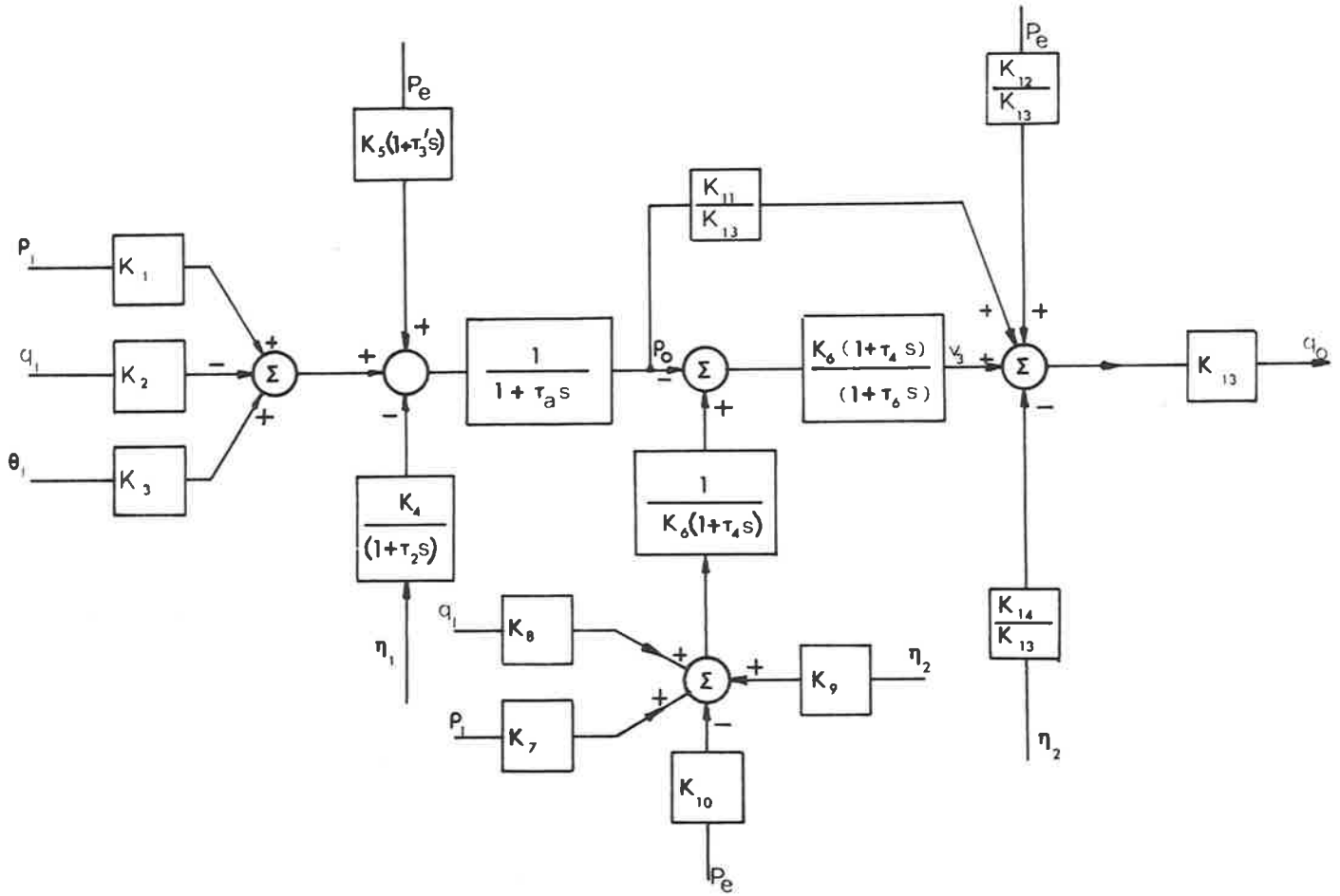

Fig.19 Open-loop block diagram of evaporator.

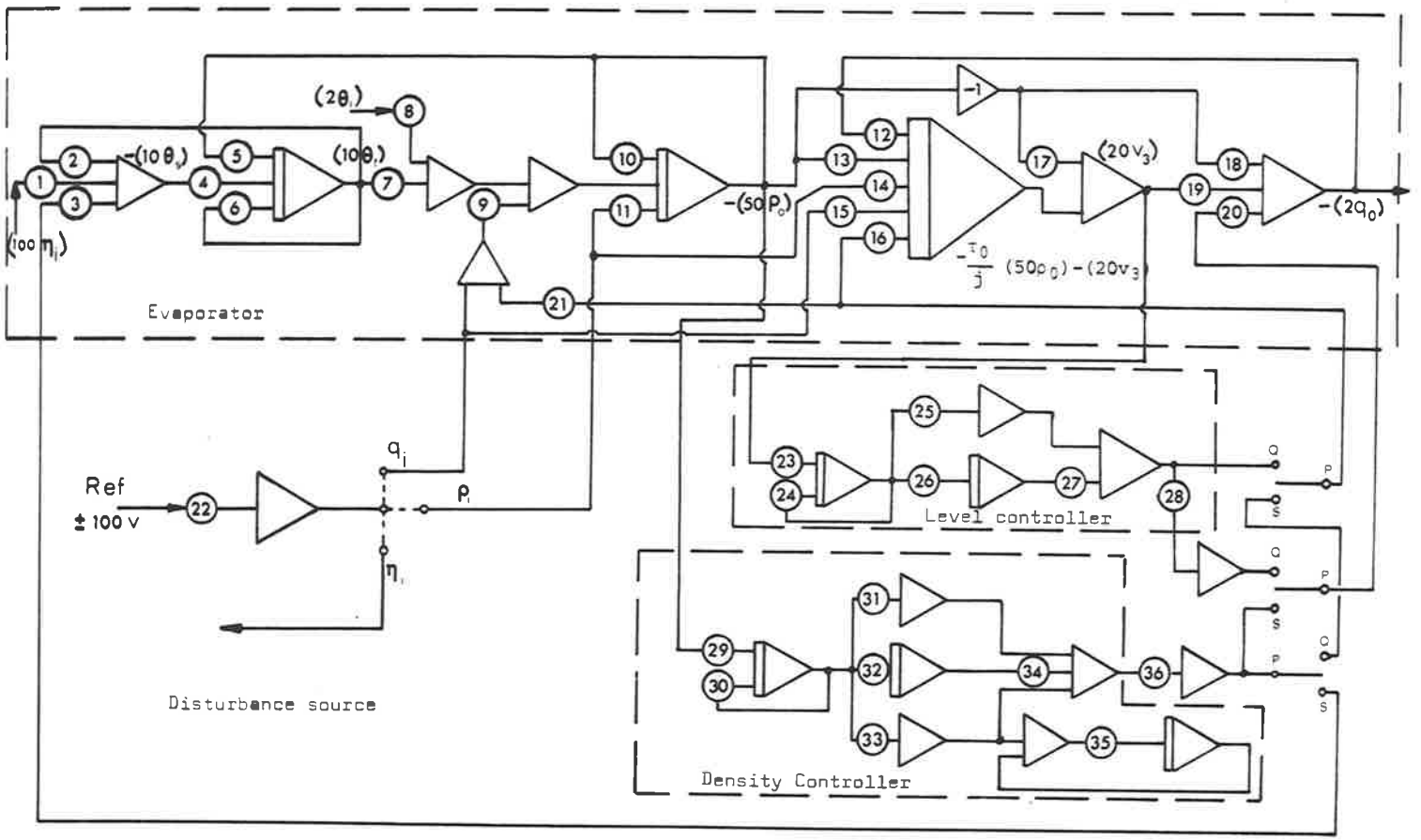

Fig 20. Analogue Computer diagram. Natural-circulation unit with controllers.

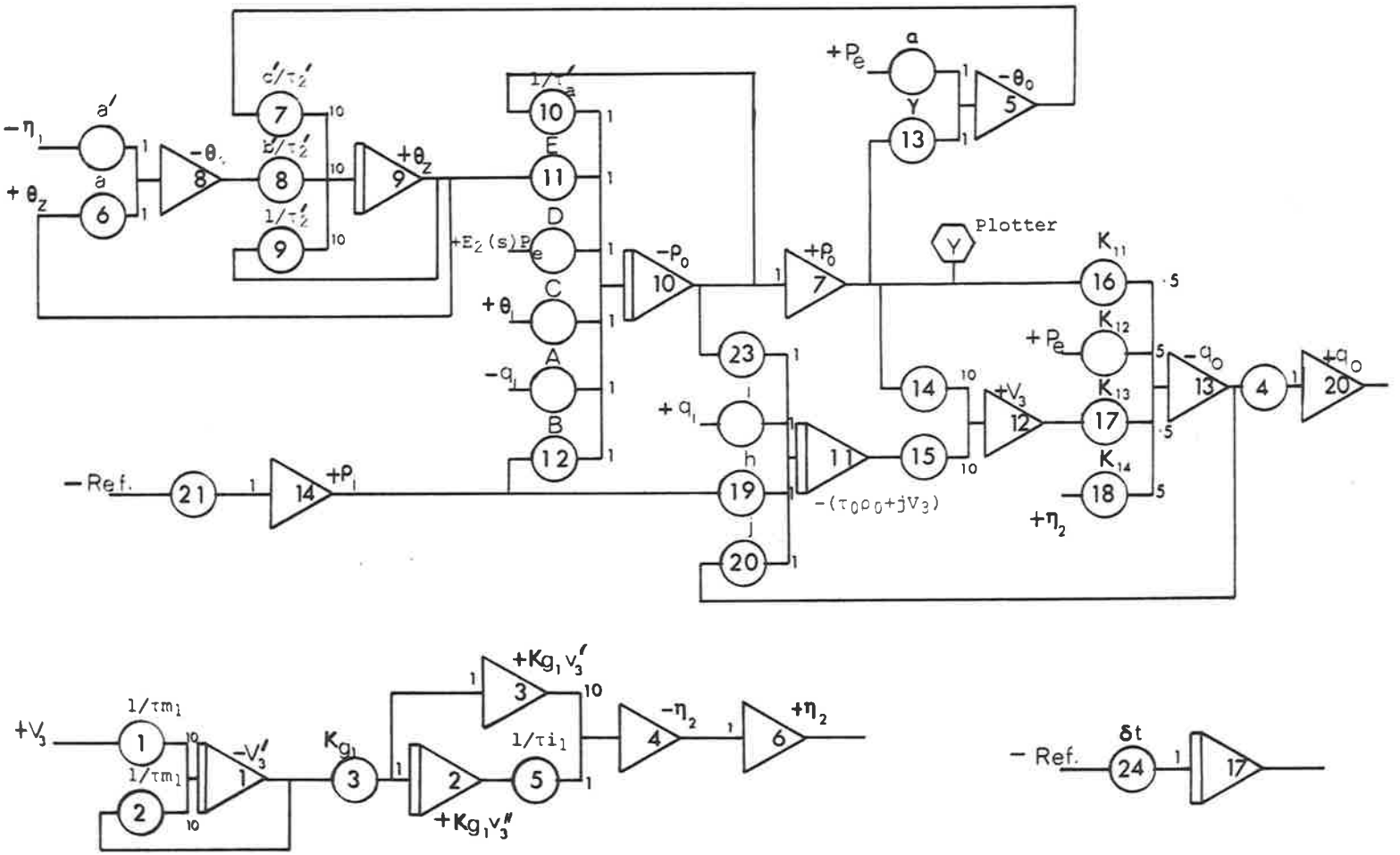

Fig.21. Circuit for use of PACE machines for simulation of standard evaporator and controller.

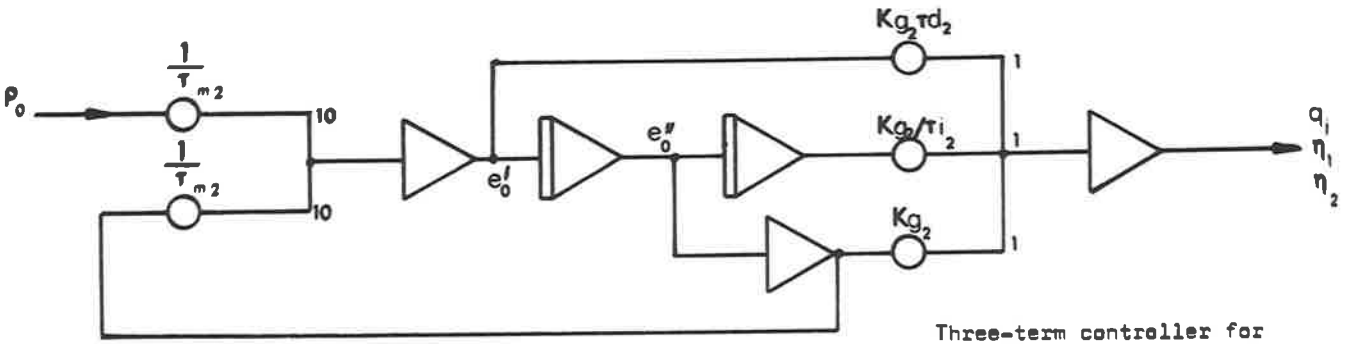

Three-term controller for density loop

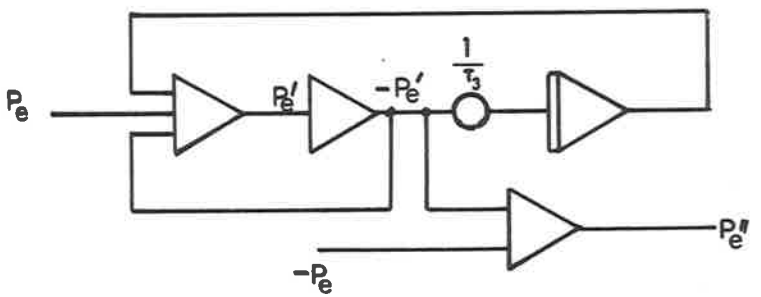

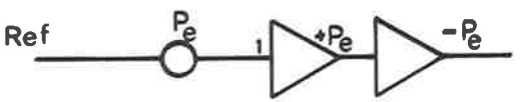

Circuit for generation of Pe.

Fig. 22 Additional circuitry to add three-term density controller and to introduce Pe.

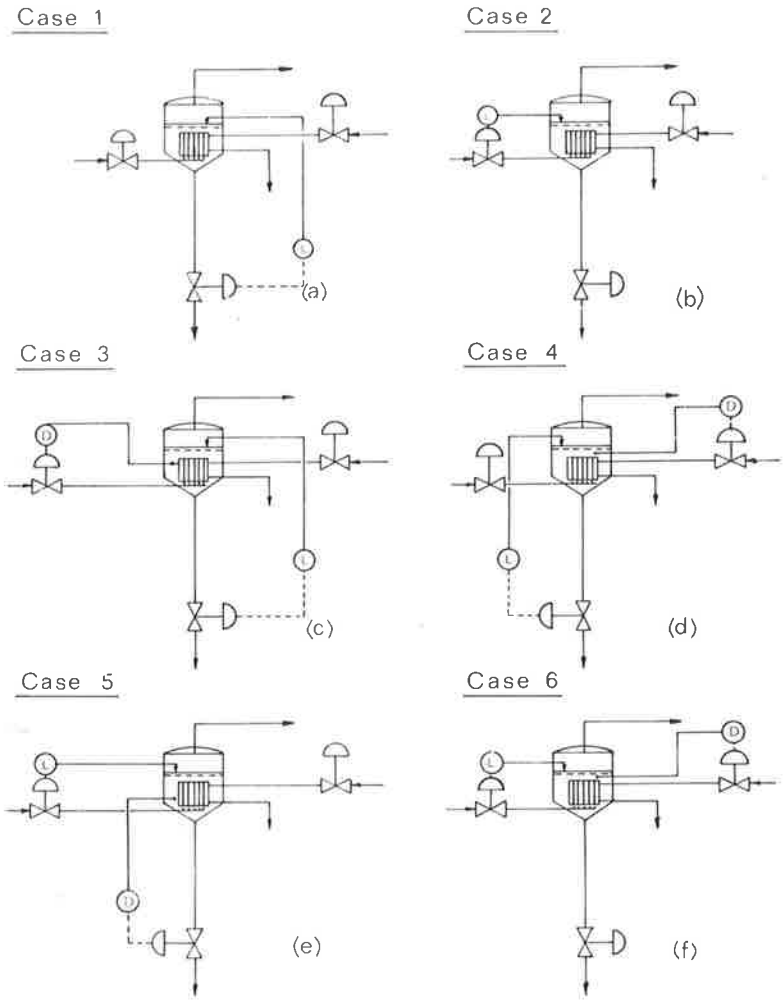

Fig 23. Basic evaporator control schemes.

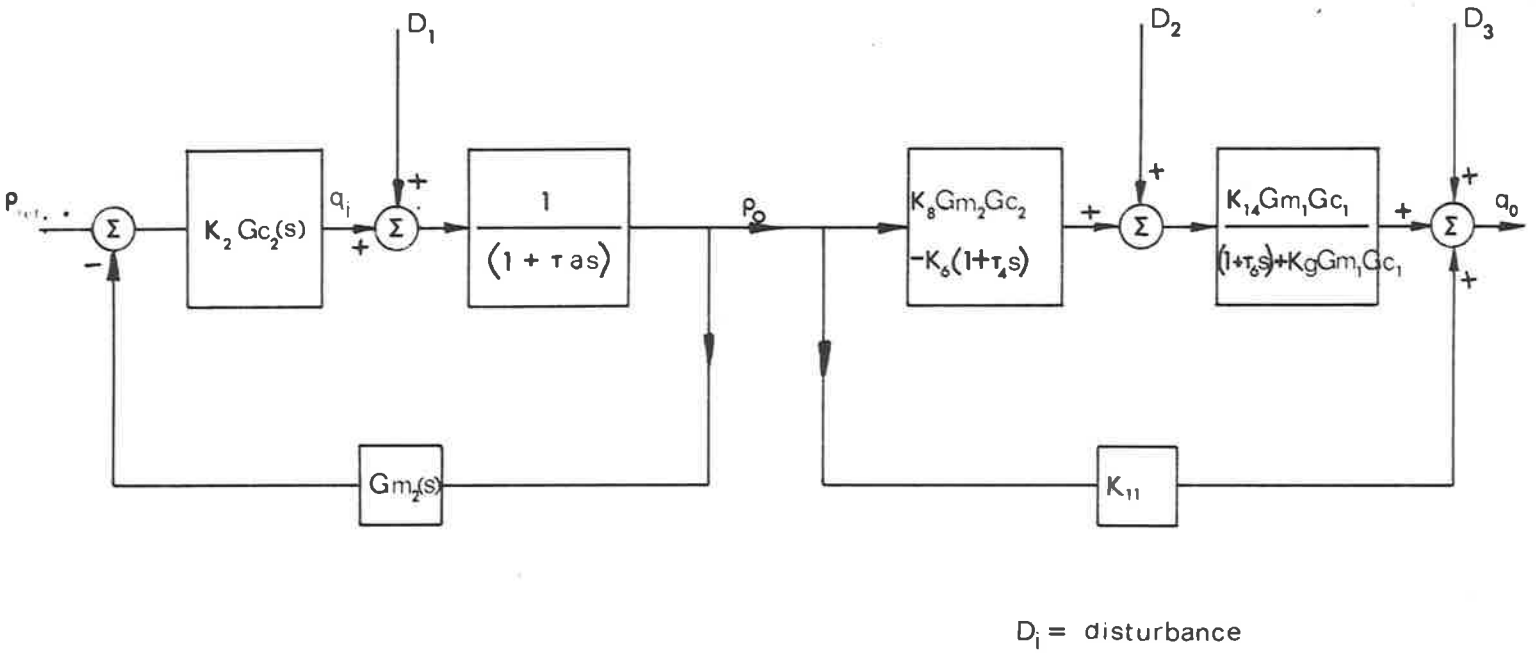

Fig. 24 Closed - loop block diagram of evaporator - Case3.

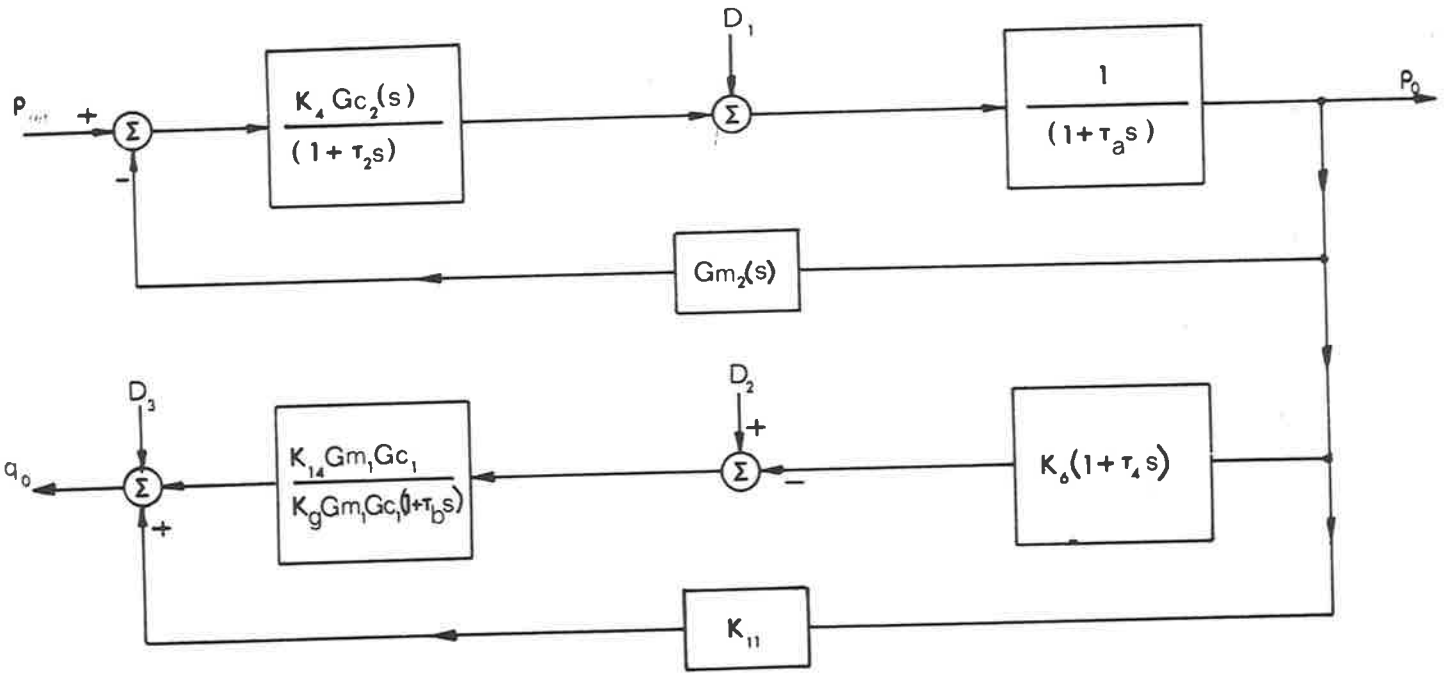

Fig. 25 Closed loop block diagram of evaporator - Case 4.

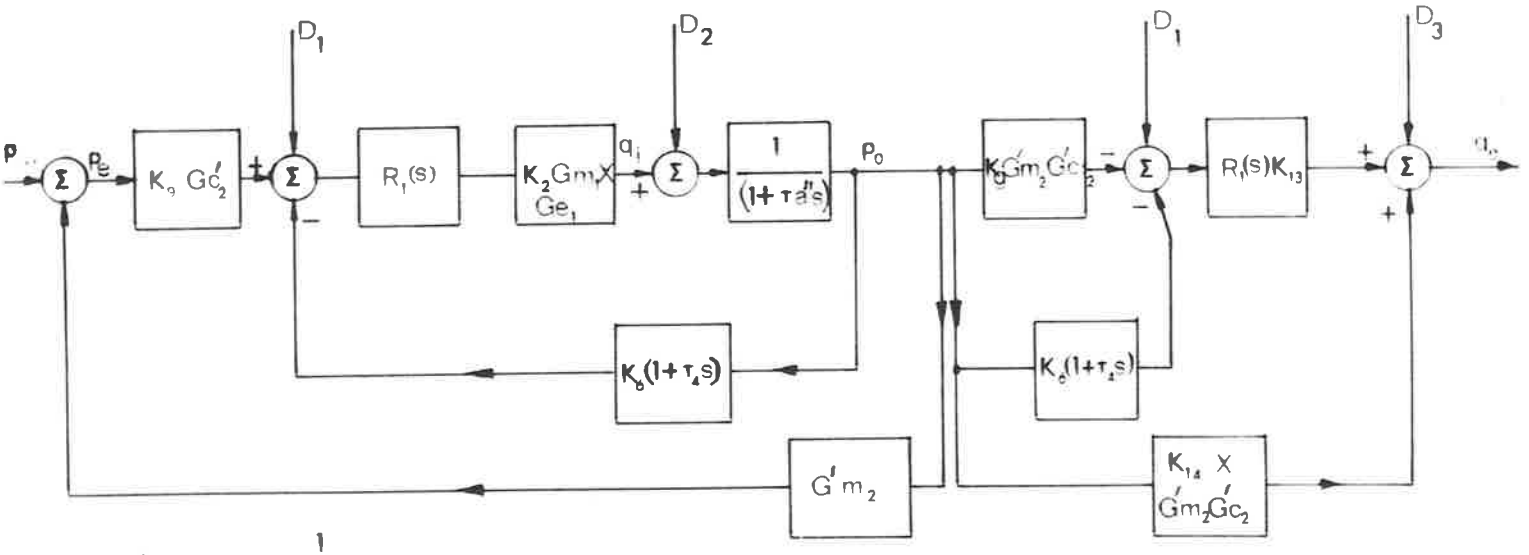

$$R_1(s) = \frac{1}{\tau_0 s - 1 + K_3 G'm_1 Gc_1}$$

$$D_1 = K_7 p_i - K_{10} P_0$$

$$D_2 = K_1 p_1 + K_3 \theta_i - K_5(\tau_3' s - 1) P_e - K_4 \eta_1$$

$$D_3 = K_{12} P_e$$

Fig. 26 Closed - loop block diagram of evaporator - Case 3.

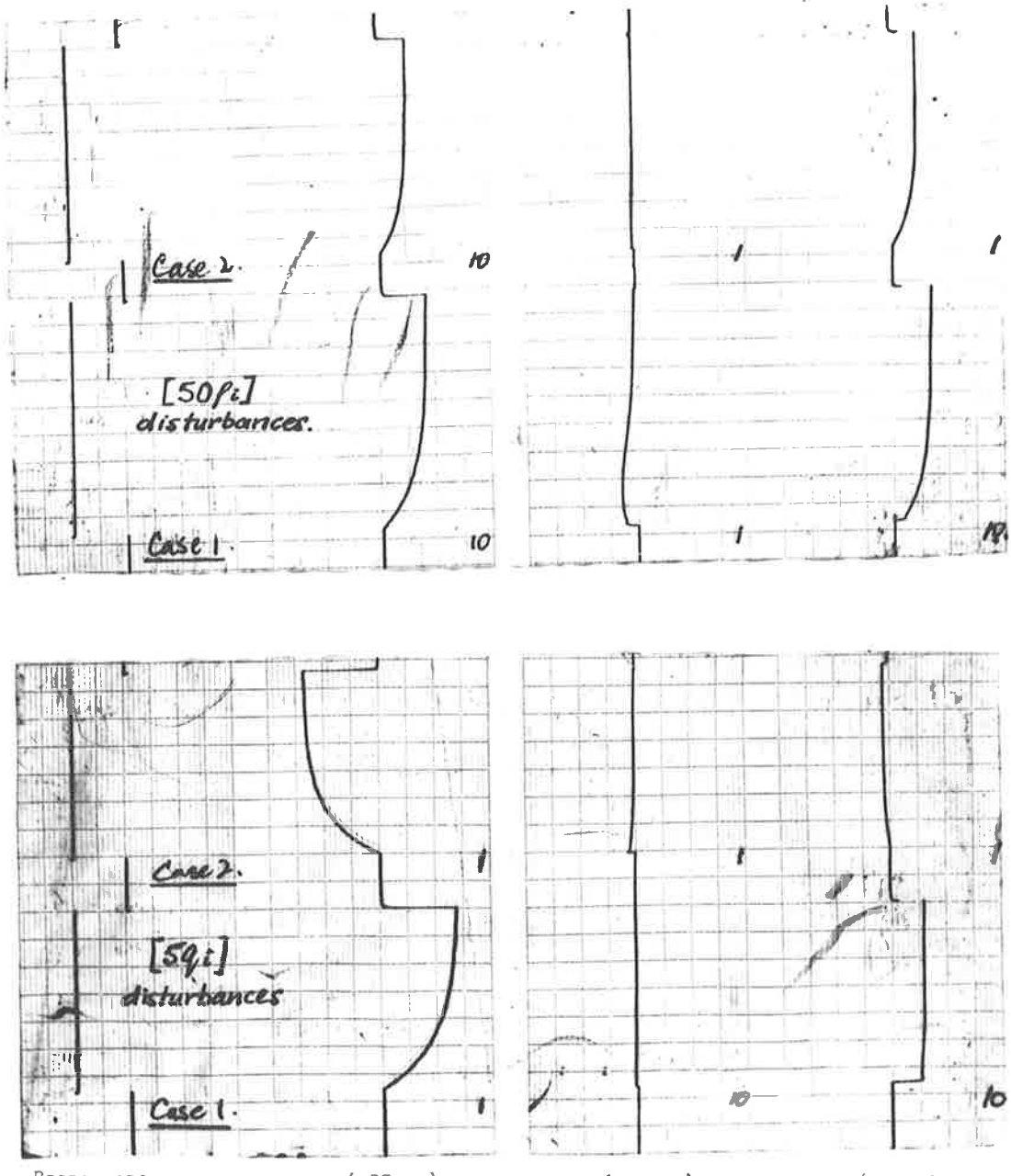

Responses: ($50\rho_0$) ($20\ v_3$) ($5\ c_0$)

Chart Speed: 0.4 mm/sec.

Controller Settings: as published $Kg_1 = 62.3$ $Ti_1 = 0.8$ hours

Fig. 27 Response of control schemes cases 1 & 2 for natural circulation evaporator.

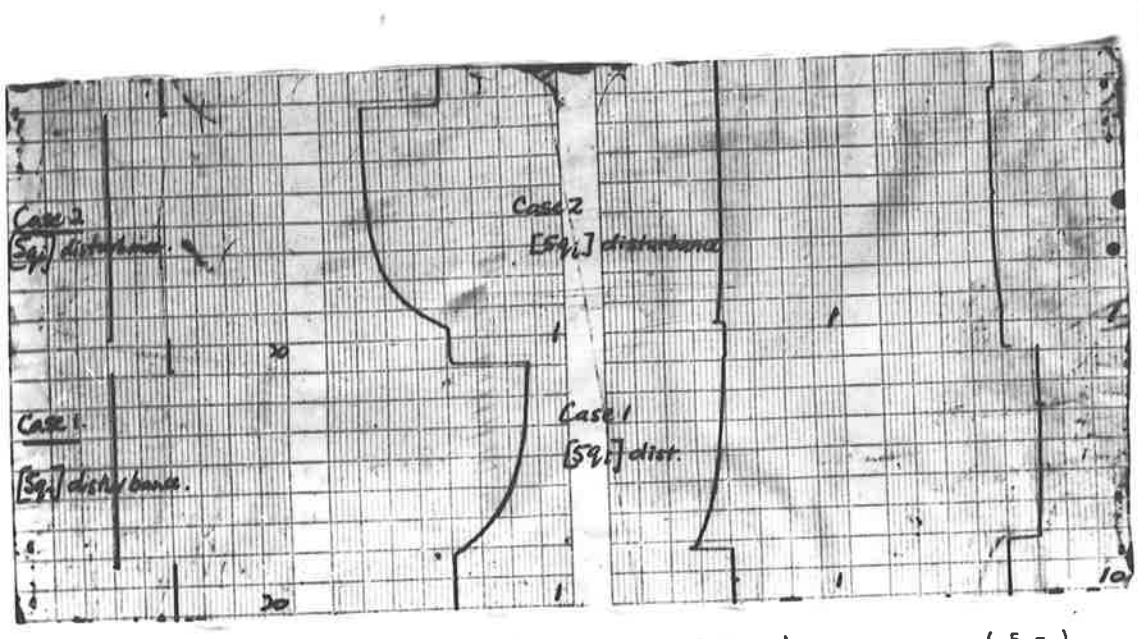

(50ρ) (20 v_3) (5 q_0)

Level Controller Settings: Kg_1 = 57.5
Ti_1 = 0.8 hours

Chart Speed: 0.4 mm/sec.

Fig. 28 Response of control schemes cases 1 & 2 for natural - circulation evaporator.

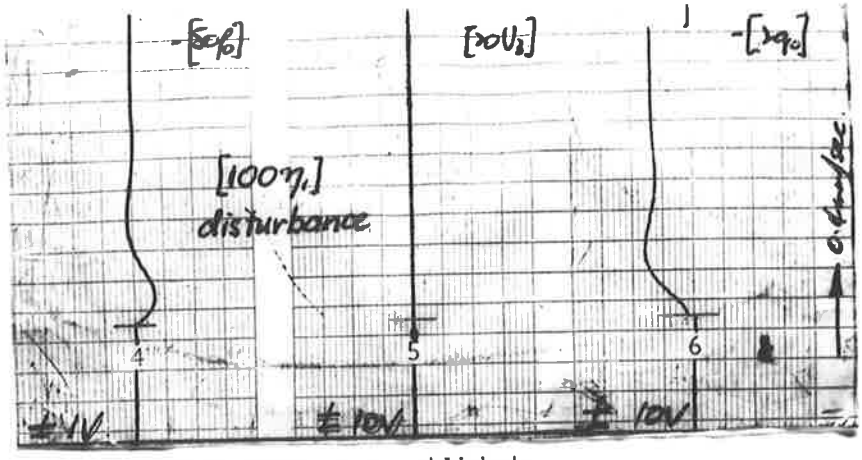

Controller Settings: as published.

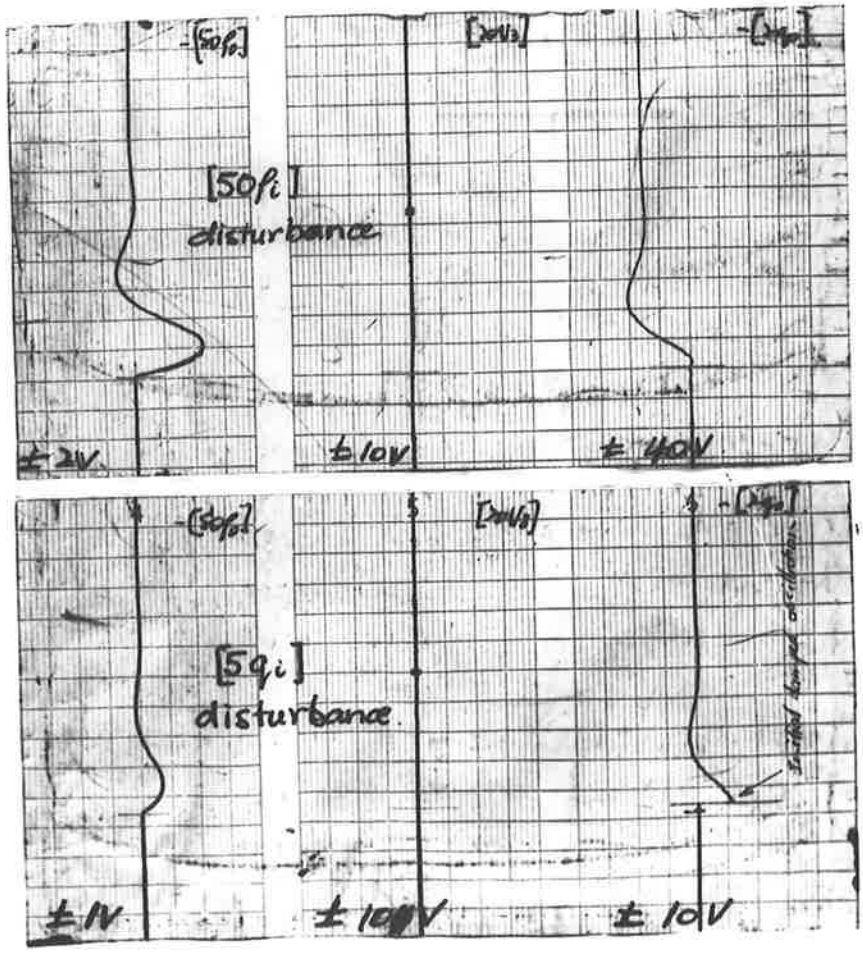

Fig. 29 Response for Case 3, natural circulation evaporators all disturbances.

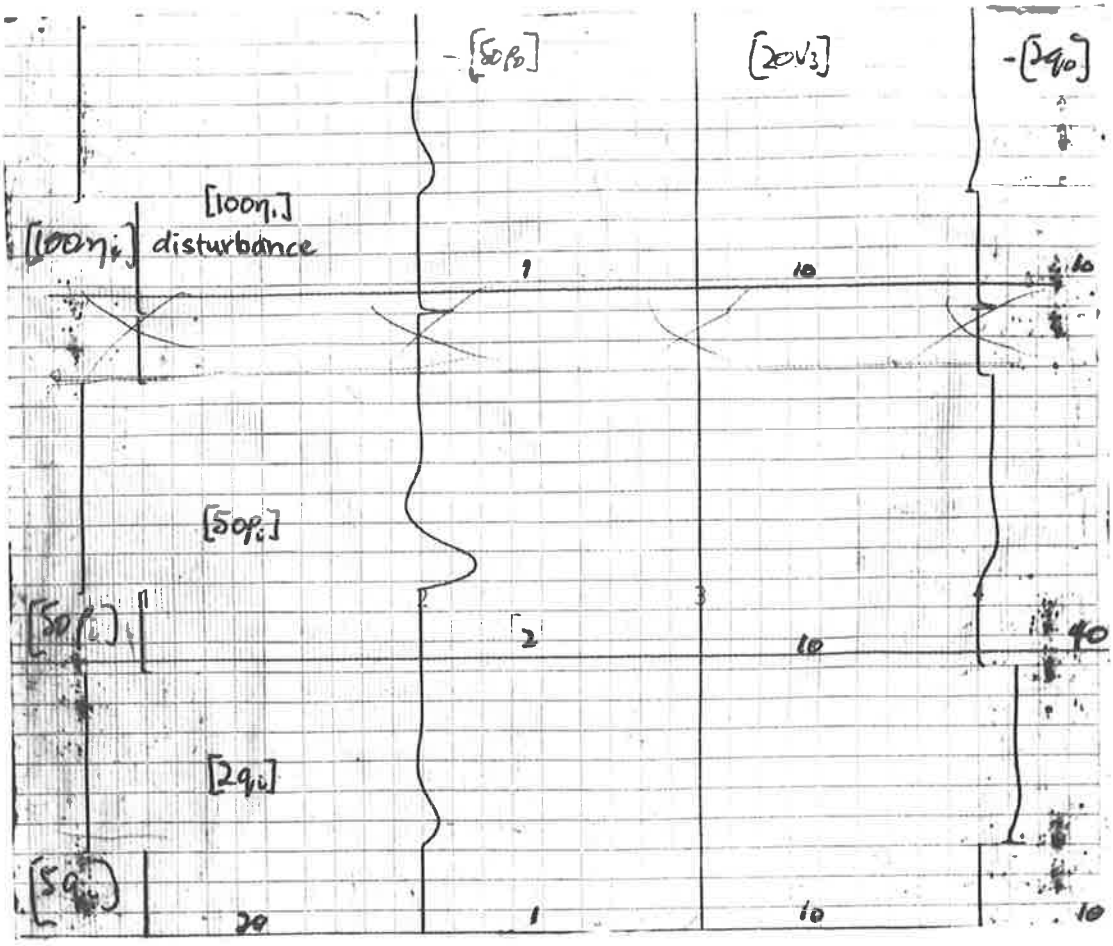

Chart Speed: 0.2 mm/sec.

Controller Settings: as published

K_{g_1} = 62.3
T_{I_1} = 0.8 hours

K_{g_2} = 22.5
T_{I_2} = 0.2 hours
TD_2 = 0.033 hours

Fig. 30 Responses for Case 4 natural - circulation evaporator - all disturbances.

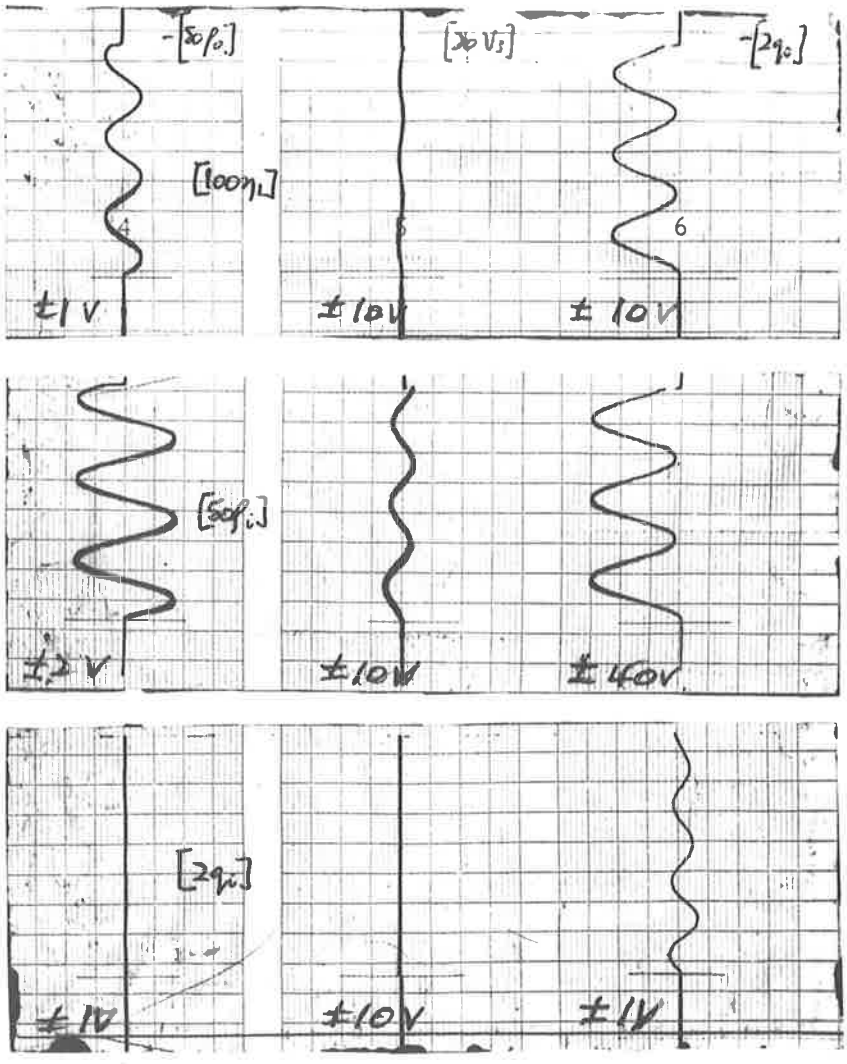

Disturbances(form top) ($100\eta_1$) ($50\rho_i$) ($5q_i$)

Chart Speeds: 0.4 mm/sec.

Controller Settings: as published

Fig. 31 Responses for Case 5 - natural circulation evaporator - all disturbances.

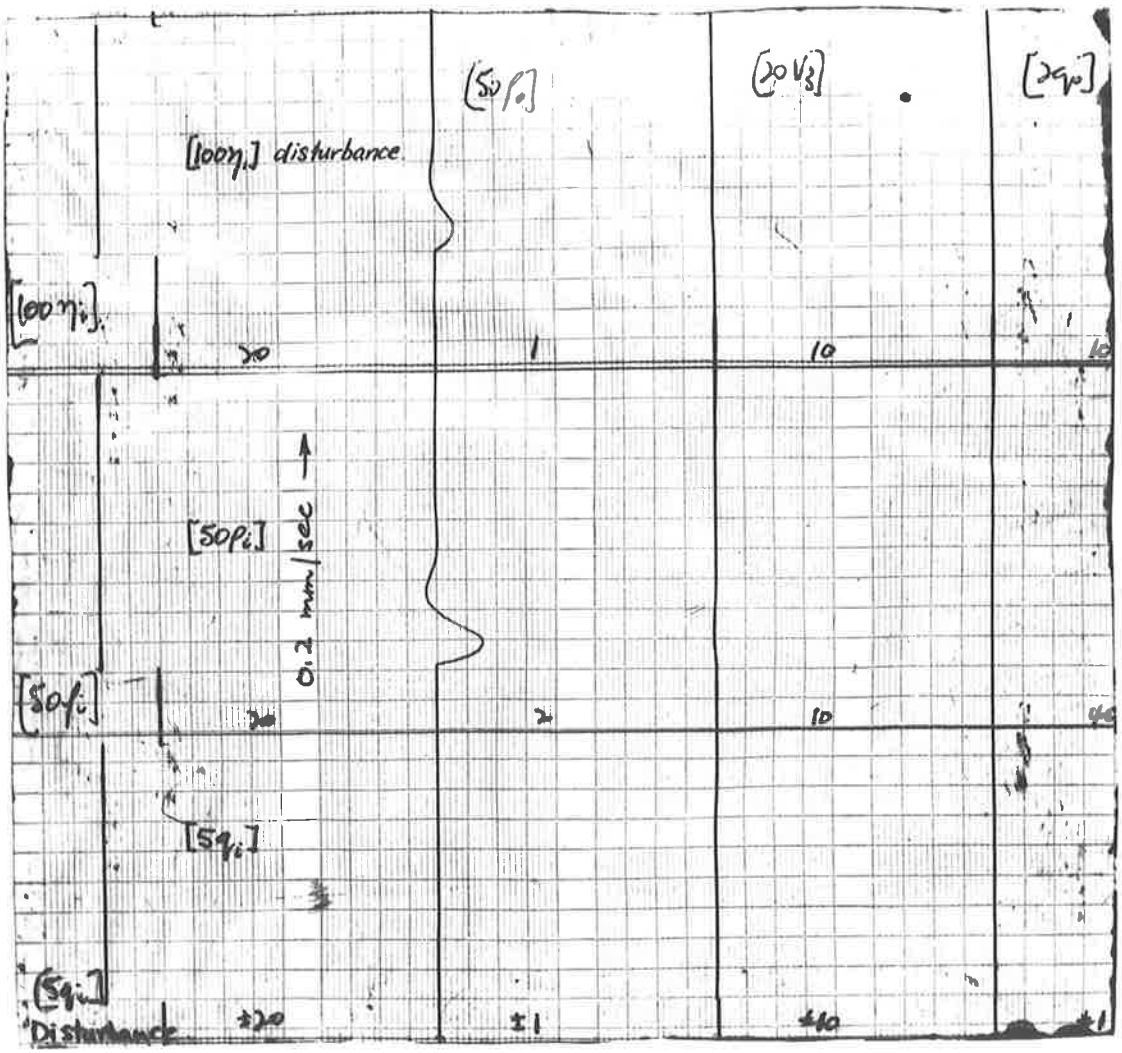

Controller Settings: K_{g1} = 62.3 K_{g2} = 22

Ti_1 = 0.8 hours Ti_2 = 0.2 hours

Td_2 = 0.033 hours

Fig. 32 Case 6. Natural - circulation evaporator.
Responses using settings detailed for
Case 3 - all disturbances.

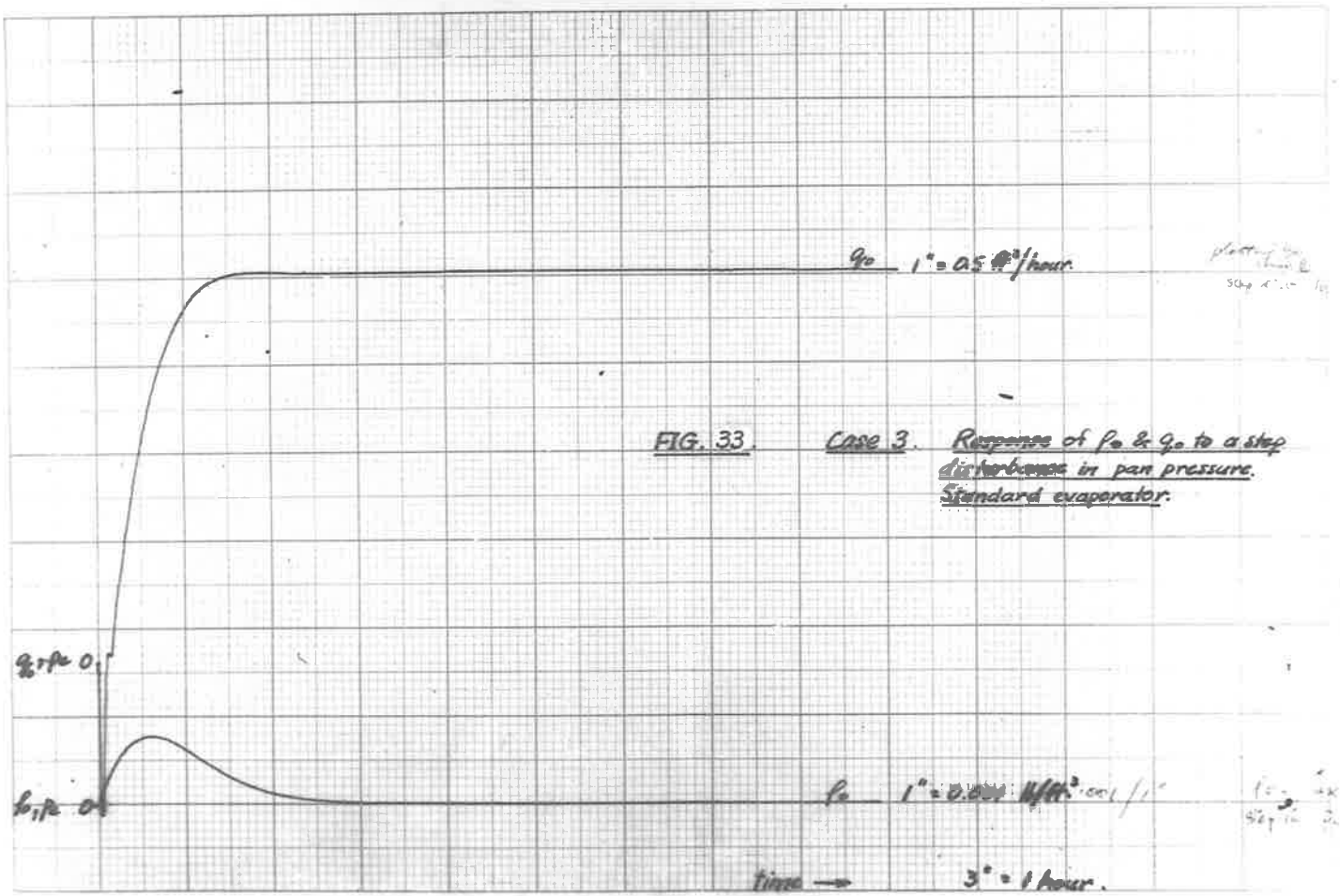

FIG. 33. Case 3. Response of f_o & q_o to a step disturbance in pan pressure. Standard evaporator.

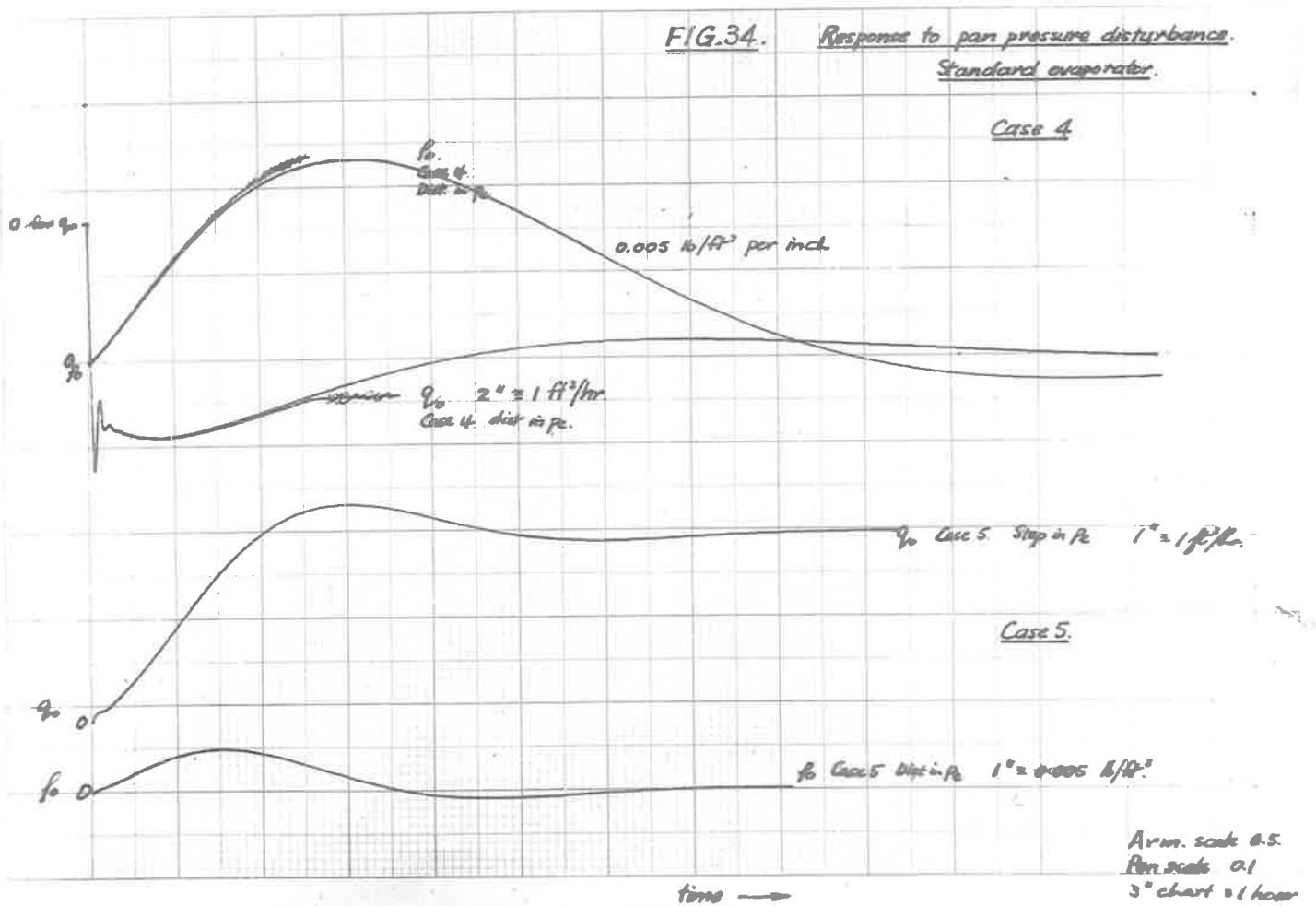

FIG.34. Response to pan pressure disturbance. Standard evaporator.

Arm. scale 0.5
Pan scale 0.1
3" chart = 1 hour

FIG 35. Response of p_o & q_o to step change in pan pressure.
Standard evaporator
Case 6.

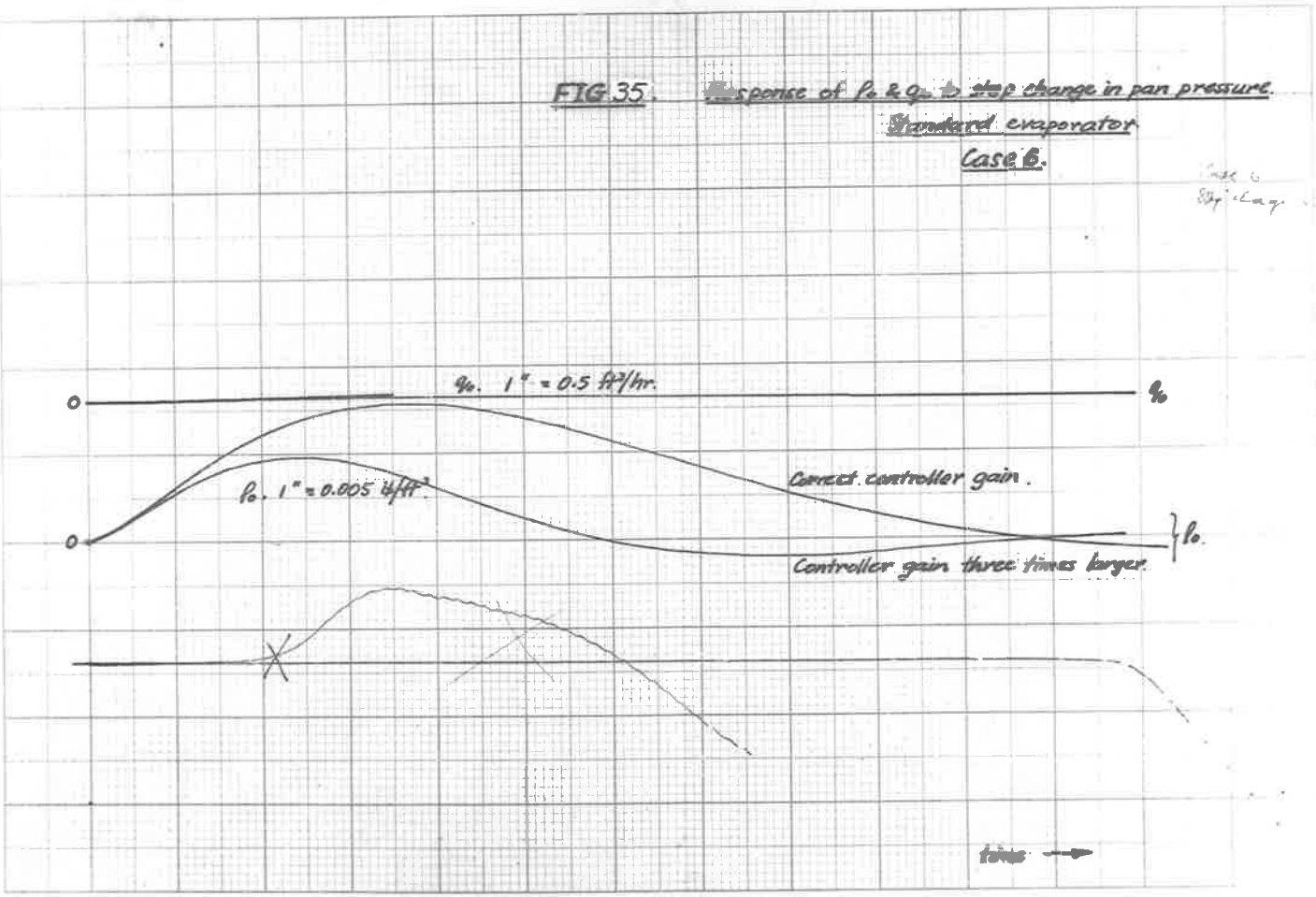

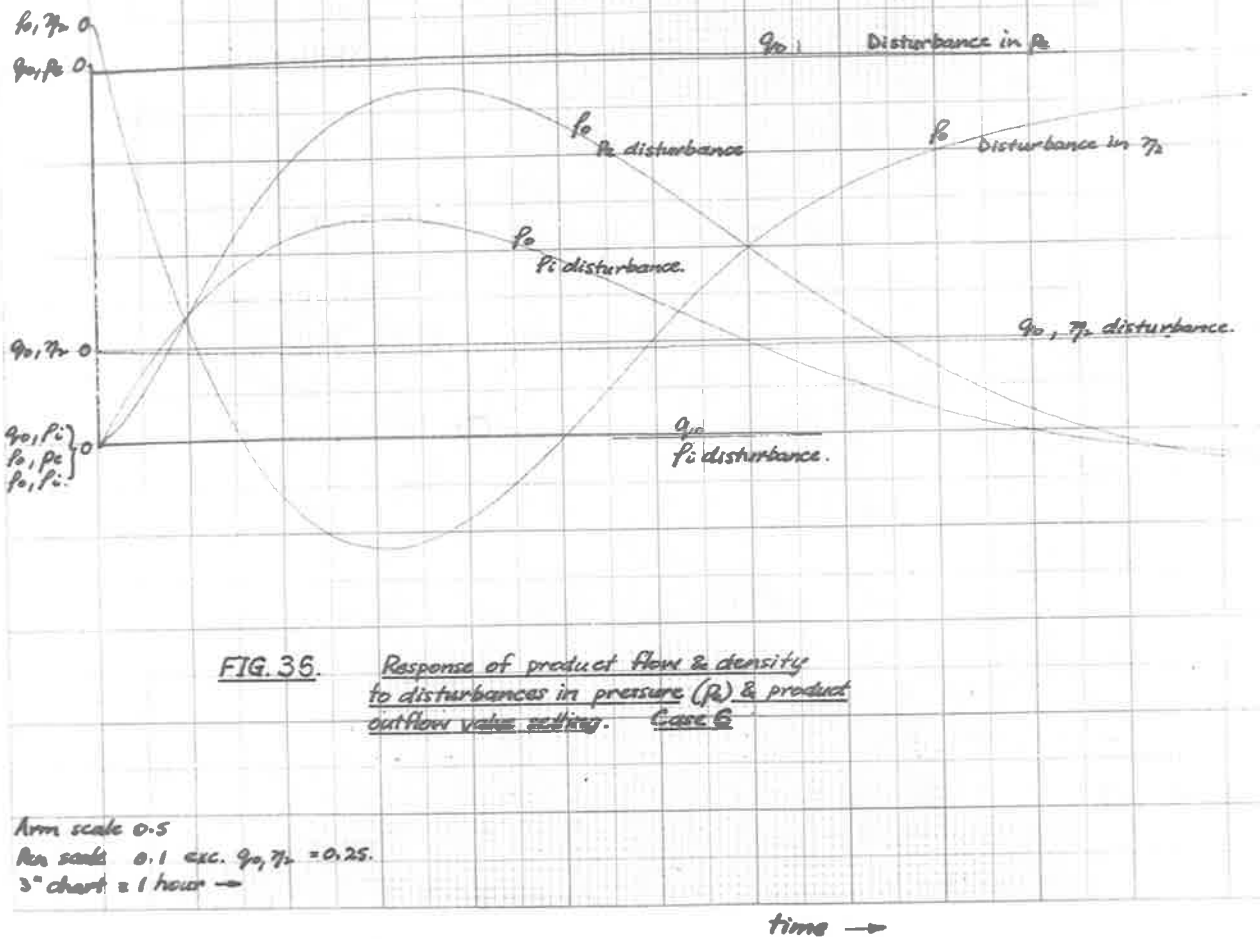

FIG. 36. Response of product flow & density to disturbances in pressure (p_2) & product outflow valve setting. Case 6

Arm scale 0.5
Res scale 0.1 exc. q_o, η_2 = 0.25.
3" chart = 1 hour →

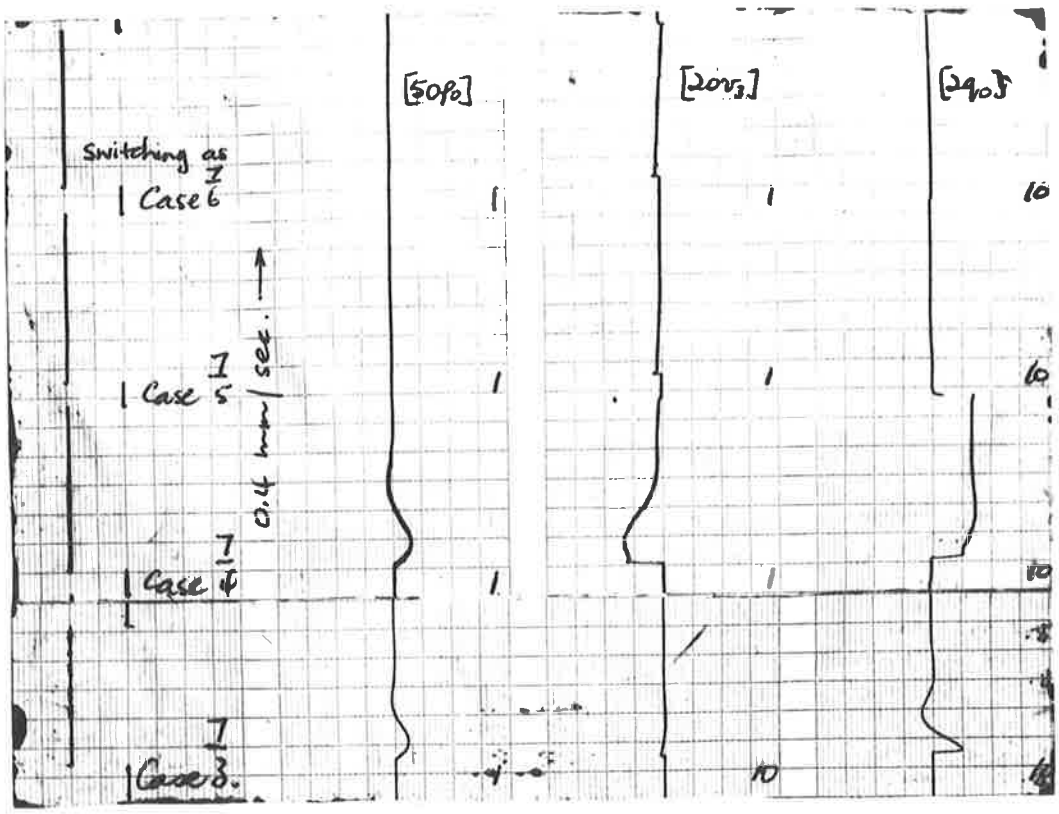

($5q_i$) disturbance

Fig. 37 Cascade control scheme Cases 7 - 3 to 7 - 6.
Response to feed flow disturbance.

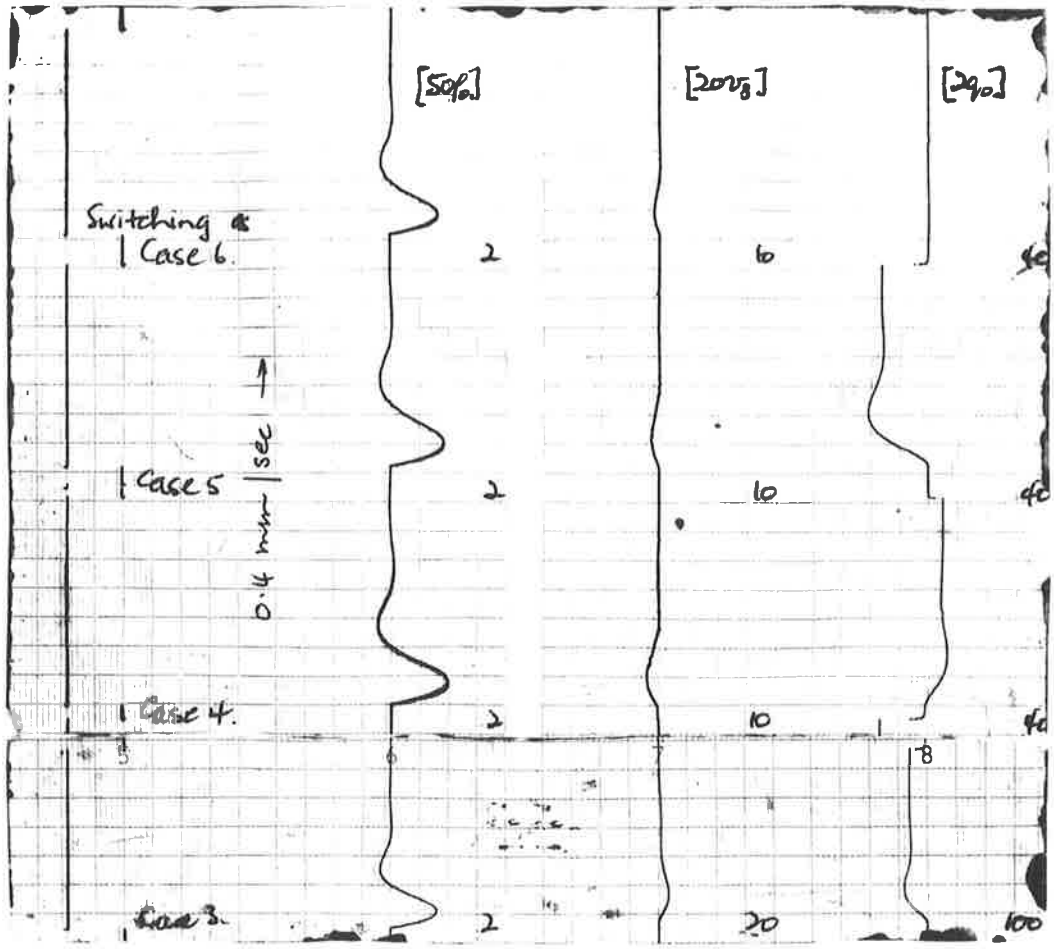

($50\rho_i$) disturbance.

Fig. 38 Cascade control scheme Cases 7 - 3 to 7 - 6.
Response to feed density disturbance.

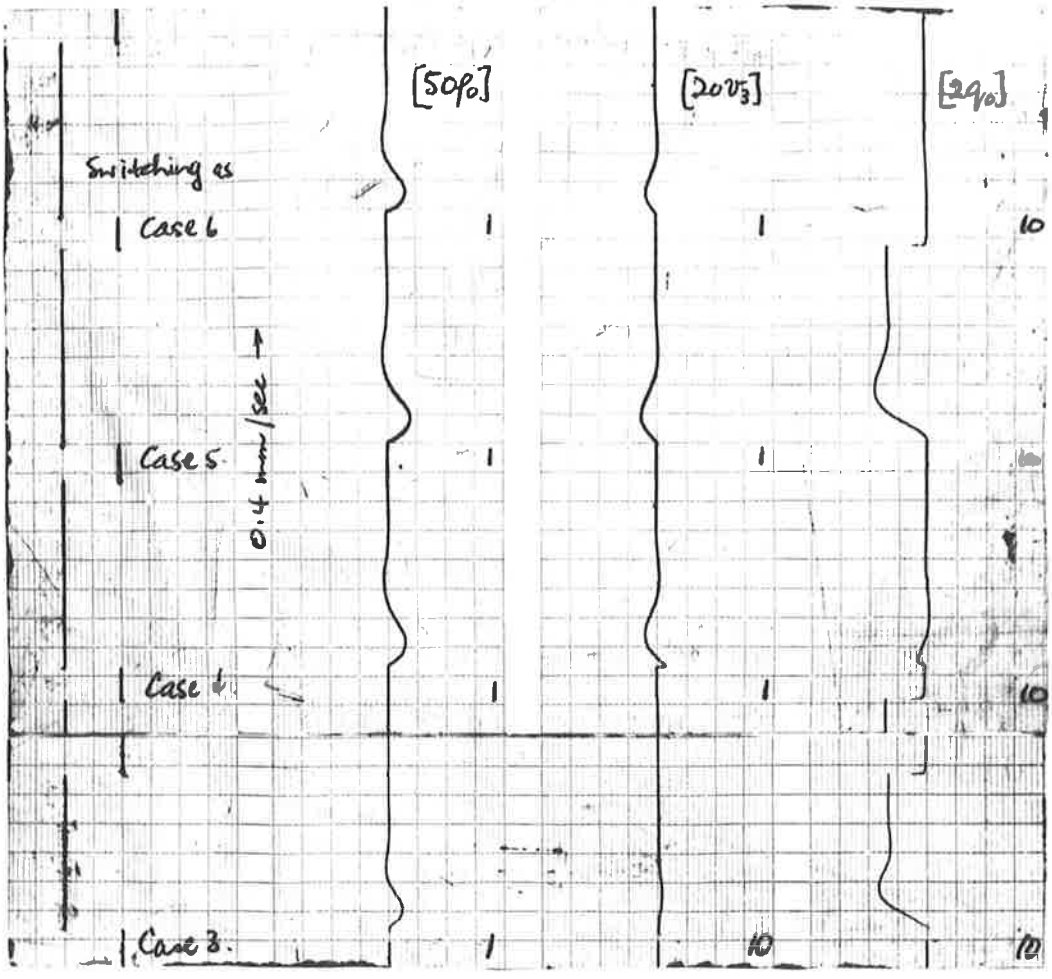

($100\eta_1$) disturbance.

Density controller cascades onto level controller.

Fig. 39 Cascade control scheme Cases 7 - 3 to 7 - 6

Response to steam supply disturbance.

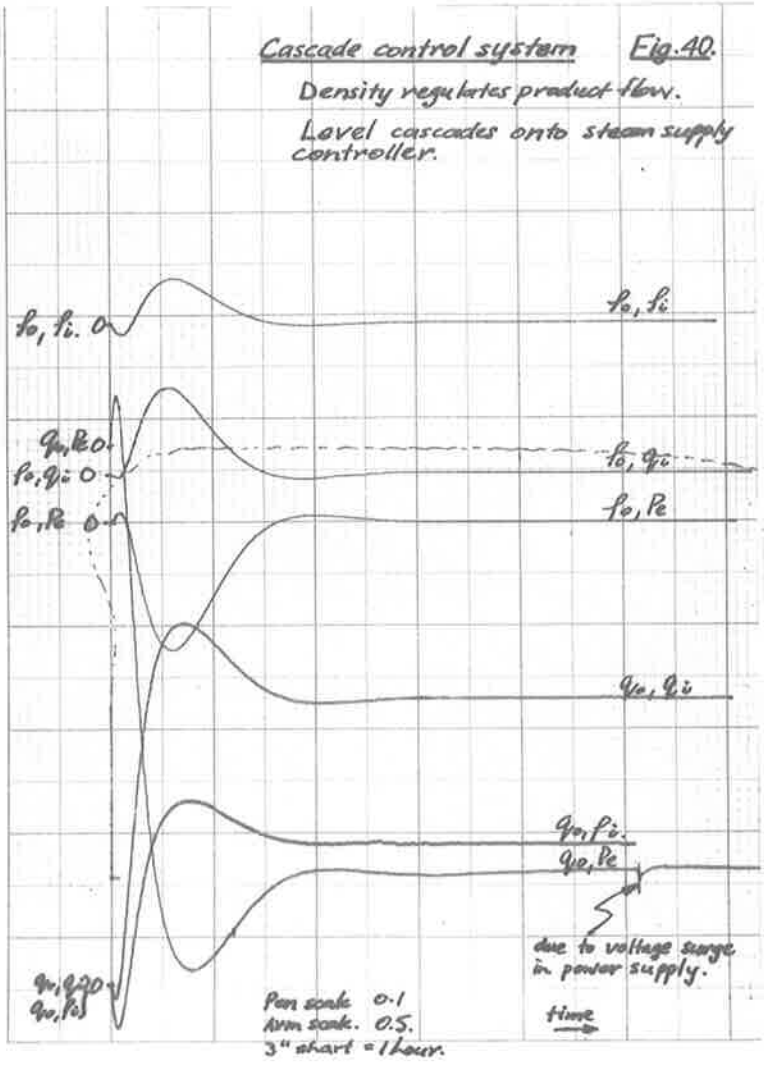
Cascade control system Fig.40.
Density regulates product flow.
Level cascades onto steam supply controller.
f_o, f_i. 0
f_o, f_i
q_o, q_i 0
f_o, q_i
f_o, P_e 0
f_o, P_e
q_o, q_i
q_o, P_i.
q_o, P_e
due to voltage surge in power supply.
q_o, q_i 0
q_o, P_e
Pen scale 0.1
Arm scale. 0.5.
3" chart = 1 hour.
time

FIG. 41. Feed-forward control.
Case 3 with density modifying level controller.

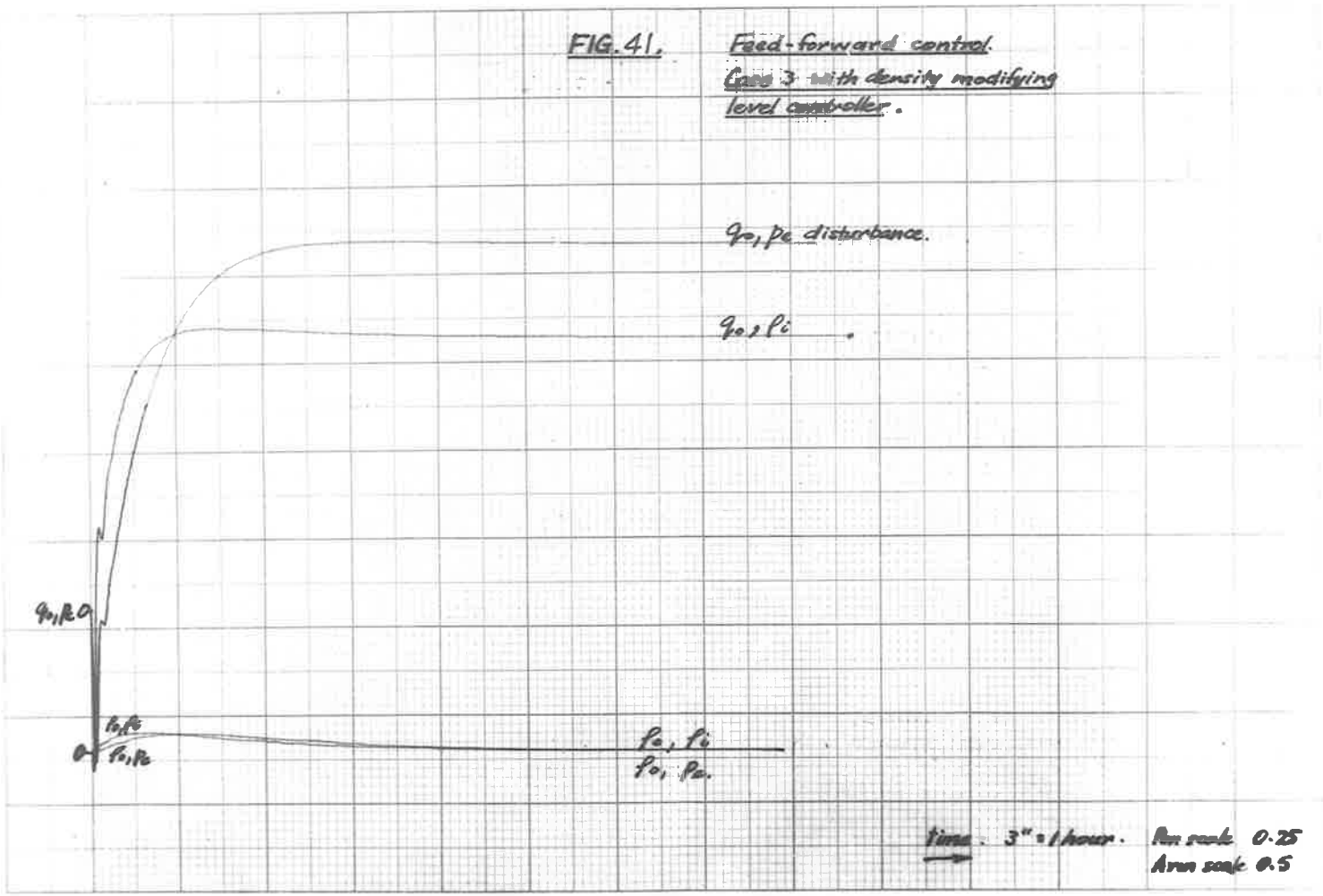

FIG. 42.

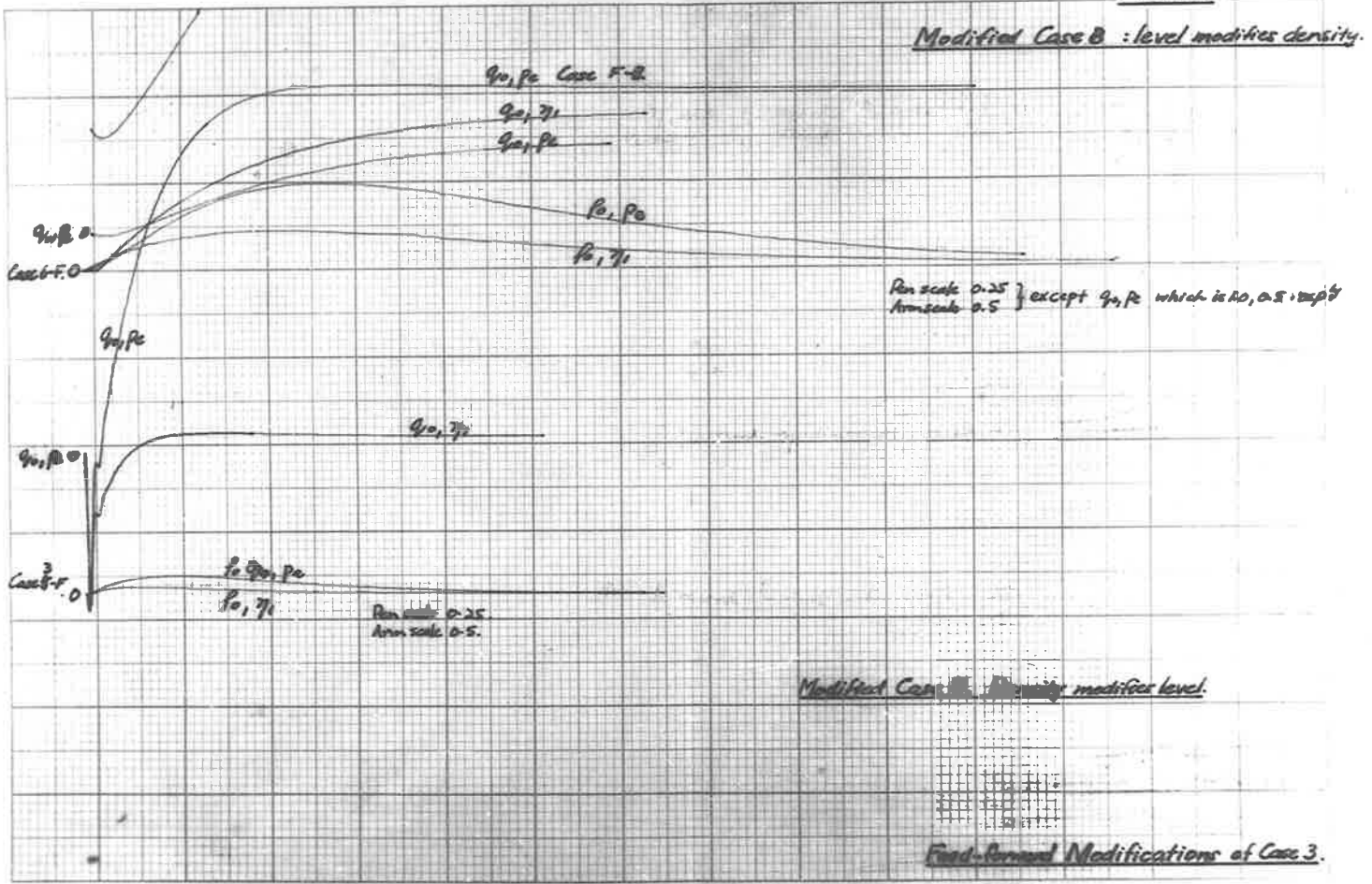
Modified Case 8 : level modifies density.
q_0, p_e Case F-8
q_0, η_1
q_0, p_e
p_0, p_0
p_0, η_1
$q_0 p_0$
Case 6-F.0
Pen scale 0.25
Arm scale 0.5
except q_0, p_e which is 1.0, 0.5 respectively
q_0, p_e
q_0, η_1
q_0, p_e
Case 3-F.0
p_0 q_0, p_e
p_0, η_1
Pen scale 0.25
Arm scale 0.5.
Modified Case [redacted] modifies level.
Feed-forward Modifications of Case 3.

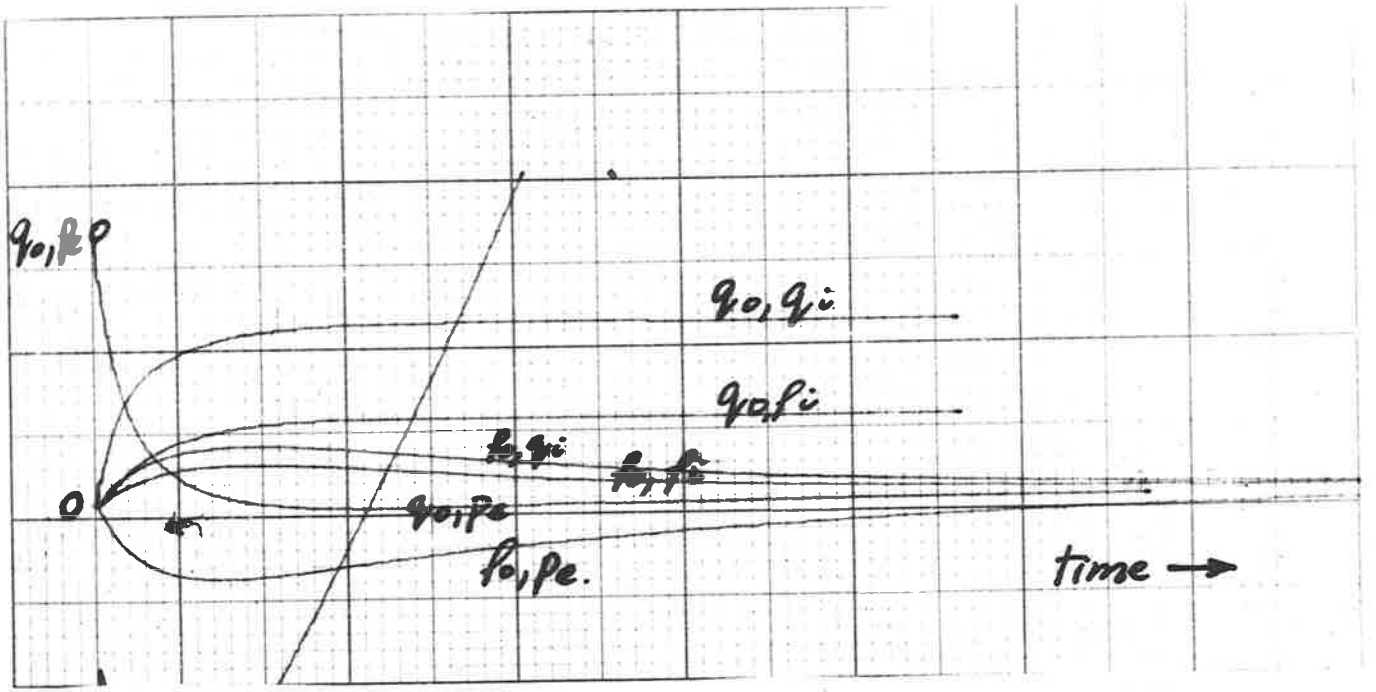

FIG.43. Case 4 : level modifies density.

Pen scale 0.25
Arm scale 0.5.
3" chart = 1 hour.

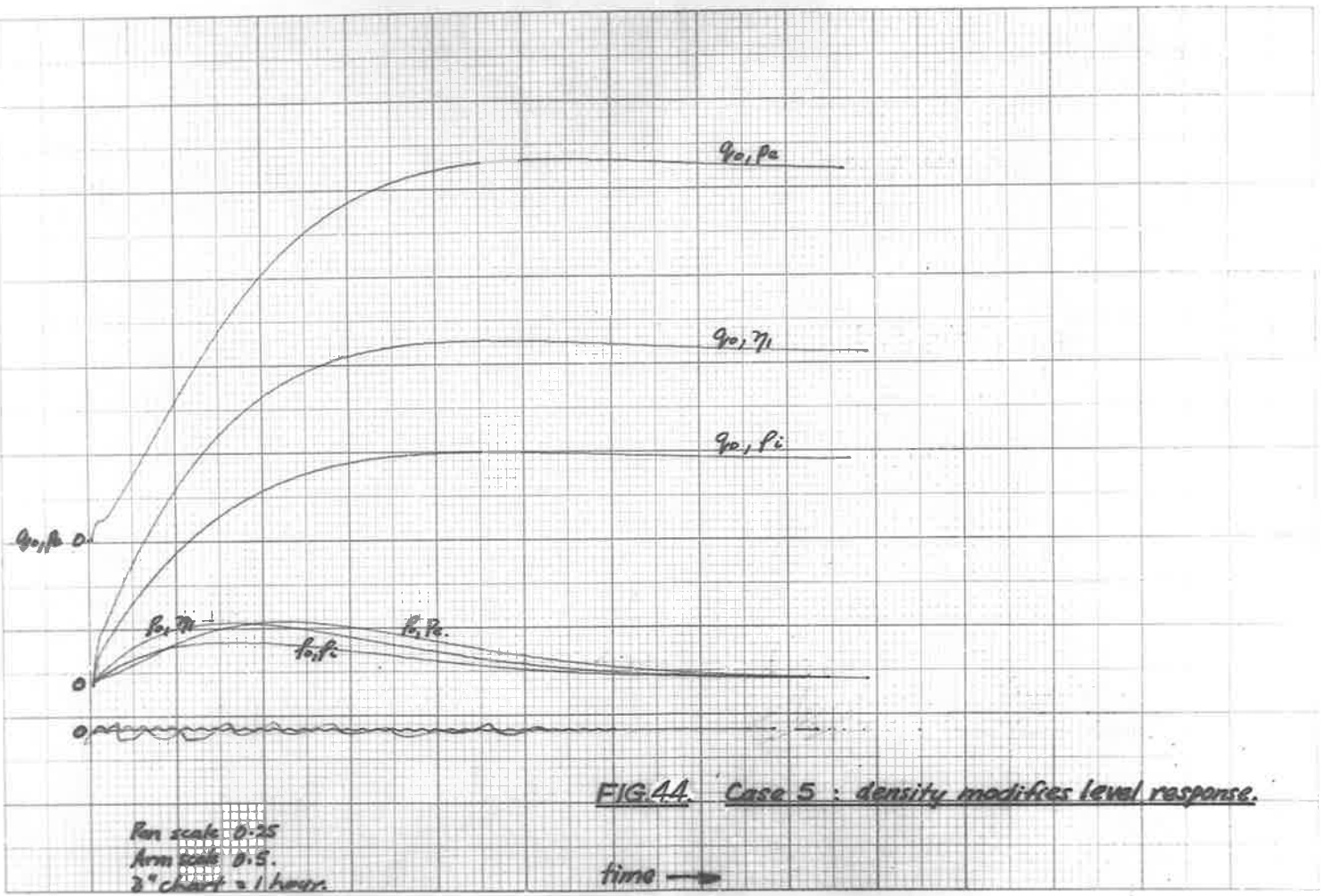

FIG 44. Case 5 : density modifies level response.

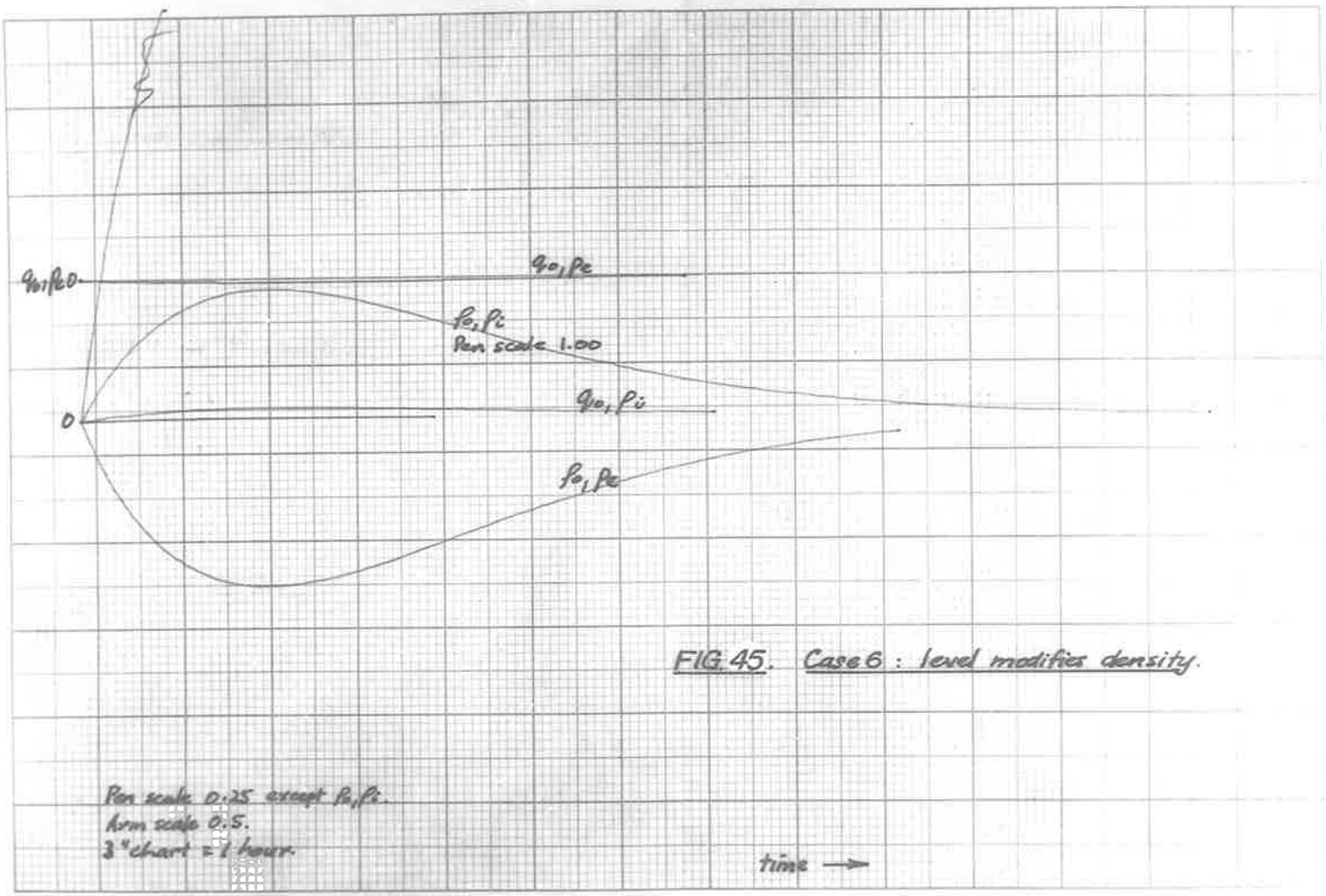

FIG. 45. Case 6 : level modifies density.

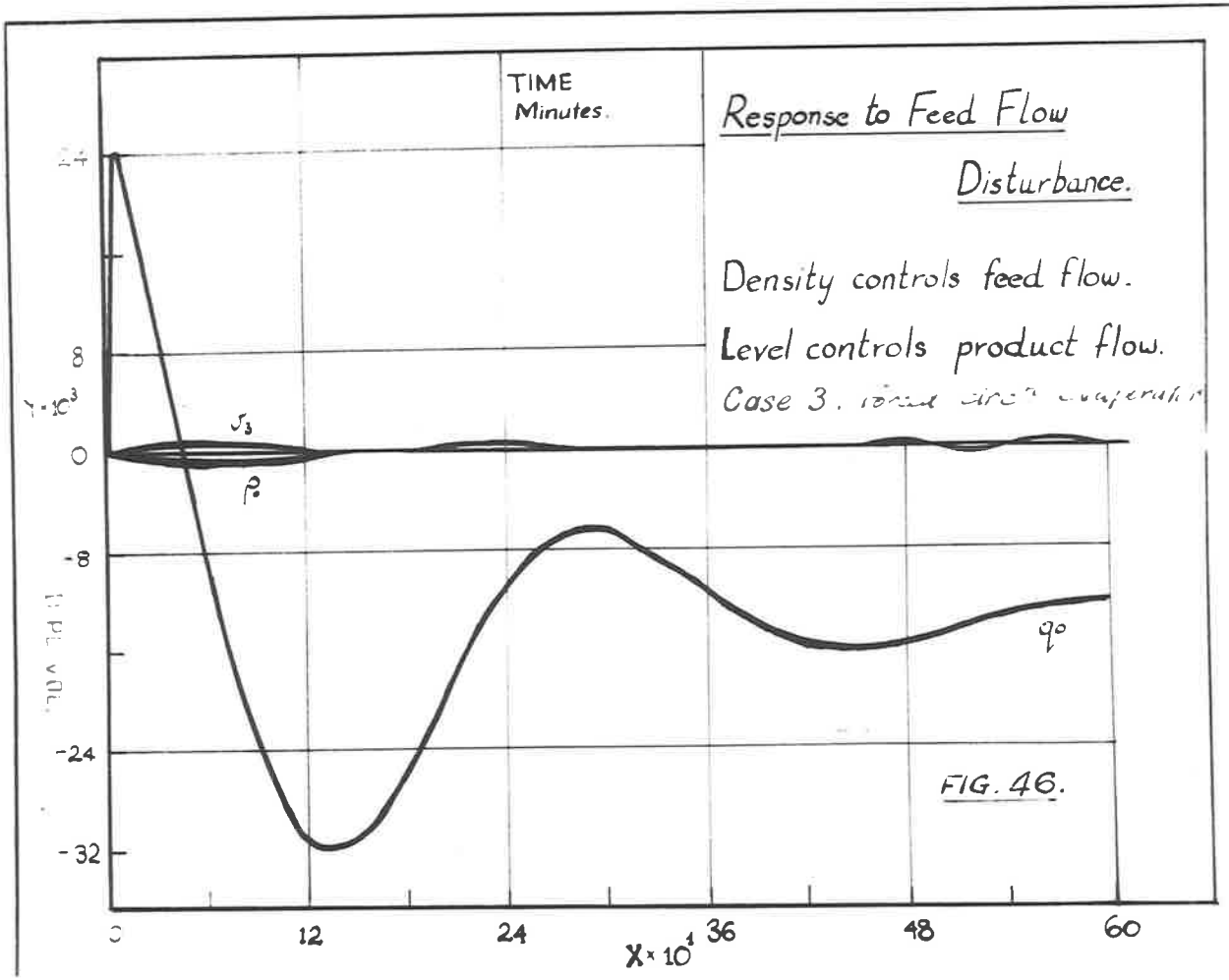
TIME
Minutes.
Response to Feed Flow
Disturbance.
Density controls feed flow.
Level controls product flow.
Case 3.
f_3
ρ
q_0
24
8
0
-8
-24
-32
12
24
36
48
60
$X \times 10^4$

FIG. 46.

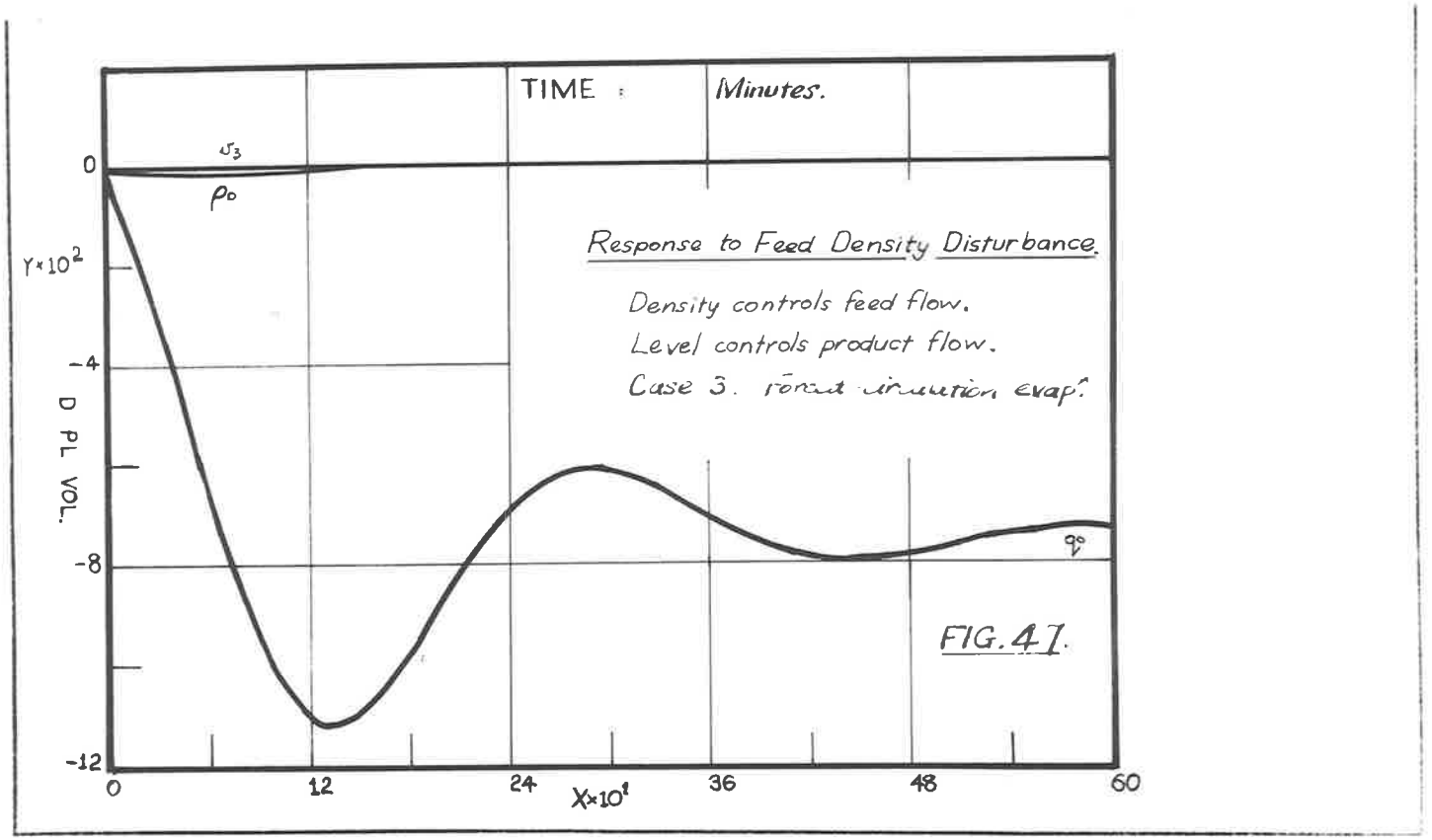
TIME : Minutes.
v_3
ρ_0
Response to Feed Density Disturbance.
Density controls feed flow.
Level controls product flow.
Case 3. Forced circulation evap.
q_0
FIG. 41.
0
-4
-8
-12
$Y \times 10^2$
D PL VOL.
0
12
24
36
48
60
$X \times 10^1$

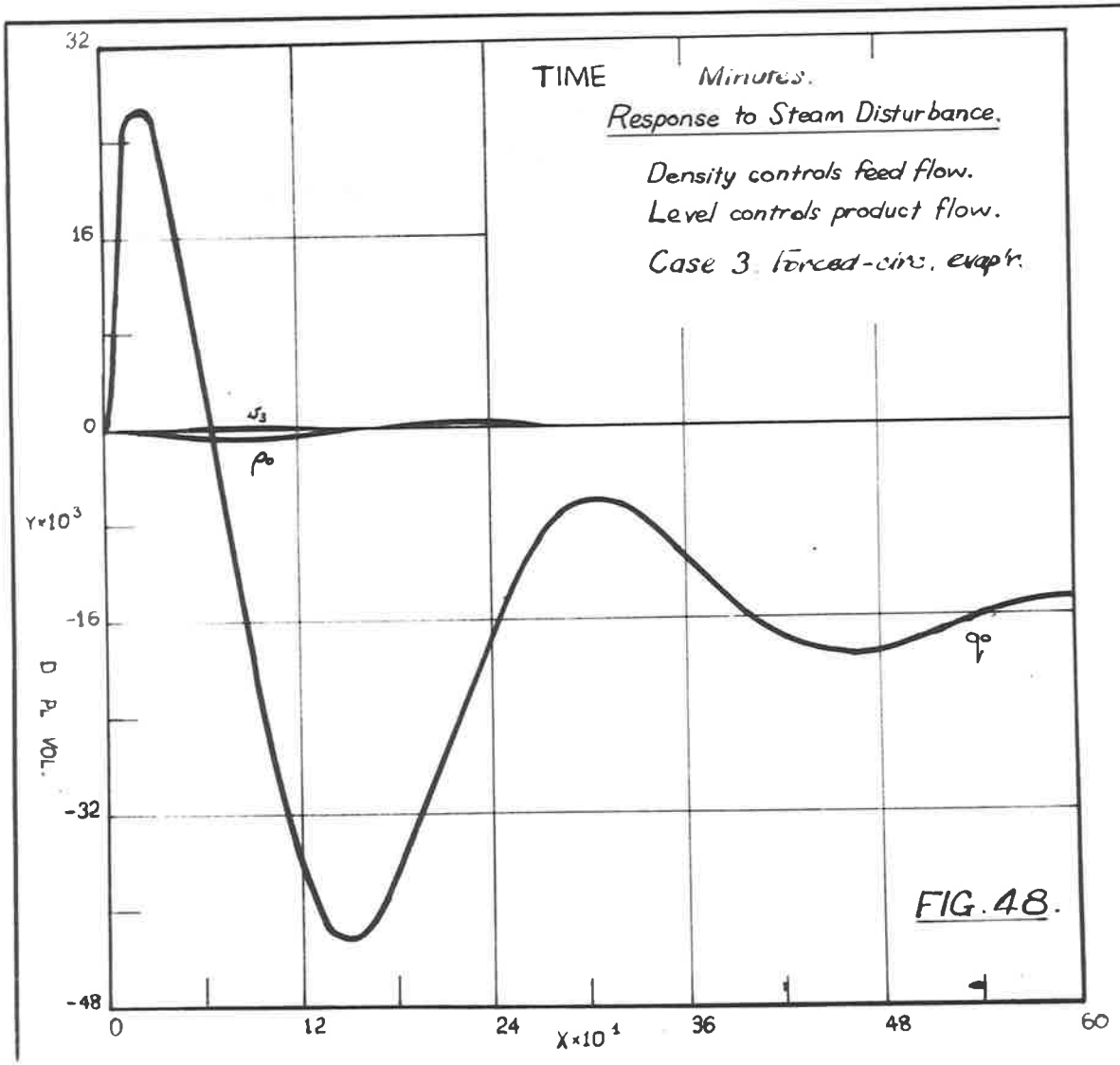
TIME Minutes.
Response to Steam Disturbance.
Density controls feed flow.
Level controls product flow.
Case 3. forced-circ. evap'r.
32
16
0
-16
-32
-48
Y×10³
DEVN.
0
12
24
36
48
60
X×10¹
ρ₀
FIG. 48.

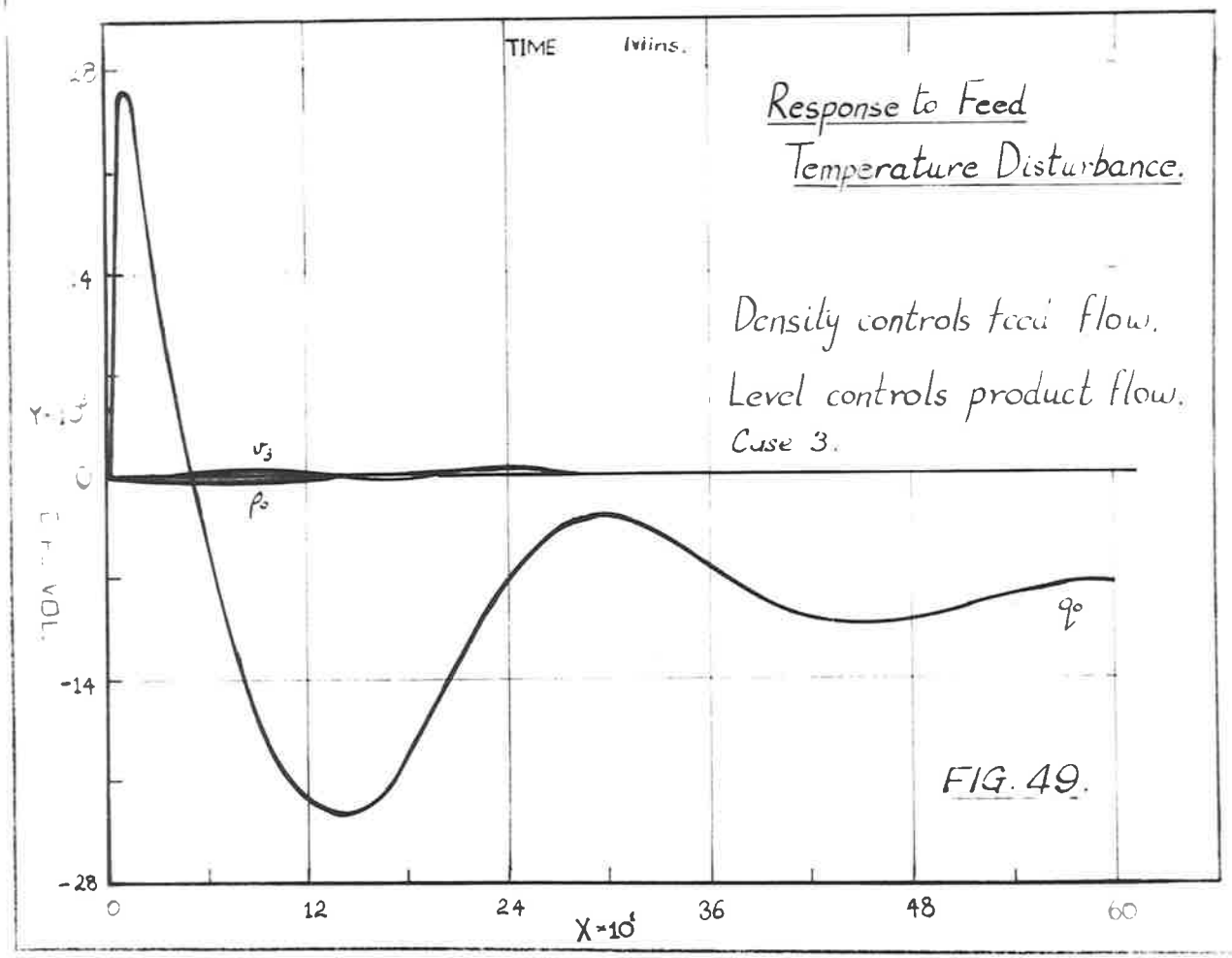
TIME Mins.
Response to Feed
Temperature Disturbance.
Density controls feed flow.
Level controls product flow.
Case 3.
v_3
ρ_0
q_0
FIG. 49.
.8
.4
-14
-28
0
12
24
36
48
60
X=10⁴

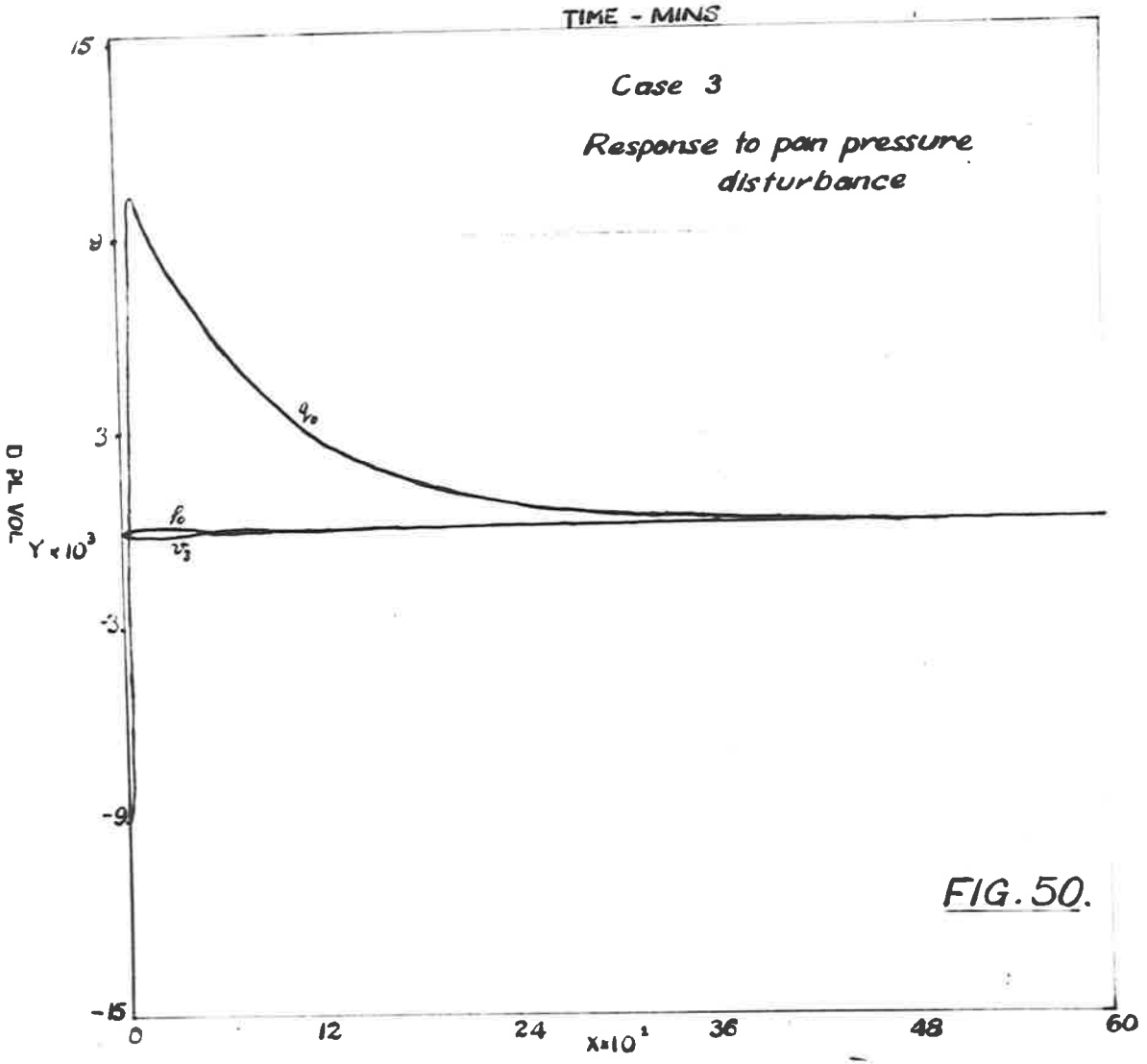
TIME - MINS
Case 3
Response to pan pressure disturbance
15
3
-3
-9
-15
0
12
24
36
48
60
$X \times 10^1$
$Y \times 10^3$
q_0
p_0
v_3

FIG. 50.

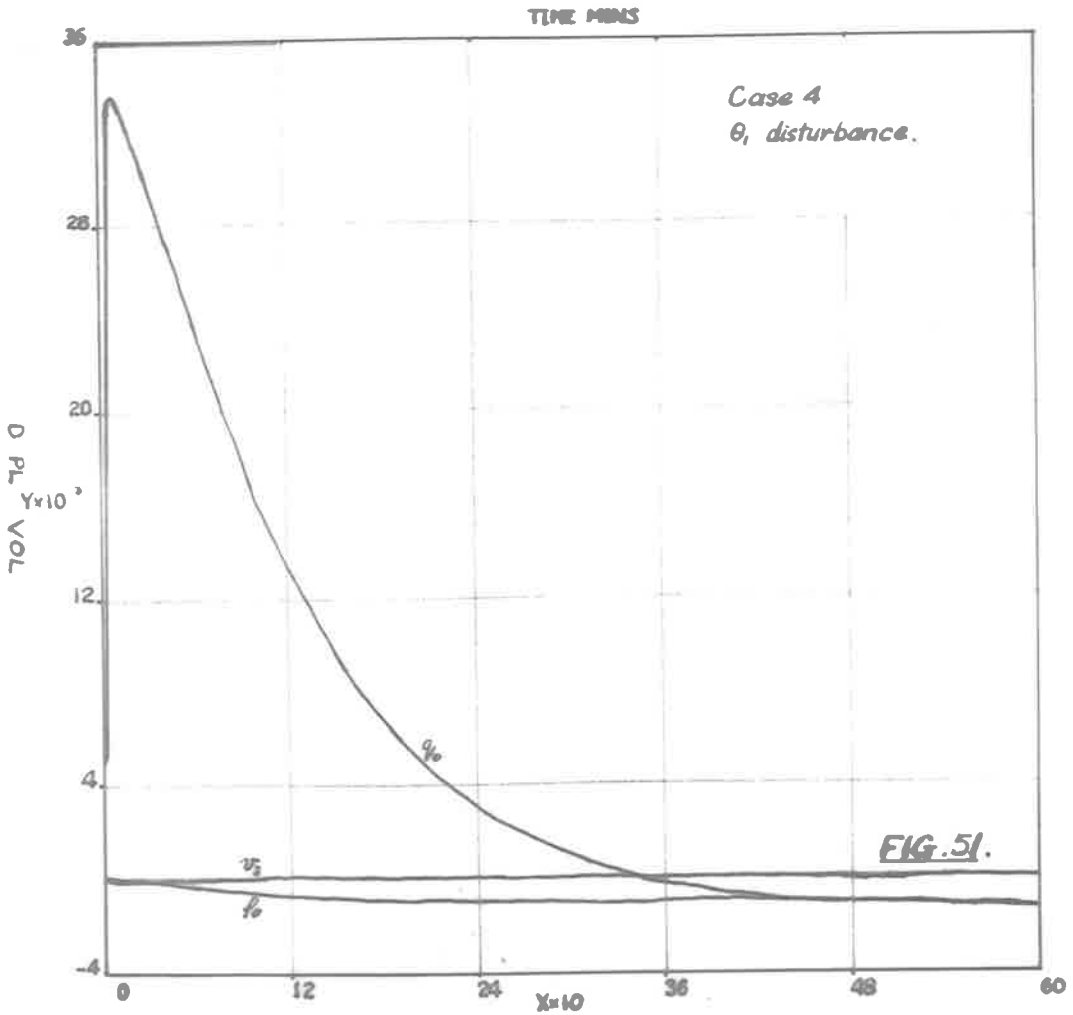
TIME MINS
Case 4
θ, disturbance.
36
28
20
12
4
-4
0
12
24
36
48
60
X×10
Y×10³
D PL VOL
q₀
v₀
h₀

FIG. 51.

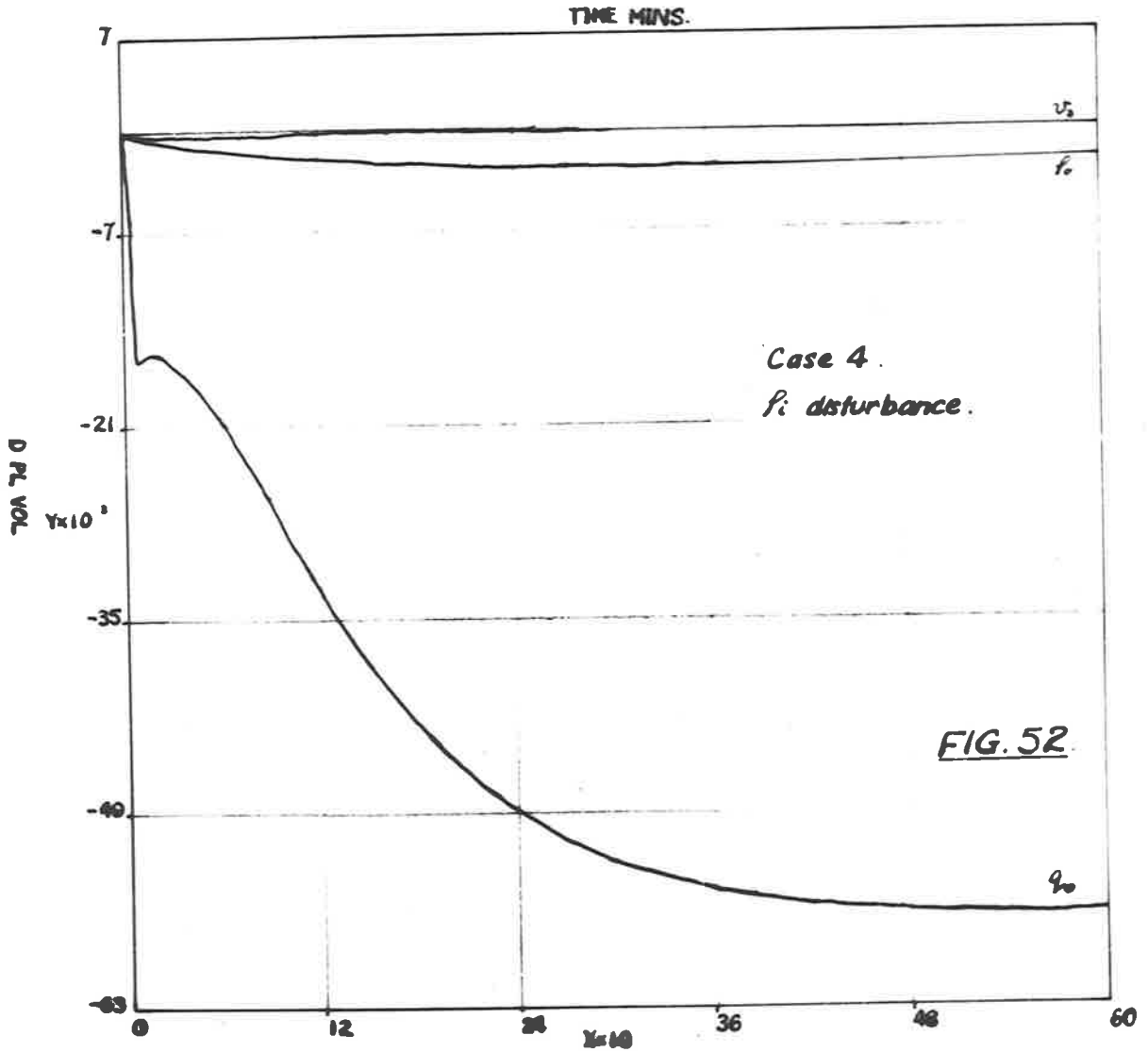
TIME MINS.
7
-7
-21
-35
-49
-63
D PL VOL
Y×10³
0
12
24
36
48
60
X×10
Case 4.
fi disturbance.

FIG. 52

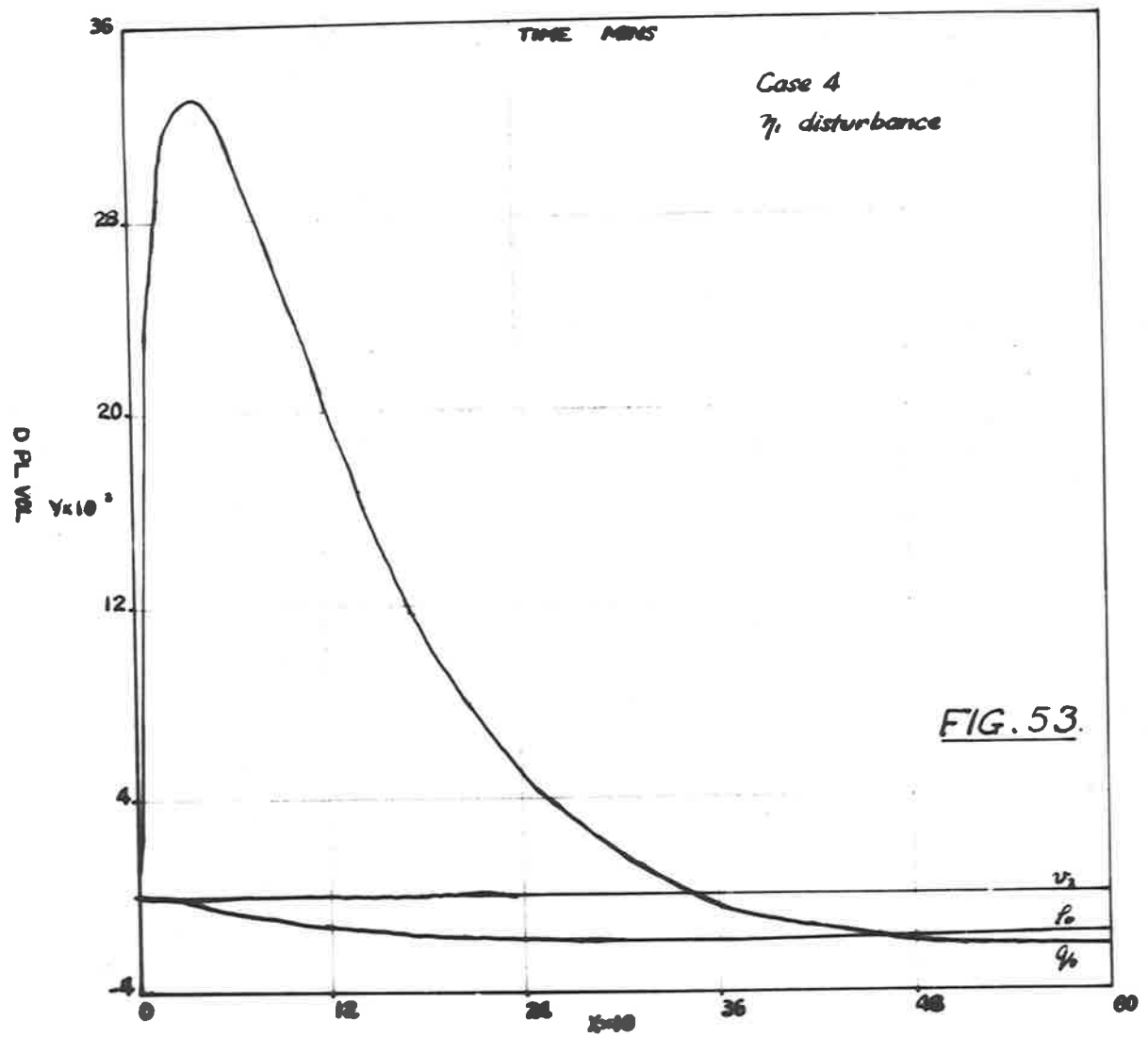
TIME MINS
Case 4
η_1 disturbance
36
28
20
12
4
-4
0
12
24
36
48
60
D PL VEL
Y×10 ³
X×10
v_1
p_0
q_0

FIG. 53.

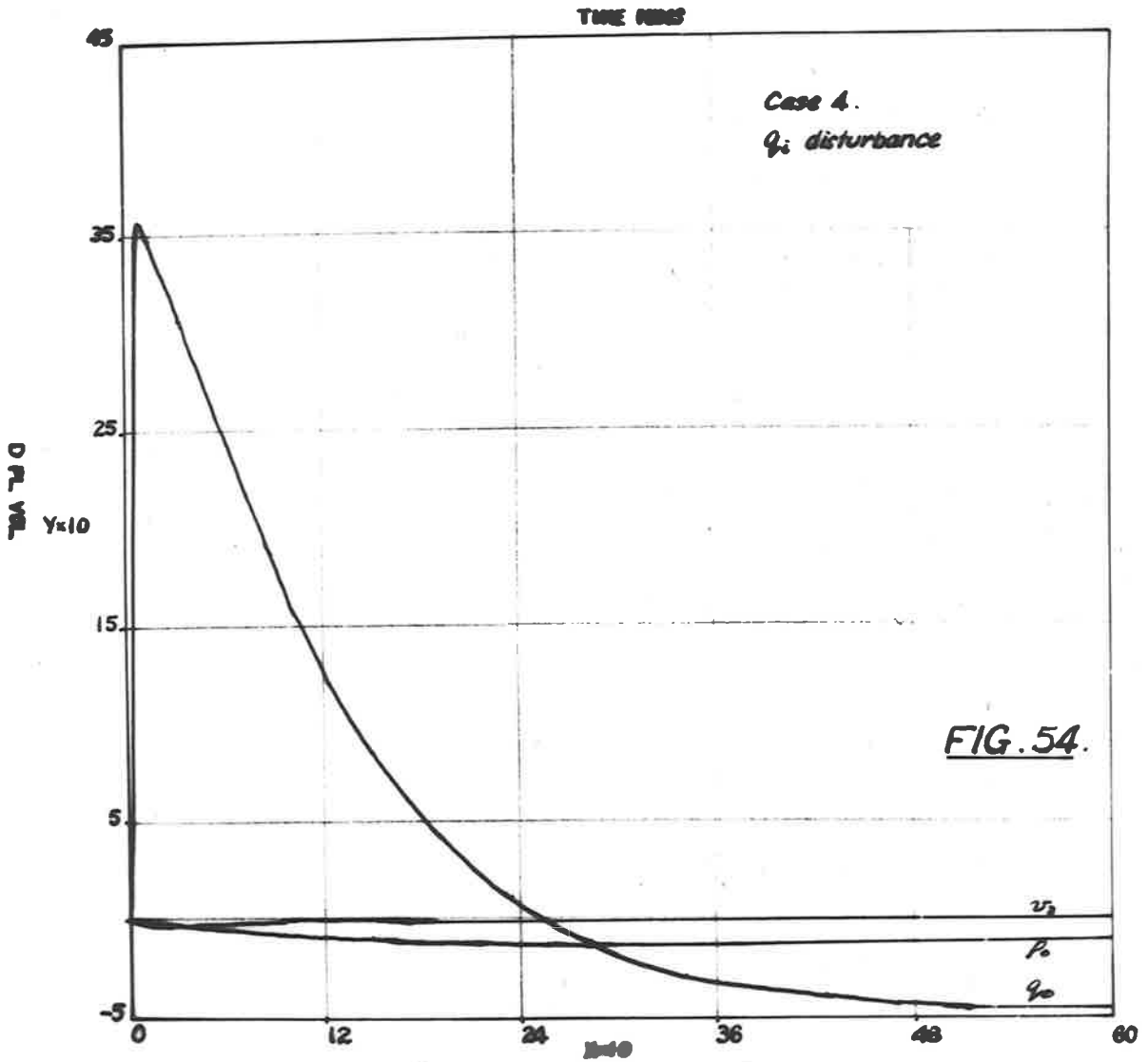
TIME MINS
45
35
25
15
5
-5
DEL VAL
Y×10
0
12
24
36
48
60
Case 4.
q_i disturbance
v_2
P_o
q_o

FIG. 54.

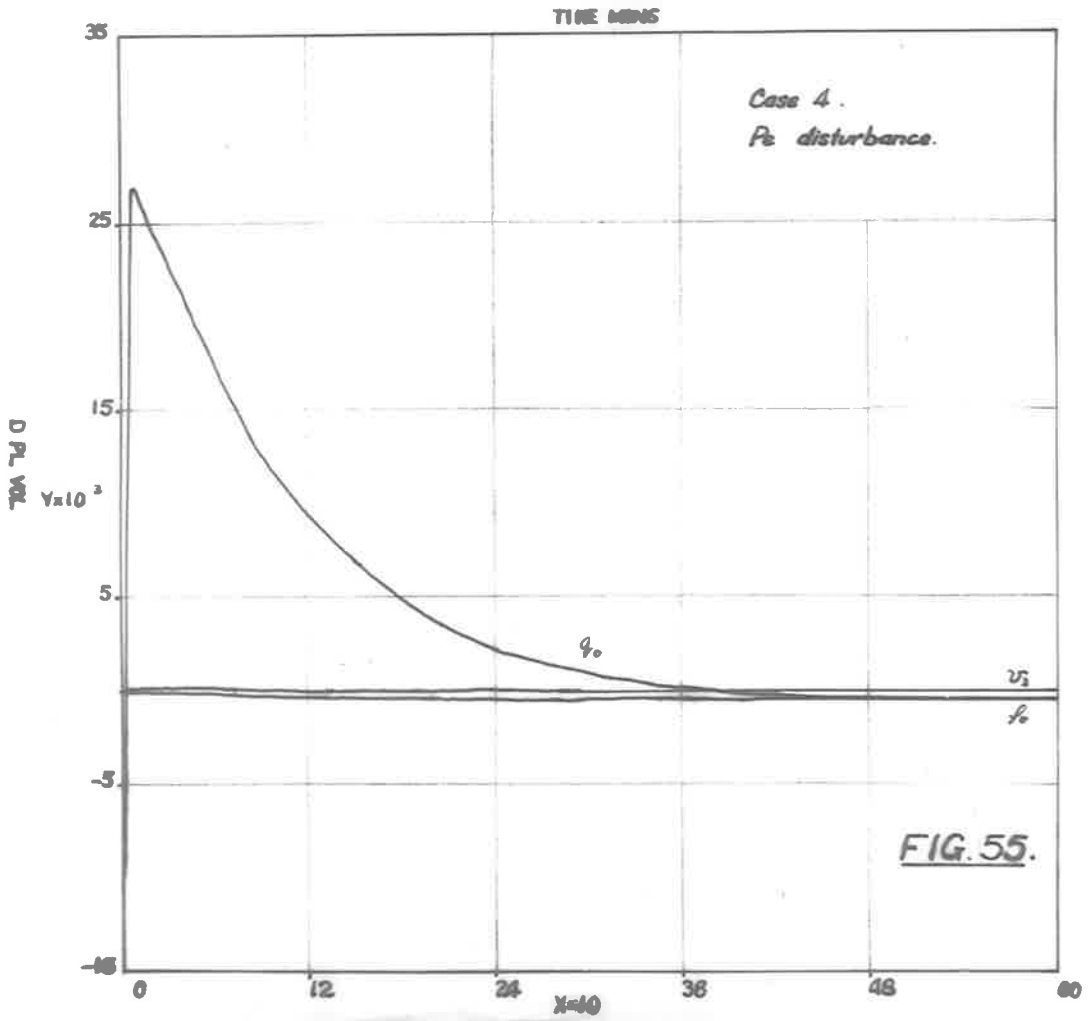
TIME MINS
35
25
15
5
-5
-10
D PL. VEL. Y x 10³
0
12
24
36
48
60
X=40
Case 4.
Pe disturbance.
q_0
v_1
f_0

FIG. 55.

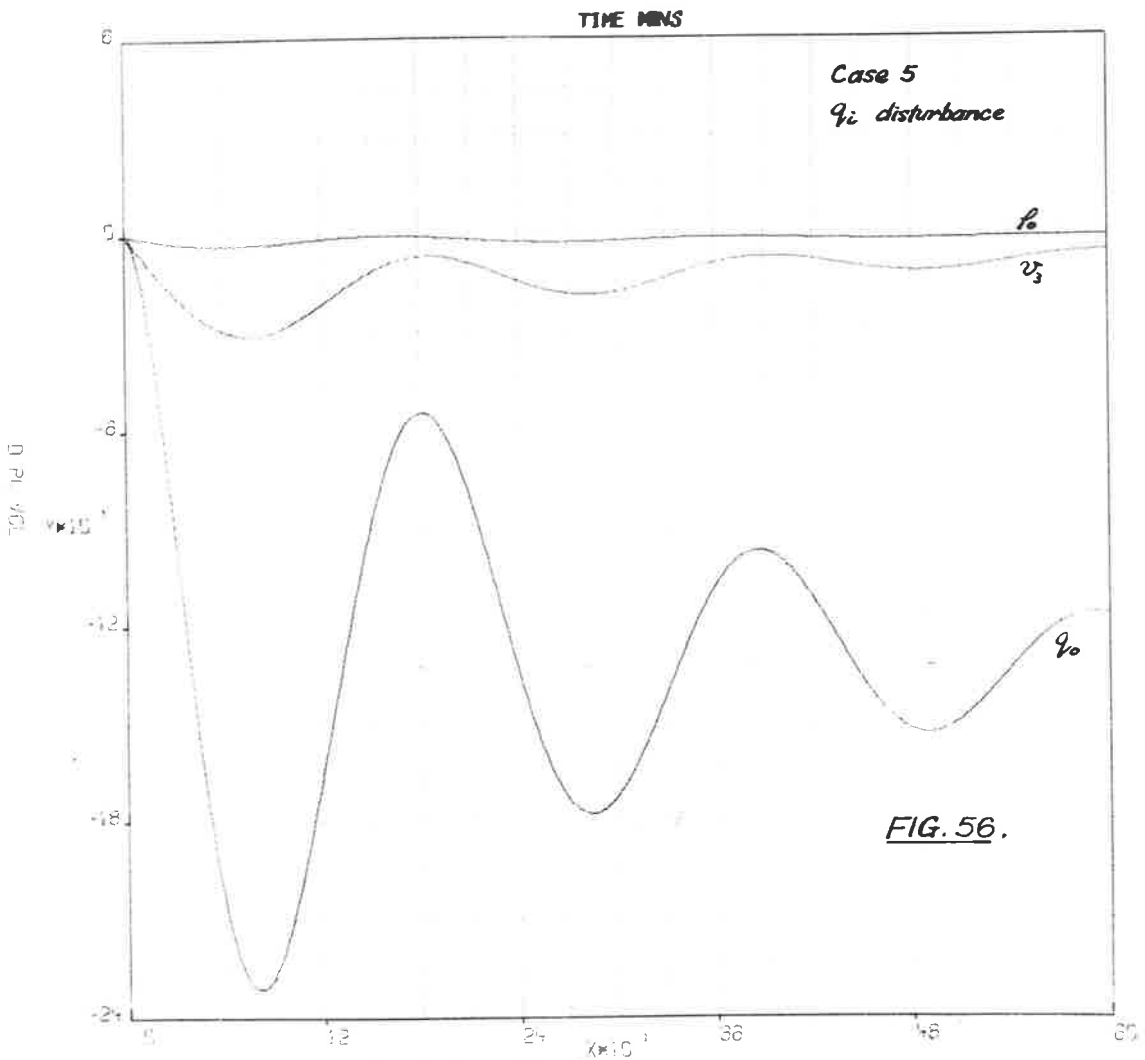
TIME MINS
Case 5
q_i disturbance
h_o
v_3
q_o
0
12
24
36
48
60
-6
-12
-18
-24

FIG. 56.

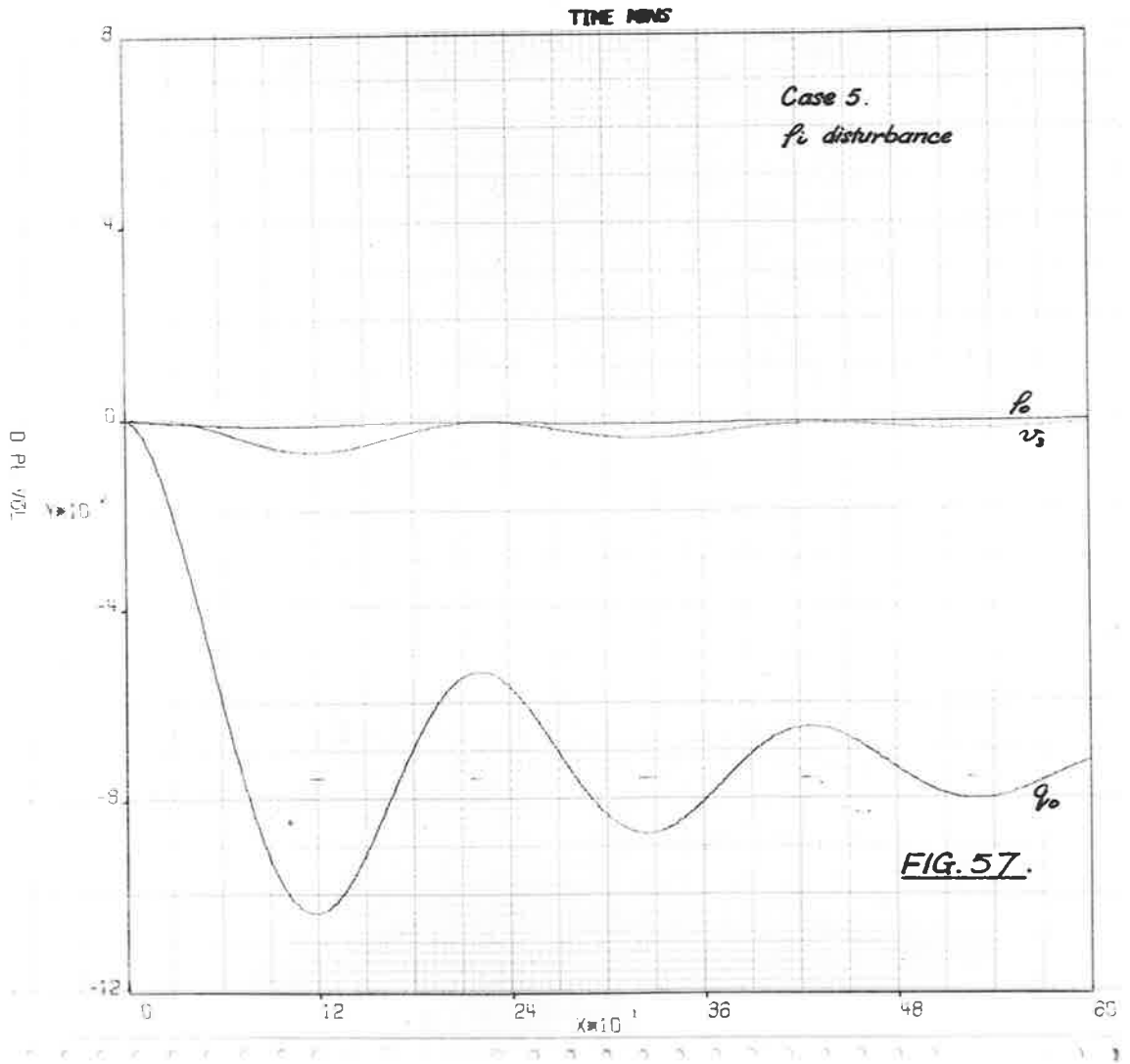
TIME MINS
Case 5.
fi disturbance
fo
vs
qo
8
4
0
-4
-8
-12
0
12
24
36
48
60
X=10

FIG. 57.

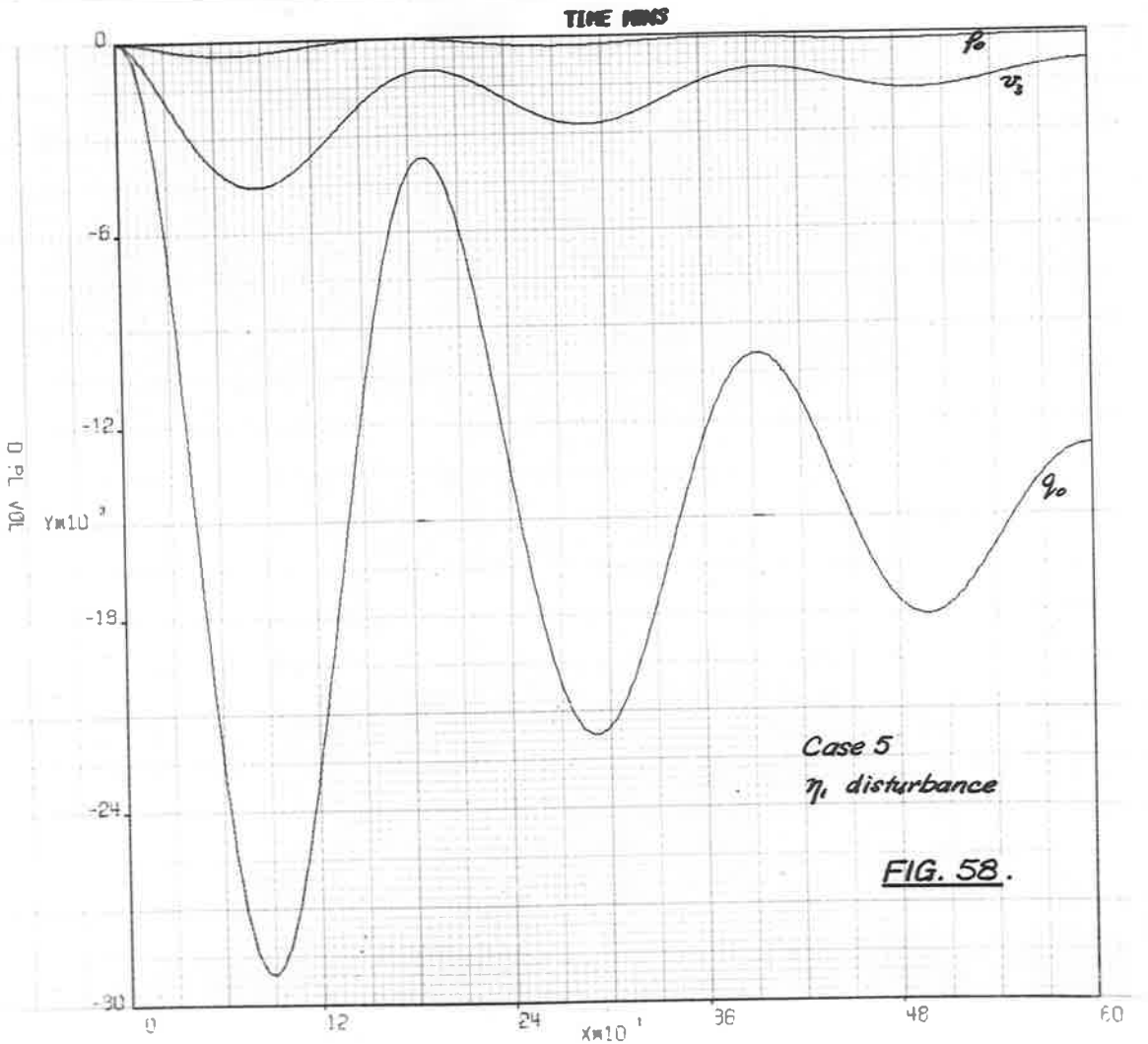
TIME MINS
0
-6
-12
-18
-24
-30
Ym10 ³
0
12
24
36
48
60
Xm10 ¹
p_0
v_3
q_0
Case 5
η_1 disturbance

FIG. 58.

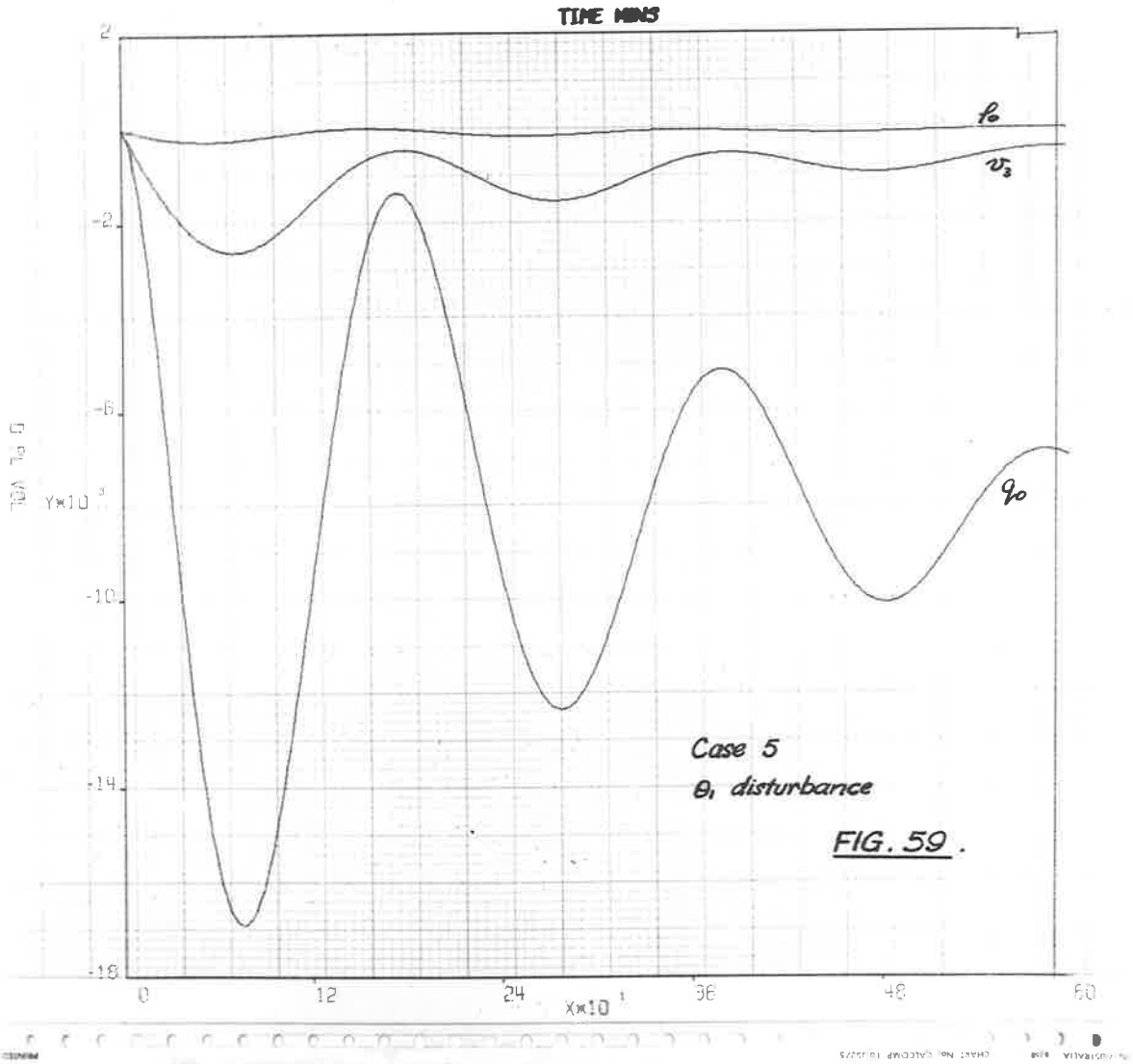
TIME MINS
2
-2
-6
-10
-14
-18
Y*10
0
12
24
36
48
60
X*10
θ_0
v_3
q_0
Case 5
θ_1 disturbance

FIG. 59 .

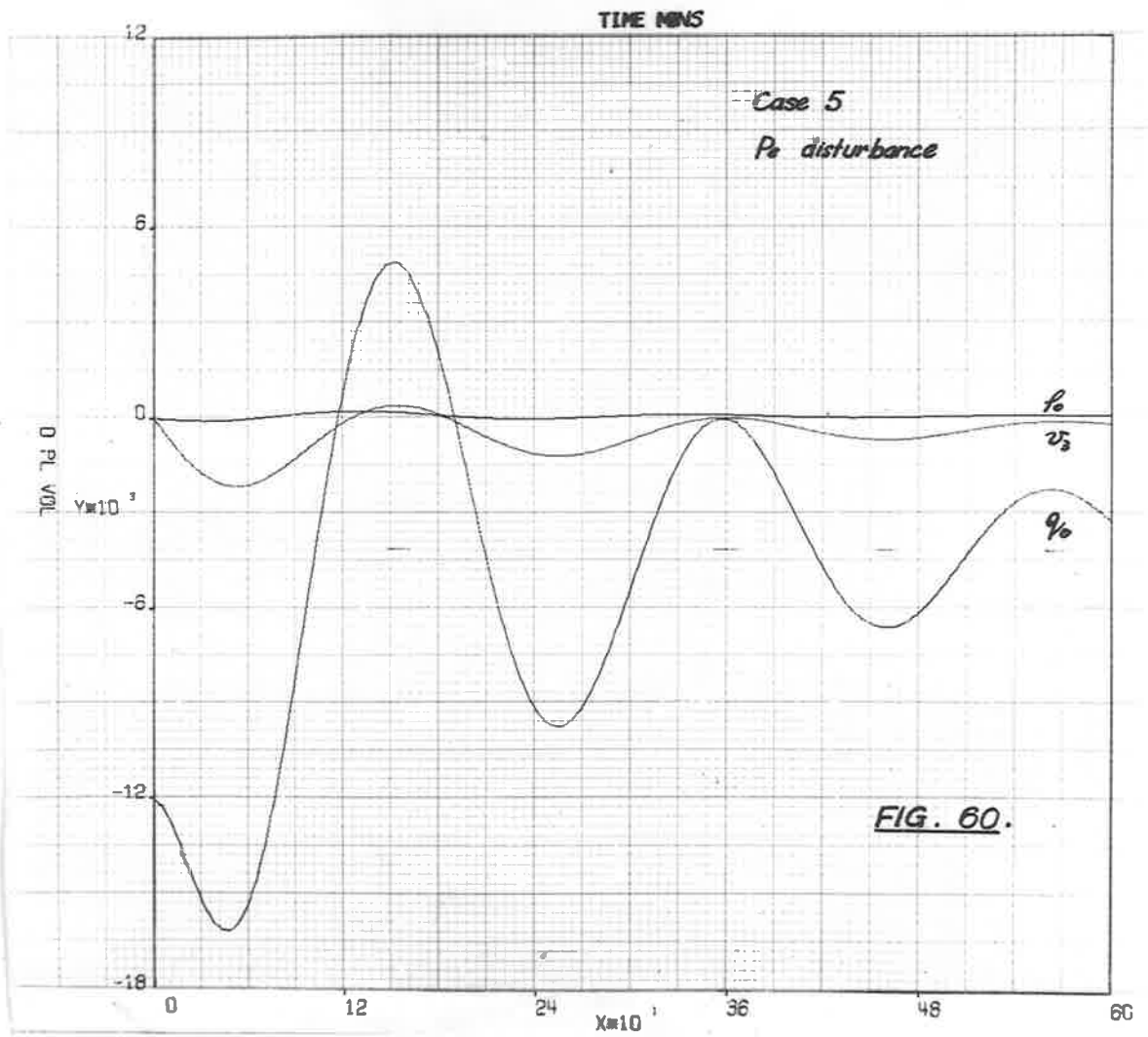
TIME MINS
Case 5
Pe disturbance
12
6
0
-6
-12
-18
0
12
24
36
48
60
Y=10 ³
X=10 ¹
δf
δv₃
δθ

FIG. 60.

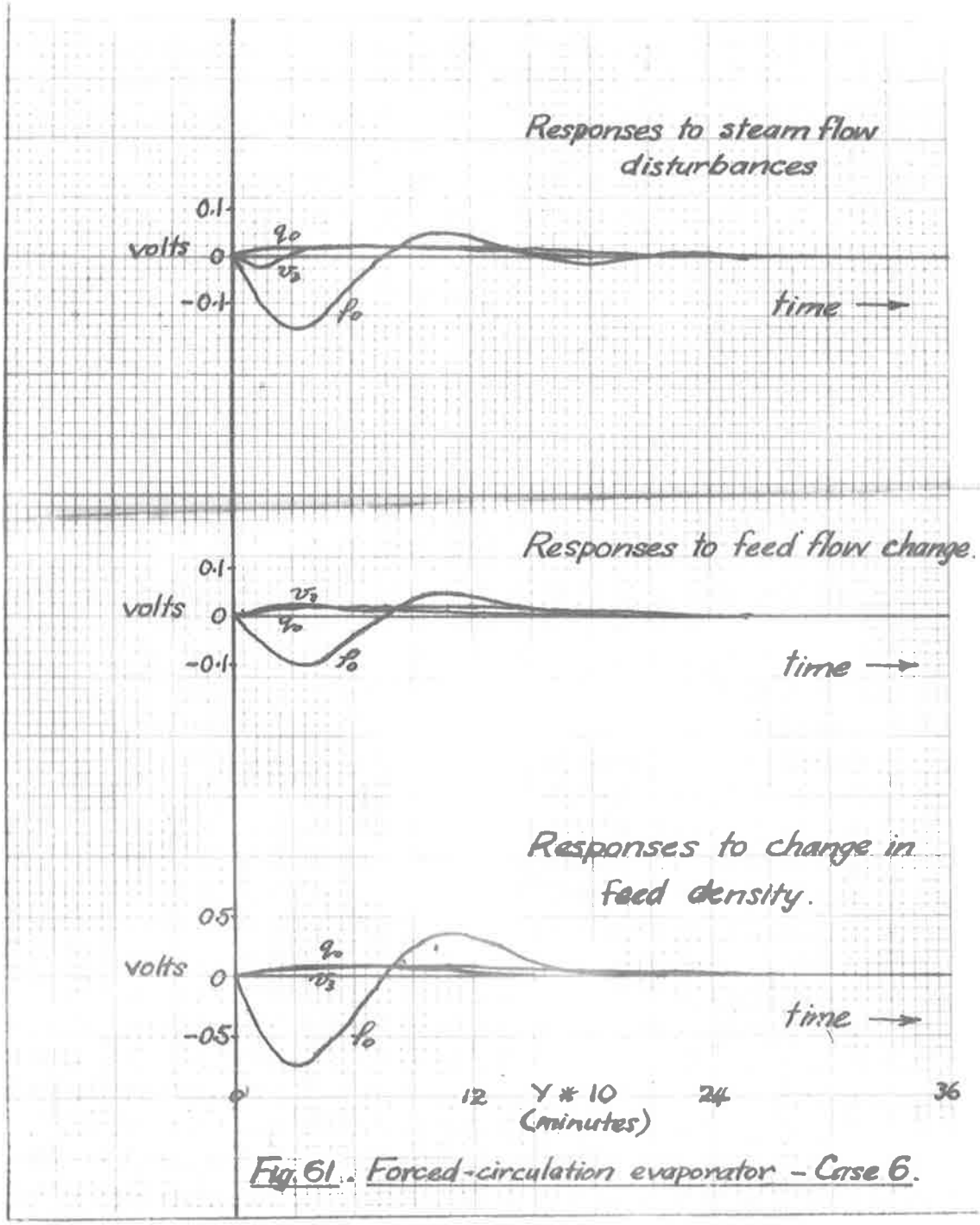

Fig. 61. Forced-circulation evaporator – Case 6.

NOMENCLATURE

This table contains only the total values or steady state values of variables. In general small variations about the steady state values are represented by the corresponding lower case letters. The principal exceptions are temperature where the variations are represented by θ, and density where the mean values are written ρ. Where confusion might arise Laplace transforms are indicated by tilde variables, e.g. $\tilde{\theta}$, and the Laplace operator is s except for those equations transformed with respect to distance and time where the operators are (p,s).

The equation constants, including gain constants and time constants, are tabulated separately and defined during the development of the mathematical model. Certain symbols defined during discussion but not appearing in the final model have not been included in the table.

A	Tube cross-sectional area
$A_{i,o}$	Inside, outside area of evaporator tubes
A_p	Cross-sectional area of pan or flash vessel
$A_{1,2}$	Coefficients in density-concentration
Cp_i	Specific heat of feed liquor
Cp_o	Specific heat of product liquor
Cp_s	Specific heat of process steam
Cp_t	Specific heat of evaporator tube material
Cp_w	Specific heat of water
Cp_1	Specific heat of shell wall material
H_1	Difference in height between pan height and discharge point datum level
H_c	Specific enthalpy of steam condensate
H_s	Specific enthalpy of steam

K	Constant in density-concentration relationship
K_i	Concentration of feed liquor
K_o	Concentration of product liquor
K_{1-n}	Gain constants of plant
K_{c1-n}	Controller gain constants
L	Length of evaporator tube
M_1	Mass of shell wall
M_{cj}	Mass of steam condensate in jacket
M_c	Mass flow rate of steam condensate
M_i	Mass flow rate of feed liquor
M_o	Mass flow rate of product liquor
M_s	Mass flow rate of process steam
M_v	Mass flow rate of solvent vapour
P_a	Atmospheric pressure
P_e	Pressure in evaporator
P_i	Perimeter inside tube
P_o	Steam supply pressure
P_s	Process steam pressure
Q_i	Volumetric flow rate of feed liquor
Q_o	Volumetric flow rate of product liquor
Q_s	Volumetric flow rate of process steam
Q_{sh}	Heat flux to shell wall
R_1	Flow resistance of steam valve
R_2	Flow resistance of product withdrawal valve
T_i	Temperature of feed liquor
T_o	Temperature of product liquor

T_s Temperature of process steam

T_t Temperature of evaporator tube wall

U_s Specific internal energy of process steam

V Process liquor flow rate

V_c Volume of condensate in calandria steam space

V_o Volume of liquor in evaporator tube

V_s Volume of calandria steam space

V_t Volume of metal in tube walls

V_3 Volume of pan contents

$d_{i,o}$ Inside, outside diameters of evaporator tube

$h_{i,o}$ Inside, outside heat transfer coefficients

$k_a = \frac{\partial \rho_s}{\partial T_s}$, change in process steam density with steam temperature

$k_b = \frac{\partial U_s}{\partial T_s}$, change in specific internal energy of steam with steam temperature

$k_c = \frac{\partial H_s}{\partial T_s}$, change in specific enthalpy of steam with steam temperature

$k_d = \frac{\partial H_c}{\partial T_c}$, change in specific enthalpy of steam condensate with condensate temperature

s Laplace operator

t Time

z Axial distance along tube from entrance

$\alpha = \frac{\partial T_o}{\partial P_e}$, change in boiling point of evaporator contents with evaporator pressure

$\beta = \frac{\partial P_s}{\partial T_s}$, change in process steam pressure with steam temperature

$\gamma = \frac{\partial T_o}{\partial \rho_o}$, change in boiling point of process liquor with density

$\eta_1 = \frac{r_1}{R_1}$, relative change in steam valve resistance

$\eta_2 = \frac{r_2}{R_2}$, relative change in product offtake valve resistance

θ Small variations in temperature

κ Thermal diffusivity of metal

λ Latent heat of vaporization of solvent

λ_s Latent heat of condensation of steam

ρ_i Density of feed liquor

ρ_o Density of product liquor

ρ_{sl} Density of saturated solution

ρ_{s2} Density of solid material

ρ_s Density of process steam

ρ_t Density of evaporator tube material

ρ_w Density of water

τ Time constant

τ_{dl-n} Derivative action time of controllers

τ_{il-n} Integral action time of controllers

τ_D Distance-velocity lag

τ_{ml-n} Measurement lags

APPENDIX A

PLANT PARAMETERS FOR FORCED-CIRCULATION EVAPORATOR

Calandria Steam Space

A_i	1.6	ft^2
A_o	1.83	ft^2
Cp_s	0.45	Btu/lb ^oF
M_s	105	lb/hr
P_o	4320	lb/ft^2
P_s	3740	lb/ft^2
R_1	0.354	lb hr/ft^5
T_s	242	^oF
h_o	2958	Btu/ft^2 ^oF hr
V_s	0.49	ft^3
β	0.059	$^oF^{-1}$
k_a	0.0011	lb/ft^3 ^oF
k_b	0.279	Btu/lb/^oF
k_c	0.348	Btu/lb/^oF
k_d	1.0	Btu/lb/^oF
λ_s	950.7	Btu/lb
ρ_s	0.064	lb/ft^3
Q_s	1640	ft^3/hr

Calandria tube walls

Cp_t	0.0942	Btu/lb ^oF
h_i	3280	Btu/ft^2 ^oF hr
L	6	ft
V_2	0.0078	ft^3

V_t	0.0013	ft^3/ft
p_t	556	lb/ft^3

Pan

A_p	2.0	ft^2
A_1	0.424	
A_2	0.026	
Cp_i	0.5	Btu/lb ^oF
Cp_o	0.5	Btu/lb ^oF
h_i	3280	Btu/ft^2 ^oF hr
H_1	10	ft
K_i	0.75	
K_o	0.88	
M_i	9720	lb/hr
M_o	9640	lb/hr
M_v	80	lb/hr
P_e	2,120	lb/ft^2
Q_i	121	ft^3/hr
Q_o	113	ft^3/hr
R_2	0.00078	lb hr^2/ft^5
T_i	210	^oF
T_o	212	^oF
V_3	3.0	ft^3
α	0.0444	^oF ft^2/lb
γ	13.3	^oF ft^3/lb
λ	970	Btu/lb
ρ_i	80	lb/ft^3
ρ_o	85	lb/ft^3
V	10.35	ft/sec

EQUATION CONSTANTS FOR FORCED-CIRCULATION EVAPORATOR

N_1	3702	Btu/^{o}F hr
a	1.46	
a^1	27	^{o}F
N_2	2274	Btu/^{o}F hr
b	64.3	^{o}F
c	2.292	
N_3	11,400	Btu/^{o}F hr
b^1	0.46	
c^1	0.475	
N_4	1565000	Btu/ft^3/lb hr
d	0.00334	lb/^{o}F ft^3
e	0.0031	lb/^{o}F ft^3
f_1	0.000685	hr/ft^3
f_2	0.086	
g	0.0583	lb hr/ft^6
N_5	3.09	
h	0.99	
i	0.172	lb hr/ft^6
j	0.214	lb hr/ft^6
N_6	0.0668	ft^5/lb^2
N_7	0.00267	ft^6/lb hr
N_8	0.855	

Gain constants	
K_1	0.159
K_2	0.00625
K_3	0.00265
K_4	0.184
K_5	0.00054
K_6	1.65
K_7	1.63
K_8	0.284
K_9	20
K_{10}	0.024
K_{11}	0.0027
K_{12}	0.067
K_{13}	2.84
K_{14}	56.6

Time constants	
τ_o	0.027 hrs
τ_1	0.0015 "
τ_2	0.00003 "
τ'_2	negligible hrs
τ_3	negligible "
τ_4	0.0002 hrs
τ_5	0.0022 "
τ_6	0.00023 "
τ_7	0.00108 "
τ_8	0.0127 "
τ_9	0.0126 "
τ_{10}	0.0036 "
τ_a	0.0128 "
τ_b	0.352 "
τ_c	0.0266 "
$\tau_{ml,2}$	0.0083 "

APPENDIX B

Evaporation with solids present

The presence of solids in an evaporator actually makes the mathematical model simpler because the boiling-point of the slurry will be independent of density.

The assumptions made previously need to be modified as follows:

(1) The liquid is saturated or contains suspended solids.

(2) The heat of formation of the solids is small compared with the latent heat of vaporisation of the solvent.

(3) There is a linear relationship between density and concentration.

The effect of these assumptions is that the expression

$$\gamma = \frac{\partial T_o}{\partial \rho_o} \quad ,$$

i.e. the change in boiling point of the pan contents with density, appearing in the density-boiling point relationship, becomes zero. This is reflected in the elimination of the term γp_o from dynamic equation (3.6). The product concentration (K_o) which appears in dynamic equation (3.8) may be re-defined as the weight of solids per unit weight of slurry, in which case, by applying assumption (3) it is possible to write

$$K_o = N_9 \, (\rho_o - \rho_{s1}) = \frac{\rho_o - \rho_{s1}}{\rho_{s2} - \rho_{s1}}$$

where $$N_9 = \frac{1}{\rho_{s2} - \rho_{s1}}$$

In addition the principal time constant of the system, τ_a, becomes equal to the volume-throughput ratio, τ_o.

The equating of γ to zero has certain effects on the reduced equations, hence on the transfer functions.

The major effects are the following:

Steam side

Equation (4.4) is modified to

$$E_1(s)\ \tilde{\theta}_t = c\ \alpha\tilde{p}_e - b\tilde{n}_1 \qquad (7.1)$$

Heat balance

In the same way substitution of the modified relationship for θ_o in equation (3.5) together with the substitutions for m_v, m_i and m_o from equations (3.7) (3.8) and (3.11) leads to a modified form of (4.5) namely:

$$-\frac{g}{\rho_o}\ s\ (v\tilde{\rho}_o) = -\tilde{\rho}_o + d\tilde{\theta}_t + g\ \tilde{q}_o - f_1\ \bar{Q}_i\ \tilde{\rho}_i - f_1\ \bar{\rho}_i\ \tilde{q}_i + e\tilde{\theta}_i \qquad (7.2)$$

Apart from the equation certain of the equation constants are also modified. τ_7 and f_2 are eliminated, while

$$N_4{}^1 = -\bar{Q}_o\ (\lambda + T_o\ (Cp_w - Cp_o)$$

and d, e, f_1, and g are modified through this revised N_4.

Mass balance on solute

If the equation (7.2) is divided by the equation constant g, and the equation (4.6) is divided by equation constant j, the following pair of equations result.

$$\left.\begin{aligned} -\frac{1}{\rho_o}\ s\ (v\tilde{\rho}_o) &= -\frac{1}{g}\tilde{\rho}_o + \frac{d}{g}\tilde{\theta}_t + \tilde{q}_o - \frac{f_1\bar{Q}_i}{g}\tilde{\rho}_i - \frac{f_1\bar{\rho}_i}{g}\tilde{q}_i + \frac{e}{g}\tilde{\theta}_i \\ \frac{\tau_o}{j}\ \frac{\bar{\rho}_o\ A_2}{K_o + \rho_o\ A_2}\ s\ \tilde{\rho}_o + \frac{1}{\rho_o}\ s\ (v\tilde{\rho}_o) &= -\frac{1}{j}\tilde{\rho}_o - \tilde{q}_o + \frac{h}{j}\tilde{\rho}_i + \frac{i}{j}\tilde{q}_i \end{aligned}\right\} \qquad (7.3)$$

Adding these two equations eliminates $(\tilde{v_3\rho_o})$ and $\tilde{q}_o$ yielding,

$$\frac{\tau_o}{j}\frac{\bar{\rho}_o A_2}{\bar{K}_o + \bar{\rho}_o A_2} s\tilde{\rho}_o = -\left(\frac{1}{g} + \frac{1}{j}\right)\tilde{\rho}_o + \frac{d}{g}\tilde{\theta}_t - \left(\frac{f_1\bar{Q}_i}{g} - \frac{h}{j}\right)\tilde{\rho}_i$$

$$- \left(\frac{f_1\bar{\rho}_i}{g} - \frac{i}{j}\right)\tilde{q}_i + \frac{e}{g}\tilde{\theta}_i$$

$$= \frac{d}{g}\tilde{\theta}_t - \left(\frac{j+g}{gj}\right)\tilde{\rho}_o - \left(\frac{jf_1\bar{Q}_i - hg}{gj}\right)\tilde{\rho}_i - \left(\frac{jf_1\bar{\rho}_i - ig}{gj}\right)\tilde{q}_i + \frac{e}{g}\tilde{\theta}_i$$

i.e.

$$\frac{\tau_o}{j}\left(\frac{\bar{\rho}_o A_2}{\bar{K}_o + \rho_o A_2}\right) s\tilde{\rho}_o = \frac{1}{gj}\left(dj\tilde{\theta}_t - (j+g)\tilde{\rho}_o - (jf_1\bar{Q}_i - gh)\tilde{\rho}_i\right.$$

$$\left. - (jf_1\tilde{\rho}_i - ig)\,\tilde{q}_i + ej\,\tilde{\theta}_i\right) \qquad (7.4)$$

This equation (7.4) differs from the equation (5.1) by the elimination of the $\tilde{p}_e$ term. Since equation (7.4) describes the response of the product density under the postulated conditions, one must conclude that when solids are present product density is unaffected by disturbances originating in the pan pressure.

Because of the changed form of this equation the transfer function for product density response will be modified in several particulars. Thus equation constant N_8 will be changed, which will introduce consequential changes in the system gains K_1, K_2, K_3, and K_4, while K_5 will be eliminated altogether.

In other words, when solids are present, the transfer functions for product density response are unchanged compared with the original model, with the exception of the disappearance of the function involving pan pressure disturbances. In the complete model for the evaporator with solids present the pan pressure still appears in the system through the equations defining the pan level and product flow responses.

APPENDIX C

SPECIMEN DIGSIM PROGRAMME

```
DOC PROGRAM
      READ FROM<CR/ATLAS%
      MASTER DIGSIM
C     USE OF FORTRAN 11 FORM DIGSIM                                          2
C     REQUIRES FUNCTIONS TIME AND S (2ND. ORDER RUNGE-KUTTA)                 3
      DIMENSION W(301),U(301,3)
      DIMENSION X(25),YIC(25),P(50)
      COMMON I,INPASS,H,HON2,YIC,X,T
      READ(1,12)(P(I),I=1,30)
      READ(1,13)START,STEP,FINISH
   12 FORMAT(10F8.4)
   13 FORMAT(3F6.3)
   14 FORMAT(4F10.4)
C     CASE 5 DENSITY CONTROLS PRODUCT FLOW ...LEVEL CONTROLS FEED FLOW
C     IMPULSE DISTURBANCE IN FEED DENSITY
C     START OF PGM PROPER                                                    66
      INPASS=0
      YIC(2),YIC(3),YIC(4),YIC(8),YIC(10),YIC(12),YIC(14)=0.0
      GO,Y1,Y2,Y3,Y4,Y5,Y6,Y7,Y8,Y9,Y10,STM,THETA,DRC,VRC,QI,RHOI=0.0
      ZO,ETA1,Y11,Y12,Y13,Y14,Y15,Y16,Y17,Y18,Y19=0.0
      J = 0
      P(1)=1.0
      P(9)=0.031
      P(9)=-P(9)
      P(20)=0.75
      P(23)=88.0
      P(24)=88.0
      P(25)=0.042
      P(28)=15.6
      P(29)=15.6
      P(30)=0.167
      P(3) = 6.96
      P(5) = 9.33
      RHOI=0.0
   10 T=TIME(START,STEP,FINISH,GO)                                           67
      IF(GO)51,40,51
```

```
C     STATEMENTS DESCRIBING SYSTEM BEING SIMULATED
   51 CONTINUE
      X(2)=P(4)*Y3+P(3)*Y1+P(5)*Y2
      Y2=S(X(2),YIC(2))
      Y2=-Y2
      X(3)=P(6)*THETA+P(7)*APE+P(8)*Y2+P(9)*QI+P(10)*RHOI+P(11)*Y3
      X(3)=AQI+X(3)
      Y3=S(X(3),YIC(3))
      Y3=-Y3
      X(8)=P(21)*Y3+P(22)*Y8
      Y8=S(X(8),YIC(8))
      Y8=-Y8
      X(10)=P(24)*Y8
      Y10=S(X(10),YIC(10))
      Y10=-Y10
      X(4)=P(13)*Y6+P(12)*Y3+P(14)*RHOI+P(15)*QI
      X(4)=AQI+X(4)
      Y4=S(X(4),YIC(4))
      Y4=-Y4
      X(12)=P(26)*Y5+P(27)*Y12
      Y12=S(X(12),YIC(12))
      Y12=-Y12
      X(14)=P(28)*Y12
   20 Y14=S(X(14),YIC(14))
      Y14=-Y14
      Y1=ETAI+P(2)*Y2+P(1)*STM
      Y1=-Y1
      Y9=P(23)*Y8
      Y9=-Y9
      Y11=Y9+P(25)*Y10
      Y11=-Y11
      ETA2=Y11
      Y7=-Y3
      Y5=P(16)*Y7+Y4
      Y5=-Y5
      Y13=P(29)*Y12
```

```
      Y13=-Y13
      Y15=Y13+P(30)*Y14
      Y15=-Y15
      QI=Y15
      Y6=P(18)*Y7+P(17)*Y5+P(19)*APE+P(20)*ETA2
      Y6=-Y6
C     STATEMENTS PROCESSING END RESULTS EACH RUN                              89
      IF(INPASS)10,10,30
   30 WRITE(2,8)T,Y3,Y5,Y6
    8 FORMAT(6H TIME=,E16.9,6X,8HDENSITY=,E16.9,6X,7HVOLUME=,E16.9,6X,
     113HPRODUCT FLOW=,E16.9)
      J = J+1
      W(J) = T
      U(J,1) = Y3
      U(J,2) = Y6
      U(J,3)=Y5
      IF(J.GE.11)GO TO 35
      IF(J.LE.5) GO TO 31
      IF(J.LE.10) GO TO 34
   34 RHOI=1.0
      WRITE(2,33)RHOI,AQI,ETAI
   33 FORMAT(1H0,*VARIABLES=*,3F10.3)
      GO TO 31
   35 RHOI=0.0
   31 CONTINUE
      GO TO 10                                                             87
   40 CONTINUE
      CALL QUICKPLOT(2,W,U,+301,+3,8H TIME HR,8H D,FLO,V)
      STOP
      END
C     2ND ORDER RUNGE KUTTA INTEGRATION ROUTINE                             9
C     TYPICALLY     Y=S(X,YIC)                                             10
C     WHERE X=INPUT,Y=OUTPUT,YIC=INITIAL CONDITION                         11
C     X MUST NOT BE AN EXPRESSION BUT S MAY BE PART OF A LARGER EXPRESSION 12
C     MAX NO OF INTEGRATORS=100                                            13
      FUNCTION S(B,A)
```

```
      DIMENSION XO(100),YO(100)
      COMMON I,INPASS,H,HON2,YIC,X,T
      I=I+1                                                              17
      IF (INPASS-1)2,1,3                                                 18
C     INITIAL PASS                                                       19
    1 YO(I)=A
      S=A
      RETURN                                                             22
C     PREDICT PASS                                                       23
    2 XO(I)=B
      S=YO(I)+H*B
      RETURN                                                             26
C     CORRECT PASS                                                       27
    3 Z=YO(I)
      YO(I)=Z+HON2*(XO(I)+B)
      S=YO(I)
      RETURN                                                             80
      END                                                                31
C     PASS CONTROL ROUTINE                                               32
C     TYPICAL USAGE     T=TIME(START,STEP,FINISH,GO)                     33
C     T INCREASES FROM START IN INCREMENTS OF STEP UNTIL IT REACHES      34
C     FINISH OR GO BECOMES ZERO, WHICHEVER IS SOONER.                    35
C     ROUTINE CAUSES A SERIES OF INITIAL, PREDICT,AND CORRECT PASSES     36
C     APPROP TO THE INTEGRATION METHOD TO BE MADE THRU THE SIMULATION    37
C     PROPER.                                                            38
      FUNCTION TIME (START, STEP, FINISH, GO)                            39
      COMMON I,INPASS,H,HON2,YIC,X,T
      I=0                                                                41
      IF (INPASS) 300,100,200                                            42
C     PREPARE FOR INITIAL PASS                                           43
  100 H=STEP                                                             44
      HON2=H/2.0                                                         45
      T=START                                                            46
      GO=1.0                                                             47
      INPASS=1                                                           48
      GO TO 500                                                          49
```

```
C     PREPARE FOR A PREDICT PASS
  200 IF(GO)210,410,210
  210 IF(T-FINISH+HON2)220,400,400
  220 T=T+H
      INPASS=-1
      GO TO 500
C     PREPARE FOR A CORRECT PASS
  300 IF(GO) 310,410,310
  310 INPASS=2
      GO TO 500
C     FINISH RUN BUT ALLOW FOR ANOTHER
  400 GO=0.0
  410 INPASS=0
  500 TIME=T
      RETURN
      END
      FINISH
```

APPENDIX D

COMPUTER PROGRAMME IMPULSE

Programme for the determination of the time-domain response of a system given its s-plane constellation and overall gain.

Summary

From a system transfer function the programme determines the impulse response by inverse Fourier transformation and convolves this with the input time function to plot the output time response.

Basis of method

Any system can be represented thus:

$$\underset{X(i\omega)}{x(t)} \quad \boxed{\underset{H(i\omega)}{h(t)}} \quad \underset{Y(i\omega)}{y(t)}$$

where $x(t)$, $y(t)$ and $h(t)$ represent the input and output signals and impulse response in the time domain respectively and $(i\omega)$ indicates the frequency domain.

Also $x(t)$ is the inverse Fourier transform of $X(i\omega)$ and similarly for $h(t)$ and $y(t)$.

Thus, writing (ω) to indicate the frequency domain for convenience,

$$Y(\omega) = H(\omega) \cdot X(\omega) \qquad (1)$$

and

$$y(t) = h(t) * x(t) \qquad (2)$$

where $*$ indicates convolution.

The second expression is equivalent to the statement

$$y(t) = \int_{-\infty}^{\infty} x(\tau).h(t-\tau)d\tau \qquad (3)$$

where τ can be regarded as a dummy variable which disappears on integration. If $H(\omega)$ is known, inverse Fourier transformation gives $h(t)$, thus

$$h(t) = \frac{1}{2\pi} \int_{-\infty}^{\infty} H(\omega)\ e^{i\omega t}\ d\omega \qquad (4)$$

Having h(t) and knowing the input x(t), equations (2) and (3) can be used to find y(t).

Also from the diagram

$$H(\omega) = \frac{Y(\omega)}{X(\omega)}$$

That is, H(ω) is equal to the system transfer function and can be found if the locations of the system poles and zeros are known.

If the system gain and the locations of its poles and zeros is input to the computer, the programme presented will compute H(ω) and use the value in conjunction with equation (4) to obtain h(t). Equation (3) is then used together with the input x(t) to find the time-domain response y(t).

The impulse response

Writing $H(i\omega) = |H(i\omega)|e^{i\beta(\omega)}$

h(t) can be found by inverse Fourier transformation as follows.

$$h(t) = \frac{1}{2\pi} \int_{-\infty}^{\infty} H(i\omega)\ e^{i\omega t}\ d\omega$$

$$= \frac{1}{2\pi} \int_{-\infty}^{\infty} |H(i\omega)| e^{i\omega t} \cdot e^{i\beta(\omega)}\ d\omega$$

$$= \frac{1}{2\pi} \int_{-\infty}^{\infty} |H(i\omega)| \cos(\omega t + \beta(\omega))\ d\omega$$

$$+ \frac{1}{2\pi} \int_{-\infty}^{\infty} |H(i\omega)| \sin(\omega t + \beta(\omega))\ d\omega$$

The integral can be split leading to,

$$h(t) = \frac{1}{2\pi} \int_{-\infty}^{0} |H(i\omega)| e^{i(\omega t + \beta\omega)}\ d(\omega)$$

$$+ \frac{1}{2\pi} \int_{0}^{\infty} |H(i\omega)| e^{i(\omega t + \beta\omega)}\ d\omega$$

The negative integral was omitted from the programme because its inclusion added substantially to the computation time with little effect on the response, particularly as in most engineering problems the choice of initial time (t=0) is open to the operator. However the negative frequency range can be added if desired.

Writing the positive integral as a summation

$$h(t) = \frac{1}{2\pi} \sum_j |H(\omega_j)| e^{i(\omega_j t + \beta(\omega_j))} \Delta\omega_j$$

and making the $\Delta\omega_j$ equal gives

$$h(t) = \frac{\Delta\omega}{2\pi} \sum_{j=0} |H(\omega_j)| e^{i(\omega_j t + \beta(\omega_j))} . \qquad (5)$$

This is the equation used in the programme to obtain the impulse response h(t).

Now for a real stable system h(t) must converge, hence H(ω) can be considered over a restricted frequency range and h(t) over a limited time span. Having h(t), y(t) can be found.

From equations (2) and (3), if x(t) = 0 for t<0

$$y(t) = \int_0^\infty x(\tau)\, h(t-\tau)\, d\tau$$

and proceeding as before,

$$y(t) = \sum_0^\infty x(\tau_j)\, h(t-\tau_j)\, \Delta\tau_j .$$

Since $\Delta\omega_j$ is constant, $\Delta\tau_j$ will be constant, hence,

$$y(t) = \Delta\tau \sum_j^m x(\tau_j)\, h(t-\tau_j)\, \Delta\tau_j . \qquad (6)$$

Equations (5) and (6) are used to compute the time domain responses given the s-plane constellation and K.

The programme

The pole and zero locations and system gain, K, are input on data cards. The programme then calculates the magnitude and phase for nominated frequencies. The impulse response is calculated using equation (5). The input function is generated from the equation

$$x(t) = \sum_j x(\tau_j)\ \Delta\tau.$$

The values of h(t) and x(t) are stored as arrays and used to compute y(t) from equation (6), this also being stored as an array. Finally y(t) is plotted using a very flexible subroutine.

The choice of maximum time and frequency, and of their increments, is quite arbitrary. The maximum time adopted was four times the largest time constant as indicated by the pole near the origin. A period of four time constants allow most stable systems to approach their final steady state value. The time increment was chosen on the assumption that 900 points would give a reasonably smooth plot. This fixes the frequency parameters. Of course these parameters can be varied for any particular case.

The flow diagram for the programme is shown on the following page.

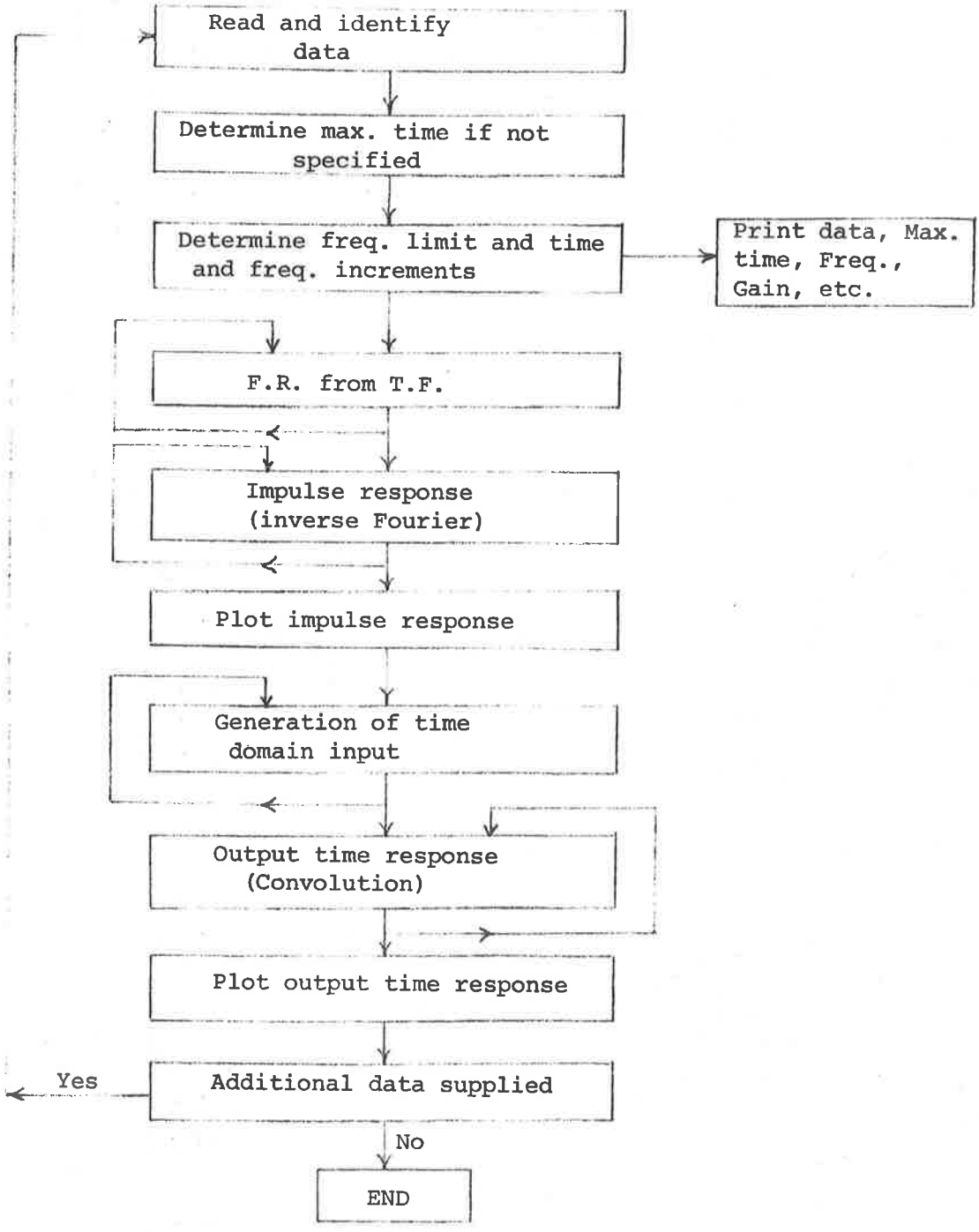
Read and identify data
Determine max. time if not specified
Determine freq. limit and time and freq. increments
Print data, Max. time, Freq., Gain, etc.
F.R. from T.F.
Impulse response (inverse Fourier)
Plot impulse response
Generation of time domain input
Output time response (Convolution)
Plot output time response
Additional data supplied
Yes
No
END

Data Input

All data except external functions must be of the following format.

Column 1 carries the identification code, which must be one of P, Z, K, T or I. P and Z indicate a pole or zero respectively and are omitted if an external function is assumed. K = gain, and has a default value of 1. T indicates the maximum time to be considered; if omitted the programme calculates a value for T_{max}. I indicates an input function.

Columns 7-16, 17-26, 27-36 carry numerical input data in floating-point form (Segments A,B,C).

The pole and zero locations are read in using the P and Z identified cards with the real and imaginary coordinates of the singularities punched in segments A and B.

In the absence of P or Z cards the programme assumes that an external function called TF is provided, e.g.

```
FUNCTION TF (ALPHA)
COMPLEX  TF  etc...
```

the function being placed just before the DATA cards. The system gain K is punched in segment A in floating-point form.

The programme can generate its own input function. Alternatively an I card can be used where the A, B, C segments are used to produce step, ramp, and/or parabolic inputs. For example a card punched

I, 1.0, 0.2, 0.5 would generate the function

$$X(t) = 1.0\ u(t) + 0.2t + 0.5t^2.$$

If the I card is blank an external function is assumed, e.g.

```
      FUNCTION TIP (TIME)
      TIP = 2.0 * (TIME * * 3) + TIME/2.0
      RETURN
      END.
```

The input for t<0 is assumed to be zero. The data cards may be placed in any order except that the I card must be last.

```
DOC PROGRAM
      READ FROM <CR/ATLAS%
      MASTER IMPULSE
      COMPLEX P(20),Z(20),SINGUL,HF(900),HTT(900)
      COMPLEX HT(900)
      INTEGER POLE,ZERO,TIME
      DIMENSION XT(900),YT(900),X(900),Y(1,900),XX(900)
      DATA POLE,ZERO,KAIN,INPT,TIME/1HP,1HZ,1HK,1HI,1HT/
      DATA IPOLE,IZERO/4HPOLE,4HZERO/
      EXTERNAL TTP,TF
 1000 CONTINUE
      TMAX=0.0
      NP,NZ,INEXT=0
      GAIN= 1.0
    1 READ(1,2)IDENT,SINGUL,A
    2 FORMAT(A1,5X,3F10.5)
      IF(IDENT.EQ.POLE)GO TO 3
      IF(IDENT.EQ.ZERO)GO TO 5
      IF(IDENT.EQ.KAIN)GO TO 7
      IF(IDENT.EQ.TIME)GO TO 6
      IF(IDENT.EQ.INPT)GO TO 8
      INEXT =1
    3 NP=NP+1
      P(NP)=SINGUL
      GO TO 1
    5 NZ=NZ+1
      Z(NZ) =SINGUL
    7 GAIN=REAL(SINGUL)
      GO TO 1
    6 TMAX=REAL(SINGUL)
      GO TO 1
    8 STEP=REAL(SINGUL)
      RAMP=AIMAG(SINGUL)
      PBOLIC=A
      IF(STEP+RAMP*PBOLIC.EQ.0.0)INEXT=1
C     DETERMINING AN UPPER FREQUENCY LIMIT
```

```
      M1=900
      M2=900
      BIG=0.0
      SMALL=1.E+20
      DO 10 J=1,NP
      A=CABS(P(J))
      IF(A.GT.BIG)BIG=A
      A=ARS(REAL(P(J)))
   10 IF(A.LT.SMALL)SMALL=A
      DO 12 J=1,NZ
      A=CABS(P(J))
   12 IF(A.GT.BIG)BIG=A
      IF(TMAX.GT.0.0)GO TO 17
      TMAX = 20.0/BIG
      IF(SMALL.NE.0.0)TMAX=8.0/SMALL
   17 CONTINUE
      OMEGA=6.28318531*M2/TMAX
      DOMEGA=OMEGA/M1
C     DETERMINING TIME INCREMENT     DT=TMAX/M1.
      DT=TMAX/M1
      CALL DATE(A)
      WRITE(2,13)A
   13 FORMAT(1H1//5X,5HDATE ,A8)
      WRITE(2,14)IPOLE,(P(J),J=1,NP)
      IF(NZ.GE.1)WRITE(2,14)IZERO,(Z(J),J=1,NZ)
   14 FORMAT(///10X,A4,*LOCATIONS ON S-PLANE*/17X,*REAL*,9X,*IMAG*,/
     1(E25.4,E12.4))
      WRITE(2,114)GAIN
  114 FORMAT(//10X,*LOOP SENSITIVITY*/ E25.4)
      WRITE(2,15)TMAX,OMEGA
   15 FORMAT(//10X,*TIME PERIOD CONSIDERED*/E25.4,*SECONDS*//10X,
     1*MAXIMUM FREQUENCY CONSIDERED*/F25.4,*RADIANS/SECOND*)
      WRITE(2,111) DOMEGA,DT
  111 FORMAT(//10X,*FREQ INCREMENT=*,F8.4,6X,*TIME INCREMENT=*,F8.4)
      IF(INEXT.EQ.1)WRITE(2,116)
  116 FORMAT(//10X,*INPUT   EXTERNAL*)
```

```
      IF(INFXT.EQ.0)WRITE(2,117)STEP,RAMP,PBOLIC
  117 FORMAT(//10X,≠INPUT FORM≠/E25.4,≠UNIT STEP≠/E25.4,
     1≠UNIT RAMP≠/E25.4,≠UNIT PARABOLA≠)
C     DETERMINING FREQ. RESPONSE FROM S-PLANE CONSTELLATION
      BIG=0.0
   18 DO 23 J=1,M1
      HF(J)=CMPLX(GAIN,GAIN)
      X(J)=DOMEGA*(J-1)
      IF(NZ.EQ.0)GO TO 20
      DO 19 JA=1,NZ
   19 HF(J)=HF(J)*(CMPLX(0.0,X(J))-Z(JA))
   20 DO 21 JA=1,NP
   21 HF(J)=HF(J)/(CMPLX(0.0,X(J))-P(JA))
      D=CABS(HF(J))
      IF(D.GT.BIG)BIG=D
      IF(D.GT.BIG/100.0)GO TO 23
      MAXF=J+1
      WRITE(2,46)J,JA,MAXF,M1
   46 FORMAT(4I4)
      DO 22 JA=MAXF,M1
   22 HF(JA)=CMPLX(0.0,0.0)
      GO TO 27
   23 CONTINUE
   27 CONTINUE
C     CALCULATING IMPULSE TIME RESPONSE
      BIG=0.0
      DO 26 J=1,M2
      XX(J)=(J-1)*DT
      HT(J)=CMPLX(0.0,0.0)
      DO 24 JA=1,MAXF
   24 HT(J)=HT(J)+HF(JA)*CEXP(CMPLX(0.0,X(JA)+XX(J)))
      D=ABS(HT(J))
      IF(D.GT.BIG)BIG=D
      IF(J.LE.2)GO TO 26
      DD=ABS(HT(J-2))+ABS(HT(J-1))+D
      IF(DD.GT.BIG/50.0)GO TO 26
```

```
      MAXT=J+1
      DO 25 JA=MAXT,M2
   25 HT(JA)=CMPLX(0.0,0.0)
      GO TO 28
   26 CONTINUE
   28 CONTINUE
      CALL TOLP(MAXT,1,XX,Y,1,1.0,4HTIME,8HRESPONSE)
C     GENERATION OF TIME DOMAIN INPUT (XT)
      IF(INEXT.EQ.0.0)GO TO 38
      DO 39 J=1,MAXT
      XT(J),Y(1,J)=TIP(DT*(J-1))
   39 X(J)=DT*(J-1)
      GO TO 41
   38 DO 37 J=1,MAXT
      A=(J-1)*DT
   37 XT(J)=STEP+RAMP*A+PROLIC*A*A
   41 IF(J.EQ.1)XT(1)=0.0
C     DETERMINING OUTPUT TIME RESPONSE
      DO 50 J=1,MAXT
      YT(J)=0.0
      DO 40 JA=1,J
   40 YT(J)=YT(J)+REAL(XT(JA)*HT(J-JA+1))
   45 YT(J)=YT(J)*DT
      X(J)=(J-1)*DT
   50 Y(1,J)=YT(J)
      CALL TOLP(MAXT,1,X,Y,1,1.0,4HTIME,8HRESPONSE)
      GO TO 1000
      STOP
      END
      SUBROUTINE TOLP(N,J,X,Y,LOG,PAGE,XLABEL,YLABEL)
C     N=NO. PTS   J=NO GRAPHS   X AND Y COORDS
C     LOG  1=ALL LINEAR, 2=X LOG, 3=Y LOG, 4=ALL LOG
C     PAGE=NO OF PAGES   XLABEL AND YLABEL LABEL THE AXES.
      INTEGERS,BLANK,SIDE, VERT,HORIZ
      DIMENSION X(N),Y(J,N),LINE(145),S(10)
      DATA BLANK,SIDE,VERT,HORIZ/1H ,1H0,1H1,1H-/
```

```
      DATA S(1),S(2),S(3),S(4),S(5),S(6),S(7),S(8),S(9),S(10)
     1/1H*,1H.,1H+,1HX,1H0,1H-,1H=,1H0,1HS,1HT/
      DATA XSCALE,YSCALE,XXSCALE,YYSCALE/2*6HLOG    ,2*6HLINEAR/
C     FINDING MAX AND MIN
      XMIN,XMAX=X(1)
      YMIN,YMAX=Y(1,1)
      DO 5 IA=1,N
      IF(X(IA).LT.XMIN)XMIN=X(IA)
      IF(X(IA).GT.XMAX)XMAX=X(IA)
      DO 5 IB=1,J
      IF(Y(IB,IA).LT.YMIN)YMIN=Y(IB,IA)
      IF(Y(IB,IA).GT.YMAX)YMAX=Y(IB,IA)
    5 CONTINUE
      YA=YMAX
      YI=YMIN
      XA=XMAX
      XI=XMIN
C     LOGGING IF REQUIRED
      IF(XMIN.LE.0.0.AND.LOG.EQ.2)LOG=1
      IF(XMIN.LE.0.0.AND.LOG.EQ.4)LOG=3
      IF(YMIN.LE.0.0.AND.LOG.EQ.3)LOG=1
      IF(YMIN.LE.0.0.AND.LOG.EQ.4)LOG=2
      GO TO(22,8,15,8),LOG
    8 XMAX=ALOG10(XMAX)
      XMIN=ALOG10(XMIN)
      DO 10 IA=1,N
   10 X(IA)=ALOG10(X(IA))
      GO TO(22,22,15,15),LOG
   15 YMAX=ALOG10(YMAX)
      YMIN=ALOG10(YMIN)
      DO 20 IA=1,N
      DO 20 IB=1,J
   20 Y(IB,IA)=ALOG10(Y(IB,IA))
C     SCALING AXES
   22 XRANGE=XMAX-XMIN
      YRANGE=YMAX-YMIN
```

```
      IF(XRANGE*YRANGE.GT.0.0)GO TO 26
   24 WRITE(2,28)
   28 FORMAT(////51X,≠TRIVIAL DATA--PLOT SUPPRESSED≠//////)
      GO TO 100
   26 NL=55.0+(PAGE-1.0)*63.0
      NN=NL+1
      XSCFA=142./XRANGE
      YSCFA=NL/YRANGE
      NNN=NN/2
      DO 30 IA=1,N
      X(IA)=(X(IA)-XMIN)*XSCFA
      X(IA)=IFIX(X(IA))+2
      DO 30 IB=1,J
      Y(IB,IA)=(Y(IB,IA)-YMIN)*YSCFA
   30 Y(IB,IA)=IFIX(Y(IB,IA))+1
C     DETERMINING ORIGIN
      XORIGN, YORIGN =-10.0
      IF(XMIN.GT.0.0.AND.XMAX.LT.0.0)GO TO 34
   32 XORIGN=-XMIN * XSCFA
      XORIGN=IFIX(XORIGN)+2
      II=XORIGN
   34 IF(YMIN.GT.0.0.AND.YMAX.LT.0.0)GO TO 38
   36 YORIGN =-YMIN*YSCFA
      YORIGN=IFIX(YORIGN)+1.0
   38 CONTINUE
      IF(LOG.EQ.1.OR.LOG.EQ.3)CALL COPY(6,XSCALE,1,XXSCALE,1)
      IF(LOG.LE.2)CALL COPY(6,YSCALE,1,YYSCALE,1)
      WRITE(2,45)XSCALE,YSCALE,YA
   45 FORMAT(1H1,65X,4HTOLP/95X,4HX -  ,A6,10X,4HY -  ,A6//
     11X,E10.3,1X,145(1H0))
C     SETTING UP LINE
      LINE(1),LINE(145)=SIDE
      DO 65 L=1,NN
      YA= NN-L+1
      IF(L.EQ.NNN)WRITE(2,47) YLABEL
   47 FORMAT(1H+,A10)
```

```
      DO 50 LL=2,144
   50 LINE(LL)=BLANK
      IF(XORIGN.GE.0)LINE(II)=VERT
      IF(YORIGN.NE.YA)GO TO 56
   55 DO 60 LL=2,144
   60 LINE(LL)=HORIZ
   56 DO 62 IB=1,J
      DO 62 IA=1,N
      IF(Y(IB,IA).NE.YA)GO TO 62
   61 LA=X(IA)
      LINE(LA)=S(IB)
   62 CONTINUE
   65 WRITE(2,70)LINE
   70 FORMAT(12X,145A1)
      WRITE(2,80)YI,XI,XA,XLABEL
   80 FORMAT(1X,E10.3,1X,145(1H0)/8X,E10.3,132X,E10.3/75X,A10)
  100 RETURN
      END
      FUNCTION TIP(TIME)
      TIP=1.0
      RETURN
      END
      FUNCTION TF(ALPHA)
      COMPLEX TF
C     THE DESIRED EXTERNAL FN. IS PLACED JUST BEFORE DATA..
C     MC. ASSUMES SUCH A FN. IN ABSENCE OF P OR Z CARDS..
C     THE SYSTEM GAIN IS PUNCHED IN FLOATING POINT FO/M IN THE X-SEG..
      RETURN
      END
      FINISH
```

BIBLIOGRAPHY

1. Andersen, J.A., Glasson, L.W.A. & Lees, F.P.
   Trans.Soc.Inst.Tech. 12, 1. 1960.

2. Benyon, P.R.
   Simulation. 6, 20. 1966.

3. Boarts, R.M., Badger, W.L. & Meisenburg, S.J.
   Ind.Eng.Chem. 29, 912. 1937.

4. Bonilla, C.F., Cervi, A., Colven, T.J., & Wang, S.J.
   CEP Symp. Series, No. 5. 49, 127. 1953.

5. Campbell, D.P. "Process Dynamics". Wiley N.Y. 1958.

6. Catheron, A.R., Goodhue, S.H. & Hansen, P.D.
   Trans. ASME. Paper 59 - IRD - 14.

7. Chantry, W.A. & Church, D.M.
   Chem.Eng.Prog. 54, 64. 1958.

8. Cohen, W.C. & Johnson, E.F.
   CEP Symp. Series No. 36. 57, 86. 1961.

9. idem
   Ind.Eng.Chem. 48, 1031. 1956.

10. Danilova, G.N. & Belsky, V.K.
    Khol.Tekh, 39, 7. 1962.

11. Day, R.L.
    "Plant and process dynamics characteristics" pp 29-55.
    Butterworth, London. 1957.

12. De Frate, L.A. & Hoerl, A.E.
    CEP Symp. Series, No. 21, 55, 43. 1959.

13. Finlay, I.C.
    Chem.& Proc.Eng. (Heat Transfer Survey), 437. 1964.

14. Gould, L.A.
    "Chemical Process Control". Addison-Wesley. 1969.

15. Hazlerigg, A.D.G. & Noton, A.R.M.
    Proc. I.E.E. 112, 2385. 1965.

16. Hempel, A.
    Trans.ASME. D83, 244. 1961.

17. Johnson, D.E.
ISA Journal. 7, 46. 1960.

18. Johnson, E.F.
"Automatic Process Control." McGraw-Hill. NY. 1967.

19. Keenan, J.H., Neumann, E.F. & Lustwerk, F.
J.Appl.Mech., Trans.ASME. 67, A 170, 299. 1950.

20. Knight, G.B.
Chem. Eng. 66, 171. 1959.

21. Koppel, L.B.
Ind.Eng.Chem.Fundas. 1, 131. 1962.

22. idem. ibid. 4, 269. 1965.

23. Law, W.M.
Neue Tech. 4, 34. 1962.

24. Lees, S. & Hougen, J.O.
Ind.Eng.Chem. 48, 1064. 1956.

25. Linebarger, R.N. & Brennan, R.D.
Simulation. 3, 6. 1964.

26. Logan, L.A., Fragen, N. & Badger, W.L.
Ind.Eng.Chem. 26, 1044. 1934.

27. McAdams, W.H.
"Heat Transmission" pp 161. McGraw-Hill, NY. 1933.

28. Mallinson, J.H.
Chem.Eng. 70, 75. 1963.

29. Moore, J.G. & Pinkel, E.B.
Chem.Eng.Prog. 64, 39. 1968.

30. Mostinski, I.L.
Tepleoenergetika No. 4, 66. 1963.

31. Mozley, J.H.
IEC. 48, 1035. 1956.

32. Newman, H.H.
ibid 64, 33. 1968.

33. Parker, N.H.
Chem.Eng. 70, 135. 1963.

34. Paynter, H.M. & Takahashi, Y.
Trans.ASME. 78, 749. 1956.

35. Perry R.H. Chilton C.H. & Kirkpatrick S.D.
"Chem.Engrs.Handbook" 4 edn. McGraw-Hill. NY. 1963.

36. Petrick, M.
Am.I.Ch.E.Journal. 9, 253. 1963.

37. Privott, W.J. & Farrell J.K.
CEP Symp. Series. 62, 200. 1966.

38. Pulling, D.J. & Collier, J.G.
Indust.Chem. 39, 129. 1963.

39. Selfridge, R.G.
Proc.Western Joint Conf. pp 82. 1955.

40. Shmelev, Yn.S., Kostareva, I.V. & Kitaeva, F.I.
Int.Chem.Eng. 6, 308. 1966.

41. Stainthorp, F.P. & Axon, A.G.
Chem.Eng.Sci. 20, 107. 1965.

42. Starczewski, J.
Brit.Chem.Eng. 10, 523. 1965.

43. Stermole, F.J. & Larson, M.A.
Am.I.Ch.E.Journal. 10, 688. 1964.

44. idem
Ind.Eng.Chem.Fundas. 2, 489. 1963.

45. Thal-Larsen, H.T.
Trans.ASME. 82, 489. 1960.

46. Thomasson, R.K.
J.Mech.Eng.Sci. 6, 13. 1964.

47. Williams, T.J. & Morris, H.J.
CEP Symp. Series No. 36. 57, 20. 1961.

48. Wilson, E.E.
Trans.ASME. 37, 47. 1915.

49. Yang, Wen-Jei.
ASME. Paper No. 63-UT-21.

50. idem
Trans.ASME. C 86, 133. 1964.

51. Young, A.J.
"An Intro. to Proc. Control System Design".
Longmans. London. 1955.